Process studies of the carbonate system in coastal and ocean environments of the Atlantic Ocean.

Process studies of the carbonate system in coastal and ocean environments of the Atlantic Ocean

PhD thesis

to obtain the degree of PhD at the
University of Groningen
on the authority of the
Rector Magnificus Prof. E. Sterken
and in accordance with
the decision by the College of Deans.

This thesis will be defended in public on

Friday 21 March 2014 at 12:45 hours

by

Lesley Anne Salt

born on 7 March 1986
in Nottingham, England.

Supervisors
Prof. H. J. W. de Baar
Prof. H. Thomas

Assessment committee
Prof. E. P. Achterberg
Prof. M. González Dávila
Prof. J. B. M. Middelburg

"The fact that we live at the bottom of a deep gravity well, on the surface of a gas covered planet going around a nuclear fireball 90 million miles away and think this to be normal is obviously some indication of how skewed our perspective tends to be."

Douglas Adams.
The Salmon of Doubt: Hitchhiking the Galaxy One Last Time.

Contents

Chapter 1

Introduction

Carbon is the most fundamental building block of life on this planet and the fourth most abundant element in the universe. Of the global carbon reservoir, the vast majority of carbon is stored in carbonate rocks, where it has such a long residence time that it affects climate only on geological time scales (>100 kyear). The next most substantial portion is stored in fossil organic carbon deposits, of which only a small percentage is recoverable as fossil fuel. Other significant carbon stores, which are subject to fluxes over shorter time scales, include the oceans, atmosphere, and the terrestrial biosphere. With the onset of the Industrial Revolution at the end of the 18th Century, human beings have been rapidly releasing naturally, long-term stores of fossil organic carbon by combustion to carbon dioxide (CO_2) that is emitted into the atmosphere. Over the 20th Century the atmospheric CO_2 concentration increased by more than 20%, and the rate of increase is still rising. The Intergovernmental Panel on Climate Change (IPCC) predict atmospheric CO_2 partial pressure to be between 490 – 1,250 ppm by the end of the 21st Century, which would place concentrations at least ~190 ppm higher than has been seen in the past 100,000 years (Petit et al., 1999; Macfarling Meure et al., 2006). The consequences of the escalation of atmospheric CO_2 are not fully understood, thus we are now partaking in a, potentially very risky, global biogeochemical experiment.

1.1   Carbon dioxide in the ocean-atmosphere system

In geological history a close link has been observed between the climate and atmospheric CO_2 concentrations over the glacial-interglacial cycle (Petit et al., 1999). Prior to 1800 the atmospheric CO_2 concentration had been quite stable between 272 and 284 ppm (Macfarling Meure et al., 2006), at the peak of an inter-glacial period. Since then there has been an exponential increase in anthropogenically-produced CO_2 (Keeling and Whorf, 2004) with the current atmospheric concentration having just reached over 400 µatm (Manoa Loa Observatory, *http://co2now.org/Current-CO2/CO2-Now/noaa-mauna-loa-co2-data.html*). Carbon dioxide is a *greenhouse* gas, meaning that it absorbs the sun's energy when it is emitted from the land as infrared radiation, thus trapping a portion of the sun's energy as heat within the atmosphere. A number of gases contribute to this process (e.g. H_2O, CH_4, N_2O), however, due to its sheer amount, CO_2 is the second overall most effective, after water vapor (Finlayson-Pitts and Pitts, 2000). The temperature increase is proportional to the enhanced radiative forcing caused by higher CO_2 concentrations. The effects of increasing temperatures include changes in precipitation patterns, a reduction in snow cover and sea ice, and an overall reduction in the effectiveness of the ocean to absorb anthropogenic CO_2.

It was proposed at the beginning of the 20th Century that a portion of the CO_2 produced from fossil fuel combustion was being taken up by the oceans, which has since proved to be the case. Of the total 300 Pg C (Pg = 10^{15}g) that humankind has already released (Archer, 2005), it has been shown, through a variety of techniques, that approximately 40% has been taken up by the world ocean (Sabine, 2004), which currently amounts to approximately 120 PgC. The transfer of CO_2 from the atmosphere into the ocean is primarily driven by a simple thermodynamic flux, caused by the differential in partial pressure between the two mediums. At equilibrium the CO_2 in surface waters can be described by Henry's Law:

$$[CO_2] = K_0 \cdot fCO_2, \hspace{3cm} \text{(equation 1)}$$

where K_0 is the solubility coefficient in seawater and fCO_2 is the fugacity of CO_2 in µatm. That is to say that when, due to continuing CO_2 emissions by mankind, the atmospheric pCO_2 is higher than the oceanic pCO_2, there will continue to be a flux into the ocean. In reality this pCO_2 equilibrium between the ocean and atmosphere is modified by winds, biological uptake and temperature, leading to large heterogeneity of surface ocean pCO_2 in different regions of the global ocean.

The accumulation of carbon dioxide in the oceans leads to the phenomenon known as *ocean acidification* (Doney et al., 2009; Raven, 2005). This term can be misleading, as the oceans will never become *acidic* (i.e. reach a pH below 7). In fact it refers more to the increase in proton (H^+) concentration and decrease in hydroxide ion (OH^-) concentration as a result of the formation and subsequent dissociation of carbonic acid. The uptake of anthropogenic CO_2 has already caused a drop of 0.1 pH units in surface ocean pH (Orr et al., 2005) and is estimated to cause a further reduction of ~0.3-0.5 by the end of the century (Caldeira and Wickett, 2005). The concurrent depletion in carbonate ion concentration is also predicted to have a detrimental effect on a number of calcifying organisms (Fabry et al., 2008) and is already having an impact in some areas of the Southern Ocean (Bedarnsk et al., 2012). Recent findings by Wootton et al. (2008) indicate that ocean acidification may be taking place at a faster rate than previously predicted in the coastal regions. Due to the large amount of primary production taking place in these regions it is becoming increasingly important to further our understanding of the fate of carbon in coastal and shelf systems.

1.2   Carbon dioxide in seawater

Of the combined ocean-atmosphere system 98% of the carbon is stored in the ocean (Zeebe and Wolf-Gladrow, 2001). The ocean acts as a very effective store of carbon due to the

behavior of the dissolved chemical carbon species. When carbon dioxide (CO_2) dissolves in water it forms carbonic acid (H_2CO_3), which is a weak, diprotic acid. It thus partially dissociates in solution, releasing one or two protons (H^+) as shown in equations 2 and 3.

$$H_2CO_3 \xleftarrow{} K_1 \xrightarrow{} HCO_3^- + H^+ \qquad \text{(equation 2)}$$

$$HCO_3^- \xleftarrow{} K_2 \xrightarrow{} CO_3^{2-} + H^+ \qquad \text{(equation 3)}$$

These equations represent a buffering system whereby further addition of carbonic acid, carbon dioxide, or carbonate shifts the respective equilibriums towards the bicarbonate state, which is the dominant carbonate specie in the pH range found in the oceans. The K_1 and K_2 are the acid dissociation constants of carbonic acid, which can be defined by the following two equations:

$$K_1 = [HCO_3^-][H^+]/[H_2CO_3] \qquad \text{(equation 4)}$$

$$K_2 = [CO_3^{2-}][H^+]/[HCO_3^-] \qquad \text{(equation 5)}$$

These dissociation constants, sometimes referred to in the logarithmic form as pK_1 and pK_2, are heavily dependent upon salinity, temperature and pressure. One of the challenges of quantifying the carbonate system is that many of the chemical species cannot be directly measured and thus must be indirectly calculated using the aforementioned equations.

There are four measurable carbonate parameters: total alkalinity (TA, A_T), dissolved inorganic carbon (DIC, C_T), pH and pCO_2. The latter two provide direct concentrations of $[H^+]$ and $[CO_2(aq)*]$, where the * represents a combination of $CO_2(aq)$ and H_2CO_3, as the two species can not be analytically differentiated. The definitions of these four parameters are as follows:

A_T = $[HCO_3^-]$ + $2[CO_3^{2-}]$ + $[B(OH)_4^-]$ + $[OH^-]$ + $[HPO_4^{2-}]$ + $2[PO_4^{3-}]$ + …$[H_3SiO_4^-]$ + … $[NH_3]$ + $[HS^-]$ +… - $[H^+]$ – $[HSO_4^-]$ – $[HF]$ – $[H_3PO_4]$ – $[HNO_2]$ + … (Dickson, 1981).

$$\text{(equation 6)}$$

DIC = $\sum[H_2CO_3]$ + $[HCO_3^-]$ + $[CO_3^{2-}]$ $\qquad$ (equation 7)

pH = $-\log_{10}[H^+]$ $\qquad$ (equation 8)

pCO_2 = $x(CO_2) \cdot p,$ $\qquad$ (equation 9)

where $x(CO_2)$ represents the mole fraction of CO_2 and p represents the pressure of equilibration. From any two of these measured variables, with complementary hydrographic data and K_1 and K_2 parameterizations, it is possible to calculate the other two variables. Where more than two parameters are determined it becomes possible to assess how *internally consistent* the system is (i.e. how well the calculated values represent the measured values). A number of studies into this have demonstrated that significant differences are obtained when using different determinations of the dissociation constants. These differences are frequently larger than the error associated with measuring them, as such, measuring as many parameters as possible is generally favorable. The lack of ideal closure in the carbonate system remains an issue in the inorganic marine carbon community (see Chapter 2).

The vast majority of inorganic carbon in seawater is riverine in origin, accumulated downstream from the chemical weathering and dissolution of carbonate rocks. Due to the dominance of the carbonate and bicarbonate ions in the alkalinity equation, this chemical weathering and dissolution also represents the dominant supply of total alkalinity to the ocean. A result of this is that in coastal regions with strong riverine influence there is a strong negative correlation between salinity, DIC and A_T. In contrast, in the surface waters of the open ocean this relationship is reversed, as the conservative nature of DIC, A_T mean that they are influenced in the same way as salinity to physical processes, such as, mixing and evaporation, leading to a tight co-correlation. In the presence of biological activity however, both parameters can show substantial deviations from conservative behavior.

The DIC is taken up by phytoplankton in photosynthesis and, in some organisms, for the formation of calcium carbonate. It can similarly be released in the respective reverse processes of respiration and dissolution, as shown in the equations below.

$$106 \, CO_2 + 122 \, H_2O + 16 \, HNO_3 + H_3PO_4 \leftarrow\rightarrow$$

$$[(CH_2O)_{106}(NH_3)16H_3PO_4]_{organic} + 138 \, O_2$$

(equation 10)

$$Ca^{2+} + 2HCO_3^- \leftarrow\rightarrow CaCO_3 + [CO_2{*}]$$ (equation 11)
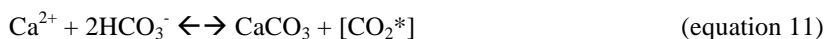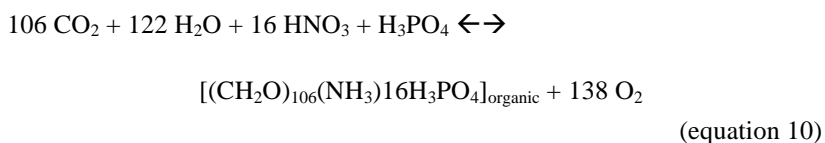
Depending on the amount of phytoplankton present, the process of photosynthesis can lead to large deficits of DIC in surface waters and a lowering of pCO_2 causing a subsequent flux of CO_2 from the atmosphere into the ocean. The majority of the biologically sequestered carbon is released back into the water column following respiration by bacteria. The amount

of carbon that is transported into deeper water layers and ultimately to the seafloor depends on a number of factors, such as, the phytoplankton class group (Jin et al., 2006; Klaas and Archer, 2002), and the depth of the water column (Reimer et al., 1999; Beck and Brumsack, 2012). Further degradation takes place in the sediment, through the following series of electron acceptors: O_2, SO_4^{2-}, MnO, FeOOH, H_2S and CO_2 (Mackin et al., 1989). The ratio of remineralization which takes place in the water column compared to the sediment is largely dependent on the depth of the water column, and ranges from 99% in the open ocean (Dunne et al., 2007) to 30% in the German Bight (Reimer et al., 1999) and 50% in the Wadden Sea (van Beusekom et al., 1999).

The formation and dissolution of calcium carbonate helps to regulate the carbonate system on much longer time scales (Archer, 2005). There are two forms of calcium carbonate; aragonite and calcite. Calcite is the more stable form and thus the depth at which dissolution rapidly increases (chemical lysocline) is approximately 2km deeper than that of aragonite in the Atlantic Ocean. Above this depth, the formation of $CaCO_3$ is the dominant process due to the presence of calcifying phytoplankton and zooplankton. At greater depths a combination of increasing pressure, lower temperatures and decreasing pH leads to the dissolution of $CaCO_3$. Despite this general trend, the analysis of high-quality A_T data from the Atlantic has also shown that a significant proportion of $CaCO_3$ dissolution occurs at depths shallower than the chemical lysocline (Chung et al., 2003). Shallow water dissolution is potentially significant as the generation of A_T in surface waters helps to buffer the changes in the carbonate system caused by increasing pCO_2. However, in shelf systems it has been shown that shallow water $CaCO_3$ dissolution is much less significant compared to the A_T produced from other processes, such as sulfate reduction (Chen, 2002).

In contrast to DIC and A_T, pH and pCO_2 show great variability with temperature and pressure changes, making them ideal to monitor smaller, and short term, variations in surface waters. Normally pH and pCO_2 show a strong anti-correlation to one another due to the associated decrease in pH with increasing CO_2 concentrations. For these reasons A_T and DIC are the preferred parameters to measure for deep ocean work, whereas pH and pCO_2 can reveal more subtle dynamics on shorter time scales in the surface ocean (Thomas et al., 2012).

1.3   Coastal and Oceanic systems

The coastal and the oceanic carbonate systems obey the same thermodynamic principles, however, external influences and inputs lead to significant differences between the two. DIC has a residence time of less than a decade in surface waters, from a decade to a century in intermediate waters and up to millennia in deep waters. The natural variability of DIC in each of these waters reflects this stability, meaning that coastal regions and shelf seas undergo natural changes on much shorter time scales compared to the open ocean. The closer proximity of the waters to the atmosphere also means that anthropogenic changes are likely to be greater in the shallow coastal seas than in the deep oceans. This then creates two separate challenges in these two environments: distinguishing large changes in a system with large natural variability and distinguishing very small changes in a system that is very stable.

Furthermore, surface waters in coastal regions tend to be subjected to more varied and direct influences due to their close proximity with the atmosphere and sediment. These influences also experience variability on long and short time scales making a very multi-disciplined approach necessary. On the other hand, studying deep waters brings the inherent problem that we do not know the full range of the natural variability. This problem is then compounded by the fact that at the present time, some of the changes we expect to see are the same size as the error margin of our techniques. These problems highlight the need to a multi-faceted approach to improve our knowledge of the global carbon cycle in both coastal and oceanic areas.

The situation becomes further complicated when taking into account how large scale forcing interacts with local forcing. The North Atlantic Oscillation index is a measure of the pressure differential between Iceland and the Azores, thus giving an indication of the strength of the westerly winds between years. It has been shown that the NAO impacts surface hydrographic properties of the North Atlantic Ocean, which affect the carbonate system through pCO_2 uptake [Belkin, 2004; Lefèvre et al., 2004; Schuster and Watson, 2007; Thomas et al., 2008]. The NAO also exerts a large influence on wind and precipitation patterns across the Northwest Atlantic Ocean [Ionita et al., 2011; Hurrell and Deser, 2009]. Due to the large role that riverine inputs have in the coastal and shelf areas, the NAO can cause significant changes in the coastal regions, as well as in the open oceans [Patsch et al., 2002; Kuhn et al., 2010; Lenhart et al., 2004]. Further imposed on this is the potential change in temperature, stratification and water advection [Hordair and Meijer, 2010; Winther and Johannessen, 2006]. Resolving all of these interactions is inherently difficult as many exert opposing

influence, for example, warmer temperatures increasing the summertime pCO_2, but greater water advection of water with lower DIC, thus decreasing summertime pCO_2. Attempting to quantify each of these roles is fundamental in understanding the variability of the carbonate system in coastal and oceanic systems.

1.3.1   Coastal systems, shelf seas and continental shelves

Despite the relatively small area occupied by continental shelves (7%), these regions support a large amount of marine primary production (15-30%, Gattuso et al., 1998). The potential sink of carbon dioxide that these areas represent makes them significant on a global scale with regards to carbon cycling. The continental shelf can be sub-divided into estuaries and shelf, or marginal, seas and further categorized by latitude band. However, as this thesis only deals with continental shelves in the temperate region, high- and low-latitude continental shelves will not be discussed further.

Cai (2011) defines estuaries as areas between the river mouth and tidewater, where freshwater mixes with seawater. The generally shallow water depth in these areas means that there is close interaction between the sediment, water column and the atmosphere, making estuaries biogeochemically very active. It also means that the water column is relatively easily mixed through wind-forcing and tides. Estuarine regions usually support high levels of biological activity due to the input of nutrients and organic carbon from land, entering the sea either from rivers or runoff. Despite this production estuaries have been defined as overall CO_2 sources, opposed to sinks, supplying 0.25 Pg C m^{-2} y^{-1} (Borges et al., 2005; Cai, 2011). When particularly large concentrations of inorganic nutrients are supplied to these regions, eutrophication can occur, leading to greater heterotrophy than autotrophy. The Northwest European continental shelf saw a large increase in incidences of eutrophication from the 1950's to the 1980's with increasing use of fertilizers and urbanization. Eutrophication has been shown to favor larger phytoplankton species (Grover, 1997) and shifts in community structure have been observed in connection with changing nutrient concentrations (Philippart et al., 2000; Philippart et al., 2007).

Beyond the estuaries, but where the effects of terrestrial input are still felt, are the shelf, or marginal, seas, which can be described as the transition zone between the coast and the open ocean. The Atlantic Ocean has the highest concentration of shelf seas of all the oceans in the world, which include the North Sea, Baltic Sea, Irish Sea, Scotia Sea, and the Mediterranean

Sea. At temperate latitudes the shelf seas show large intra-annual variations in the carbonate system related to the seasonally-driven phytoplankton blooms (Prowe et al., 2009; Ishii et al., 2011; Shadwick et al., 2011; Huertas et al., 2006]. How productive a region is exerts large control over how much carbon is drawn down from the atmosphere. The heterogeneity between continental shelves means that observed air to sea CO_2 fluxes range from 32g C m^{-2} a^{-1} in the East China Sea and the Gulf of Biscay (Tsunogai et al., 1999; Frankignoulle and Borges, 2001) to 17g C m^{-2} a^{-1} in the North Sea (Thomas et al., 2004). The fate of the carbon sequestered in phytoplankton and zooplankton determines whether the overall system acts as a CO_2 source or sink.

In the estuarine/coastal system, it is vital to determine the pathway and fate of the sequestered carbon in order to extrapolate whether regions are overall CO_2 sinks or sources. A shallow water column often means that any CO_2 taken up in biomass is likely to be remineralized and released back to the atmosphere before being transported to the open ocean. The North Sea has been determined an overall CO_2 sink (Bozec et al., 2005) and an example of a *continental shelf pump*, a term coined by Tsunogai, in 1999, who noted the "export" potential of shelf seas with respect to CO_2. It is used to describe the export of carbon drawn down on the shelf and subsequently transported into the deep, adjacent ocean. The northern North Sea performs this operation very effectively, however, the shallower southern North Sea is limited by high remineralization rates in the water column. Contrastingly, shallow regions, and larger classes of phytoplankton, are associated with larger carbon contributions to the sediment (Riegman et al., 1993) where a variable fraction can be remineralized or buried. The higher flux of organic matter to the sediment can also lead to anoxic conditions resulting in the generation of A_T through denitrification or sulfate reduction (Thomas et al., 2009). Such A_T generation could lead to an enhanced buffering capacity of overlying waters, if produced in sufficient quantities, again highlighting the need of a multi-disciplinary approach to carbonate studies in these areas.

1.3.2   Open Ocean

While continental shelves have been shown to hold substantial anthropogenic carbon stores (Lee et al., 2011) they cannot compete with the vastness of the larger oceans. The Atlantic Ocean currently contains ~38% of the total global C_{ant} inventory (Sabine et al., 2004) making it the largest store of all the oceans. In the North Atlantic the deep water formation is largely responsible for the majority of C_{ant} uptake, whereas in the South Atlantic the most effective uptake occurs in the SubAntarctic Zone (McNeil et al., 2007), where large amounts of C_{ant}

are injected into intermediate depths. Despite this efficiency the volume of Antarctic Bottom Water means that this water mass represents one of the most significant stores of C_{ant} in the Southern Ocean (Rios et al., 2012). On a global scale ~50% of C_{ant} accumulation resides in the upper 400 m (Sabine et al., 2004) and this number is predicted to rise as the flux into the ocean accelerates with increasing atmospheric concentrations.

The open ocean generally shows the least variation over short time scales, however, arguably the most over longer time scales. Climatic forcing is one relatively short-term driver, which affects the carbonate system in the surface waters of ocean basins. The NAO index shows strong correlations to temperature and salinity anomalies across the North Atlantic subtropical gyre (Thomas et al., 2008) and to the circulation pattern and inflow rates of the North Sea (Winther and Johannasson, 2006). A shift from a predominantly negative NAO index to predominantly positive index has been suggested as being responsible for a notable decline in ΔpCO_2 (pCO_{2sea} – pCO_{2air}) observed over the past decade in the North Atlantic Ocean (Lefèvre et al., 2004; Corbiere et al., 2007; Watson et al., 2009). As the effects on the two sides of the North Atlantic subtropical gyre were different, and it takes time for the water to travel, one must consider the immediate effects but also the longer-term lag effects, depending on where and when one is measuring. Such effects have been noted at the European Station for Time series in the Ocean at the Canary Islands (ESTOC) station (Santana-Casiano et al., 2007) and the Bermuda Atlantic Time Series (BATS) station (Bates, 2001) and have also been shown to have an impact on the C_{ant} uptake of the region (Perez et al., 2010).

1.3 Objectives of this thesis

This thesis was designed to build upon an extensive dataset of carbonate system measurements obtained in the North Sea over 5 years, and examine changes in the buffering capacity. Covering the same stations at the same time of year (late summer 2001, 2005 and 2008) allowed direct comparison of the carbonate system and the distribution of carbonate parameters. This work was further complemented with the development of a time-series station adjacent to the North Sea, in the Marsdiep basin of the Wadden Sea, and by continuous pCO_2 measurements on the other side of the North Atlantic basin. Two cruises covering the southwest Atlantic provided further opportunity to examine the processes operating in shelf seas compared to those in the ocean.

1.4 Thesis Outline

This thesis deals with the buffering capacity of coastal and oceanic systems with regard to the continual increase in anthropogenic, atmospheric CO_2 concentrations. The effects of rising CO_2 concentrations are placed in the context of natural carbon variability in a number of environments of the Atlantic Ocean.

In **Chapter 2** we first describe the techniques used to measure the four carbonate variables and assess how robust our basic assumptions of the carbonate system are based on the consistency between the measured and calculated variables. This internal consistency study uses 6 data sets from the North Sea, including four seasonal data sets, to assess how these calculations hold up throughout the year and in different salinity environments within the North Sea. A number of similar studies have been undertaken in the laboratory and in the open ocean, however, here we present the results from the first such study to take place in a coastal or shelf-sea environment.

The Wadden Sea exerts a large influence on the southern North Sea, supplying large quantities of DIC and A_T. In **Chapter 3** we use two and a half years worth of time series data from the Marsdiep basin of the Wadden Sea to examine the seasonal controls on DIC and A_T. This was done in light of recent evidence that coastal sediments could produce significant fluxes of A_T to the overlying waters, facilitating a degree of buffering against increasing CO_2 concentrations. The effects of phytoplankton succession during the spring bloom on DIC and A_T were also investigated.

Having examined the local contributions to the carbon dynamics of the North Sea, placing it in the context of larger scale forcing is also necessary. **Chapter 4** employs three reoccupations of the North Sea during late summer in 2001, 2005 and 2008, during years of differing North Atlantic Oscillation states. We attempt to deconvolute a number of internal and external forcings on the shelf sea to investigate how these conditions control the effectiveness of the North Sea as a 'shelf pump' of CO_2.

Time series are often limited by resolution of sampling, thus in **Chapter 5** we use continuous, high-frequency measurements from a CARIOCA buoy coupled with data from a SeaHorse profiler to examine the diel CO_2 cycling occurring on the Scotian shelf throughout the year. We show how temperature and light controls the seasonal, and daily cycle of CO_2 drawdown by phytoplankton.

In **Chapter 6** we examine the increase in anthropogenic carbon, which has taken place over the past 17 years, in the southwest Atlantic Ocean. Here we use the benchmark dataset from the World Ocean Circulation Experiment (WOCE) in 1994 to perform an extended Multi Linear Regression (eMLR) in comparison with the more recent West Atlantic Geotraces section (2010/11). The anthropogenic influx is placed into the context of the buffering capacity of differing water masses. We show that the anthropogenically-driven decrease in pH is not directly proportional to the amount of carbon added to seawater, but relies heavily on other water mass characteristics.

Finally, the main conclusions from this body of research is summarized and placed in the wider context of the field. The implications and recommendations for future research are also discussed.

References

Archer, D. (2005). Fate of fossil fuel CO_2 in geologic time. *J. Geophys. Res.* 110, C09S05.

Bates, N. R. (2001). Interannual variability of oceanic CO_2 and biogeochemical properties in the Western North Atlantic subtropical gyre. *Deep-Sea Res. II* 48, 1507-1528.

Beck, M., and H. –J. Brumsack, (2012). Biogeochemical cycles in sediment and water column of the Wadden Sea: The example Spiekeroog Island in a regional context. *Ocean Coast. Manage.* 68, 102-113.

Bednaršek, N., G.A. Tarling, D.C.E. Bakker, S. Fielding, E.M. Jones, H.J. Venables, P. Ward, A. Kuzirian, B. Lézé, R.A. Feely and E.J. Murphy (2012). Extensive dissolution of live pteropods in the Southern Ocean. *Nat. Geosc.* 5, 881-885.

Belkin, I. M. (2004). Propagation of the "Great Salinity Anomaly" of the 1990s around the Northern Atlantic. *Geophys. Res. Lett.* 31, L08306.

van Beusekom, J.E.E.., U.H. Brockmann, K.-J. Hesse, W. Hickel, K. Poremba, and U. Tillmann (1999). The importance of sediments in the transformation and turnover of nutrients and organic matter in the Wadden Sea and German Bight. *Ger. J. Hydrogr.* 51, 245-266.

Borges, A.V., B. Delille, and M. Frankignoulle (2005). Budgeting sinks and sources of CO_2 in the coastal ocean: Diversity of ecosystems counts. *Geophys. Res. Lett*. 32, L14601.

Bozec, Y., H. Thomas, K. Elkalay and H.J.W. de Baar (2005). The continental shelf pump for CO_2 in the North Sea – evidence from summer observation. *Mar. Chem.* 93, 131-147.

Cai, W., (2011). Estuarine and Coastal Ocean Carbon Paradox: CO_2 Sinks or Sites of Terrestrial Carbon Incineration? *Ann. Rev. Mar. Sci.* 3**,** 123-145.

Caldeira, K. and M. E. Wickett (2005). Ocean model predictions of chemistry changes from carbon dioxide emissions to the atmosphere and ocean. *J. Geophys. Res.* 110, C09S04.

Chen, C.-T.A. (2002). Shelf-vs. dissolution-generated alkalinity above the chemical lysocline, *Deep-Sea Res. II* 49, 5365-5375.

Chung, S.-N., K. Lee, R.A. Feely, C.L. Sabine, F.J. Millero, R. Wanninkhof, J.L. Bullister, R.M. Key, and T.-H. Peng (2003). Calcium carbonate budget in the Atlantic Ocean based on water column inorganic carbon chemistry. *Global Biogeochem. Cycles* 17(4), 1093.

Corbière, A., N. Metzl, G. Reverdin, C. Brunet and T. Takahashi (2007). Interannual and decadal variability of the oceanic carbon sink in the North Atlantic subpolar gyre. *Tellus* 59B, 168-178.

Dickson, A.G. (1981). An exact definition of total alkalinity and a procedure for the estimation of alkalinity and total inorganic carbon from titration data, *Deep-Sea Res., 28A* (6), 609-623.

Doney, S.C., V.J. Fabry, R.A. Feely and J.A. Kleypas (2009). Ocean acidification: the other CO_2 problem. *Ann. Rev. Mar. Sci.* 1, 169-192.

Dunne, J.P., J.L. Sarmiento, and A. Gnanadesikan (2007). A synthesis of global particle export from the surface ocean and cycling through the ocean interior and on the seafloor. *Global Biogeochem. Cycles* 21, GB4006.

Fabry, V.J., B.A. Seibel, R.A. Feely, and J.C. Orr (2008). Impacts of ocean acidification on marine fauna and ecosystem processes. *ICES J. Mar. Sci.* 65, 414-432.

Finlayson-Pitts, B.J., and J.N. Pitts (1999). *Chemistry of the Upper and Lower Atmosphere*. Academic Press: New York, 1999.

Frankignoulle, M., and A.V. Borges (2001). European continental shelf as a significant sink for atmospheric carbon dioxide. *Global. Biogeochem. Cycles* 15(3), 569-576.

Gattuso, J.-P., M. Frankignoulle, and R. Wollast (1998). Carbon and carbonate metabolism in coastal aquatic ecosystems. *Ann. Rev. Ecol. Syst.* 29, 405–434.

Grover, J.P (1997). Resource competition. London: Chapman and Hall, 342.

Hordoir, R., and H.E.M. Meier (2010). Freshwater fluxes in the Baltic Sea: A model study. *J. Geophys. Res.* 115, C08028.

Huertas, I.E., G. Navarro, S. Rodríguez-Gálvez and L.M. Lubián (2006). Temporal patterns of carbon dioxide in relation to hydrological conditions and primary production in the northeastern shelf of the Guld of Cadiz (SW Spain). *Deep-Sea Res. II* 53, 1344-1362.

Hurrell, J.W. (1995). Decadal trends in the North Atlantic Oscillation: Regional temperatures and precipitation. *Science* 269, 676–679.

Hurrell, J.W. and C. Deser (2010). North Atlantic climate variability: The role of the North Atlantic. *J. Mar. Syst.* 79, 231-244.

Ionita, M., N. Rimbu, and G. Lohmann (2011). Decadal variability of the Elbe River streamflow. *Int. J. Climatol.* 31, 22-30.

IPCC (2007). Climate Change 2007: The Physical Science Basis. Contribution of Working Group I to the Fourth Assessment. Report of the Intergovernmental Panel on Climate Change. Edited by: S. Solomon, D. Qin, M. Manning, Z. Chen, M. Marquis, K.B. Averyt, M. Tignor and H.L. Miller. Cambridge University Press, Cambridge, United Kingdom and New York, NY, USA.

Ishii, M., N. Kosugi, D. Sasano, S. Saito, T. Midorikawa and H. Y. Inoue (2011). Ocean acidification off the south coast of Japan: A result from time series observations of CO_2 parameters from 1994 to 2008. *J. Geophys. Res.* 116, C06022.

Jin, X., N. Gruber, J.P. Dunne, J.L. Sarmiento, and R.A. Armstrong (2006). Diagnosing the contribution of phytoplankton functional groups to the production and export of

particulate organic carbon, $CaCO_3$, and opal from global nutrient and alkalinity distributions. *Global Biogeochem. Cycles* 20, GB2015.

Klaas, C., and D.E. Archer (2002). Association of sinking organic matter with various types of mineral ballast in the deep sea: Implications for the rain ratio. *Global Biogeochem. Cycles 16(4)*, 1116.

Kühn, W., J. Pätsch, H. Thomas, A.V. Borges, L.–S. Schiettecatte, Y. Bozec and A.E.F. Prowe (2010). Nitrogen and carbon cycling in the North Sea and exchange with the North Atlantic-A model study, Part II: Carbon budget and fluxes. *Cont. Shelf Res.* 30, 1701-1716.

Lee, K., C.L. Sabine, T. Tanhua, T.–W. Kim, R.A. Feely and H.–C. Kim (2011). Roles of marginal seas in absorbing and storing fossil fuel CO_2. *Energy Environ. Sci.* 4, 1133.

Lefèvre, N., A.J. Watson, A. Olsen, A.F. Ríos, F.F. Pérez and T. Johannessen (2004). A decrease in the sink for atmospheric CO_2 in the North Atlantic. *Geophys. Res. Lett.* 31, L07306.

Lenhart, H.J., J. Pätsch, W. Kühn, A. Moll, and T. Pohlmann (2004). Investigation on the trophic state of the North Sea for three years (1994-1996) simulated with the ecosystem model ERSEM – the role of a sharp NAOI decline. *Biogeosciences Discuss.* 1, 725-754.

Macfarling Meure, C., D. Etheridge, C. Trudinger, P. Steele, R. Langenfelds, T. van Ommen, A. Smith and J. Elkins (2006). Law Dome CO_2, CH_4 and N_2O ice core records extended to 2000 years BP. *Geophys. Res. Lett.* 33, L14810.

Mackin, J.E., and K.T. Swider (1989). Organic matter decomposition pathways and oxygen consumption in coastal marine sediments. *J. Mar. Res.* 47, 681-716.

McNeil, B.I., N. Metzl, R.M. Key, R.J. Matear, and A. Corbiere (2007). An empirical estimate of the Southern Ocean air-sea CO_2 flux. *Global Biogeochem. Cycles* 21, GB3011.

Pätsch, J., W. Kühn, G. Radach, J.M. Santana Casiano, M. Gonzalez Davila, S. Neuer, T. Freudenthal and O. Llinas (2002). Interannual variability of carbon fluxes at the North Atlantic Station ESTOC. *Deep-Sea Res. II* 49, 253-288.

Pérez, F.F., M. Vázquez-Rodríguez, H. Mercier, A. Velo, P. Lherminier, and A.F. Ríos (2010). Trends of anthropogenic CO_2 storage in North Atlantic water masses. *Biogeosciences* 7, 1789-1807.

Petit, J.R., J. Jouzel, D. Raynaud, N.I. Barkov, J.–M. Barnola, I. Basile, M. Benders, J. Chappellaz, M. Davis, G. Delaygue, M. Delmotte, V.M. Kotlyakov, M. Legrand, V.Y. Lipenkov, C. Lorius, L. Pépin, C. Ritz, E. Saltzman and M. Stievenard (1999). Climate and atmospheric history of the past 420,000 years from the Vostok ice core, Antarctica. *Nature* 399, 429-436.

Philippart, C.J.M., G.C. Cadée, W. van Raaphorst, and R. Riegman (2000). Long-term

phytoplankton-nutrient interactions in a shallow coastal sea: algal community structure, nutrient budgets, and denitrification potential. *Limnol. Oceanogr.* 45, 131-144.

Philippart, C.J.M., J.J. Beukema, G.C. Cadée, R. Dekker, P.W. Goedhart, J.M. van Iperen, M.F. Leopold, and P.M.J. Herman (2007). Impacts of nutrient reduction on coastal communities. *Ecosystems* 10, 95-118.

Prowe, A.E.F., H. Thomas, J. Pätsch, W. Kühn, Y. Bozec, L.–S. Schiettecatte, A.V. Borges, and H.J.W. de Baar (2009). Mechanisms controlling the air–sea CO_2 flux in the North Sea. *Cont. Shelf Res*. 29, 1801-1808.

Orr, J.C., V.J. Fabry, O. Aumont, L. Bopp, S.C. Doney, R.A. Feely, A. Gnanadesikan, N. Gruber, A. Ishida, F. Joos, R.M. Key, K. Lindsay, E. Maier-Reimer, R. Matear, P. Monfray, A. Mouchet, R.G. Najjar, G.-K. Plattner, K.B. Rodgers, C.L. Sabine, J.L. Sarmiento, R. Schlitzer, R.D. Slater, I.J. Totterdell, M.-F. Weirig, Y. Yamanaka and A. Yool (2005). Anthropogenic ocean acidification over the twenty-first century and its impact on calcifying organisms. *Nature* 437, 681-686.

Raven, J. (2005). Ocean acidification due to increasing atmospheric carbon dioxide, Document No. 12/05, The Royal Society, London, 2005.

Reimer, A., S. Brasse, R. Doerfer, C.-D. Dürselen, S. Kempe, W. Michaelis, H.-J. Rick, and R. Seifert (1999). Carbon cycling in the German Bight: An estimate of transformation processes and transport. *Ger. J. Hydrogr.* 51, 313-329.

Riegman, R., B.R. Kuipers, A.A.M. Noordeloos, and H.J. Witte (1993). Size-differential control of phytoplankton and the structure of plankton communities. *Neth. J. Sea Res.* 31, 255-265.

Ríos, A.F., A. Velo, P.C. Pardo, M. Hopema and F.F. Pérez (2012). An update of anthropogenic CO_2 storage rates in the western South Atlantic basin and the role of Antarctic Bottom Water. *J. Mar. Syst.* 94, 197-203.

Santana-Casiano, J.M., M. González-Dávila, M.–J. Rueda, O. Llinás and E.–F. González-Dávila (2007). The interannual variability of oceanic CO_2 parameters in the northeast Atlantic subtropical gyre at the ESTOC site. *Global Biogeochem. Cycles* 21, GB1015.

Sabine, C.L., R.A. Feely, N. Gruber, R.M. Key, K. Lee, J.L. Bullister, R. Wanninkhof, C.S. Wong, D.W.R. Wallace, B. Tilbrook, F.J. Millero, T.-H. Peng, A. Kozyr, R. Ono and A.F. Rios (2004). The Oceanic Sink for Anthropogenic CO_2. *Science* 305, 367-371.

Schuster, U., and A.J. Watson (2007). A variable and decreasing sink for atmospheric CO_2 in the North Atlantic. *J. Geophys. Res.* 112, C11006.

Schuster, U., A.J. Watson, N.R. Bates, A. Corbiere, M. Gonzalez-Davila, N. Metzl, D. Pierrot, and M. Santana-Casiano (2009). Trends in North Atlantic sea-surface fCO_2 from 1990 to 2006. *Deep-Sea Res. II* 56, 620-629.

Shadwick, E.H., H. Thomas, K. Azetsu-Scott, B.J.W. Greenan, E. Head, and E. Horne (2011). Seasonal variability of dissolved inorganic carbon and surface water pCO_2 in the Scotian Shelf region of the Northwestern Atlantic. *Mar. Chem.* 124, 23-37.

Thomas, H., A.E.F. Prowe, I.D. Lima, S.C. Doney, R. Wanninkhof, R.J. Greatbatch, U. Schuster and A. Corbière (2008). Changes in the North Atlantic Oscillation influence CO_2 uptake in the North Atlantic over the past 2 decades. *Global Biogeochem. Cycles* 22, GB4027.

Thomas, H., L.-S. Schiettecatte, K. Suykens, Y.J.M. Koné, E.H. Shadwick, A.E.F. Prowe, Y. Bozec, H.J.W. de Baar, and A.V. Borges (2009). Enhanced ocean carbon storage from anaerobic alkalinity generation in coastal sediments. *Biogeosciences* 6, 267-274.

Thomas, H., S.E. Craig, B.J.W. Greenan, W. Burt, G.J. Herndl, S. Higginson, L. Salt, E.H. Shadwick, and J. Urrego-Blanco (2012). Direct observations of diel biological CO_2 fixation in the oceans. *Biogeosciences Discuss.* 9, 2153-2168.

Tsunogai, S., S. Watanabe, and T. Sato (1999). Is there a "continental shelf pump" for the absorption of atmospheric CO_2? *Tellus* 51B, 701–712.

Watson, A.J., U. Schuster, D.C.E. Bakker, N.R. Bates, A. Corbière, M. González-Dávila, T. Friedrich, J. Hauck, C. Heinze, T. Johannessen, A. Körtzinger, N. Metzl, J. Olafsson, A. Olsen, A. Oschlies, X.A. Padin, B. Pfeil, J.M. Santana-Casiano, T. Steinhoff, M. Telszewski, A.F. Rios, D.W.R. Wallace and R. Wanninkhof (2009). Tracking the variable North Atlantic sink for atmospheric CO_2. *Science* 326 (5958), 1391–1393.

Winther, N.G. and J.A. Johannessen (2006). North Sea circulation: Atlantic inflow and its destination. *J. Geophys. Res.* 111, C12018.

Wollast, R. (1998). Evaluation and comparison of the global carbon cycle in the coastal zone and in the open ocean, p. 213-252. In K.H. Brink and A.R. Robinson (eds.), The Global Coastal Ocean. John Wiley & Sons.

Wootton, J.T., C.A. Pfister, and J.D. Forester (2008). Dynamic patterns and ecological impacts of declining ocean pH in a high-resolution multi-year dataset. *Proc. Natl. Acad. Sci.* 105, 18848-18853.

Zeebe, R.E. and D. Wolf-Gladrow (2001). CO_2 in Seawater: Equilibrium, Kinetics, Isotopes, Amsterdam: Elsevier Science, B.V. pp 346.

Chapter 2

The internal consistency of the North Sea carbonate system

Lesley A. Salt, Helmuth Thomas, Yann Bozec, Alberto V. Borges,

and Hein J. W. de Baar.

Abstract

A number of repeat observations of the seawater carbonate system in the North Sea has allowed quantitative assessment of its internal consistency on an inter- and intra-annual scale. In 2002 (February) and 2005 (August) the full suite of carbonate system parameters (Total Alkalinity (A_T), Dissolved Inorganic Carbon (DIC), pH, and partial pressure of CO_2 (pCO_2) were measured on two re-occupations of the entire North Sea basin, and three parameters (A_T, DIC, pCO_2) measured on an additional four re-occupations in 2001 (August, November), 2002 (May) and 2008 (August), which completed coverage of all four seasons. Here we examine the ability of six different sets of carbonic acid dissociation constants, to accurately and precisely, reproduce measurements taken in a variety of biogeochemical environments. Overall the carbonic acid dissociation constants of Mehrbach et al. (1973), refit by Dickson and Millero (1987), produced the most consistent results, however, in lower salinity environments (salinity<34.5) those of Mojica-Prieto and Millero (2002) start to outperform those of Mehrbach et al. (1973), refit by Dickson and Millero (1987). For most of the year there is a similar level of internal consistency, with A_T being calculated to within ± 6 µmol kg^{-1} with DIC and pH, DIC to ±6 µmol kg^{-1} with A_T and pH, pH to ±0.008 with A_T and pCO_2, and pCO_2 to ±8 µatm with DIC and pH. In spring, however, we observe a significant decline in the ability to accurately calculate the carbonate system, with A_T being calculated to ±27.3 µmol kg^{-1}, DIC to ±23.3 µmol kg^{-1}, and pCO_2 to ±41.3 µatm. A significant correlation is present between the internal consistency of DIC and pCO_2, to the A_T/DIC ratio during this time, which follows a latitudinal pattern, however, the deviations between the calculated and measured A_T values remain constant throughout the basin. There is no clear explanation for this, but we suggest that these patterns are the result of a number of contributing factors, such as, the presence of interfering terrestrial compounds, organic matter and measurement biases.

1 Introduction

Increasing atmospheric carbon dioxide (CO_2) has been partly mitigated by oceanic uptake, which currently accounts for 25-30% of the total CO_2 emissions (Sabine et al., 2004; Canadell et al., 2007). The uptake of CO_2 in surface waters causes a shift in the chemistry of seawater, notably increases in [H^+] and a decrease in [CO_3^{2-}] leading to the phenomenon known as ocean acidification (OA)(Caldeira and Wickett, 2003, 2005; Raven, 2005). Recent findings of Wootton et al. (2008) indicate that ocean acidification is proceeding in coastal areas more rapidly than has been predicted. The associated changes related to OA have been shown to have a variety of effects on marine phytoplankton (Fabry et al., 2008). The coastal zone is responsible for a disproportionately large amount of primary production per surface area as compared to the open ocean (Wollast, 1998) and has been shown to be responsible for a similarly large proportion of carbon export (Dunne et al., 2007). As such, understanding how these waters respond to acidification is vital in accurately predicting the future consequences of continued CO_2 increase.

The North Sea has been identified as an effective continental shelf-pump of CO_2 (Tsunogai et al., 1999; Thomas et al., 2004) and has thus undergone intensive study with respect to the CO_2 system. The high seasonal variability of the carbonate system in the North Sea (Bozec et al., 2006; Prowe et al., 2009) makes the use of high temporally-resolved datasets necessary to understand the observed signals. The use of Voluntary Observing Ships (VOS) to collect underway pCO_2 data have been used extensively in the North Sea (Omar et al., 2010) complemented by measurements of one other of the measurable carbonate variables (total alkalinity (A_T), dissolved inorganic carbon (DIC), and pH). The carbonate system can then be fully solved and quantified using equilibrium equations and constants (Park, 1969) from at least two measured variables (a combination pair of A_T, DIC, pH and pCO_2) that are integrated in computer programs such as CO2SYS (Lewis and Wallace, 1998). These computed parameters are prone to error, which have been well documented (Millero et al., 1993; Lee et al., 2000; Koeve et al., 2011; Hoppe et al., 2012). These errors stem from the accuracy of the two measured variables and to the reliability of the first and second dissociation constants of carbonic acid. The assessment of the reliability of dissociation constants can be achieved with internal consistency studies.

The first internal consistency studies took place in the open ocean and focused on the reliability of the various sets of carbonic acid dissociation constants, which are used to

calculate the distribution of inorganic carbon species. These constants have been determined over a variety of salinities and temperatures, in artificial seawater (Roy et al., 1993; Goyet and Poisson, 1989; Hansson, 1973) and in natural seawater (Mehrbach et al., 1973) and the data were later refitted using improved computer-generated models (Dickson and Millero, 1987). Assessments and comparisons of each set of constants has taken place in several locations, including the equatorial Pacific (Millero et al., 1993) and the North Atlantic (Lee et al., 1997), and spanning across several ocean basins (Wanninkhof et al., 1999; Millero et al., 2002) with little difference in the results. At sea studies have been complemented by further work using laboratory set-ups (Lee et al., 1996; Lueker et al., 2000) and more recently investigations into inconsistencies in culture experiments (Hoppe et al., 2012; Koeve et al., 2011).

The conclusion from these studies is that the pK values of Mehrbach et al. (1973), refit by Dickson and Millero (1987), are the most reliable when calculations involve pCO_2, that is pCO_2 is being calculated or is being used to calculate another parameter (Wanninkhof et al., 1999; Lee et al., 1996). These constants were the only ones determined in natural seawater and the difference has been attributed to the lack of boric acid in the artificial seawaters. In solution the majority of dissolved boron is present in two forms; boric acid and borate, following the equilibrium relationship below:

$$B(OH)_3 + H_2O \longleftrightarrow B(OH)_4^- + H^+ \qquad \text{(equation 1)}$$
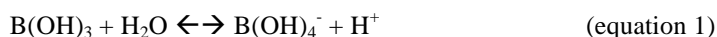
In natural seawater boric acid interacts with HCO_3^- and CO_3^{2-} to lower the activity of HCO_3^- and thus pK_2 ($pK = -\log_{10} K$). In contrast, when the computations use pH, A_T, and DIC, the best dissociation constants have been found to be Roy et al., (1993) or Goyet and Poisson (1989) (Lee et al., 1997; Clayton et al. 1995). Despite this, in an attempt to homogenize the way carbon chemists carry out these calculations, it is now the recommended standard procedure to use the constants of Mehrbach et al. (1973), refit by Dickson and Millero (1987), on the Total pH scale (Dickson et al., 2007).

Beyond the scope of dissociation constants, additional errors have been associated with high DIC/A_T ratios (>1.10)(Lee et al., 1996), the interference of fatty acids (Gripenberg, 1960), and contribution from organic acids and bases to A_T (Hernandez-Ayon et al., 2007; Koeve et al., 2011). The latter errors are only thought to be a problem in cultures, where dissolved organic carbon (DOC) reaches particularly high concentrations (Koeve et al., 2011). Similarly, the contributions of fatty acids and high DIC/A_T ratios in the open ocean are so

low that internal consistency remains within the same order of magnitude as the measurement precision. However, in cultures, unaccounted for errors have been much larger, and thus coastal areas where high primary production takes place, could also be susceptible to large errors in calculations of the carbonate system. Furthermore, the recommended constants of Mehrbach et al., (1973) were only determined to salinities above 26. In the coastal ocean it is not uncommon to find salinities falling below this value, which could be introducing further errors in carbonate system calculations. Here we present the first internal consistency study performed in coastal waters with seasonal resolution over a range of salinities and biogeochemical regimes.

2 Methods

2.1 Hydrography

The hydrographic properties in the surface waters of the North Sea demonstrate the presence of 3 different water masses, acknowledged in the literature as North Atlantic water, Baltic water, and German Bight water, with the resulting composite water mass known as Central North Sea Water (Kempe and Pegler, 1991; Bozec et al., 2006). In the northern North Sea, North Atlantic water flows over the Shetland Shelf bringing characteristic warm and high saline waters into the North Sea. In the southeast the Skagerrak water mass, a mixture of Central North Sea water and Baltic water, is easily identifiable through much lower salinities and temperatures than the central North Sea. The German Bight water comes from the Northwest European continental, coastal region in the southern North Sea, where the riverine influence is strongest in the North Sea.

The North Sea can be divided into two biogeochemical regimes, which are dictated in behavior by depth (Thomas et al., 2005; Prowe et al., 2009; Omar et al., 2010). The northern North Sea (nNS)(north of ~56°N) is deeper than the south (50-400 dbar) and experiences more ocean-like behavior, e.g. higher salinity and seasonal stratification. The southern North Sea (sNS) is much shallower (<50 dbar) and remains well-mixed throughout the year. Both regions receive nutrient and organic carbon inputs from terrestrial sources, facilitating high primary production that leads to overall annual autotrophy in the nNS and near balanced trophic status in the sNS (Bozec et al., 2005; Schiettecatte et al., 2007).

2.2 Measurements and comparisons

The data used in this study comes from 6 separate re-occupations of the North Sea, taking

place in August 2001, November 2001, February 2002, May 2002, August 2005 and August 2008. All four carbonate parameters were measured on two of these cruises; February 2002, and August 2005, with precision of $\pm 2-3$ μmol kg^{-1} for A_T, $\pm 1-2$ μmol kg^{-1} for DIC, ± 0.001 for pH, and ± 1 μatm for pCO_2, respectively.

For all of the afore-mentioned cruises, A_T was measured by potentiometric titration to the second end-point (pK_2) of carbonic acid, using 0.1M hydrochloric acid as the titrant. For the cruises taking place in August 2001, November 2001, February 2002, May 2002 and August 2005 the samples for A_T were filtered on GF/F shortly after sampling, prior to analysis. The resultant acid volumes and corresponding e.m.f values are fitted to a Gran titration plot using least squares (Gran, 1952). An uncertainty of $\pm 2-3$ μmol kg^{-1} was found for all cruises. The concentrations of silicate and phosphate are required to account for their contribution to A_T, which can be of the order of up to 1 μmol kg^{-1} in the North Sea. All of the DIC data collected in the North Sea was analyzed by the coulometric method of Johnson et al. (1993), with an overall uncertainty of $\pm 1-2$ μmol kg^{-1} for all cruises. For quality control and calibration of DIC and A_T, Certified Reference Material (CRM), of known DIC and A_T, acquired from Prof. Andrew Dickson (Scripps Institute of Oceanography, USA) were used.

In 2002 and 2005, discrete samples were taken from the CTD and analyzed for pH potentiometrically on the total hydrogen ion scale, calibrated using TRIS (2-amino-2-hydroxymethyl-1,3-propanediol) and AMP (2-aminopyridine) buffers prepared at a salinity of 35 according to Dickson (1993). The accuracy of this method is strongly dependent on the sensitivity of the pH meter and how accurately the two buffer solutions are made up. For the measurements used in this work a precision of ± 0.001 pH units was attained. For all North Sea cruises pCO_2 was measured continuously, underway, from surface waters, providing the greatest coverage of data. The instrument used continuous equilibration with a head-space and infrared detection with an accuracy of ± 1 μatm (Körtzinger et al., 1996). The calibration of pCO_2 measurements was carried out regularly (every 2-3 hours) using National Oceanic and Atmospheric Administration (NOAA, Global Monitoring Division, Carbon Cycle Greenhouse Gases Group) calibrated gas standards. For all cruises a minimum of 3 calibration gases were used, spanning a concentration range from 0 ppm to 750 ppm.

2.3   Calculations

The internal consistency was assessed using the measured in-situ salinity, temperature, and

pressure values. The KSO_4 constants of Dickson (1990) were used and pH values are given throughout on the total hydrogen ion scale. Not all station positions were occupied and measured in all six cruises that are compared here. In order to overcome this the percentage of data points considered internally consistent is often used to allow direct comparison without the loss of data. The calculations were performed using the CO2_SYS program (Lewis and Wallace, 1998), adapted for MATLAB (van Heuven, 2009). All calculated parameters as a function of two input parameters were explored, thus consisting of: $A_T(DIC,pH)$, $A_T(DIC,pCO_2)$, $A_T(pH,pCO_2)$, $DIC(A_T,pH)$, $DIC(A_T,pCO_2)$, $DIC(pH,pCO_2)$, $pH(DIC,A_T)$, $pH(DIC,pCO_2)$, $pH(A_T,pCO_2)$, $pCO_2(DIC,A_T)$, $pCO_2(DIC,pH)$, and $pCO_2(A_T,pH)$, for the following six different sets of carbonic acid dissociation constants: Roy et al. (1993)(ROY), Goyet and Poisson (1989)(GP), Hansson (1973), refit by Dickson and Millero (1987)(HAN), Mehrbach et al. (1973), refit by Dickson and Millero (1987)(MEH), Hansson and Mehrbach, refitted by Dickson and Millero (1987)(HM) and Mojico-Prieto and Millero (2002)(MM). In the remaining text, for simplicity, the constants will be referred to by the abbreviations (ROY, GP, HAN, MEH, HM and MM).

2.4   Assessment

The internal consistency of the carbonate system can be considered in a number of different ways. Here, we assess how accurate and precise it is by comparing measured parameters to calculated parameters. An accurate but imprecise system would be indicated by a low average (absolute) difference between the measured and calculated values, but with a high standard deviation (noise) around this average. A precise but inaccurate system, however, is indicated by a low standard deviation of differences, between calculated and measured parameters, but with a high average difference. Alternatively, the system can be accurate and precise, resulting in a small average difference between the measured and calculated values, accompanied by a low standard deviation of differences. The measured and calculated values of each parameter, for each set of dissociation constants, was fitted to the form $Y = a.X$, by means of linear regression, the results are shown in Table 1.

2.5   Error Propagation

When the term 'internally consistent' is used, it refers to whether the calculated values and associated errors fit within the limits of the errors propagated through the calculations from the initial measurements. Measurement errors are carried through in the calculations and depending on the input parameter combination lead to different error margins in the resultant

values. These margins vary insignificantly over the range of conditions (e.g. temperature, salinity) observed in the North Sea, thus average margins were calculated using basin-wide average temperature, salinity, silicate and phosphate concentrations. The carbonate parameters were set to minimum or maximum values (average measured values ± error) to obtain the largest error margin possible. This carried through calculation error (CE) was then divided by two to create an error margin on both sides, which then had the respective measurement error (ME) of the calculated parameter added on. The variation in CE for different carbonic acid dissociation constants is less than 0.5% of the parameter, thus the same CE was applied for all the dissociation constants.

2.6 Total Borate Calculations

To independently calculate the total borate contribution from each water mass, the individual water mass fractions were first calculated, following Friis et al. (2005). The German Bight constitutes a complex mixture of different water masses, with input from several rivers, thus distinguishing an end member is impossible. Instead, for our purposes, we used the salinity and A_T data from the station closest to the German Bight to form a regression line with the Central North Sea end member. We then extrapolated this down to a salinity of 0 to get a representative freshwater end member. This assumes that all the fresh water present comes from the same source, however, due to other rivers in the region having a similar catchment lithology we assume that the chemical signal of the water will be similar. Comparing the regressed value with recent seasonal A_T data from the Elbe (Thorben Amann, *pers. comm.*) we find end member values in the same range as that calculated here, thus we assume our estimation is sufficient for the purpose of the calculation.

The borate alkalinity (BAlk) was then calculated for the end members, using the equations of Barth (1998) (equations 8 and 9) for the salinity-borate relationship in the German Bight, and that modified from Gripenberg (1960) (equations 10 and 11) for the Baltic salinity-borate relationship. At a salinity of 35 the two seasonal linear relationships of Barth (1998), for summer (September, 1994) and winter (February, 1995), yield an average difference of 50 µmol kg^{-1} in the calculated borate. As such, for our calculations, equation 8 was used for the calculations of August 2005 (summer), and equation 9 for the calculation of February 2002 (winter). The water mass fractions were then multiplied by the theoretical BAlk contribution and summed to obtain the actual BAlk of the sample.

$$B = 0.13*S + 0.18 \text{ (for sept, 1994)} \qquad\qquad \text{(equation 8)}$$

$$B = 0.14*S + 0.17 \text{ (for feb, 1995)} \qquad \text{(equation 9)}$$

The salinity-borate relationship in the Baltic is less well documented, however, the following equation was regressed from the data presented by Grippenberg (1960):

$$B = 14.0111*S - 3.3103 \qquad \text{(equation 10)}$$

with an R^2 value of 0.9, where B represents boric acid measured in meq kg^{-1} and salinity has been converted from chlorinity using Lewis (1980, S = 1.80655 Cl‰). The data of Grippenberg (1960) was obtained mainly in the Baltic proper and into the Bothnian Sea, the latter of which, Beldowski et al. (2010) show, has a much steeper salinity-alkalinity relationship than the Baltic Proper. Borate demonstrates conservative behavior, similar to alkalinity, thus we assume a constant relationship between alkalinity and borate throughout the Baltic. We can then use the ratio of B/A_T from the data of Grippenberg, adapted to the regression of Beldowski et al. (2010), for the Baltic proper, to form an equation between borate and salinity. The resulting equation for the total boron in the Baltic is:

$$B = 1.8848*S + 95.741 \qquad \text{(equation 11)}$$

where B represents total boron in µmol kg^{-1}.

For the North Atlantic fraction the traditional seawater relationship of Uppstrom (1974) was used:

$$B = (0.000232./10.811)*(S./1.80655) \qquad \text{(equation 12)}$$

3 Results and Discussion

3.1 A seasonal comparison

The two seasons with data from four measured carbonate parameters are winter (February) and summer (August), allowing us to compare the internal consistency in two very different conditions in terms of values of the carbonate variables, and water temperature. As the North Sea is a temperate coastal sea, it is characterized by high primary production during summer and very low, or no, production in winter. The average DIC in February 2002 was 64 µmol kg^{-1} higher than that in August. The average A_T changed by just 2 µmol kg^{-1}, however, the various contributions to A_T showed greater variability. We calculated the different A_T contributions in the North Sea in February 2002 and August 2005 (Figures 1a and 1b). For

average annual conditions in the North Sea, the HCO_3^- and CO_3^{2-} species are by far the greatest contributors to A_T, supplying ~2212 μmol kg^{-1}, followed by borate $(B(OH)_4^-)$(~68 μmol kg^{-1}), hydroxide (OH^-)(~3 μmol kg^{-1}), phosphate (PO_4^{3-})(~0.07 μmol kg^{-1}) and silicate $(SiO(OH)_3^-)$(~0.04 μmol kg^{-1}). The largest change between the two seasons was in carbonate alkalinity $(HCO_3^- + 2.CO_3^{2-})$, which was significantly lower in August, when photosynthesis occurred. The contributions of silicate and phosphate were also much smaller then, due to uptake by phytoplankton. The borate contribution was slightly higher in August, which is mainly the effect of temperature on K_B.

The change in average pCO_2 was just 8 μatm, however, this is not representative of the entire North Sea, as the pCO_2 range is two times greater in August (287 – 455 μatm) compared to February (315 – 396 μatm). The greater range in summer reflects the two biogeochemical regimes within the North Sea: the stratified nNS, where stratification enables prolonged phytoplankton growth causing a large drawdown of CO_2, shows very low pCO_2 values, whereas in the sNS, very low pCO_2 values are observed only in spring and a combination of remineralization and higher temperatures lead to much higher pCO_2 in August (Bozec et al., 2005; Thomas et al., 2004, 2005; Schiettecatte et al., 2007). In February, the water column is well-mixed throughout, and biological activity is lower thus leading to a more homogenous horizontal distribution of pCO_2.

The results from all internal consistency calculations using the 4 carbonate parameters, with various dissociation constants, in the February 2002 and August 2005 data sets are shown in Tables 1 and 2, respectively. The regressed data fitted the calculated values to measured values (measured value on the y-axis and calculated value on the x-axis), thus a regression with a slope >1 indicates that the measured value is greater than the calculated value. A regression slope of 1.000 is achieved with several combinations in both seasons; 6 times in winter and 3 times in summer. In February, when the parameters involved are DIC, A_T and pCO_2, we find that the constants of MEH are the most suitable, whereas when DIC, A_T and pH are involved the constants of GP outperform the others. The largest deviations and residuals are consistently observed when the input parameters are pH and pCO_2, with MM producing the most accurate reproduction of measurements. In August the constants of MEH are, again, the best choice when the parameter combination is A_T, DIC and pCO_2 but also when A_T, DIC and pH are all involved. However, for calculations involving pH and pCO_2 the constants of GP or HAN are most appropriate.

Figure 1a. The distribution of total alkalinity in the North Sea and respective contributions to total alkalinity by carbonate species, borate, silicate, phosphate and ammonia in February 2002.
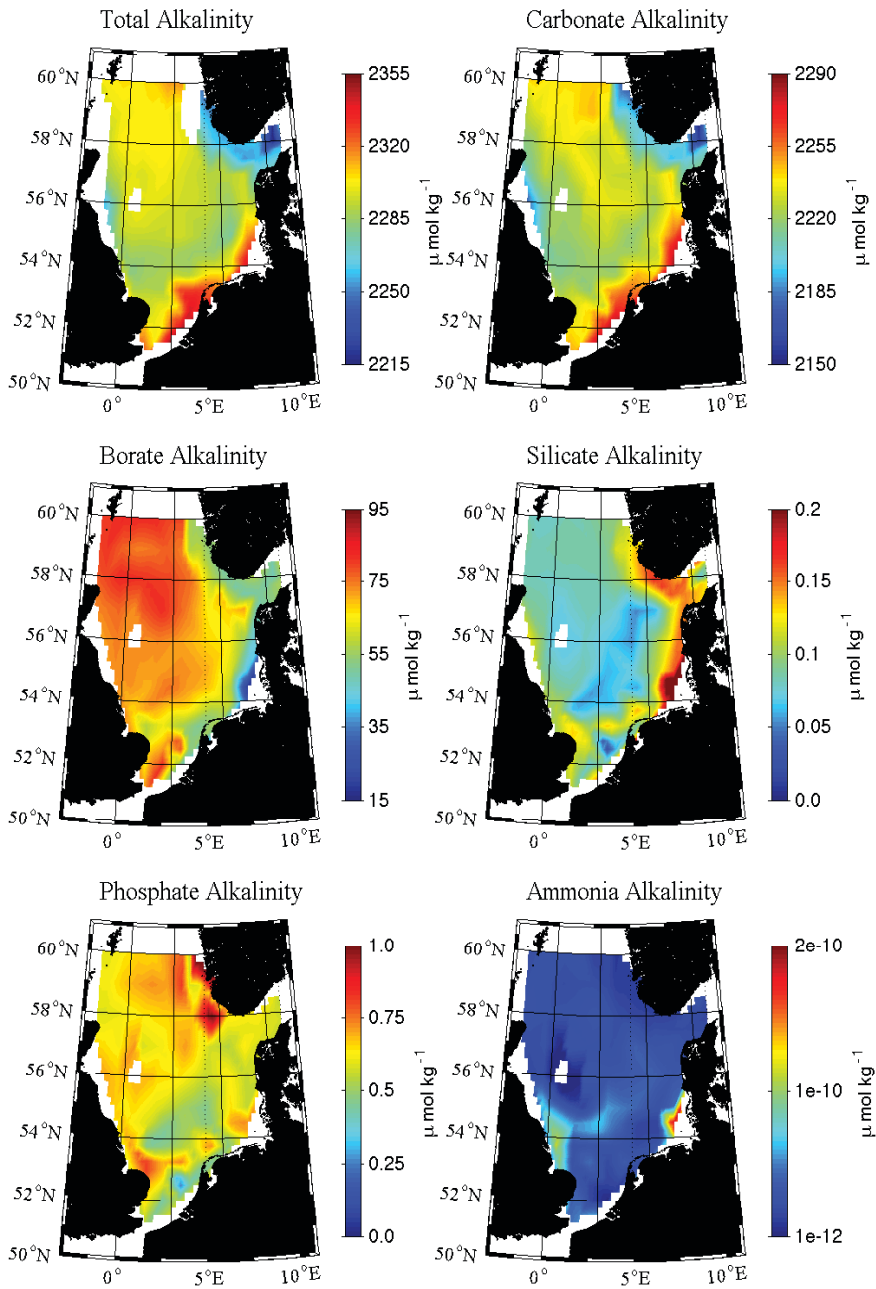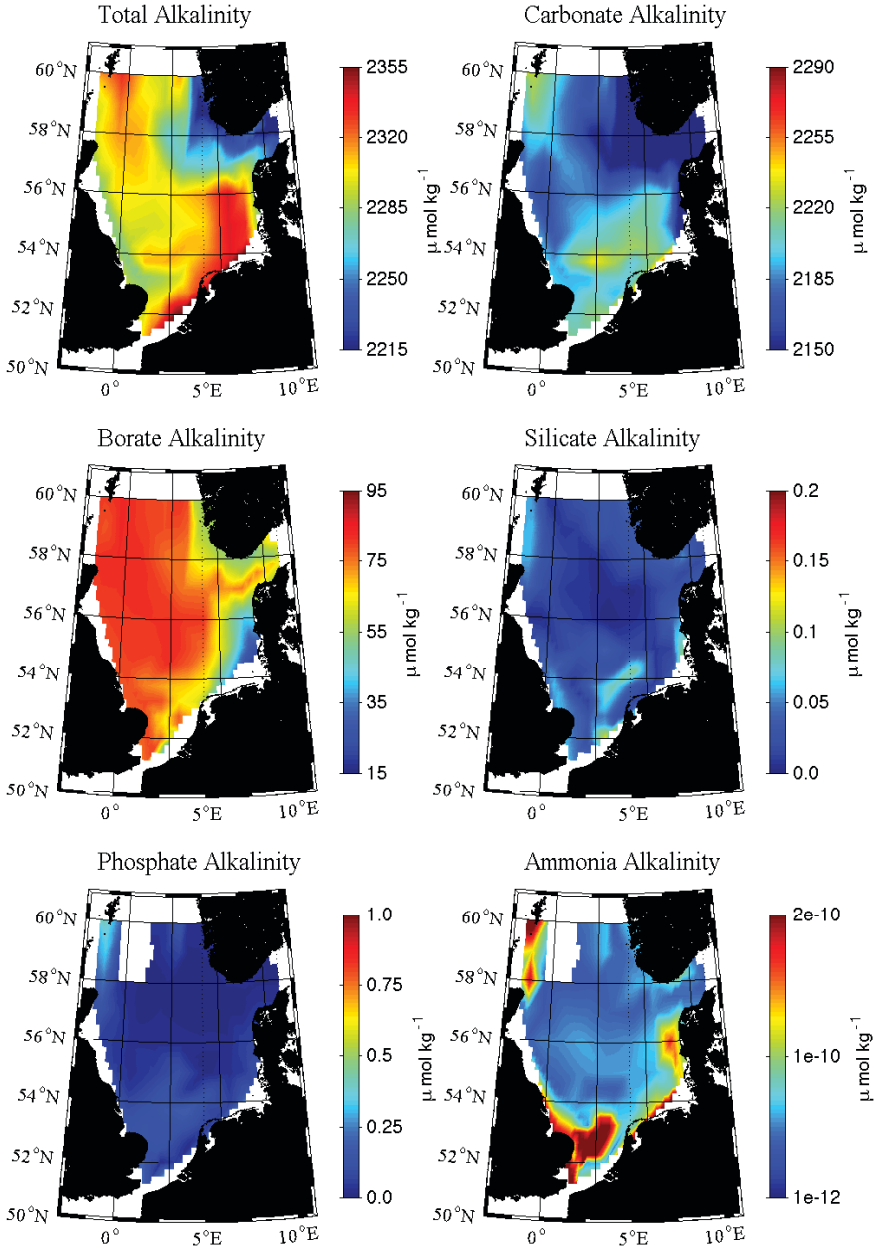
30

Figure 1b. The distribution of total alkalinity in the North Sea and respective contributions to total alkalinity by carbonate species, borate, silicate, phosphate and ammonia in August 2005.

Table 1. Calculated statistics for all calculated values of carbonate parameters compared to the measured values in February 2002, calculated with various carbonic acid dissociation constants. The linear regression was performed using least squares fitting.

			Roy	GP	HAN	MEH	HM	MM
A_T	**Regress**	DIC,pH	0.999	1.000	0.998	1.001	0.999	0.999
		DIC,pCO$_2$	0.997	0.997	0.995	1.000	0.997	0.998
		pH, pCO$_2$	1.022	1.035	1.042	1.013	1.031	1.009
	Residuals (Average)	DIC,pH	3.01	0.61	3.74	-1.75	1.68	3.28
		DIC,pCO$_2$	7.69	7.60	12.32	0.85	7.97	5.62
		pH, pCO$_2$	-50.10	-79.43	-93.15	-31.88	-70.35	-22.92
	STDV	DIC,pH	8	8	7	7	8	8
		DIC,pCO$_2$	9	9	9	8	9	8
		pH, pCO$_2$	63	62	62	60	61	61
DIC	**Regress**	A_T, pH	1.001	1.000	1.002	0.999	1.001	1.001
		A_T, pCO$_2$	1.003	1.003	1.005	1.000	1.003	1.002
		pH, pCO$_2$	1.024	1.036	1.045	1.013	1.033	1.011
	Residuals (Average)	A_T, pH	-2.84	-0.56	-3.54	1.69	-1.58	-3.10
		A_T, pCO$_2$	-6.68	-6.60	-10.71	-0.72	-6.93	-4.88
		pH, pCO$_2$	-50.39	-76.05	-91.96	-28.66	-68.42	-24.86
	STDV	A_T, pH	7	7	7	7	7	7
		A_T, pCO$_2$	8	8	7	7	8	7
		pH, pCO$_2$	59	58	57	55	57	56

		Roy	GP	HAN	MEH	HM	MM
pH	**Regress**						
	DIC, A_T	1.001	1.000	1.001	0.999	1.000	1.001
	A_T, pCO_2	0.999	0.998	0.998	0.999	0.998	1.000
	DIC, pCO_2	0.999	0.998	0.998	0.999	0.998	0.999
	Residuals (Average)						
	DIC, A_T	-0.006	-0.001	-0.008	0.004	-0.004	-0.007
	A_T, pCO_2	0.009	0.014	0.016	0.006	0.012	0.004
	DIC, pCO_2	0.010	0.015	0.018	0.006	0.014	0.005
	STDV						
	DIC, A_T	0.017	0.017	0.017	0.017	0.017	0.017
	A_T, pCO_2	0.011	0.011	0.011	0.010	0.011	0.011
	DIC, pCO_2	0.012	0.012	0.012	0.011	0.011	0.011
pCO_2	**Regress**						
	A_T, pH	0.959	0.959	0.936	0.994	0.957	0.969
	A_T, pCO_2	0.975	0.963	0.956	0.985	0.967	0.987
	pH, pCO_2	0.976	0.963	0.957	0.985	0.967	0.989
	Residuals (Average)						
	A_T, pH	15.03	14.85	24.32	1.56	15.63	11.00
	A_T, pCO_2	9.03	13.69	16.64	5.16	12.28	4.49
	pH, pCO_2	8.55	13.61	16.02	5.47	12.02	3.98
	STDV						
	A_T, pH	18	18	17	17	17	17
	A_T, pCO_2	10	11	11	10	10	10
	pH, pCO_2	11	11	11	10	11	10

Table 2. Calculated statistics for all calculated values of carbonate parameters compared to the measured values in August 2005, calculated with various carbonic acid dissociation constants. The linear regression was performed using least squares fitting.

			Roy	GP	HAN	MEH	HM	MM
A_T	**Regress**	DIC,pH	0.992	0.994	0.996	0.997	0.995	0.995
		DIC,pCO$_2$	0.994	0.994	0.995	1.001	0.996	0.999
		pH, pCO$_2$	0.977	0.991	0.999	0.962	0.998	0.960
	Residuals (Average)	DIC,pH	17.46	13.79	9.81	6.80	10.95	11.59
		DIC,pCO$_2$	13.86	13.31	10.79	-1.18	9.27	3.28
		pH, pCO$_2$	53.06	19.01	0.95	88.52	28.01	95.76
	STDV	DIC,pH	7	7	6	6	6	6
		DIC,pCO$_2$	9	9	9	9	9	9
		pH, pCO$_2$	52	51	51	52	51	52
DIC	**Regress**	A$_T$, pH	1.008	1.006	1.004	1.003	1.005	1.005
		A$_T$, pCO$_2$	1.006	1.005	1.004	0.999	1.004	1.001
		pH, pCO$_2$	0.984	0.997	1.004	0.964	0.992	0.963
	Residuals (Average)	A$_T$, pH	-16.08	-12.72	-9.07	-6.29	-10.11	-10.71
		A$_T$, pCO$_2$	-11.57	-11.12	-9.03	1.02	-7.76	-2.74
		pH, pCO$_2$	32.77	4.78	-8.24	75.67	15.74	77.75
	STDV	A$_T$, pH	6	6	6	6	6	6
		A$_T$, pCO$_2$	7	7	7	7	7	7
		pH, pCO$_2$	48	47	47	48	47	48

		Roy	GP	HAN	MEH	HM	MM
pH							
Regress	DIC, A_T	1.004	1.003	1.002	1.002	1.002	1.003
	A_T, pCO_2	1.001	1.000	1.000	1.002	1.001	1.002
	DIC, pCO_2	1.001	1.000	1.000	1.002	1.000	1.002
Residuals (Average)	DIC, A_T	-0.031	-0.024	-0.018	-0.012	-0.020	-0.021
	A_T, pCO_2	-0.009	-0.003	0.000	-0.014	-0.005	-0.015
	DIC, pCO_2	-0.006	-0.001	0.002	-0.014	-0.003	-0.015
STDV	DIC, A_T	0.012	0.012	0.012	0.012	0.012	0.012
	A_T, pCO_2	0.009	0.008	0.008	0.008	0.008	0.008
	DIC, pCO_2	0.009	0.009	0.009	0.009	0.009	0.009
pCO_2							
Regress	A_T, pH	0.939	0.942	0.952	1.004	0.959	0.984
	A_T, pCO_2	1.014	1.000	0.994	1.035	1.006	1.036
	pH, pCO_2	1.022	1.006	0.998	1.038	1.011	1.041
Residuals (Average)	A_T, pH	22.40	21.51	17.37	-1.82	14.93	5.26
	A_T, pCO_2	-5.23	-0.51	1.72	-12.29	-2.40	-12.61
	pH, pCO_2	-7.93	-2.67	0.18	-13.31	-4.10	-14.35
STDV	A_T, pH	15	14	14	13	14	13
	A_T, pCO_2	8	8	8	8	8	8
	pH, pCO_2	8	8	8	8	8	8

In general the difference in precision (represented by the standard deviation) between the dissociation constants was minor compared to the differences obtained with various input parameter combinations. The results for both February and August are consistent, showing that the best calculation combination for A_T was (DIC,pH), for DIC it was (A_T,pH), for pH it was (A_T,pCO$_2$) and for pCO$_2$ it was (DIC,pH). The results from February show a slight decrease in precision, represented by a higher standard deviation, compared to that obtained in August, however, the regressions indicate a lower accuracy. The standard deviations of the differences between the calculated and measured parameters (Δ) for February 2002 and August 2005 (shown in brackets, respectively) are approximately double to those found in the open ocean by Lee et al. (1997), of ± 3 μmol kg^{-1} in A_T (± 6, 7 μmol kg^{-1}), ± 3 μmol kg^{-1} in DIC (± 6, 7 μmol kg^{-1}), and $\pm 1.3\%$ of pCO$_2$ (± 3, 2 %).

3.1.1   The effects of salinity on dissociation constants

Different salinity and temperature parameterizations used in the determination of pK_1 and pK_2 are largely responsible for the deviations in the calculations between dissociation constants. Plotting the difference in ΔA_T ($A_{T,meas} - A_{T,calc}$), ΔDIC, ΔpH and ΔpCO$_2$ between results from different dissociation constants shows an exponential increase around a salinity of ~34.5, indicating that at higher salinities the choice of dissociation constants becomes more significant. To investigate the performance of the six dissociation constants at different salinities, the North Sea data from August and February were split into two groups; low salinity waters, with salinities less than 34.5, and high salinity waters, with salinities greater than or equal to 34.5. The same linear regressions were then applied again to the two different groups. The 1 standard deviation (sd) of ΔA_T, ΔDIC, ΔpH and ΔpCO$_2$ is greater, for all parameters and in both seasons, for low salinity waters compared to high salinity waters. In high salinity waters in February the sd of ΔA_T decreases by 2 μmol kg^{-1}, DIC by 1 μmol kg^{-1}, pH by 0.002 and pCO$_2$ by 2 μatm. In the less saline waters, there is an increase in the sd of ΔA_T, ΔDIC, ΔpH and ΔpCO$_2$ by 2 μmol kg^{-1}, 1 μmol kg^{-1}, 0.003, and 2 μatm, respectively. The same pattern is observed in August, however, the differences are smaller, with the sd of ΔA_T decreasing by 1 μmol kg^{-1}, DIC by 1 μmol kg^{-1}, pH by 0.002 and pCO$_2$ by 1 μatm in high salinity waters, and increasing the sd of A_T by <1 μmol kg^{-1}, DIC by <1 μmol kg^{-1}, pH by 0.001 and pCO$_2$ by 2 μatm in low salinity waters.

Furthermore, in February, a clear separation appears between the different dissociation constants in low and high salinity waters. As previously mentioned, over the total dataset, when DIC, A_T and pH are involved in calculations, the constants of GP produce the least

deviation between measured and calculated parameters, however, in high salinity waters the constants of MEH become more appropriate and in the lower salinity waters the constants of ROY outperform the others. Despite these changes, the constants of MM show little variation in performance between the two salinity environments. For August there was no difference between the most suitable constants for the entire dataset compared to the different salinity regimes regarding measurements with DIC, A_T and pH, with GP still most closely representing the measurements. With regard to measurements of pH, pCO_2 and DIC, however, in the lower salinity waters the constants of HAN outperformed those of GP. Similarly to February, the constants of MM also perform well and show the best consistency across the entire salinity range.

At lower salinities the ratio of K_1/K_2 is greater [Mosley et al. 2010; Zeebe and Wolf-Gladrow, 2001] leading to relatively greater HCO_3^- concentrations compared to CO_2 and CO_3^{2-}. This ratio is used directly in the calculation of pH and A_T from DIC and pCO_2. Due to the different parameterizations of K_1 and K_2 for the different constants, the difference in this ratio between constants may become larger or smaller at lower salinities. This will lead to greater or smaller differences between the measured and calculated parameters. As such, at lower salinities, one would expect, overall, greater variation between the calculations from the different dissociation constants, as is observed here. The salinity range does not change between the two seasons, however, in February, 2002 a 3.5 fold higher Elbe river discharge was recorded compared to August, 2005 (GKSS, 2012, http://coast.gkss.de/staff/kappenberg /elbe/abfluss/elbe.abfluss). A greater proportion of freshwater in the North Sea could explain why a greater difference is observed between the two salinity environments during this time. Based on these results, for datasets that cover a large range of salinities, for consistency, one can achieve the best overall results using the constants of MM in carbonate system calculations.

3.1.2   The Role of Borate Alkalinity

The ratio of K_1/K_2 varies between parameterizations of dissociation constants partly, depending on whether the constants were determined in artificial seawater or natural seawater. In natural seawater interactions between borate and carbonate cause a decrease in K_1 and an increase in K_2 (Prieto & Millero, 2002), which does not occur in artificial seawater due to the lack of boron. Thus, the fact that the constants of ROY and MM outperform those of MEH in less saline waters may be indicative of their lower borate concentration, thus the difference in pK_2 is not as large as in more saline waters. Borate has a long residence time in

the oceans leading to a conservative relationship with salinity, thus in carbonate system calculations the total boron contribution is calculated as a linear function of salinity, and the borate then calculated using K_B. In the North Sea, the Baltic input through the Skagerrak, and the Elbe input in the German Bight, have demonstrated non-conventional salinity-borate relationships (Barth, 1998). Figure 1 shows clearly that borate is the second largest non-carbon contributor to A_T, constituting ~4% (Zeebe and Wolf-Gladrow, 2001), thus deviations from the true borate concentration can potentially cause substantial errors in calculations involving A_T. Furthermore, the K_B of the boric acid system is very close to ocean pH, thus any miscalculation of $[H^+]$ can also lead to significant errors in the calculation of $[B(OH)_3]$ and $[B(OH)_4^-]$ concentrations.

To evaluate the potential error introduced into calculations of the carbonate system in the North Sea by unaccounted-for borate, the borate concentrations in the Elbe- and Baltic-influenced areas of the North Sea were calculated using the water mass fractions and borate-salinity equations from the literature (see section 2.5). This 'pre-calculated' borate contribution to alkalinity ($BAlk_{pre}$) was then implemented into CO2_SYS, replacing the salinity-borate calculation (Uppstrom et al., 1974), which the program normally uses. For comparative purposes BAlk was also calculated using the traditional equation (Uppstrom et al., 1974) with various $[H^+]$ determinations, including that from direct pH measurements, using DIC and A_T as inputs and using A_T and pCO_2 as inputs (DIC/pCO_2 produce the same results as A_T/pCO_2, hence have not been included). We found that the $BAlk_{pre}$ calculations showed little change from the BAlk concentrations, the difference showing a normal distribution with 0 as the absolute mean and 2σ of 8 μmol kg^{-1}. The equations of Barth (1998) are very similar to the oceanic relationships, thus no significant difference was observed in the German Bight between the two calculations. The greatest difference occurs in the Skagerrak where CO2_SYS over-estimates the BAlk compared to the equation derived from Gripenberg's data. This was particularly so in August 2005, when the Uppstrom et al. (1974) ratio overestimated the BAlk contribution by up to 8 μmol kg^{-1}. Despite these differences, using our derived $BAlk_{pre}$ values did not improve the internal consistency. In fact it led to greater deviations between the measured and calculated parameters, reducing the number of internally consistent stations for all input combinations. We thus conclude that the non-conservative salinity-borate relationships in the North Sea are not significant contributors to the lack of internal consistency.

For our second 'experiment', the $[H^+]$ concentration from pH measurements was used to calculate BAlk directly, and this value is implemented in CO2SYS, however, again this

resulted in a reduction in internal consistency. On the other hand, when the BAlk calculated using [H$^+$] from (DIC, A$_T$) is implemented the internal consistency improves notably if DIC or A$_T$ are being calculated, for both February and August. The number of internally consistent (IC) stations in February and August, for A$_T$(DIC,pH) and DIC(A$_T$,pH), increased by 7 and 29 stations respectively, which represent a respective 11% and 36% increase in internal consistency. The internal consistency of A$_T$(DIC,pCO$_2$) increased by 5 (8%) and 15 (19%) stations for February and August, respectively, and DIC(A$_T$,pCO$_2$) increased by 4 (6%) and 13 (16%) stations, respectively. It should be noted that the [H$^+$] calculated from (DIC, A$_T$) is only used to calculated the BAlk, whereas the [H$^+$] used in the other calculations is calculated from the stated input parameters. These results indicate that it is the effect of miscalculation of [H$^+$] on the BAlk concentration that contributes to the lack of internal consistency for (A$_T$, pCO$_2$) and (DIC, pCO$_2$). This can be illustrated by Figure 2, where the change in ΔA$_T$ between the measured and calculated values are plotted against the change in BAlk between that calculated from (DIC, A$_T$) and (DIC, pCO$_2$). When the BAlk from (DIC, A$_T$) is implemented the ΔA$_T$ values are shifted towards the x-axis (0), indicative of the improvement in internal consistency. The reason for such a bias is unknown, and may be caused by an undetected bias in one of the measured parameters.

Of the observed increases in internal consistency, the Skagerrak region shows no change with the new BAlk concentrations. Using the additional seasonal datasets, the largest fraction of Baltic water found in the Skagerrak is present in May (17%), during which time there is a significant (R^2=0.55, p=0.008) positive correlation between the Baltic fraction and the deviation between calculated and measured parameters (Figure 2(b)). Despite this, in May, the internal consistency could also not be improved by changing the BAlk calculation. Gripenberg (1960) concluded, from back titrations of alkalinity, that whilst borate did not directly affect the accuracy of the A$_T$ titrations, the interactions between boric acid and organic material could lead to underestimated alkalinity values. Thus in May, the lack of internal consistency could stem from some interaction between boric acid and the additional organic material in the water at this time of year. This would lead to unpredictable and random variations in the total alkalinity, however, there would be no pattern to the lack of internal consistency and no way to correct for such an effect.
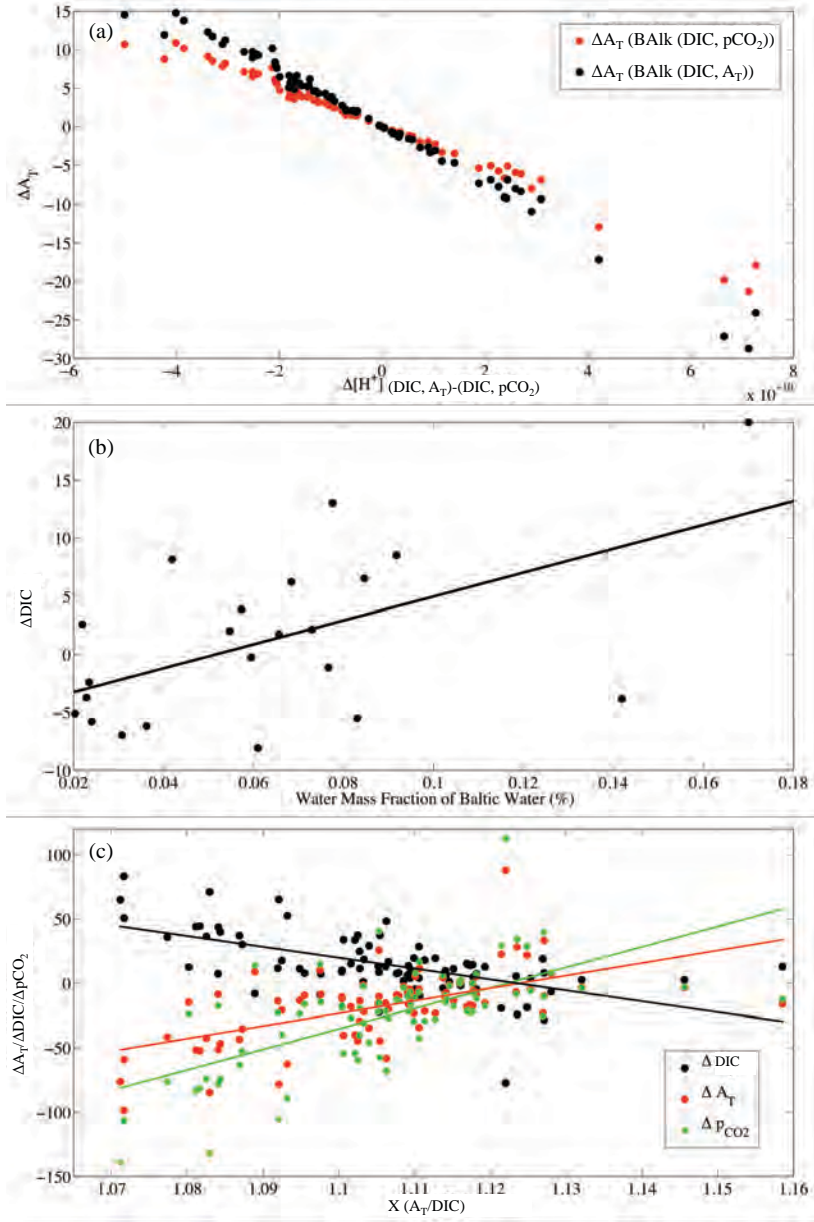
Figure 2. (a) The change in ΔA_T caused by the difference in $[H^+]$ calculated using (DIC, A_T) and (DIC, pCO_2). (b) Regression of ΔDIC with the calculated water mass fraction of Baltic water, selectively displaying those with a fraction of 2% or higher. (c) The change in ΔDIC, ΔA_T, and ΔpCO_2 observed with a varying ratio of A_T/DIC (X).

3.2 Seasonal comparison (A$_T$, DIC, and pCO$_2$)

3.2.1 Seasonal Internal Consistency

The results from the internal consistency study from all 6 data sets, using just three carbonate parameters (A$_T$, DIC and pCO$_2$) show a clear dominance of the constants of MEH outperforming the others. The results of the seasonal calculations with the use of MEH constants are given in Table 3. These statistics indicate that the internal consistency of the North Sea follows a slightly seasonal pattern, with May - the most biologically productive time period - producing the most inconsistent calculations and the rest of the year displaying a very similar level of consistency. These findings are in agreement with those of Koeve et al. (2011) and Hoppe et al. (2012), whom have similarly noted significant inconsistencies in the carbonate system in waters of high biological activity.

Table 3. Derived linear regressions (regress) and standard deviations (stdv) of differences between measured and calculated parameters with the percentage of internally consistent stations (IC) for all six cruises. The calculations were performed using the acid dissociation constants of Mehrbach et al., (1973), refit by Dickson and Millero, (1987).

		Aug '01	Nov '01	Feb '02	May '02	Aug '05	Aug '08
(DIC, pCO$_2$)	A$_T$ regress	0.999	1.001	1.000	0.993	1.001	1.000
	A$_T$ stdv	28.5	8.3	8.2	27.3	8.6	9.0
	A$_T$ IC (%)	15.5	47.7	43.5	9.4	34.9	50.2
(A$_T$, pCO$_2$)	DIC regress	1.000	0.999	1.000	1.007	1.000	1.000
	DIC stdv	23.7	7.2	7.2	23.3	7.2	7.6
	DIC IC (%)	17.2	47.7	43.5	9.4	38.7	52.3
(DIC, A$_T$)	pCO$_2$ regress	0.976	1.004	0.994	0.906	1.004	0.998
	pCO$_2$ stdv	40.7	14.9	16.6	41.3	13.3	15.1
	pCO$_2$ IC (%)	25.9	50.0	40.3	20.0	48.7	56.8

As the North Sea consists of two different biogeochemical regimes, the northern North Sea (nNS) and the southern North Sea (sNS), we investigated whether these two environments contributed towards a difference in the internal consistency of the carbonate system. The North Sea was subsequently divided along the 56°N latitude and the internal consistency re-examined in both areas (Table 4). In May there is a significant increase in the standard deviation of ΔDIC and ΔpCO_2 in the north compared to the south, however, ΔA_T shows no difference. It is in the nNS that larger phytoplankton blooms are maintained for long periods due to seasonal, thermal stratification in contrast to the sNS where rapid remineralization takes place in the permanently well-mixed water column. As previously mentioned there is also greater freshwater influence in the sNS however, the difference observed between the north and south is greater than the difference previously mentioned between oceanic and estuarine waters. Errors have previously been associated with intense biological activity (Hoppe et al., 2012), thus we are inclined to suggest that this may have a similar effect here, however, it is interesting that the errors in ΔA_T are not affected on a latitudinal gradient, as ΔpCO_2 and ΔDIC are.

The different regimes also influence the dominant phytoplankton species present in each location. Calcifying organisms and coccolithophore blooms are well documented in the nNS where their growth is controlled by North Atlantic influence and the stratification of the water column (Houghton et al., 1991; Burkill et al., 2002). These organisms influence the A_T/DIC (X) ratio of the waters through calcification which removes one mole of DIC per 2 moles of A_T. Lee et al. (1996, 1997) found that high X (>1.10) values have an impact on the sensitivity of pK_2, thus affecting the consistency between measured and calculated carbonate parameters. The range of X found in the North Sea varies from 1.06 - 1.16 throughout the year with largest range (1.07 - 1.16) found in May. During this season X also shows a positive linear correlation with ΔDIC, ΔA_T and ΔpCO_2 with R^2 values of -0.6, 0.6 and 0.7, respectively (Figure 2 (c)). The size of the error introduced by varying X can be up to 5 μmol kg^{-1}, as found by Lee et al. (1996), which would contribute a large proportion of the errors we observe. In the North Sea, the presence of coccolithophores may also contribute to errors in DIC measurements if in the sample, while A_T samples were filtered. As the method relies on the acidification of the sample, the added acid may conceivably dissolve any $CaCO_3$ present, introducing noise into the method (Dickson et al., 2007).

The range of X does not impact the errors in A_T, which remain elevated throughout the basin. The A_T is altered by the uptake and release of NO_3^- and $NH_4^\pm$ during photosynthesis (Brewer and Goldman, 1976), contributing up to 33 μmol kg^{-1} to A_T in some regions (Wolf-Gladrow

Table 4. Calculated internal consistency statistics for each data set divided into northern North Sea stations (nNS)(latitude>56°N) and southern North Sea stations (sNS)(latitude≤56°N). The calculations were performed using the acid dissociation constants of Mehrbach et al., (1973), refit by Dickson and Millero, (1987).

		Aug '01	Nov '01	Feb '02	May '02	Aug '05	Aug '08
nNS (lat>56°N)	A_T (DIC, pCO$_2$) regress	1.00	1.00	1.00	0.99	1.00	1.00
	A_T (DIC, pCO$_2$) std	26.7	8.3	8.2	27.3	8.6	9.0
	A_T (DIC, pCO$_2$) IC (%)	16.0	52.8	44.7	7.4	34.8	48.1
	DIC (A_T, pCO$_2$) regress	1.00	1.00	1.00	1.01	1.00	1.00
	DIC (A_T, pCO$_2$) std	22.1	6.5	6.2	26.8	7.3	8.7
	DIC (A_T, pCO$_2$) IC (%)	16.0	52.8	44.7	7.4	28.3	44.4
	pCO$_2$ (A_T, DIC) regress	1.01	1.01	0.99	0.87	1.01	1.00
	pCO$_2$ (A_T, DIC) regress	29.7	13.0	14.1	47.8	13.0	16.5
	pCO$_2$ (A_T, DIC) regress	32.0	54.7	39.5	14.8	45.7	53.7
	# of stations in province	25	53	38	54	46	54
sNS (lat≤56°N)	A_T (DIC, pCO$_2$) regress	1.00	1.00	1.00	0.99	1.00	1.00
	A_T (DIC, pCO$_2$) std	29.0	8.3	8.2	27.3	8.6	9.0
	A_T (DIC, pCO$_2$) IC (%)	20.6	41.7	38.5	10.3	44.1	56.8
	DIC (A_T, pCO$_2$) regress	1.00	1.00	1.00	1.00	1.00	1.00
	DIC (A_T, pCO$_2$) std	24.2	7.9	8.1	11.8	7.2	6.9
	DIC (A_T, pCO$_2$) IC (%)	17.6	41.7	38.5	10.3	44.1	56.8
	pCO$_2$ (A_T, DIC) regress	0.96	1.00	1.00	0.97	1.00	1.00
	pCO$_2$ (A_T, DIC) regress	46.1	16.8	19.2	18.8	13.8	14.8
	pCO$_2$ (A_T, DIC) regress	23.5	47.2	38.5	25.6	52.9	59.5
	# of stations in province	34	36	26	39	34	37

et al., 2008; Hydes et al., 2012). Fraga & Alvarez-Salgado (2005) quantified the change in A_T during photosynthesis and found that the differences are caused predominantly by N_2 fixation, DMSP production and $CaCO_3$ formation, of which the latter contributes the greatest. Samples were filtered before A_T analysis, thus eliminating the possibility of an error being introduced if some of the $CaCO_3$ shell is dissolved during the A_T titration. Futhermore, in other studies (Hoppe et al., 2012) where samples were filtered for A_T, this did not result in improved internal consistency, suggesting that dissolution of $CaCO_3$ during the titration may not be a dominant factor in deviations between the measured and calculated carbonate parameters.

The North Sea receives a high input of allochthonous dissolved organic matter, for which analysis of colored dissolved organic matter (CDOM) indicates a large proportion is of terrigenous sources (Stedmon et al., 2009) and thus may contain terrestrial "titratable" compounds not accounted for in our analysis. It has been suggested that fatty acids may contribute to measured A_T and in the Baltic Sea there is a higher than average concentration of fatty acids. The contribution of these to A_T has been fairly extensively examined by Osterroht (1993) and maximum contributions of 5 nM A_T were found, which is insufficient to cause the inconsistencies observed here. Muller et al. (2008), using the technique of Hernandez-Ayon et al. (2005) on fjord surface waters, compared the A_T estimation of DIC to the measured value and found that organic alkalinity can contribute from 2-22 μmol kg^{-1} in regions of high organic matter. This could account for the differences observed here in May, however, an additional alkalinity component not accounted for would lead to a larger measured A_T values not lower. As such any organic compound would not be contributing to A_T but detracting from it. As such, it is likely a number of factors contributing to the observed pattern.

4   Conclusions

On a basin-wide scale in the North Sea we find that the dissociation constants of carbonic acid of Mehrbach et al. (1973), refit by Dickson and Millero, (1987), provide the best internal consistency in agreement with previous findings (Lee et al., 1996; Wanninkhof et al., 1999). In regions of lower than average ocean salinity (34.5), there is markedly less deviation between the internal consistency of the different constants and the constants of MM outperform those of MEH. At high salinities these two sets of constants are comparable in performance, thus over datasets with a wide variety of salinities, we recommend the use of MM constants for more consistent calculations.

In the North Sea in general we find that the internal consistency of the carbonate system is much less than that found in the open ocean, by approximately 2-fold, which is unsurprising considering the additional input of terrestrial compounds in coastal areas, and generally higher biological productivity. The internal consistency is relatively constant throughout the year, with the exception of May, where there is a marked decrease in our ability to accurately calculate the carbonate system. This is consistent with previous findings of reduced internal consistency in the presence of high biological activity. A significant correlation with X (A_T/DIC) is found during this period, which is likely to contribute to the errors observed. Calcification, calcifying organisms, changes to A_T due to photosynthesis may all also be a contributing factor to noise during this time of year, however, no definitive conclusions can be drawn here.

References

Barth, S. (1998). $^{11}B/^{10}B$ variations of dissolved boron in a freshwater-seawater mixing plume (Elbe Estuary, North Sea). *Mar. Chem.* 62, 1 - 14.

Beldowski, J., A. Löffler, B. Schneider and L. Joensuu (2010). Distribution and biogeochemical control of total CO_2 and total alkalinity in the Baltic Sea. *J. Mar. Syst.* 81, 252-259.

Borges, A.V. and N. Gypens (2010). Carbonate chemistry in the coastal zone responds more strongly to eutrophication than to ocean acidification. *Limnol. Oceanogr.* 55, 346-353.

Bozec, Y., H. Thomas, K. Elkalay, and H.J.W. de Baar (2005). The continental shelf pump for CO_2 in the North Sea - evidence from summer observation. *Mar. Chem.* 93, 131-147.

Bozec, Y., H. Thomas, L.-S. Schiettecatte, A.V. Borges, K. Elkalay, and H.J.W. de Baar (2006). Assessment of the processes controlling seasonal variations of dissolved inorganic carbon in the North Sea. *Limnol. Oceanogr.* 51, 2746-2762.

Brewer, P.G., and J.C. Goldman (1976). Alkalinity changes generated by phytoplankton growth. *Limnol. Oceanogr.* 21, 108-117.

Burkill, P.H., S.D. Archer, C. Robinson, P.D. Nightingale, S.B. Groom, G.A. Tarran, and M.V. Zubkov (2002). Dimethyl sulphide biogeochemistry within a coccolithophore bloom (DISCO): an overview. *Deep-Sea Res. II* 49, 2863-2885.

Caldeira, K., and M.E. Wickett (2003). Anthropogenic carbon and ocean pH. *Nature* 425, 365.

Caldeira, K., and M.E. Wickett (2005). Ocean model predictions of chemistry changes from carbon dioxide emissions to the atmosphere and ocean. *J. Geophys. Res.* 110, C09S04.

Canadell, J.G., C. Le Quere, M.R. Raupach, C.B. Field, E.T. Buitenhuis, P. Ciais, T.J. Conway, N.P. Gillett, R.A. Houghton and G. Marland (2007). Contributions to accelerating atmospheric CO_2 growth from economic activity, carbon intensity, and efficiency of natural sinks, *Proc. Natl. Acad. Sci.* 104, 18866-18870.

Clayton, T.D., R.H. Byrne, J.A. Breland, R.A. Feely, F.J. Millero, D.M. Campbell, P.P. Murphy, and M.F. Lamb (1995). The role of pH measurements in modern oceanic CO_2-system characterizations: precision and thermodynamic consistency. *Deep-Sea Res.* 42, 411-431.

Dickson, A.G., and F.J. Millero (1987). A comparison of the equilibrium constants for the dissociation of carbonic acid in seawater media. *Deep-Sea Res.* 34, 1733-1743.

Dickson, A.G. (1990). Standard potential of the reaction: $AgCl(s) + 1/2H_2(g) = Ag(s) + HCl(aq)$, and the standard acidity constant of the ion HSO_4^- in synthetic seawater from 273.15 to 318.15K. *J. Chem. Thermodyn.* 22,113-127.

Dickson, A.G. (1993). pH buffers for sea water media based on the total hydrogen ion

concentration scale. *Deep-Sea Res. A* 40, 107-118.

Dickson, A.G., C.L. Sabine, and J.R. Christian (2007). *Guide to best practices for ocean CO₂ measurements*. PICES Special Publication 3. 191 pp.

Dunne, J.P., J.L. Sarmiento and A. Gnanadesikan (2007). A synthesis of global particle export from the surface ocean and cycling through the ocean interior and on the seafloor. *Global Biogeochem. Cycles* 21, GB4006.

Fabry, V.J., B.A. Seibel, R.A. Feely, and J.C. Orr (2008). Impacts of ocean acidification on marine fauna and ecosystem processes. *ICES J. Mar. Sci.* 65, 414-432.

Fraga, F., and X.A. Alvarez Salgado (2005). On the variation of alkalinity during phytoplankton photosynthesis. *Ciencias Marinas*, Universidad Autonoma de Baja California.

Friis, K., A. Körtzinger and D.W.R. Wallace (2003). The salinity normalization of marine inorganic carbon chemistry data. *Geophys. Res. Lett.* 30(2), 1085.

Goyet, C. and A. Poisson (1989). New determination of carbonic acid dissociation constants in seawater as a function of temperature and salinity. *Deep Sea Res. I* 36, 1635-1654 .

Gran, G. (1952). Determination of the equivalence point in potentiometric titrations of seawater with hydrochloric acid. *Oceanol. Acta*. 5, 209-218.

Gripenberg, S. (1960). On the Alkalinity of Baltic Waters. *ICES J. Mar. Sci*. 26(1), 5-20.

Hansson, I. (1973). A new set of acidity constants for carbonic acid and boric acid in sea water. *Deep Sea Res. I* 20, 461-478.

Hernandez‑Ayon, J.M., A. Zirino, A.G. Dickson, T. Camiro-Vargas, and E. Valenzuela-Espinoza (2007). Estimating the contribution of organic bases from microalgae to the titration alkalinity in coastal seawaters. *Limnol. Oceanogr-Meth.* 5, 225-232.

van Heuven, S., D. Pierrot, E. Lewis, and D.W.R. Wallace (2009). MATLAB Program developed for CO₂ system calculations. ORNL/CDIAC-105b. Carbon dioxide information analysis center. Oak Ridge National Laboratory, U.S. Department of Energy, Oak Ridge.

Hoppe, C.J.M., G. Langer, S. D. Rokitta, D.A. Wolf-Gladrow, and B. Rost (2012). Implications of observed inconsistencies in carbonate chemistry measurements for ocean acidification studies. *Biogeosciences* 9, 2401-2405.

Hoppema, M. (1991). The seasonal behaviour of carbon dioxide and oxygen in the coastal North Sea along the Netherlands. *Neth. J. Sea Res.* 28(3), 167-179.

Houghton, S.D. (1991). Coccolith sedimentation and transport in the North Sea. *Mar. Geol.* 99, 267-274.

Kempe, S. and K. Pegler (1991). Sinks and sources of CO₂ in coastal seas: the North Sea. *Tellus* 43B, 224 - 235.

Koeve, W., H.-C. Kim, K. Lee and A. Oschlies (2011). Potential impact of DOC accumulation on fCO₂ and carbonate ion computations in ocean acidification

experiments. *Biogeosciences Discuss*. 8, 3797-3827.

Körtzinger, A., H. Thomas, B. Schneider, N. Gronau, L. Mintrop, and J.C. Duinker (1996). At-sea intercomparison of two newly designed underway pCO_2 systems – encouraging results. *Mar. Chem.* 52, 133-145.

Lamb, M.F., C.L. Sabine, R.A. Feely, R. Wanninkhof, R.M. Key, G.C. Johnson, F.J. Millero, K. Lee, T.-H. Peng, A. Kozyr, J.L. Bullister, D. Greeley, R.H. Byrne, D.W. Chipman, A.G. Dickson, C. Goyet, P.R. Guenther, M. Ishii, K.M. Johnson, C.D. Keling, T. Ono, K. Shitashima, B. Tilbrook, T. Takahashi, D.W.R. Wallace, Y.W. Watanabe, C. Winn, and C.S. Wong (2002). Consistency and synthesis of Pacific Ocean CO_2 survey data. *Deep-Sea Res. II* 49, 21-58.

Lee, K., and F. Millero (1995). Thermodynamic studies of the carbonate system in seawater. *Deep-Sea Res. I* 42, 2035-2061.

Lee, K., F.J. Millero, and D.M. Campbell (1996). The reliability of the thermodynamic constants for the dissociation of carbonic acid in seawater. *Mar. Chem.* 55, 233-245.

Lee, K., F. Millero, and R. Wanninkhof (1997). The carbon dioxide system in the Atlantic Ocean. *J. Geophys. Res.* 102, 15693-15707.

Lee, K., F.J. Millero, R.H. Byrne, R.A. Feely, and R. Wanninkhof (2000). The recommended dissociation constants for carbonic acid in seawater. *Geophys. Res. Lett.* 27(2), 229-232.

Lewis, E.L. (1980). The practical salinity scale 1978 and its antecedents. *IEEE J. Oceanic Eng.* OE-5 (1), 3-8.

Lewis, E.L. and D.W.R. Wallace (1998). Program developed for CO_2 system calculations, ORNL/CDIAC-105. Carbon dioxide information analysis center, Oak Ridge National Laboratory, U.S. Department of Energy, Oak Ridge.

Liss, P.S. and M.J. Pointon (1973). Removal of dissolved boron and silicon during estuarine mixing of sea and river waters. *Geochim. Cosmochim. Ac.* 37, 1493-1498.

Lueker, T.J., A.G. Dickson and C.D. Keeling (2000). Ocean pCO_2 calculated from dissolved inorganic carbon, alkalinity, and equations for K_1 and K_2: validation based on laboratory measurements of CO_2 in gas and seawater at equilibrium. *Mar. Chem.* 70, 105-119.

Mehrbach, C., C.H. Culberson, J.E. Hawley, and R.M. Pytkowicz (1973). Measurement of the apparent dissociation constants of carbonic acid in seawater at atmospheric pressure. *Limnol. Oceanogr.* 18, 897-907.

Millero, F.J., R.H. Byrne, R. Wanninkhof, R. Feely, T. Clayton, P. Murphy and M.F. Lamb (1993). The internal consistency of CO_2 measurements in the equatorial Pacific. *Mar. Chem.* 44, 269-280.

Millero, F.J., D. Pierrot, K. Lee, R. Wanninkhof, R. Feely, C.L. Sabine, R.M. Key, and T. Takahashi (2002). Dissociation constants for carbonic acid determined from field

measurements. *Deep-Sea Res. II* 49, 1705-1723.

Millero, F.J., T.B. Graham, F. Huang, H. Bustos-Serrano and D. Pierrot (2006). Dissociation constants of carbonic acid in seawater as a function of salinity and temperature. *Mar. Chem.* 100, 80-94.

Mojica-Preito F.J., and F.J. Millero (2002). The values of pK_1 and pK_2 for the dissociation of carbonic acid in seawater. *Geochim. Cosmochim. Ac.* 66, 2529-2540.

Mosley, L.M., B.M. Peake and K.A. Hunter (2010). Modelling of pH and inorganic carbon speciation in estuaries using the composition of the river and seawater end members. *Environ. Modell. Softw.* 25, 1658-1663.

Muller F.L.L. and B. Bleie (2008). Estimating the organic acid contribution to coastal seawater alkalinity by potentiometric titrations in a closed cell. *Analytica Chimica Acta*, **619**: 183-191 (2008).

Omar, A.M., A. Olsen, T. Johannessen, M. Hoppema, H. Thomas, and A.V. Borges (2010). Spatiotemporal variations of fCO_2 in the North Sea. *Ocean Sci.* 6, 77-89.

Osterroht, C. (1993). Extraction of dissolved fatty acids from sea water. *Fresenius J Anal Chem.* 345, 773-779.

Park, K.P. (1969). Oceanic CO_2 System: An evaluation of ten methods of investigation. *Limnol. Oceanogr.* 14, 179-186.

Prieto, F.J.M., and F.J. Millero (2002). The values of pK_1 and pK_2 for the dissociation of carbonic acid in seawater. *Geochim. Cosmochim. Ac.* 66, 2529 - 2540.

Prowe, A.E.F., H. Thomas, J. Pätsch, W. Kühn, Y. Bozec, L.-S. Schiettecatte, A.V. Borges, and H.J.W. de Baar (2009). Mechanisms controlling the air-sea CO_2 flux in the North Sea. *Cont. Shelf Res.* 29, 1801-1808.

Raven, J. (2005). Ocean acidification due to increasing atmospheric carbon dioxide. Document No. 12/05, The Royal Society, London, 2005.

Roy, R.N., L.N. Roy, K.M. Vogel, C. Porter-Moore, T. Pearson, C.E. Good, F.J. Millero and D. Campbell (1993). Determination of the ionization constants of carbonic acid in seawater. *Mar. Chem.* 44, 249-259.

Sabine, C.L., R.A. Feely, N. Gruber, R.M. Key, K. Lee, J.L. Bullister, R. Wanninkhof, C.S. Wong, D.W.R. Wallace, B. Tilbrook, F.J. Millero, T.–H. Peng, A. Kozyr, T. Ono and A.F. Rios (2004). The Oceanic Sink for Anthropogenic CO_2. *Science* 305, 367-371.

Schiettecatte, L.-S., H. Thomas, Y. Bozec, and A.V. Borges (2007). High temporal coverage of carbon dioxide measurements in the Southern Bight of the North Sea. *Mar. Chem.* 106, 161-173.

Seidel, M.P., M.D. DeGrandpre, and A.G. Dickson (2008). A sensor for in situ indicator-based measurements of seawater pH. *Mar. Chem.* 109, 18-28.

Stedmon, C.A., C.L. Osburn, and T. Kragh (2010). Tracing water mass mixing in the Baltic-North Sea transition zone using the optical properties of coloured dissolved organic

matter. *Estuar. Coast. Shelf S.* 87, 156-162.

Thomas, H., Y. Bozec, K. Elkalay, and H.J.W. de Baar (2004). Enhanced Open Ocean Storage of CO_2 from Shelf Sea Pumping. *Science* 304, 1005-1008.

Thomas, H., Y. Bozec, K. Elkalay, H.J.W. de Baar, A.V. Borges and L.-S. Schiettecatte (2005). Controls of the surface water partial pressure of CO_2 in the North Sea. *Biogeosciences* 2, 323-334.

Thomas, H., L.-S. Schiettecatte, K. Suykens, Y.J.M. Koné, E.H. Shadwick, A.E.F. Prowe, Y. Bozec, H.J.W. de Baar and A.V. Borges (2009). Enhanced ocean carbon storage from anaerobic alkalinity generation in coastal sediments. *Biogeosciences* 6, 267-274.

Tsunogai, S., S. Watanabe, and T. Sato (1999). Is there a "continental shelf pump" for the absorption of atmospheric CO_2? *Tellus* 51B, 701-712.

Uppstrom, L.R. (1974). The boron/chlorinity ratio of deep-sea water from the Pacific Ocean. *Deep-Sea Res.* 21, 161-162.

Wanninkhof, R., E. Lewis, R.A. Feely, and F.J. Millero (1999). The optimal carbonate dissociation constants for determining surface water pCO_2 from alkalinity and total inorganic carbon. *Mar. Chem.* 65, 291–301.

Wollast, R. (1998). Evaluation and comparison of the global carbon cycle in the coastal zone and in the open ocean. In: Brink, K. H., Robinson, A. R. (Eds.), The Sea. John Wiley & Sons, New York, pp. 213-252.

Wootton, J.T., C.A. Pfister, and J.D. Forester (2008). Dynamic patterns and ecological impacts of declining ocean pH in a high-resolution multi-year dataset. *Proc. Natl. Acad. Sci.* 105, 18848-18853.

Zeebe, R.E., and D. Wolf-Gladrow (2001). CO_2 in Seawater: Equilibrium, Kinetics, Isotopes. Elsevier, Amsterdam.

Chapter 3

Seasonal carbon dynamics in the Marsdiep basin of the Wadden Sea

Lesley A. Salt, Helmuth Thomas, Astrid Hoogstraten, Katja Phillippart,

Josje Snoek, and Hein J. W. de Baar.

Abstract

Seasonal and inter-annual variations of dissolved inorganic carbon (DIC) and total alkalinity (A_T) are analyzed for a 30-month time series station in the Marsdiep basin of the Wadden Sea. Undersaturation of the surface water partial pressure of CO_2 (pCO_2), relative to the atmosphere, occurs at the time of the spring diatom bloom causing a significant CO_2 drawdown. The diatom bloom had a calculated NCP of 0.95 mol C m^{-2} in 2009, and 1.24 mol C m^{-2} in 2010. The difference in NCP between the two years is attributed to a higher wintertime silicate concentration in 2010. The DIC continues to decrease after the diatom bloom, with the successive *Phaeocystis globosa* bloom, however, a combination of pelagic remineralization and increasing temperature increases the pCO_2 in the Marsdiep above that of the atmosphere. The DIC signal shows the same seasonal pattern as that in the adjacent southern North Sea (sNS), indicative of similar controls. In contrast the A_T signal demonstrates inverse seasonality compared to that of the adjacent sNS, which we attribute to the substantial impact of ongoing redox reactions related to the nitrogen cycle. The decline in A_T observed from spring to summer is likely to be caused by a combination of nitrification and ammonia uptake, however, rapid remineralization and recycling of nitrate and ammonia make quantification of each process problematic. From autumn through to winter A_T can be well constrained from DIC concentrations, with the ratio between the two strongly indicative of a dominance of denitrification driving the remineralization process.

1   Introduction

The coastal zone is an important biogeochemical pathway of carbon from land to sea, delivering up to 32 T mol (1 T mol = 10^{12} mol) of dissolved inorganic carbon (DIC) and 20.5 T mol of dissolved organic carbon (DOC) every year (Maybeck, 1982, 1993). The concomitant supply of inorganic nutrients stimulates a large amount of primary production, meaning that coastal regions facilitate up to 30% of total oceanic primary production (Wollast, 1991; Gattuso et al., 1998). In temperate regions, large intra- and inter-annual variability leads to large fluxes of CO_2 between the ocean and atmosphere (Thomas et al., 2004; Chen and Borges, 2009; Gypens et al., 2011; Shadwick et al., 2011) making these regions significant to the global carbon budget. In an extensive literature survey by Borges et al. (2005), coastal seas have overall been classified as CO_2 *sinks,* and estuaries as *sources*. It has been calculated that continental shelves represent a CO_2 sink of -0.25 Pg C m^{-2} y^{-1} whereas estuaries act as a source of +0.25 Pg C m^{-2} y^{-1} (Cai, 2011). Despite this broad generalization there is great heterogeneity between coastal systems, with differences in CO_2 uptake ranging from 32g C m^{-2} a^{-1} in the Gulf of Biscay (Frankignoulle and Borges, 2001) to 17g C m^{-2} a^{-1} in the North Sea (Thomas et al., 2004), thus highlighting the need to study coastal and estuarine systems on an individual basis.

The North Sea is an effective shelf pump of CO_2 (Thomas et al., 2004), which is significantly influenced by the numerous coastal systems, which border it. The Wadden Sea is a shallow system of tidal flats, located off the coast of the Netherlands and Germany, and delivers approximately 62 x 10^9 Gmol y^{-1} DIC (Brasse et al., 1999), and circa 73 Gmol y^{-1} of A_T (Thomas et al., 2009) to the German Bight, in the southern North Sea (sNS). In the shallow Wadden Sea, where depth ranges from 2-3m, it has been estimated that 48% of the organic matter is turned over in the sediment compared to just 10% in the German Bight (van Beusekom et al., 1999). Benthic remineralization thus has a much larger impact on carbon metabolism in the Wadden Sea compared to that on the shelf or in the open ocean, making it just as important as pelagic remineralization (Heip et al., 1995). Benthic remineralization of organic matter quickly depletes oxygen in the sediment, following which, nitrate (NO_3^-), manganese oxide (MnO_2), iron oxide (FeOOH), and sulfate (SO_4^{2-}) are used as electron acceptors, in that order (Richards et al., 1965). The increasing anoxic conditions thus stimulate the release of dissolved Mn, Fe, PO_4^{3-} and H_2S through reduction, as has been observed in the Marsdiep basin of the Wadden Sea (Schoemann et al., 1998; Kowalski et al., 2011). Due to the seasonal biological production in the Marsdiep, the sediment also undergoes a yearly cycle of redox reactions (Schoemann et al., 1998), largely dependent

upon the oxygen penetration into the sediment. The extent of exchange, of the reactants and products of these reactions, between the sediment and water column relies largely upon the type of sediment and the hydrography (Beck and Brumsack, 2012).

In coastal environments the nitrogen cycle is closely linked to the carbon cycle (Fennel, 2010; Pätsch and Kühn, 2008), particularly through riverine contributions (Hofman et al., 2009). It has been observed that in shelf environments the generation of total alkalinity (A_T) from calcium carbonate dissolution is significantly less than that generated from other shelf processes (Chen, 2002). Via a number of redox reactions in the nitrogen cycle, such as denitrification, nitrification and through the assimilation of nitrogen species by phytoplankton or bacteria, a significant amount of total alkalinity (A_T) can be generated or removed (Chen and Wang, 1999; Wolf-Gladrow et al., 2007; Thomas et al., 2009). Nitrogen species thus have an indirect influence on pH in riverine and estuarine systems (Hofmann et al., 2009). In the southern North Sea a maximum in benthic denitrification has been identified near the mouths of the rivers Rhine and Elbe (Proctor et al., 2003) and it has been calculated that a combination of sulfate reduction and denitrification in sediments of the sNS could facilitate 20-25% of the CO_2 uptake in the North Sea (Thomas et al., 2009) making these processes significant to the marine carbonate system.

The European riverine supply of nitrogen to the coastal zone increased notably from the 1950's onwards but has shown a decline since the 1980's (Loebl et al., 2009 (and more references herein); Borges and Gypens, 2010). Terrestrial loading of nutrients can lead to a greater increase in heterotrophy than in autotrophy (Cai, 2011), and has also been shown to influence the community structure of the present phytoplankton species (Bakker et al., 1994; Philippart et al., 2000; Philippart et al., 2007). Eutrophication favors large-celled phytoplankton species (Grover, 1997), which are associated with greater fluxes to the sediment than small-celled organisms (Riegman et al., 1993). One species that can compete with the larger cells is the Haptophyte *Phaeocystis*, which forms large colonies resistant to zooplankton grazing. An increase in *Phaeocystis globosa* abundance was observed in the Marsdiep during the 1970's, associated with eutrophication (Cadée and Hegeman, 2002). As such, changes in riverine flows or loads of inorganic nutrients can have a significant impact on coastal primary production and carbon metabolism (Cadée, 1992; Loebl et al., 2009).

The main objective of the present paper is to investigate the seasonal processes governing the carbon dynamics in the Marsdiep basin, using a 30-month time-series. Loebel et al. (2007)

noted that the seasonality in the Wadden Sea leads to the area being predominantly heterotrophic in autumn and winter and net autotrophic in spring and summer. As such, yearly data sets are required to resolve the dynamics of this region and fully understand the biogeochemical coupling between the benthic and pelagic environments. The analysis performed here was undertaken in conjunction with supplementary data from the CANOBA project and CARBOOCEAN, which covered the entire North Sea basin during all 4 seasons from 2001-2002 (Thomas et al., 2005; Bozec et al., 2006) and a late summer cruise in 2008.

2   Methods

2.1   Area of Study

The time-series station is located in the Marsdiep basin, which is the largest tidal basin of the Wadden Sea, located southeast of the Wadden island Texel, adjacent to the North Sea (Figure 1). It is a shallow, estuarine environment with approximately 50% of the area consisting of tidal flats (van Beusekom et al., 1999). The Marsdiep is a distinctly unique environment due to the temporally variable input of freshwater from lake IJssel through the sluices of the Afsluitdijk. There are less significant freshwater inputs from the rivers Elbe, Weser and Ems (Lenhart et al., 1996) in the eastern Wadden Sea, and a fraction of Rhine river water is present, mixed in with the

Figure 1. Location of time series station in the Marsdiep basin of the Wadden Sea.

southern North Sea water (de Jonge, 1990). The main water exchange between the North Sea and the Wadden Sea occurs by tidal exchange in the southwest of the basin, through the Marsdiep basin (Ridderinkhof et al., 1990). The North Sea enters from the west, flowing along the southern boundary and mixes with the Wadden Sea water from the south, after which a fraction of this mixed water exits the basin along the northern boundary, where the sampling station is located (Figure 1).
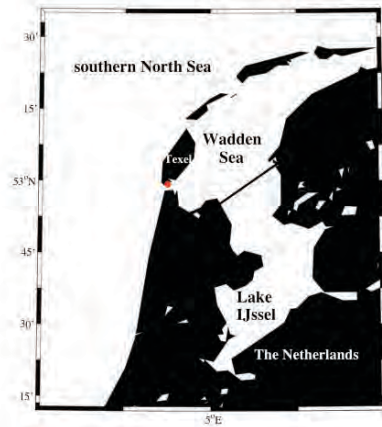
The western Wadden Sea is a very turbulent region due to tidally dominated currents and irregular topographical features. The time-series site is shallow with an average water depth of 7m (Schoemann et al., 1998) and the sediment is sandy with a silty surface layer

(Kieskamp et al., 1991). Primary production estimates show a wide range over several years, from 120 gC m^{-2} y^{-1} (Philippart et al., 2007) to 440 gC m^{-2} y^{-1} (Cadée and Hegeman, 2002). It has been estimated that 48% of the remineralization takes place in the sediment (van Beusekom et al., 1999), of which rates are highest in the summer months (Kowalski et al., 2012).

2.2   Sampling and Analysis

Samples were collected from ~1m depth using a niskin bottle on a fixed winch. The water column remains mixed all year-round, thus we assume that the 1m surface samples are representative of the entire water column. During the winter months (December - February) samples were taken on a monthly basis, increasing to weekly resolution through spring and summer (March - August) and then decreasing to bi-weekly sampling in autumn (September - November). Sampling consistently took place at high water, when the coastal southern North Sea water is the dominant water mass. Samples were chemically analyzed for dissolved oxygen, inorganic nutrients (ammonium (NH_4), nitrite (NO_2), nitrate (NO_3), phosphate (PO_4), silicate ($Si(OH)_4$)), chlorophyll α, dissolved inorganic carbon (DIC) and total alkalinity (A_T), and measurements of temperature and salinity were taken at the time of sampling.

The A_T and DIC samples were measured on a VINDTA 3C (Marianda, Kiel), which uses potentiometric titration with 0.1M hydrochloric acid to determine A_T and measures DIC using the coulometric method of Johnson et al. (1993). These parameters are measured with a precision of ±2 µmol kg^{-1} and ±1 µmol kg^{-1}, respectively. Samples were collected in 250 ml durex glass bottles using tygon tubing following the standard sampling procedure outlined in DOE (Dickson, 2007). The samples were poisoned with 0.25 ml $HgCl_2$ after a volume of 5.25 ml was removed, creating a headspace of 5 cm^3. Samples were taken in duplicate or triplicate and stored, in the dark, until analysis. All samples were measured within a year of sampling in batches of ~100 or more. Data quality was controlled using certified reference material (CRM, Batches #'s 86, 89, 100), acquired from Prof. Andrew Dickson at Scripps Institute of Oceanography (San Diego, California). The A_T titration data was re-processed after analysis to allow the inclusion of nutrient concentrations and salinity calibrations.

2.3 pCO$_2$ and pH calculations

From any two of the four measurable carbonate parameters it is possible to calculate the remaining two using thermodynamic principles. Here, measurements of A$_T$ and DIC were used to calculate pCO$_2$ and pH using the Matlab version of CO2_SYS (Lewis & Wallace, 1998; van Heuven, 2009) with the carbonic acid dissociation constants of Mehrbach et al., (1973), refit by Dickson and Millero (1987). Both pH and pCO$_2$ were calculated at *in-situ* temperature and pressure and pH is reported on the total pH scale. The pCO$_2$ normalized to a constant, annual average temperature of 12˚C (pCO$_2$@12˚C) is also computed, to remove the temperature-driven changes in pCO$_2$.

2.4 Water mass calculations

The seasonal data from the CANOBA project was used to obtain a seasonally averaged salinity value in the region south of 56ºN and west of 6ºE. A simple mixing line was then applied between the measured salinity values in the Marsdiep and the relevant seasonal sNS end member to calculate the fraction of fresh water versus North Sea water.

3 Results

3.1 Seasonal and temporal patterns in the Marsdiep basin

Figure 2 shows the time series observations of temperature, salinity, ammonium (NH$_4^+$), nitrate (NO$_3^-$), nitrite (NO$_2^-$), silicate (Si(OH)$_4$), phosphate (PO$_4^{3-}$), apparent oxygen utilization (AOU = [O$_2$]$_{sat}$ − [O$_2$]$_{obs}$), chlorophyll α, DIC, A$_T$, pCO$_2$ and pCO$_2$@12˚C from May 2008 to October 2010. The seasonally averaged values of selected parameters are shown in Table 1, with the average monthly freshwater discharges from the sluices at Den Oever, at the Afsluitdijk.

Temperature follows the annual solar irradiance pattern of the northern hemisphere, with peak temperatures occurring in late summer (August) and the yearly minima occurring early in the year at the end of winter (February). The maximum temperatures for the three years showed little variation, peaking at 20.1ºC for both 2008 and 2009, and 20.2ºC in 2010. There is a general annual trend of lower salinities occurring in the Marsdiep in winter and a period of higher salinities throughout summer, with the annual peak in July. This pattern is consistent with decades of observations (Patsch and Lenhart, 2004) and explained through higher rainfall over the southwest European continent leading to higher river runoff during
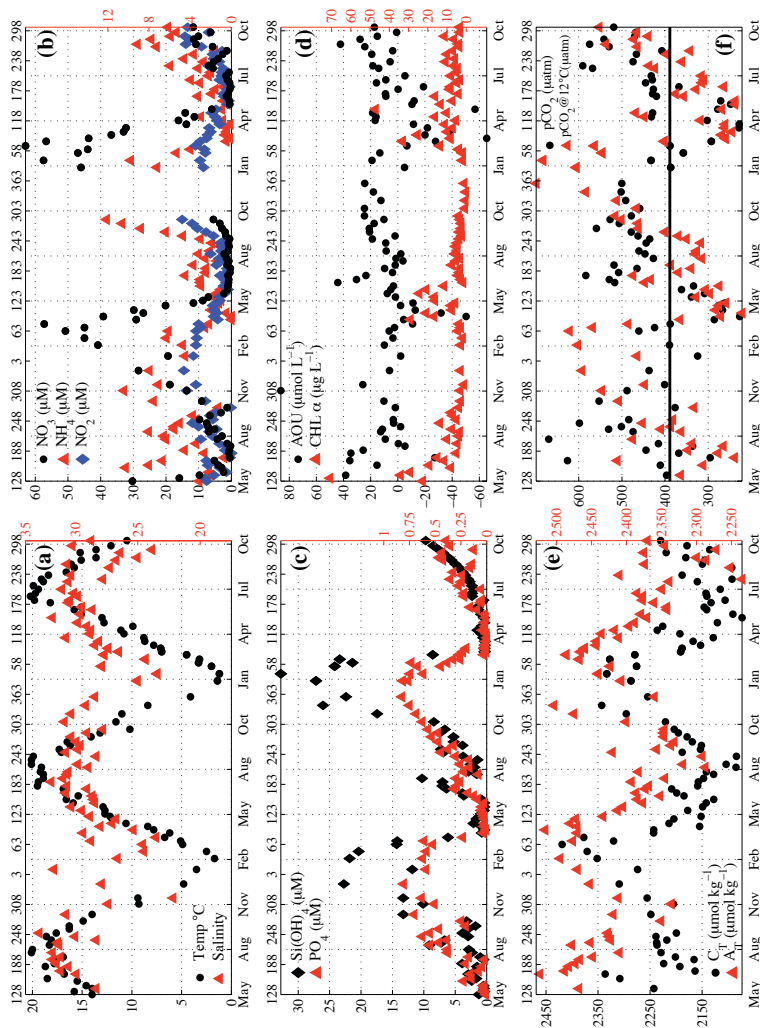
Figure 2. 30 Month time series plots of temperature (°C), salinity, ammonium (µmol l⁻¹), nitrate (µmol l⁻¹), nitrite (µmol l⁻¹), silicate (µmol l⁻¹), phosphate (µmol l⁻¹), AOU (µmol l⁻¹), chlorophyll α (µg l⁻¹), DIC (µmol kg⁻¹), A_T (µmol kg⁻¹), pCO₂ (µatm) and pCO₂@12°C (µatm).

Table 1. Seasonally averaged values of measured parameters in the Marsdiep given with one standard deviation. Spring was defined as from yearday 60 to 151, summer is from yearday 152 to yearday 243, autumn is from yearday 244 to 334 and winter is from yearday 335 to 59. The numbers highlighted in red refer to the DIC and A_T samples taken during the time period, as fewer DIC and A_T samples were obtained compared to the other parameters.

Year	Season	#	Sluice Discharge ($m^3 s^{-1}$)	Salinity	Chl α ($\mu g\ l^{-1}$)	NO_3 ($\mu mol\ l^{-1}$)	$Si(OH)_4$ ($\mu mol\ l^{-1}$)	PO_4 ($\mu mol\ l^{-1}$)	NH_4 ($\mu mol\ l^{-1}$)	DIC ($\mu mol\ kg^{-1}$)	A_T ($\mu mol\ kg^{-1}$)	pCO_2 (μatm)	pCO_2 @ 12°C (μatm)
2008	Spring	6 (2)	115±89	27.80±1.5	40±22	14.58±12	0.64±0.4	0.06±0.0	2.71±0.5	2243±1	2442±2	396±8	264±10
2008	Summer	14	237±129	28.83±0.9	10±5	3.36±2.6	3.50±2.5	0.29±0.2	5.67±2.8	2234±51	2447±33	461±117	372±84
2008	Autumn	8	304±221	29.03±3.6	6±4	9.38±5.6	7.60±4.9	0.54±0.2	5.77±3.1	2209±54	2377±36	484±85	446±79
2009	Winter	4	323±253	27.87±2.8	3±1	30.22±12	18.56±5.0	0.70±0.1	6.21±1.6	2315±43	2446±19	384±56	562±77
2009	Spring	13	314±200	27.24±2.0	14±9	25.29±19	3.54±5.1	0.17±0.2	1.89±1.6	2230±93	2438±51	316±81	359±132
2009	Summer	13	142±132	29.25±1.0	6±3	1.02±0.5	4.08±2.8	0.25±0.1	2.80±0.9	2137±41	2336±34	476±66	367±63
2009	Autumn	9	127±116	29.28±1.0	3±1	3.12±1.7	8.40±3.9	0.56±0.1	8.76±3.5	2205±44	2366±43	489±38	465±68
2010	Winter	8	358±198	26.08±2.5	2±1	49.12±6.4	26.62±3.9	0.76±0.0	7.60±2.2	2297±33	2403±36	420±58	638±64
2010	Spring	18	189±276	27.93±2.2	17±12	26.86±20	4.03±9	0.12±0.2	1.44±1.3	2190±72	2410±31	286±81	346±116
2010	Summer	13	134±99	29.22±1.1	8±4	2.13±2.3	2.01±1	0.20±0.1	2.91±1.5	2133±29	2339±40	441±86	344±58
2010	Autumn	10	321±220	28.32±2.3	6±3	8.71±4.1	8.17±2.9	0.43±0.1	6.19±2.4	2187±51	2331±51	502±52	466±68

winter compared to summer. There is large variability within the seasonal cycle of salinity and despite this broad pattern the minimum salinity (18.5) was recorded in early June and the maximum salinity (33.7) in early October. The highly variable freshwater output from the Afsluitdijk, combined with the influence of wind and tidal mixing in the Marsdiep, are likely to contribute towards some of the observed variability.

The concentration of inorganic nutrients throughout the years demonstrates clear seasonality linked to photosynthesis (Figure 2 (b)(c)). The nitrate, phosphate, and silicate concentrations all show a consistent pattern with peaks in the winter and minima in the spring or summer. A minimum concentration of nitrate is reached on yearday 165 in 2009 and yearday 150 in 2010, with concentrations of 0.8 µmol l^{-1} and 0.5 µmol l^{-1}, respectively. Both years show a nitrate peak of ~60 µmol l^{-1}, on yearday 76 in 2009 and yearday 67 in 2010, which coincides with the respective minimum winter salinity value of each year. The ammonium annual trend shows a general offset to that of nitrate, however, is in phase with nitrite. Ammonium and nitrite also show a wintertime peak followed by a spring minimum, however, both fall approxiamately three months earlier than the respective peaks in nitrate. Concentrations of ammonium, in both 2009 and 2010, start to increase steadily from late spring.

In 2009, ammonium concentrations mirror the small peak in concentrations seen in phosphate, immediately following the initial depletion in spring. In 2009 there are two distinctive dips in phosphate concentration, the first closely following the peak in nitrate, on yearday 82, and the latter (yearday 216) slightly preceding the onset of increasing ammonium concentrations in late summer, which begin on yearday 231. In contrast, in 2010 a second period of decline in phosphate cannot be discerned, as the values stay close to zero throughout spring with a minimum reached on yearday 110. Phosphate concentrations show a close correlation to silicate concentrations, which are the first, of all the inorganic nutrients, to be depleted in the year, reaching values of 0.37 and 0.30 µmol l^{-1} by yearday 91 in 2009 and 95 in 2010, respectively. The respective maximum concentrations for these years, before the declines, were 21.81 µmol l^{-1}, on yearday 34 in 2009 and 32.8 µmol l^{-1} on yearday 38 in 2010, representing respective decreases of 21.44 µmol l^{-1} and 32.5 µmol l^{-1} within the first three and a half months of the year.

Chlorophyll α concentrations show a general inverse relationship with apparent oxygen utilization (AOU = $[O_2]_{sat}$ − $[O_2]_{obs}$), with both parameters showing large fluctuations over spring. Chlorophyll α peaks on yearday 85 in 2009, just before AOU reaches the yearly

minimum on yearday 91. The same pattern is seen in 2010 in early spring, with the minimum AOU (on yearday 82) closely following a peak in Chlorophyll α. However, in 2010, the yearly maximum of Chlorophyll α falls later in the year on the same day (yearday 140) as the second lowest AOU value.

The seasonal cycle of DIC and A_T in the Marsdiep reveal a tight coupling to each other, shown in Figure 2 (e) and Figure 3. Both parameters show the highest concentrations occurring in spring, when both maxima exceed their respective peaks in the adjacent southern North Sea (data not shown). Values then decrease until late summer, with minima observed in mid-August, after which, both DIC and A_T begin a steady increase again. The DIC minimum in 2009, on yearday 216, is observed much later in the year than in 2010, which falls on yearday 150. Despite the difference in timing, both DIC minima are within 10 μmol kg^{-1} of each other (2073.9 μmol kg^{-1} in 2009 and 2083.3 μmol kg^{-1} in 2010). In contrast, the DIC peak of the whole 28 months falls in the winter of 2008-2009 and is 86 μmol kg^{-1} higher than the respective winter peak of 2009-2010, representing a 25% decrease in the annual range of DIC. Due to the non-conservative behavior of DIC in the presence of biological activity (spring and summer), we took the wintertime DIC and salinity values and regressed them with values taken from the adjacent southern North Sea to obtain the following equations:

$$2009: DIC = -14.6*S + 2728 \qquad (R^2 = -0.99, \text{p-value: } 0.065)$$

$$2010: DIC = -14.3*S + 2662 \qquad (R^2 = -0.94, \text{p-value: } 0.005).$$

Both regressions show a similar relationship, however the derived zero-salinity end-member in 2009 is 66 μmol kg^{-1} higher, explaining a large portion of the greater DIC range observed in this year. The annual A_T peak decreases from 2529 μmol kg^{-1} in 2009 to 2458 μmol kg^{-1} in 2010, however, similarly the range remains similar for both years (247 μmol kg^{-1} and 223 μmol kg^{-1} for 2009 and 2010, respectively). Linear regression of salinity against A_T in the Marsdiep was insignificant, preventing us from deriving a similar A_T-salinity mixing line.

To further examine the changes in DIC and A_T throughout the year, seasonal linear regressions were performed between both parameters, revealing four statistically significant relationships (Figure 3). From summer to winter the regression slope showed little variation (0.80 – 0.93), however, with significant variation in the intercept. Such a relationship would suggest that the same processes are controlling the interaction between the two parameters for the majority of the year, but that the background A_T or DIC concentration is being further modified, independently of the other. The spring DIC-A_T relationship varied notably from
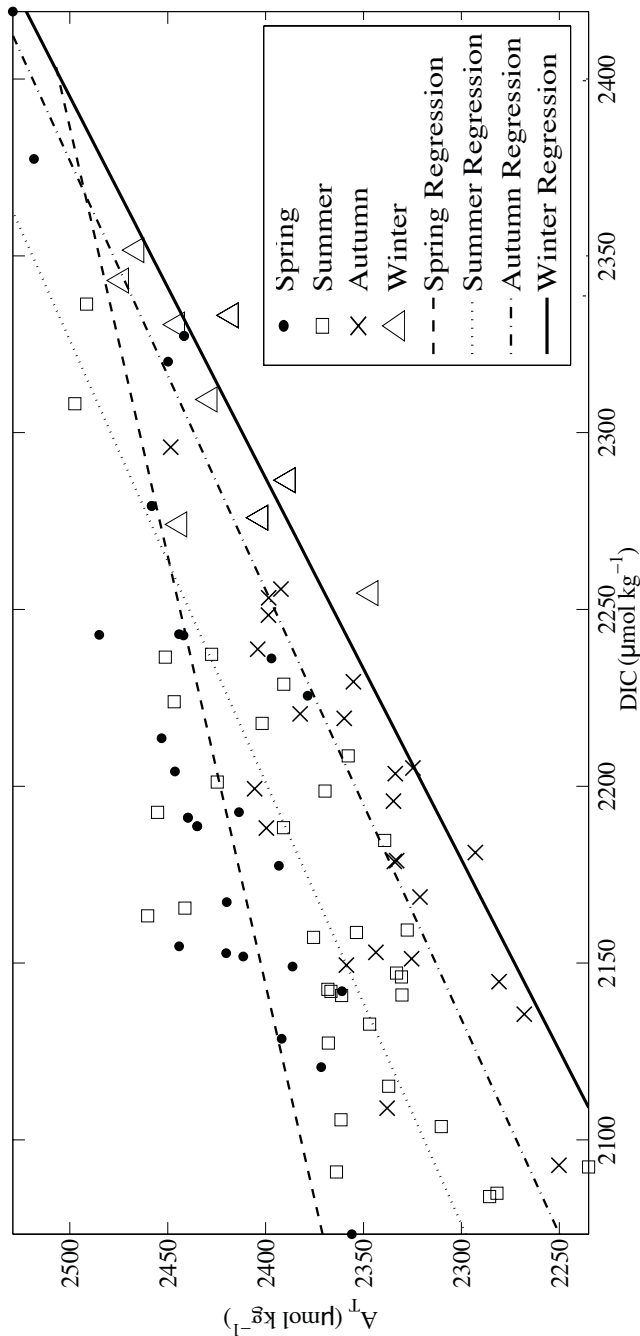
Figure 3. Seasonal linear regressions of DIC and A_T fitted using data from all three years. Fitting was performed using the least squares method, resulting in the following equations, with the correlation coefficient (R^2) and p-value given in brackets:

Winter: $A_T = 0.93DIC + 280$ [±23]   [R^2=0.76, p=0.004]
Spring: $A_T = 0.41DIC + 1515.9$ [±25]   [R^2=0.79, p=0.000]
Summer: $A_T = 0.80DIC + 638.8$ [±36]   [R^2=0.80, p=0.000]
Autumn: $A_T = 0.82DIC + 542.3$ [±29]   [R^2=0.80, p=0.000]

that of the other seasons in that the gradient was approximately half that for the rest of the year (0.41) and the highest A_T intercept is observed.

The difference in winter DIC peaks between the years appear to have a negligible effect on the following years pCO_2 distribution, with the maximum pCO_2 values calculated in 2009 and 2010 falling within 8 µatm of each other (583.7 and 590.8 µatm, respectively). The respective annual minimum pCO_2 values were 190.53 and 205.36 µatm, occurring in spring. The annual cycle of calculated pCO_2 in 2009 exhibits two clear periods of depression (Figure 2(f)), the first one occurring in late winter and the second in late spring. The first depression is smaller than the second, however, both lead to under-saturation of CO_2 with respect to the atmosphere. In contrast, in 2010 the two peaks fall later in the year, the first minima occurring in early spring and the second in early summer. There is a small peak immediately following the initial dip, most evident in the temperature-normalized plot in 2010, where pCO_2 concentrations reach 431.8 µatm before falling to 248.2 µatm again. From July, in both years, the pCO_2 increases to above atmospheric concentrations, turning the Marsdiep into a temporary source of CO_2. The temperature-normalized pCO_2 plot (Figure 2(f)) shows a similar pattern for most of the year, however, a greater portion of summer is undersaturated with respect to CO_2.

The result of the water mass analysis is shown in Figure 4 as a function of discharge from the sluices of the Afsluitdijk (data Rijkswaterstaat, Henk Zemmelink, *pers. comm.*). The minimum fraction of southern North Sea water found in the Marsdiep basin was 54% in the early summer of 2008 (yearday 160), whereas the maximum fraction of 98% was found in October of the same year. The higher rates of discharge generally occur between October to May, thus resulting in slightly fresher water in the Marsdiep during these periods. It is only during these periods of higher discharge that a relationship between the fraction of freshwater and discharge volume can be observed. At discharges greater than 450 m^3 s^{-1}, a significant linear relationship becomes apparent with an R^2 value of -0.67 (p-value of 0.006).

4   Discussion

4.1   Phytoplankton Dynamics

The depletion of silicate early in the year is caused by the first spring phytoplankton bloom of diatoms. The diatom bloom has been observed to peak close to yearday 92 (van Boekel et al., 1992), which is consistent with the silicate minima found here on yearday 91 and 95, in
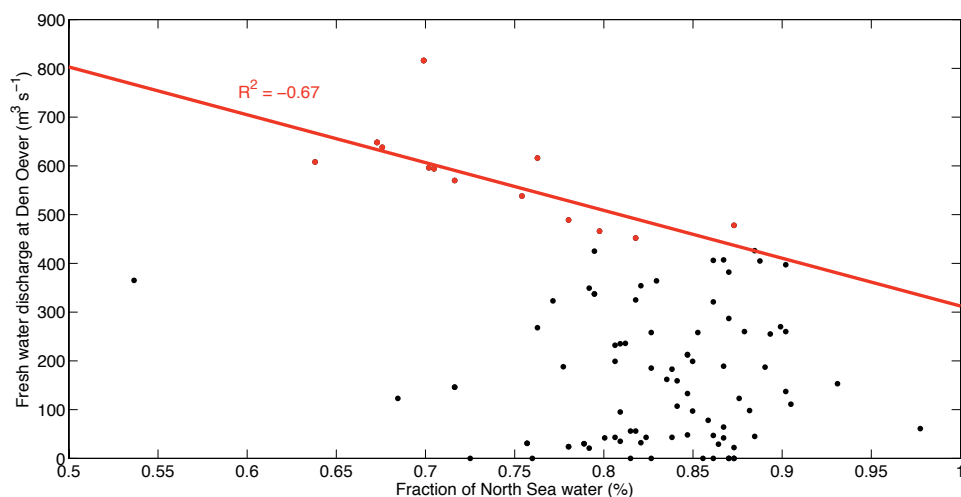
Figure 4. The fraction of North Sea water, expressed as a percentage, present in the Marsdiep against freshwater discharge from the sluices at Den Oever ($m^3 s^{-1}$). The linear regression is applied to data with a discharge greater than 450 $m^3 s^{-1}$.

2009 and 2010, respectively. Phosphate limitation in the Marsdiep has been well documented (De Jonge, 1997; Phillipart et al., 2000) and the exhaustion of silicate occurred after phosphate concentrations had reached very low levels for both years. However, linear regression of phosphate against silicate for the duration of the bloom produces a positive intercept, indicating that silicate was the limiting nutrient of the bloom. Furthermore, the decline in pCO_2 observed during this period of the year is larger in 2010, the year in which wintertime silicate concentrations peaked 11 μmol l^{-1} higher than 2009. In 2009 there was a pCO_2 decline of 162.5 μatm associated with the exhaustion of silicate, and in 2010 the decrease was 227.3 μatm. The phosphate and nitrate concentrations were similar for both years, suggesting that the greater silicate concentrations in 2010 facilitated additional primary production, supporting the argument that silicate acts as the limiting nutrient.

In both years, nitrate concentrations reveal a distinct decline immediately following silicate depletion, which is characteristic of the *Phaeocystis* bloom (van Boekel et al., 1992; Schoemann et al., 1998; Loebl et al., 2007). Linearly regressing nitrate against phosphate produces a negative intercept, which indicates nitrate was the limiting nutrient on this occasion. A substantial increase in microzooplankton is observed at the end of the *Phaeocystis* bloom (Loebl et al., 2007) and van Boekel et al. (1992) also noted a rapid increase in bacteria in the Marsdiep after the decline of the second bloom, which are indicative of the rapid uptake of the organic carbon into the microbial foodweb. Efficient remineralization is supported in our observations by increasing concentrations of ammonium occurring at the end of *Phaeocystis* bloom (Loebl et al., 2007).

The anticipated decline in pCO_2 associated with the *Phaeocystis* bloom is not as evident as that caused by the diatom bloom. In fact in 2009 there is just one data point (on yearday 118) showing a decrease in pCO_2, whilst the general trend is increasing. The same pattern is evident in $pCO_2@12°C$, although to a lesser extent, thus this increasing trend can only partly be attributed to the effect of increasing temperatures. Figure 5 shows that the increase in pCO_2 during this time is accompanied by increasing AOU, suggesting that pelagic remineralization is greater than production resulting in a net pCO_2 increase. In 2010, a slightly different pattern is apparent. After the diatom bloom, pCO_2 increases to 431.8 µatm on yearday 125, at which point a period of decrease begins until yearday 150, where the second pCO_2 minimum occurs simultaneously with nitrate exhaustion. The concurrent decrease of pCO_2 with nitrate is accompanied by a small decrease in AOU (Figure 5), indicative that in 2010 the primary production within the *Phaeocystis* bloom was sufficiently large to outcompete the effects of remineralization on AOU.
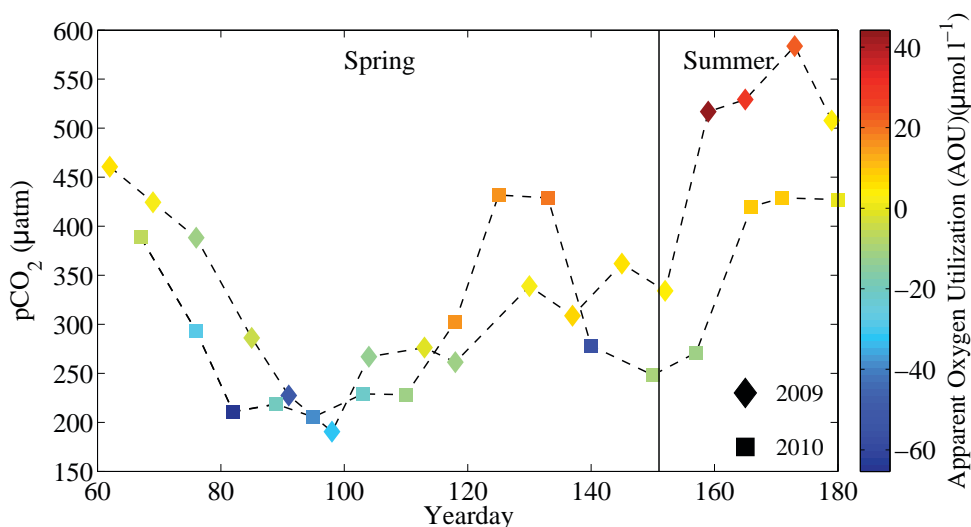

Figure 5. Calculated pCO_2 (µatm) (from A_T and DIC) values through spring (yearday 59 – 151) and into summer (yearday 152 – 243), for the years 2009 and 2010. The boundary between spring and summer is denoted by the black line. Apparent oxygen utilization (µmol l^{-1}) is represented by the colourscale.

4.2 Effects of Phytoplankton on DIC

The effects of phytoplankton succession are evident in the pCO_2 concentrations, however, it is not as clear how it impacts the DIC concentration. Net community production (NCP) is the difference between gross primary production and respiration. In the adjacent southern North Sea a very similar NCP is calculated based on DIC to that calculated using dissolved inorganic phosphate (DIP) (Bozec et al., 2006; Brockmann et al., 1990). The similarity of the two different calculations of NCP indicates that NCP is similar to new primary production

where NPP is considered as primary production associated with the assimilation of newly available nitrate in accordance to Redfield stoichiometry ((106:16), Redfield, 1963; Dugdale and Goering, 1967). During the diatom bloom there is no indication of nutrient limitation or significant remineralization, thus we use the changes in nitrate and DIC concentration (ΔNO_3 and ΔDIC), assuming Redfield Stoichiometry, to get an indication of NPP and NCP for the two years.

Using ΔDIC and a water column depth of 7m we calculate the NCP of the Marsdiep during the diatom bloom as 0.95 mol C m^{-2} in 2009 and 1.24 mol C m^{-2} in 2010. Similarly, using ΔNO_3 and the Redfield ratio we calculate NPP as 0.85 mol C m^{-2} in 2009, and 1.39 mol C m^{-2} in 2010. Comparing these sets of values, there is a lower NPP compared to NCP in 2009, indicative that only ~90% of production was in fact NPP. In contrast, in 2010 the higher estimate of NPP compared to NCP indicates that only NPP was taking place. These results are consistent with the pattern of pCO_2, however, as pCO_2 was calculated from DIC, this may contribute to the similarities. It was earlier suggested that higher silicate concentrations were responsible for facilitating a greater amount of production in 2010. As such, one would expect a relationship between the change in silicate concentration and change in NPP. Such a link is apparent when looking at the change in silicate peak from 2009 to 2010, which increased by 150% and the difference in the NPP, calculated from ΔNO_3, which increased by 163% from 2009 to 2010. Whilst this is a rough approximation of NPP, as we do not account for contributions or loss by advection, the amount of new production during the spring diatom bloom does appear to be influenced by the wintertime silicate concentrations.

If we also take into account changes in phosphate throughout the diatom bloom, production occurs with a N:P ratio of 16:0.2 in both 2009 and 2010. Such an elevated ratio of $\Delta NO_3/\Delta PO_4$ indicates that phosphate may act as a limiting nutrient. However, the fact that further production occurs, on quite a large scale, past the point of phosphate depletion indicates that preferential recycling of phosphate is taking place (Thomas et al., 1999). During the diatom bloom the $\Delta DIC/\Delta NO_3$ ratio conforms quite well to that of Redfield (106:16), with ratios of 109:16 in 2009 and 115:16 in 2010. However, post-bloom it becomes significantly higher than that of Redfield's ideal ratio. This is likely to be further indication of preferential recycling of nitrate, however, the ratio of carbon to nitrate in *Phaeocystis* blooms has been shown to deviate significantly from that of Redfield (Schoemann et al., 2005).
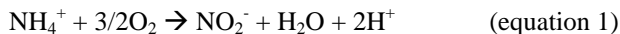
4.3　　DIC-associated variations in A_T

The seasonal relationship between A_T and DIC (Figure 3) shows a tight coupling, however, whilst DIC is strongly influenced by photosynthesis through direct uptake, the effect on A_T is smaller. Photosynthesis causes an overall positive change in A_T due to the uptake of nutrients and the shift in carbon chemistry. The production of 1 mol of organic matter (containing 106 mols of organic carbon) has been calculated to increase A_T by 17 mols (Chen et al., 1982). In the Marsdiep the observed DIC decreases by 109 µmol kg^{-1} and 182 µmol kg^{-1} during spring (yearday 60 – 151), which would correspond to A_T increases of 17.5 µmol kg^{-1} and 29.1 µmol kg^{-1}. In contrast to this, A_T shows a distinctive decreasing trend during spring in the Marsdiep basin, with an associated ΔA_T of -168 µmol kg^{-1} and -102.17 µmol kg^{-1}. The annual cycle of A_T in the Marsdiep (Figure 2(e)) is thus the direct inverse pattern to that of the A_T cycle in the sNS (Thomas et al., 2009), indicative of the dominance of different biogeochemical processes.

As we lack data for the freshwater end member of A_T and DIC it is not possible to derive a reliable linear relationship with salinity. Instead we use the seasonally derived linear relationships between A_T and DIC and the fact that both are conservative properties, with regard to temperature and pressure, to calculate the predicted changes in A_T associated with DIC changes, between seasons. Any observations deviating from these relationships are indicative of DIC-independent A_T sources or sinks operating at that time of year. Such a method should also, to an extent, take into account changes caused by fluctuations in the freshwater end member concentrations, as both parameters should co-vary with such changes. During autumn and winter, when temperature and light availability limit primary production, the DIC associated changes in A_T extend to remineralization processes. However, in spring and summer the generation of DIC through pelagic remineralization will be masked as the newly available DIC is quickly removed again from the water column by phytoplankton. Therefore, A_T generated from remineralization processes, although limited in spring and summer, will have to be considered as DIC-independent, and accounted for.

In 2009 the change from the maximum winter concentration of DIC to the minimum spring concentration of DIC is -277 µmol kg^{-1}, with a calculated associated change in A_T (ΔA_T) of -123 µmol kg^{-1}, using the seasonal DIC-A_T regressions. This value is close to the observed ΔA_T of -168 µmol kg^{-1}, leaving just -45 µmol kg^{-1} A_T unaccounted for. For 2010 the observed ΔDIC of -260 µmol kg^{-1} has a calculated, associated ΔA_T decrease of -72 µmol kg^{-1}. The observed ΔA_T decrease was -102 µmol kg^{-1}, leaving -30 µmol kg^{-1} to an independent A_T sink. As the water column is saturated with respect to oxygen throughout this
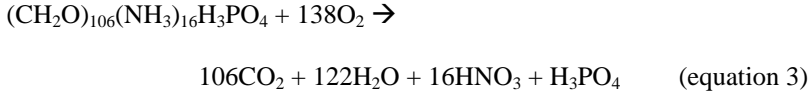
period, the two most likely processes contributing to such a decrease in A_T are nitrification and the uptake of ammonia. Nitrification is the oxidation of ammonium to nitrite and nitrate, and has been found to peak in spring and late summer in the Wadden Sea (Jensen et al., 1996), when oxygen is still readily available. Furthermore, more recently, net nitrification has also been found to take place in Dutch coastal waters during winter (Wuchter et al., 2006). For every mole of nitrate produced by nitrification, A_T decreases by 2 moles, following the below two equations:
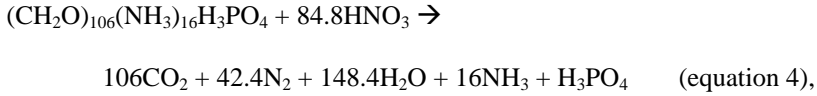
$$NH_4^+ + 3/2O_2 \rightarrow NO_2^- + H_2O + 2H^+ \qquad \text{(equation 1)}$$

$$NO_2^- + 1/2O_2 \rightarrow NO_3^- \qquad \text{(equation 2; Schlesinger, 1997)}$$

If the entirety of the unaccounted for sink of A_T was due to nitrification from remineralization there would be an equivalent, release of 360 µmol kg^{-1} of DIC in 2009 and 240 µmol kg^{-1} of DIC in 2010. The lack of an observed increase in DIC is unsurprising, as it would be largely mitigated by the ongoing primary production. The uptake of ammonia is also likely to contribute to the decrease in A_T. Over the time period in question we observe a 12 µmol l^{-1} decrease in ammonia, which, if was completely due to biological uptake would cause a decrease of 24 µmol kg^{-1} in A_T. As such, ammonia uptake could constitute half of the A_T sink, however, a proportion of the decrease in ammonium will be caused by ongoing nitrification. Thus in what ratio these processes take place cannot be determined here.

The concurrent increase of DIC and A_T from late summer to winter results in both peaking simultaneously, for both years. In 2009 the DIC concentration starts to increase from yearday 238 to its peak on yearday 340, however, in 2010 the increase starts earlier on yearday 227 peaking on yearday 350. Following the same method as from winter to spring, we assess the ΔDIC and ΔA_T from autumn, just after the DIC minimum, to winter. The total observed ΔDIC from autumn to winter, for the two years, is +192 µmol kg^{-1} and +238 µmol kg^{-1}, respectively. The concomitant observed ΔA_T is smaller, with values of +148 µmol kg^{-1} and +195 µmol kg^{-1} for 2009 and 2010, respectively. Using the DIC-A_T regressions we calculate ΔA_T values of +137 µmol kg^{-1} and +174 µmol kg^{-1}, respectively. These values are representative of the observed values, indicating that the dominant controls on A_T are accounted for by those processes related to the remineralization of DIC. The deviation between the calculated and observed values may be attributable to changes in the freshwater end member properties.

Aerobic oxidation of organic matter leads to a decrease in A_T, following the reaction:

$$(CH_2O)_{106}(NH_3)_{16}H_3PO_4 + 138O_2 \rightarrow$$

$$106CO_2 + 122H_2O + 16HNO_3 + H_3PO_4 \qquad \text{(equation 3)}$$

A high AOU in autumn makes it unlikely that this will constitute a significant process at this time of year. In the absence of oxygen the next electron acceptor is nitrate, in the process of denitrification. The reaction can be written in full as (Chen and Wang, 1999):

$$(CH_2O)_{106}(NH_3)_{16}H_3PO_4 + 84.8HNO_3 \rightarrow$$

$$106CO_2 + 42.4N_2 + 148.4H_2O + 16NH_3 + H_3PO_4 \qquad \text{(equation 4)},$$

which leads to an increase in A_T of 83.8mol per mol of organic matter. Denitrification has been observed in the sediment of the Marsdiep, beginning in late summer and increasing throughout winter (Kieskamp, 1991). Denitrification in other areas of Wadden Sea sediments have demonstrated rates up to 0.19 mmol N m^{-2} h^{-1}, and have even been found to take place in oxic conditions (Gao et al., 2010). Assuming a maximum sediment remineralization rate of 90%, which is representative of the region (van Beusekom et al., 1999), 194 μmol kg^{-1} of DIC (observed in 2009) remineralized with nitrate as electron acceptor, should release 137 μmol kg^{-1} of A_T, and 238 μmol kg^{-1} of DIC (observed in 2010) would release 169 μmol kg^{-1} of A_T. These values are very similar to the observed change in A_T, strongly indicative that the majority of organic matter was remineralized via this process.

Sulfate reduction has also been found to be responsible for a significant proportion of carbon remineralization in the sediments of the Wadden Sea (Al-Raei et al., 2009) and has also been proposed as a significant contributor of A_T generation in the Wadden Sea (Thomas et al., 2009). Sulfate reduction releases both DIC and A_T into the water column, and thus it may also contribute to the observed autumn increase in both of these parameters. Furthermore, the reduction of trace metals has also been shown to contribute significantly to A_T in the East China Sea (Chen and Wang, 1999). Schoemann et al. (1997) observe a seasonal release of dissolved Mn and Fe in the Marsdiep associated with anoxic conditions in the sediment caused by the spring diatom and *Phaeocystis* blooms. It should be noted that a large number of these processes take place in the sediment and are reversed when the products enter an aerobic environment again. Unfortunately, the contribution of A_T from the sediment cannot be distinguished from that generated in the pelagic environment without additional data.

5 Conclusions

The results of 30 months of observations in the Marsdiep basin of the Wadden Sea suggest a

very close coupling between inorganic carbon dynamics, phytoplankton succession and the nitrogen cycle. The diatom spring bloom is almost exclusively NPP resulting in substantial under-saturation with respect to pCO_2 in the surface waters and turning the Marsdiep into a seasonal sink for CO_2. The bloom is ultimately silicate limited in both years, thus in 2009 the NCP calculated for the diatom bloom was just 0.95 mol C m^{-2}, whereas in 2010, with a 48% increase in wintertime silicate concentration, the NCP was 1.24 mol C m^{-2}. Non-redfield ratios during the subsequent *Phaeocystis globosa* bloom, and ongoing preferential nutrient recycling prevent such a calculation being performed for biological production taking place later in the year.

There is a significant linear relationship between A_T and DIC for all four seasons, in both years. Whilst the annual DIC cycle mirrors that of the adjacent sNS, the A_T displays the inverse seasonal relationship to that of the sNS. We attribute A_T consumption, through spring and into summer, to nitrification and ammonia uptake, however, the ratio in which they occur cannot be constrained here, and is likely to vary within the time period. From autumn through to winter A_T is produced in quantities consistent with denitrification of 90% of the organic matter produced. While this is likely the dominant ongoing process at this time, the reduction of sulfate, manganese and iron is also likely to contribute to A_T generation and we suggest further work on sediment fluxes in the area to better constrain an A_T budget.

References:

Al-Raei, A.M., K. Bosselmann, M.E. Böttcher, B. Hespenheide, and F. Tauber, (2009). Seasonal dynamics of microbial sulfate reduction in temperature intertidal surface sediments: controls by temperature and organic matter. *Ocean Dyn.* 59, 351-370.

Bakker, C., P.M.J. Herman, and M. Vink (1994). A new trend in the development of the phytoplankton in the Oosterschelde (SW Netherlands) during and after the construction of a storm-surge barrier. *Hydrobiologia* 283, 79-100.

Beck, M., and H.-J. Brumsack (2012). Biogeochemical cycles in sediment and water column of the Wadden Sea: The example of Spiekeroog Island in a regional context. *Ocean Coast Manage.* 68, 102-113.

van Beusekom, J.E.E., U.H. Brockmann, K.-J. Hesse, W. Hickel, K. Poremba, and U. Tillmann (1999). The importance of sediments in the transformation and turnover of nutrients and organic matter in the Wadden Sea and German Bight. *Ger. J. Hydrogr.* 51, 245-266.

van Beusekom, J.E.E., and V.N. De Jong (2002). Long-term changes in Wadden Sea nutrient cycles: importance of organic matter import from the North Sea. *Hydrobiologia* 475/476, 185-194.

van Beusekom, J.E.E., M. Loebl, and P. Martens (2009). Distant riverine nutrient supply and local temperature drive the long-term phytoplankton development in a temperate coastal basin. *J. Sea Res.* 61, 26-33.

van Beusekom, J.E.E., and V.N. de Jonge (2012). Dissolved organic phosphorus: An indicator of organic matter turnover? *Estuar. Coast. Shelf S.* 108, 29-36.

van Boekel, W.H.M., F.C. Hansen, R. Riegman, and R.P.M. Bak (1992). Lysis-induced decline of a *Phaeocystis* spring bloom and coupling with the microbial foodweb. *Mar. Ecol. Progr. Ser.* 81, 269-276.

Borges, A.V., B. Delille, and M. Frankignoulle (2005). Budgeting sinks and sources of CO_2 in the coastal ocean: Diversity of ecosystems counts. *Geophys. Res. Lett.* 32, L14601.

Borges, A.V., L.-S. Schiettecatte, G. Abril, B. Delille, and F. Gazeau (2006). Carbon dioxide in European coastal waters. *Estuar. Coast. Shelf S.* 70, 375-387.

Borges, A.V., and N. Gypens (2010). Carbonate chemistry in the coastal zone responds more strongly to eutrophication than ocean acidification. *Limnol. Oceanogr.* 55, 346-353.

Bozec, Y., H. Thomas, L.-S. Sciettecatte, A.V. Borges, K. Elkalay, and H.J.W. de Baar (2006). Assessment of the processes controlling seasonal variations of dissolved inorganic carbon in the North Sea. *Limnol. Oceanogr.* 51, 2746-2762.

Bozec, Y., L. Merlivat, A.-C. Baudoux, L. Beaumont, S. Blain, E. Bucciarelli, T. Danguy, E. Grossteffan, A. Guillot, J. Guillou, M. Répécaud, and P. Tréguer (2011). Diurnal to inter-annual dynamics of pCO_2 recorded by a CARIOCA sensor in a temperate coastal ecosystem (2003-2009). *Mar. Chem.* 126, 13–26.

Brasse, S., A. Reimer, R. Seifert, and W. Michaelis (1999). The influence of intertidal mudflats on the dissolved inorganic carbon and total alkalinity distribution in the German Bight, southeastern North Sea. *J. Sea Res.* 42, 93-103.

Brockmann, U., R.W.P.M. Laane, and J. Postma (1990). Cycling of nutrient elements in the North Sea. *Neth. J. Sea Res.* 26, 239-264.

Cadée, G.C. (1992). Phytoplankton variability in the Marsdiep, The Netherlands. *ICES Mar. Sci. Symp.* 195, 213-222.

Cadée, G.C.and J. Hegeman (2002). Phytoplankton in the Marsdiep at the end of the 20th century; 30 years monitoring biomass, primary production, and *Phaeocystis* blooms. *J. Sea Res.* 48, 97-110.

Cai, W. (2011). Estuarine and Coastal Ocean Carbon Paradox: CO_2 Sinks or Sites of Terrestrial Carbon Incineration? *Ann. Rev. Mar. Sci.* 3**,** 123-145.

Chen, C.-T.A., R.M. Pytkowicz, and E.J. Olson (1982). Evaluation of the calcium problem in the South Pacific. *Geochem. J.* 16, 1-10

Chen, C.-T.A., and S.-L. Wang (1999). Carbon, alkalinity and nutrient budgets on the East China Sea continental shelf. *J. Geophys. Res.* 104, 20675-20686.

Chen, C.-T.A. (2002). Shelf-vs. dissolution-generated alkalinity above the chemical lysocline. *Deep-Sea Res. II* 49, 5365-5375.

Chen, C.-T.A., and A.V. Borges (2009). Reconciling opposing views on carbon cycling in the coastal ocean: Continental shelves as sinks and near-shore ecosystems as sources of atmospheric CO_2. *Deep-Sea Res. II* 56, 578-590.

Dickson, A.G., C.L. Sabine, and J.R. Christian (2007). Guide to best practices for ocean CO_2 measurements. PICES Special Publication, 3, Sidney.

van Engeland, T., K. Soetaert, A. Knuijt, R.W.P.M. Laane, and J.J. Middelburg (2010). Dissolved organic nitrogen dynamics in the North Sea: A time series analysis

(1995-2005). *Estuar. Coast. Shelf S.* 89, 31-42.

Dugdale, R.C., and J.J. Goering (1967). Uptake of new and regenerated forms of nitrogen in primary production. *Limnol. Oceanogr.* 12, 196-206.

Fennel, K. (2010). The role of continental shelves in nitrogen and carbon cycling: Northwestern North Atlantic case study. *Ocean Sci.* 6, 539-548.

Frankignoulle, M., and A.V. Borges (2001). European continental shelf as a significant sink for atmospheric carbon dioxide. *Global Biogeochem. Cycles* 15, 569-576.

Gao, H., F. Schreiber, G. Collins, M.M. Jensen, O. Svitlica, J.E. Kostka, G. Lavik, D. de Beer, H.Y. Zhou, and M.M. Kuypers (2010). Aerobic denitrification in permeable Wadden Sea sediments. *ISME Journal* 4(3), 417-426.

Gattuso, J.-P., M. Frankignoulle, and R. Wollast (1998). Carbon and carbonate metabolism in coastal aquatic ecosystems. *Annu. Rev. Ecol. Syst.* 29, 405–434.

Grover, J.P. (1997). Resource competition. London: Chapman and Hall, 342.

Gypens, N., G. Lacroix, C. Lancelot, and A.V. Borges (2011). Seasonal and inter-annual variability of air-sea CO_2 fluxes and seawater carbonate chemistry in the Southern North Sea. *Prog. Oceanogr.* 88, 59-77.

Heip, C.H.R., N.K. Goosen, P.M.J. Herman, J. Jromkamp, J.J. Middelburg, and K. Soetaerd (1995). Production and consumption of biological particles in temperate tidal estuaries. Oceanogr. *Mar. Biol. Ann. Rev.* 33, 1-149.

Hofmann, A.F., F.J.R. Meysman, K. Soetaert, and J.J. Middelburg (2009). pH modelling in aquatic systems with time-variable acid-base dissociation constants applied to the turbid, tidal Scheldt estuary. *Biogeosciences* 6, 1539-1561.

Hoppema, J.M.J. (1991). The Carbon Dioxide System and Dissolved Oxygen in the Coastal Waters of the Netherlands. Rijsuniversiteit Groningen.

Hoppema, J.M.J. (1990). The Distribution and Seasonal Variation of Alkalinity in the Southern Bight of the North Sea and in the Western Wadden Sea. *Neth. J. Sea Res.* 26, 11-23.

Hoppema, J.M.J. (1993). Carbon-dioxide and oxygen disequilibrium in a tidal basin (Dutch-Wadden Sea). *Neth. J. Sea Res.* 31, 221-229.

Hydes, D.J., B.A. Kelly-Gerreyn, A.C. Le Gall, and R. Proctor (1999). The balance of supply of nutrients and demands of biological production and denitrification in a temperate latitude shelf sea – a treatment of the southern North Sea as an extended estuary.

Mar. Chem. 68, 117-131.

Johnson, K.M., K.D. Wills, D.B. Butler, W.K. Johnson, and C.S. Wong (1993). Coulometric total carbon dioxide analysis for marine studies: maximizing the performance of an automated gas extraction system and coulometric detector. *Mar. Chem.* 44, 167-188.

de Jonge, V.N. (1990). Response of the Dutch Wadden Sea ecosystem to phosphorus discharges from the river Rhine. *Hydrobiologia* 195, 49-62.

de Jonge, V.N. (1997). High remaining productivity in the Dutch western Wadden Sea despite decreasing nutrient inputs from riverine sources. *Mar. Poll. Bull.* 34(6), 427-436.

Kieskamp, W.M., L. Lohse, E. Epping, and W. Helder (1991). Seasonal variation in denitrification rates and nitrous oxide fluxes in intertidal sediments of the western Wadden Sea. *Mar. Ecol. Prog. Ser.* 72, 145-151.

Kowalski, N., O. Dellwig, M. Beck, M. Grunwald, C.-D. Dürselen, T.H. Badewien, H.-J. Brumsack, J.E.E. van Beusekom, and M.E. Böttcher (2012). A comparative study of manganese dynamics in the water column and sediments of intertidal systems of the North Sea. *Estuar. Coast. Shelf S.* 100, 3-17.

Lenhart, H.-J., J. Patsch, and G. Radach (1996). Daily nutrient loads of the European continental rivers for the years 1977-1993. Berichte aus dem Zentrum fur Meeres- und Klimaforschung. Reihe B: Ozeanographie 22, 1-159.

Lewis, E.L., and D.W.R. Wallace (1998). Program developed for CO_2 system calculations, ORNL/CDIAC-105. Carbon dioxide information analysis center, Oak Ridge National Laboratory, U.S. Department of Energy, Oak Ridge.

Loebl, M., T. Dolch, and J.E.E. van Beusekom (2007). Annual dynamics of pelagic primary production and respiration in a shallow coastal basin. *J. Sea Res.* 58, 269-282.

Loebl, M., F. Colijn, J.E.E. van Beusekom, J.G. Baretta-Bekker, C. Lancelot, C.J.M. Philippart, V. Rousseau, and K.H. Wiltshire (2009). Recent patterns in potential phytoplankton limitation along the Northwest European continental coast. *J. Sea Res.* 61, 34-43.

Maybeck, M. (1982). Carbon, nitrogen, and phosphorus transport by world rivers, *Am. J. Sci.* 282, 401-450.

Maybeck, M. (1993). Riverine transport of atmospheric carbon: sources, global typology and budget. *Water Air Soil Poll.* 70, 443-463.

Pätsch, J., and H.-J. Lenhart (2004). Daily Loads of Nutrients, Total Alkalinity, Dissolved Inorganic Carbon and Dissolved Organic Carbon to the European Continental Rivers for the Years 1977-2002. Berichte aus dem Zentrum für Meeres- und Klimaforschung, Reihe B, Ozeanographie, 48, 159 pp.

Pätsch, J., and W. Kühn (2008). Nitrogen and carbon cycling in the North Sea and exchange with the North Atlantic – A model study. Part I. Nitrogen budget and fluxes. *Cont. Shelf Res.* 28, 767-787.

Philippart, C.J.M., and G.C. Cadée (2000). Was total primary production in the western Wadden Sea stimulated by nitrogen loading? *Helgol. Mar. Res.* 54, 55-62.

Philippart, C.J.M., J.J. Beukema, G.C. Cadée, R. Dekker, P.W. Goedhart, J.M. van Iperen, M.F. Leopold, and P.M.J. Herman (2007). Impacts of nutrient reduction on coastal communities. *Ecosystems* 10, 95-118.

Proctor, R., J.T. Holt, J.I. Allen, and J. Blackford (2003). Nutrient fluxes and budgets for the North West European Shelf from a three-dimensional model. *Sci Total Environ.* 314-316, 769-785.

Reimer, A., S. Brasse,, R. Doerfer, C.-D. Dürselen, S. Kempe, W. Michaelis, H.-J. Rick, and R. Seifert (1999). Carbon cycling in the German Bight: An estimate of transformation processes and transport. *Ger. J. Hydrogr.* 51, 313-329.

Richards, F.A., J.D. Cline, W.W. Broenkow, and L.P. Atkinson (1965). Some consequences of the decomposition of organic matter in Lake Nitinat, an Anoxic Fjord. *Limnol. Oceanogr.* 10, 185-201.

Ridderinkhof, H., J.T.F. Zimmerman, and M.E. Philippart (1990). Tidal exchange between the North Sea and Dutch Wadden Sea and mixing time scales of the tidal basins. *Neth. J. Sea Res*. 25(3), 331-350.

Riegman, R., B.R. Kuipers, A.A.M. Noordeloos, H. Witte, (1993). Size-differential control of phytoplankton and the structure of plankton communities. *Neth. J. Sea Res.* 31, 255-265.

Schlesinger, W.H. (1997). Biogeochemistry: An Analysis of Global Change, 2nd ed. Academic Press, San Diego. 588pp.

Schoemann, V., H.J.W. de Baar, J.T.M. de Jong, and C. Lancelot (1998). Effects of phytoplankton blooms on the cycling of manganese and iron in coastal waters. *Limnol. Oceanogr.* 43, 1427-1441.

Schoemann, V.S., S. Becquevort, J. Stefels, V. Rousseau, and C. Lancelot (2005).

Phaeocystis blooms in the global ocean and their controlling mechanisms: A review. *J. Sea Res.* 53, 43-66.

Shadwick, E.H., H. Thomas, K. Azetsu-Scott, B.J.W. Greenan, E. Head, and E. Horne (2011). Seasonal variability of dissolved inorganic carbon and surface water pCO_2 in the Scotian Shelf region of the Northwestern Atlantic. *Mar. Chem.* 124, 23-37.

Takahashi, T., J. Olafsson, J.G. Goddard, D.W. Chipman, and S.C. Sutherland (1993). Seasonal variation of CO_2 and nutrients in the high-latitude surface oceans a comparative-study. *Global Biogeochem. Cycles* 7(4), 843-878.

Takahashi, T., S.C. Sutherland, C. Sweeney, A. Poisson, N. Metzl, B. Tilbrook, N.R. Bates, R. Wanninkhof, R.A. Feely, C.L. Sabine, J. Olafsson, and Y. Nojiri (2002). Global sea-air CO_2 flux based on climatological surface ocean CO_2, and seasonal biological and temperature effects. *Deep Sea. Res. II* 49, 1601-1622.

Thomas, H., V. Ittekkot, C. Osterroht, and B. Schneider (1999). Preferential recycling of nutrients – the ocean's way to increase new production and to pass nutrient limitation? *Limnol. Oceanogr.* 44, 1999-2004.

Thomas, H., Y. Bozec, K. Elkalay, and H.J.W. de Baar (2004). Enhanced Open Ocean Storage of CO_2 from Shelf Sea Pumping. *Science* 304, 1005-1008.

Thomas, H., Y. Bozec, K. Elkalay, H.J.W. de Baar, A.V. Borges, and L.-S. Schiettecatte (2005). Controls of the surface water partial pressure of CO_2 in the North Sea. *Biogeosciences* 2, 323-334.

Thomas, H., L.-S. Schiettecatte, K. Suykens, Y.J.M. Koné, E.H. Shadwick, A.E.F. Prowe, Y. Bozec, H.J.W. de Baar, and A.V. Borges (2009). Enhanced ocean carbon storage from anaerobic alkalinity generation in coastal sediments. *Biogeosciences* 6, 267-274.

Thomas, H., S.E. Craig, B.J.W. Greenan, W. Burt, G.J. Herndl, S. Higginson, L. Salt, E.H. Shadwick, and J. Urrego-Blanco (2012). Direct observations of diel biological CO_2 fixation in the oceans. *Biogeosciences* 9, 2301-2309.

van der Zee, C., and L. Chou (2005). Seasonal cycling of phosphorus in the southern bight of the North Sea. *Biogeosciences* 2, 27-42.

Wolf-Gladrow, D.A., R.E. Zeebe, C. Klaas, A. Kortzinger, and A.G. Dickson (2007). Total alkalinity: The explicit conservative expression and its application to biogeochemical processes. *Mar. Chem.* 106, 287-300.

Wollast, R. (1991). The coastal organic carbon cycle: fluxes, sources and sinks. In:

Mantoura, R.F.C., Martin, J.M., Wollast, R. (Eds.), Ocean Margin Processes in Global Change, Wiley, Chichester, pp.365-382.

Wuchter, C., B. Abbas, M.J.L. Coolen, L. Hertford, J. van Bleiswijk, P. Timmers, M. Strous, E. Teira, G.J. Herndl, J.J. Middelburg, S. Schouten, and J.S. Sinninghe Damsté (2006). Archaeal nitrification in the ocean. *Proc. Natl. Sci. USA*, 103, 12317-12322.

Chapter 4

Variability of North Sea pH and CO$_2$ in response to North Atlantic Oscillation forcing.

Lesley A. Salt, Helmuth Thomas, A. E. Friederike Prowe, Alberto V. Borges, Yann Bozec, and Hein J. W. de Baar.

Abstract

High biological activity causes a distinct seasonality of surface water pH in the North Sea, which is a strong sink for atmospheric CO_2 via an effective shelf pump. The intimate connection between the North Sea and the North Atlantic Ocean suggests that the variability of the CO_2 system of the North Atlantic Ocean, may, in part be responsible for the observed variability of pH and CO_2 in the North Sea. In this work we demonstrate the role of the North Atlantic Oscillation (NAO), the dominant climate mode for the North Atlantic, in governing this variability. Based on three extensive observational records covering the relevant levels of the NAO index, we provide evidence that the North Sea pH and CO_2 system strongly responds to external and internal expressions of the NAO. Under positive NAO the higher rates of inflow of water from the North Atlantic Ocean and the Baltic outflow leads to a strengthened north-south biogeochemical divide. The limited mixing between the north and south leads to a steeper gradient in pH and partial pressure of CO_2 (pCO_2) between the two regions in the productive period. This is exacerbated further when coinciding with higher sea surface temperature, which concentrates the net community production in the north through shallower stratification. These effects can be obscured by changing properties of the constituent North Sea water masses, which are also influenced by NAO. Our results highlight the importance of examining inter-annual trends in the North Sea CO_2 system with consideration of the NAO state.

1.   Introduction

Coastal and marginal seas play an important role in the atmosphere-ocean carbon exchange, responsible for a disproportionately large amount of primary production relative to their surface area [*Gattuso et al.,* 1998], which is triggered by large inputs of nutrients and organic carbon from the adjacent ocean, land and atmosphere [*Wollast*, 1998; *Thomas et al.,* 2005a*; Thomas et al.,* 2008]. The export of this carbon into the adjacent open ocean, thus sequestering large quantities of anthropogenic CO_2, is known as the continental shelf pump [*Tsunogai et al.,* 1999; *Thomas et al.,* 2004]. The effectiveness of this pump is related to the physical and biological conditions governing the CO_2 disequilibrium between the atmosphere and the sea surface, which in turn is thermodynamically responsible for the CO_2 uptake and the subsequent variation in pH and partial pressure of CO_2 (pCO_2). The codependence of this variability on physical and biological factors makes it difficult to discern the increase in CO_2 solely attributable to atmospheric pCO_2 increases [*Santana-Casiano et al.,* 2007].

The North Sea is a shelf sea on the northwest European continent with links to the North Atlantic Ocean in the south and the north. The majority of water exchange with the North Atlantic occurs in the northern North Sea, where inflowing waters enter through the Orkneys-Shetland shelf, Shetland shelf and the Norwegian channel, with the Norwegian Trench providing the main exit pathway of circulated water out of the North Sea [*Otto et al.*, 1990; *Winther and Johannessen*, 2006]. The total net carbon export to the North Atlantic via the Norwegian Trench has been estimated to be $6 \pm 1 \times 10^{12}$ mol C yr^{-1} [*Wakelin et al.*, 2012], which includes more than 90% of the CO_2 drawn down from the atmosphere in the North Sea [*Thomas et al.,* 2005a]. The effectiveness of the North Sea CO_2 pump is determined principally by water mass exchange between the North Sea and the North Atlantic Ocean in combination with the export of carbon out of the surface layer, predominantly as sinking particulate organic matter [*Thomas et al.,* 2004; *Bozec et al.,* 2005]. The latter applies most significantly to the deeper (>50 m), seasonally stratified northern part of the North Sea (>56°N), where seasonality in pH is controlled by production of organic matter and its export [*Thomas et al.,* 2009]. The seasonality of pH and pCO_2 in the southern North Sea is also closely coupled to primary production, however the export of organic matter is reduced by the rapid remineralization, which takes place in the shallow (<50 m) and well-mixed water column [*Borges and Frankignoulle*, 1999, 2002; *Schiettecatte et al.*, 2006, 2007].

Over the North Atlantic Ocean, a number of atmospheric teleconnection patterns influence climate variability of which the North Atlantic Oscillation (NAO) is the most prominent. The NAO Index (NAOI) is defined as the difference of atmospheric sea level pressure (SLP) between the Icelandic low and the Azores high and accounts for the greatest proportion (>30%) of the observed SLP variance in the region from December to March [*Hurrel, 2003*]. The effects of the NAO control a number of large-scale processes at different timescales [e.g. *Hurrell*, 1995; *Hurrel and Loon*, 1997; *Greatbatch*, 2000]. Since the atmospheric pressure anomalies are most pronounced during northern hemisphere winter [*Greatbatch*, 2000] and the ratio of signal to noise is the highest [*Hurrell and Loon*, 1997], commonly (but not exclusively) the NAOI recorded during December, January and February (DJF), has been referred to in the literature yielding the most accentuated NAOI variability. Thus, although the NAOI is commonly established for DJF consequences of the NAO have been identified at various timescales. While the atmospheric realm responds at immediate, shorter timescales, for example via variability of trajectory, direction and strength of winds, the oceanic system responds at times scales from seasons to decades, for example via altered circulation patterns at various spatial scales [e.g. *Hurrel*, 1995; *Hurrel and Loon*, 1997, *Greatbatch*, 2000; *Thomas et al.*, 2008a]. Modeling studies [*Thomas et al.*, 2008; *Levine et al.*, 2011; *McKinley et al.*, 2011] and long-term observations [*Santana-Casiano et al.*, 2007; *Pérez et al.*, 2010; *Bates*, 2011] suggest that NAO-driven changes exert significant control over the inter-annual variability of hydrographic properties and in turn the uptake of CO_2.

Recently, observations from the North Sea [*Thomas et al.*, 2007] and the North Atlantic Ocean [*Watson et al.*, 2009] indicate that the surface water pCO_2 has risen faster than the atmospheric pCO_2, which has been linked to the effects of the NAO, with varying time-scales of effect across the region [*Santana-Casiano et al.*, 2007; *Thomas et al.*, 2008a]. In-depth discussions of the role of the NAO in regulating the climate and weather go beyond the scope of the present paper, and can be found elsewhere, for example in *Hurrel* [1995], or *Greatbatch* [2000]. However, within the North Sea many processes have demonstrated significant correlations with the wintertime (DJF) NAOI, which, as we later show, impact the carbonate system. The strength of the water mass exchange between the North Atlantic and the North Sea is regulated by the NAO, which in turn affects physical and chemical characteristics of the North Sea water column for the annual cycle. As a consequence of enhanced water mass exchange between North Atlantic and North Sea during years of positive NAOI (NAO+)[*Winther and Johannessen*, 2006; *Kühn et al.*, 2010], the corresponding increase of the North Sea's nutrient inventory leads to higher productivity throughout the productive season from spring until the end of summer [*Pätsch and Kühn*, 2008]. Characteristic in the North Sea's response to NAO forcing can also be a hysteresis

between cause and effect: In the North Sea NAO+ has further been associated with higher precipitation across Scandinavia with drier conditions over central Europe [*Ionita et al.*, 2011]. Changes in precipitation patterns over the drainage area of the Baltic Sea during winter will affect the runoff from the Baltic Sea into the North Sea over the relevant (runoff) seasons. Additionally, stronger westerly winds during winter, correlated with a positive wintertime NAOI, push North Sea water into the Baltic Sea, a process that in turn leads to an enhanced outflow from the Baltic Sea into the North Sea during the subsequent spring and summer [*Hordoir and Meier*, 2010]. These patterns are generally reversed during a NAO negative (NAO-) state. From these few examples it is evident that despite the fact that the NAOI is commonly established for winter (DJF), the consequences for the North Sea are complex, not restricted to the winter season, and can be (partly) masked or even overridden by local or regional weather. One of the primary aims of this paper is to unravel this complex situation and to understand the variability of the North Sea CO_2 system in front of this background.

The intra-annual variability of pCO_2 and dissolved inorganic carbon (DIC) has been well documented in the North Sea [*Frankignoulle and Borges*, 2001; *Thomas et al.*, 2005b; *Prowe et al.,* 2009; *Bozec et al.*, 2006; *Omar et al.*, 2010; *Artioli et al.*, 2012], however, on long time scales little work has been done [*Thomas et al.*, 2005a; *Thomas et al.*, 2007; *Borges and Gypens*, 2010] and despite the proximity of the North Atlantic, the drivers for inter-annual variability of the CO_2 system in relation to the North Atlantic variability, have not yet been investigated from field observations. Further, the full scope of variations in pH and pCO_2 are still difficult to constrain when attempting to reproduce them in models [*Prowe et al.*, 2009; *Gypens et al.*, 2011; *Lorkowski et al.*, 2012; *Artioli et al.*, 2012]. Relying on a unique data set covering three basin-wide occupations of the North Sea during all relevant NAO phases, we are now able to examine the influences of NAO forcing on the North Sea carbonate system, which exerts control over internal and external processes affecting the North Sea basin.

2.   Materials and Methods

The North Sea was sampled during August/September 2001, 2005 and 2008 using a station grid of approximately 90 identical stations each time [*Bozec et al., 2005, 2006*]. These years experienced NAO (DJF) indices of -1.9, 0.12 and 2.1, respectively (http://www.cgd.ucar.edu/cas/jhurrell/indices.html*, 2012*). As we examine the influence of

the NAO in the North Sea on different time scales, we assume that the wintertime NAO forcing will be responsible for producing the most prominent signal in the data on a basin-wide scale.

Due to greater spatial coverage of DIC and pCO_2 data, in all three years, compared to that of total alkalinity (A_T) and pH, the latter two were calculated from the former two, as previously done in inter-comparison studies [*Thomas et al.,* 2009]. Internal consistency studies from cruises with full carbonate parameter coverage in late summer indicate that A_T and pH can be predicted, using DIC and pCO_2, with an accuracy of ± 9 µmol kg^{-1} and ± 0.008, respectively [*L.A. Salt, manuscript in preparation,* 2014]. Only stations with valid values for DIC and pCO_2 for all of the three years were used, resulting in a total of 85 stations worth of data for comparison.

2.1   DIC and pCO_2

Samples for the carbonate parameters were obtained following the operating procedures outlined in DOE (2007). Carbonate system parameters, DIC, A_T and pH (in 2005) were determined at 8-15 depths per station, yielding approximately 700 samples per cruise. All samples were analyzed within 12 hours of sampling, and were verified for quality control using certified reference material (CRM) supplied by Prof. Andrew Dickson (Scripps Institute of Oceanography, USA). A single sample was obtained for both DIC and A_T and these were determined by coulometric and potentiometric titrations, respectively. For further details please see *Thomas et al.*, [2007].

Surface water pCO_2 was measured every minute using a flow-through system with continuous equilibration and infrared detection [*Körtzinger et al.,* 1996], yielding approximately 20000 measurements per cruise with an accuracy of ± 1 µatm. A temperature-normalization was applied to the pCO_2 data to obtain pCO_2@16°C, which is independent of temperature differences between the years [*Takahashi et al.*, 1993].

2.3 Calculations

2.3.1 Water Mass Analysis

The North Sea surface waters (5 m depth) were separated into three simpler constituents using a mixing analysis of the dominant water masses in the North Sea [*Kempe and Pegler*, 1991; *Shadwick et al.*, 2011], with North Atlantic water, Baltic Sea water and German Bight water as end-members. The latter two consist of a fraction of North Atlantic water, however, the large freshwater contribution makes both very distinct from North Atlantic water and allows us to track them into the central North Sea. In order to differentiate water mass fractions from *n* number of contributors, *n*-1 end member variables are required. As this decomposition was done for the surface waters, temperature cannot be used, because due to seasonal heating and cooling it is not a conservative tracer as used in traditional multi-parametric optimizations for analysis of deep waters. Salinity, DIC and A_T all offer sufficiently distinct end member concentrations to be used, however, the co-dependence of A_T on salinity makes DIC favorable. The DIC is non-conservative due to biological uptake/release of CO_2, however, the end members used (Table 1) are sufficiently distinct that changes in DIC concentration affected by mixing are much greater than the potential interference of primary production/respiration. This was confirmed by similar results being obtained using salinity and A_T, which is more conservative with respect to primary production.

DIC (μmol kg^{-1}) and salinity end members	2001	2005	2008
North Atlantic	2047 (35.06)	2078 (35.30)	2065 (35.13)
Baltic	1530 (8)	1530 (8)	1530 (8)
German Bight	2090 (30.36)	2012 (30.77)	2149 (32.28)

Table 1. Dissolved inorganic carbon and salinity end members. The DIC end members used for the water mass fraction calculation for the three years, with the corresponding salinity values in parentheses.

The end members for the North Atlantic and German Bight were determined individually for each year, with only the Baltic end member remaining constant. As we lacked observations in the Baltic Proper, DIC and A_T values were taken from literature for a representative salinity of 8 [*Thomas and Schneider*, 1999; *Hjalmarsson et al.*, 2008](Table 1). The North Atlantic end member was determined by the maximum surface salinity found in the northwest North Sea (Latitudes > 58°N and Longitudes < 0°E) and its corresponding DIC value. The German Bight end member was determined by the salinity and DIC value found at the station closest to the Elbe river mouth (54.75°N, 8.25°E). By using annually determined end members for the three years, we can rule out any change in water mass fractions occurring due to changes in the chemical signal of end members, which we later show does occur in the North Sea. Statistics describing the calculated water mass fractions are shown in Table 2.

Water Mass	2001			2005			2008		
	Range	Av.	Med.	Range	Av.	Med.	Range	Av.	Med.
North Atlantic	0-100	83	91	0-100	81	87	0-100	84	91
Baltic	0-16	2	0	0-15	3	1	0-20	3	7
German Bight	0-100	15	4	0-100	16	10	0-100	13	1

Table 2. Statistics of the different water mass fractions present in the North Sea in 2001, 2005 and 2008. The basin-wide range of values, average and median are given with the units representing the % of the total water present in the North Sea.

2.3.2   DIC Inventory Calculation of the North Sea

To quantify the changes in DIC between years, differences in biological activity and remineralization must be accounted for. Here we use the apparent oxygen utilization (AOU = $[O_2]_{sat} - [O_2]_{obs}$) to account for production and remineralization, applying the Redfield ratio [*Anderson and Sarmiento*, 1994] in the following equation:

DIC* = DIC – (AOU*0.7).

These values were integrated throughout the water column to a common maximum depth per station, and then station totals were extrapolated over the entire North Sea basin. To help us

better understand the changes, the International Council for the Exploration of the Sea (ICES) defined boxes [*ICES*, 1983] were used to examine the regional changes in DIC and salinity. Unless specified otherwise, boxes 1- 5 refer to the entire water column, not just the upper 30m, whereas boxes 11- 15 refer to the deep (>30 m) portion of these boxes, respectively.

2.3.3 Calculation of Brunt-Väisälä frequency squared.

To assess the vertical stability of the water column in the northern North Sea (>56°N) we utilized the Brunt-Väisälä frequency squared:

$N^2 = (-g/\rho).(\partial\rho/\partial z)$

where z is the depth (m), ρ is density (kg m^{-3}) computed following the density equation of *Fofonoff and Millard* [1983] and *g* is the gravitational acceleration (9.807 m s^{-2}). The temperature and salinity data from the conductivity-temperature-depth (CTD) casts with a 1 m resolution were smoothed using a cubic spline. The N^2 was calculated from the smoothed dataset and the depth at which the maximum N^2 occurs we defined as the mixed-layer depth.

3. Results

The main distribution pattern of the carbonate parameters is relatively constant between years (Figure 1). The brackish Baltic outflow around the Norwegian headland has low A_T and DIC signals. The German Bight, in the southwest, is distinguished by its high A_T and high DIC content. The Shetland shelf represents the main North Atlantic inflow site, and is clearly identified by notably higher A_T values than the basin-wide average (Figure 1 (b)). The anti-correlated pH and pCO_2 both show a strong gradient at the 50 m depth contour, representing the boundary at which the dominant control on pCO_2 changes from temperature, in the well-mixed south, to biology, in the stratified north [*Prowe et al.,* 2009; *Thomas et al.,* 2005b]. The gradient between the north and south is steepest in 2008, closely followed by 2001, and weakest in 2005. This pattern reflects the measured surface water temperatures in the North Sea, 2001 and 2008 being the warmest (mean surface temperatures of 16.2°C (±1.3) and 16.1°C (±1.1), respectively), and 2005 the coldest (15.4°C (±1.0)). The highest northern pH values and lowest pCO_2 values are observed in the northern North Sea in 2001, with progressively decreasing mean pH and increasing mean pCO_2 trends over time. The average surface DIC increased by 21 µmol kg^{-1}, although not uniformly, and the average surface A_T remained relatively constant, ± 4 µmol kg^{-1}, throughout all three years.
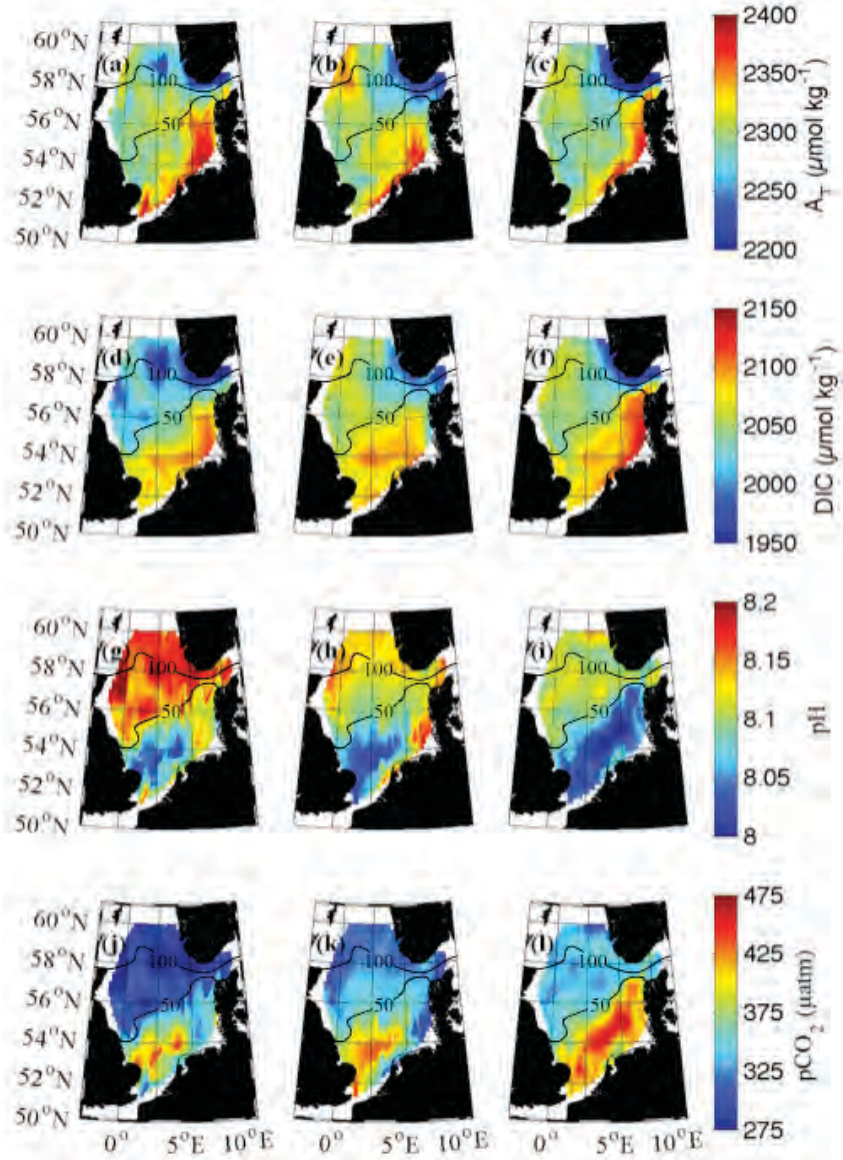
Figure 1. Surface layer distribution of carbonate parameters with 50 and 100 meter depth contours. a-c, total alkalinity (μmol kg^{-1}) for the years 2001, 2005 and 2008, **d-f**, dissolved inorganic carbon (μmol kg^{-1}) for the years 2001, 2005 and 2008, **g-i**, pH for the years 2001, 2005 and 2008, and **j-l,** partial pressure of CO_2 (pCO$_2$; μatm) for the years 2001, 2005 and 2008. The DIC and pCO$_2$ are observations, A$_T$ and pH are calculated parameters from DIC and pCO$_2$, using carbonic acid dissociation constants of *Mehrbach et al.*, 1973, refit by *Dickson and Millero* (1987), and pH is given on the Total scale. Average values for 2001, 2005 and 2008 are 2299, 2298 and 2291 μmol kg^{-1} for A$_T$, respectively, 2034, 2052 and 2055 μmol kg^{-1} for DIC, 8.129, 8.105 and 8.079 for pH and 323, 344 and 369 μatm for pCO$_2$.

The North Sea CO_2 system is largely governed by the relative contribution of different water masses composing the North Sea water as well as the rate at which these are circulated within the North Sea shelf. The mixing analysis (Figure 2(a)) clearly identifies the North Atlantic Ocean water as the dominant water mass, constituting an average 83% fraction throughout all three years (Table 2). The average, basin-wide fraction of Baltic water increases from 2% in 2001 to 3% in 2005 and 2008 (Table 2). The dominant North Atlantic inflow follows an anti-clockwise circulation from the north, mixing in the south with German Bight water. In the northeastern areas the Baltic Sea outflow plays an additional role where it is introduced to the circulation on its way out of the North Sea. This leads to the presence of two main mixing regimes, one consisting of North Atlantic and German Bight water, and the other of North Atlantic and Baltic water (Figure 2(a)). It can be seen that in 2008 these two regimes are most distinguishable, which corresponds to the year in which the maximum Baltic fraction was recorded (20%; Table 2). The formation of the two mixing environments is reflected in the formation of a dichotomy in pH measurements in 2008, which is absent in 2001 and 2005 (Figure 2(b-d)). The dichotomy divides the North Sea, with more acidic waters in the south and higher pH values in the north. The divide is formed at, approximately, the 50 m depth contour accounting for the strong gradient visible in Figure 1(i) and (l).
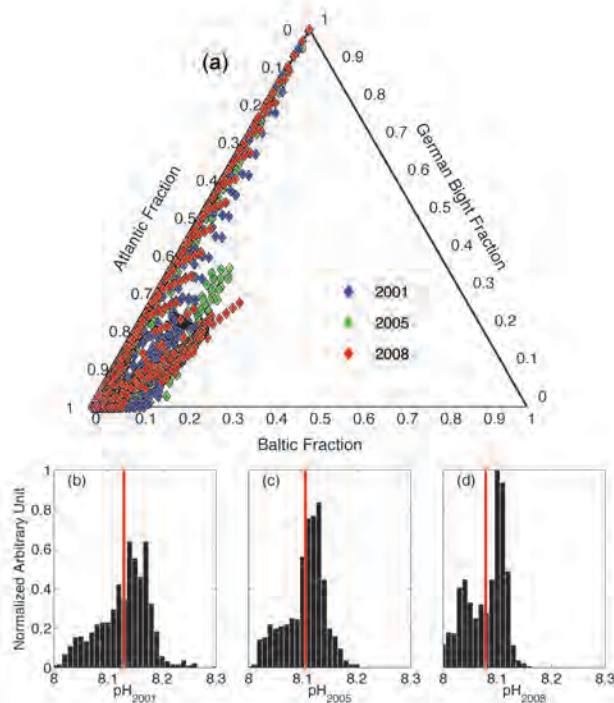

Figure 2. Water type contributions to the North Sea. (**a**) The fractions of North Atlantic water, Baltic water and German Bight water in the North Sea in 2001 (blue), 2005 (green) and 2008 (red). (**b**)-(**d**), histograms of the frequency of calculated pH values binned in 0.01 pH unit intervals with the mean value per year marked by the red line.

Examining the mixing relationship between the North Atlantic and Baltic water further reveals a change in the water mass end members from 2001 to 2005. A linear regression was applied, for each year, to data with a Baltic water mass fraction greater than the three-year average of 3% (Figure 3) revealing three statistically significant relationships. The years 2005 and 2008 show a remarkably similar mixing line with the most notable difference being a general decrease in the salinities observed in the Skagerrak in 2008 compared to 2005. Such a shift is reflective of different proportions of the two water masses but indicates that the water masses remain constant in their properties. The difference between these two years and 2001, however, is much greater. The slope of the regression line is shallower in 2001, indicative of a higher DIC Baltic end member and a lower DIC North Atlantic end member. The same relationship is reflected, between 2005 and 2008, in the A_T mixing diagram (Figure 3(b)).
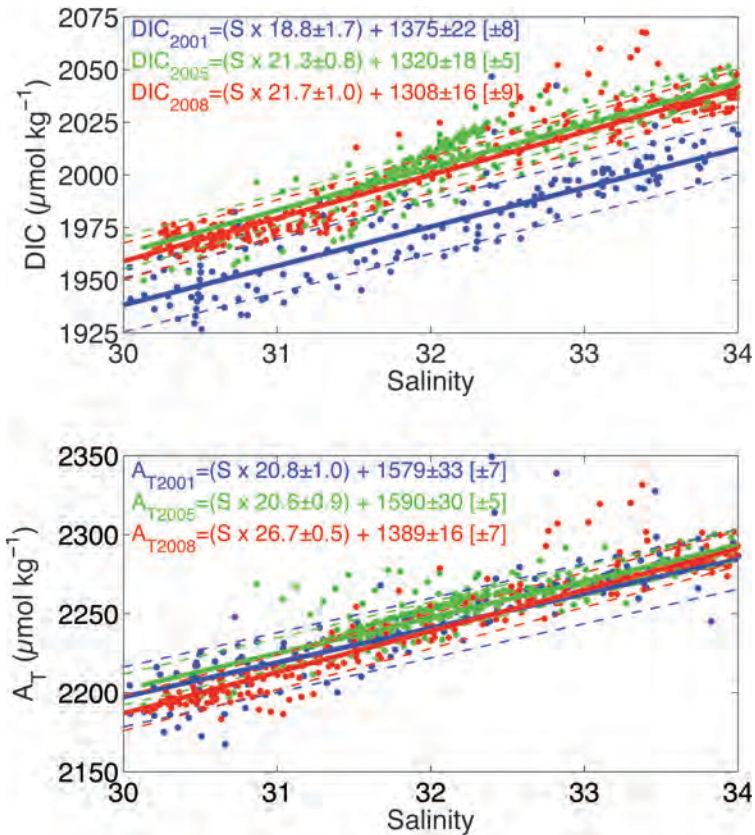

Figure 3. North Sea – Skagerrak mixing diagram. Linear fitted regressions for the mixing relationship between the Skagerrak and North Atlantic inflow in the northern North Sea. Upper graph shows DIC and lower graph shows A_T. Points were selected based on percentage of Baltic water mass fraction present (>3%). Dashed lines represent one standard deviation ($\pm 1\sigma$) of the residuals for each fit, also given in parentheses.

The inorganic carbon, after correction for metabolic DIC (calculations in section 2.3.2) and respective salinity inventories were used to quantify the changes (ΔS and ΔDIC) between the two time periods. The change in each ICES box for the two time periods showed a significant correlation coefficient of 0.903 and 0.839 (excluding Box 8) for the period 2001-2005 and 2005-2008, respectively. Box 8, heavily influenced by the German Bight, recorded very low salinities for 2008, coinciding with a larger Elbe discharge [*GKSS*, 2012, *http://coast.gkss.de/staff/kappenberg/elbe/abfluss/elbe.abfluss*]. This box is likely to be more representative of local effects thus skewing the general pattern for the rest of the North Sea (including box 8 gives a $R^2 = 0.49$). Although the increase in DIC was basin-wide from 2001 to 2005, it did not occur evenly across the basin or throughout the water column.

The greatest increases in average DIC concentration from 2001 to 2005 occurred in the central and northwestern North Sea. The latter region is significantly deeper than the southern North Sea, thus the ICES boxes were further divided into a surface (30m) and deep box. The surface boxes showed an increase of the same order of magnitude as the deep boxes, however, due to the greater DIC concentrations at depth this constitutes a lower percentage of total increase. From 2005 to 2008 the changes in DIC were much smaller and demonstrated no clear pattern. The North Sea DIC inventory was 8.11 Pg C (1 Pg = 10^{15} g) in 2001, 8.17 Pg C in 2005 and 8.18 Pg C in 2008. Hence, it increased by approximately 0.8% (+ 6 x 10^{-2} Pg C) from 2001 to 2005, while the inventory remained almost stable (+ 5 x 10^{-3} Pg C, <0.1%) between 2005 and 2008. The deep northern boxes demonstrated a greater inventory increase of 1.1% from 2001 to 2005, and a 0.0% change from 2005 to 2008. Of the entire observed change in these boxes, 97% occurred from 2001 to 2005.

The changes in the DIC concentrations in the surface also manifest in the change in temperature-normalized pCO_2 (pCO_2@16ºC) distribution (Figure 4). The increase in the average North Sea pCO_2@16ºC from 2001 to 2005 is 26 µatm, compared to 4 µatm from 2005 to 2008 (the increases for 2001 to 2005 and 2005 to 2008 for non-temperature normalized pCO_2 were 21 µatm and 25 µatm, respectively). Using an average basin-wide pCO_2@16ºC from all three years (346 µatm), these increases correspond to 7.5% and 1.0% increases, which are proportional to the calculated increase in the North Sea DIC inventory. This agreement implies that the surface expression of pCO_2@16ºC is, to a large extent, representative of the entire water column, which, due to the shallow depths of the majority of the North Sea is not surprising. Similar to the distribution of DIC increase, the majority of the increase in pCO_2@16ºC occurs in the northern North Sea, namely, where the main inflow site is for North Atlantic water. In the north (>56°N) the average surface increase from 2001
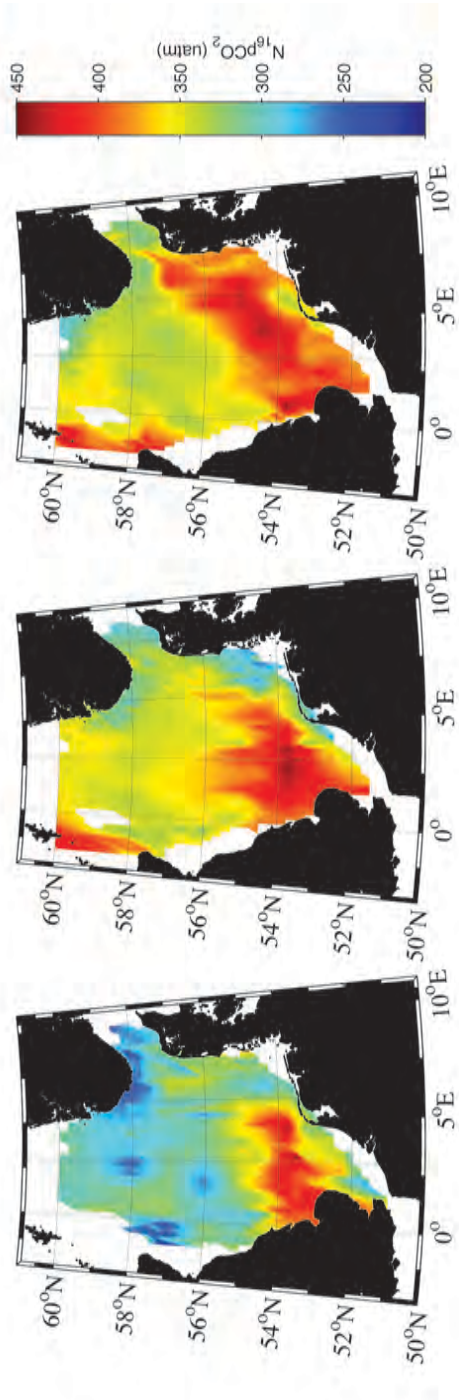
Figure 4. Distribution of temperature-normalized (16°C) pCO$_2$ in surface waters. (**a**) in 2001, (**b**) 2005, and (**c**) 2008.

to 2005 is 44 µatm, and from 2005 to 2008 the increase is 2 µatm. The southern North Sea shows much more stable increases, of 22 µatm and 18 µatm. At this time of year in the northern North Sea, pCO_2 without the effect of temperature is predominantly controlled by biology (Prowe et al., 2009). Using this parameter $pCO_2@16°C$ to investigate the differences in production between the three years would indicate a drop in primary productivity from 2001 to 2005 and 2008. However, the AOU in subsurface waters in the northern North Sea show comparable values between all three years (36.4 µmol kg^{-1} in 2001, 30.1 µmol kg^{-1} in 2005, and 31.3 µmol kg^{-1} in 2008), indicating that net community production (NCP) was similar.

5.   Discussion

Despite the similar fundamental patterns observed in 2001, 2005 and 2008, distinct differences occurred as a consequence of different DIC mixing patterns and proportions. In 2008, the year with the most positive NAO index (+2.1), the most pronounced front between the two mixing regimes occurs, where North Atlantic and German Bight waters were on the southern side and a mix of North Atlantic and Baltic Sea waters were on the northern side. This is caused by the fact that both the inflows of North Atlantic [*Winther and Johannessen,* 2006] and Baltic Sea [*Hordoir and Meier,* 2010] water into the North Sea are strongest under NAO+ conditions due to stronger westerly winds, strengthening the anti-clockwise circulation [*Lenhart et al.*, 2004; *Winther and Johannessen,* 2006]. There is subsequently an increased flow from east to west along the isoclines at 50 m, (the Dooley current [*Dooley*, 1974]), in addition to increased flow down the west coast of the UK. When these inflows weaken during neutral (2005) or NAO- (2001) phases, there is a less pronounced mixing pattern and the contrast between the two regimes is diminished with more mixing occurring in the eastern central North Sea. The front between the north and south is thus less distinct or vanished, as for example, visible in the greater presence of Baltic Sea water (Figure 2) or in the distribution of A_T (Figure 1), which is unaffected by the anthropogenic CO_2 perturbation, in contrast to the remaining CO_2 system parameters.

The biogeochemical divide along the 50 m contour, separating the northern and southern North Sea, is a well-documented feature in CO_2 distributions [*Thomas et al.*, 2004; *Bozec et al.*, 2005; *Prowe et al.*, 2009; *Omar et al.*, 2010], however here, the manifestation of this divide is shown to be strongly influenced by the NAO. The observed mixing behavior has

profound implications for the distribution of pH in the North Sea (Figure 1 (c-e)). The two aforementioned mixing regimes lead to a higher pH in the stratified northern region, where Baltic Sea and North Atlantic inflows mix, and a lower, more acidic pH, in the shallower southern region. When these inflows weaken during NAO- years, evidently more thorough mixing between these regions occurs and the pH histogram reveals a more transitional pattern.

In addition to NAO driven changes in mixing ratios and rates, the North Sea CO_2 system is further affected by the biogeochemical properties of its composing water masses. This applies especially to the DIC concentrations of the inflowing North Atlantic Ocean waters, which have demonstrated substantial variability during the recent decade [*Watson et al.,* 2009; *Thomas et al.,* 2008a; *Schuster and Watson,* 2007]. The northern North Sea CO_2 system shows a substantial increase in DIC and temperature-normalized pCO_2 and decrease in pH between 2001 and 2005 (Figures 1 and 3) in comparison to that observed from 2005 to 2008. The concomitant change in salinity with the change in DIC throughout the water column reveals that the increase is water mass driven. *Otto et al.* [1990] state that changes in salinity in the North Sea stem from either changes in the salinity of inflowing water or changes in runoff. A shift in the salinity-DIC mixing diagram confirms that the DIC concentrations in the North Atlantic end member have increased dramatically from 2001 to 2005, which we propose is a delayed response to NAO driven changes in the North Atlantic [*Thomas et al.,* 2008]. This accelerated the decrease in pH and increase in pCO_2 of the North Sea beyond that anticipated from the rise of atmospheric CO_2 concentrations alone [*Thomas et al.,* 2007]. The DIC and salinity changes between 2005 and 2008 also demonstrated a significant correlation, but were an order of magnitude smaller thus much less pronounced, yielding similar end-member DIC concentrations for 2005 and 2008, analogous to the variable behavior observed in surface pCO_2 in the North Atlantic Ocean [*Schuster et al.,* 2009].

The same pattern was less substantial in the A_T-salinity mixing line. As the increase in DIC observed in the North Atlantic, and subsequently the North Sea, is driven by air-sea pCO_2 exchange, there is no concomitant change in A_T with DIC. However, there is still some variation in the A_T-salinity mixing lines, which could be associated with the noted change in salinity [*Thomas et al.*, 2008a]. The NAO also exerts large influence over precipitation patterns over Europe so that NAO+ leads to drier conditions across Europe but wetter conditions over Scandinavia [*Hurrell and Loon*, 1997]. It follows that in 2008 we would expect more rainfall and runoff in the northern area of the Baltic drainage basin, which is

associated with granite rocks and has lower A_T values compared to the south [*Hjalmarsson et al.*, 2008]. This would lead to lower A_T in 2008 compared to 2001, which is consistent with our computed A_T end members (Figure 3(b)). These changes in precipitation patterns over Europe and thus riverine runoff into the North Sea may additionally alter salinity and DIC patterns in the southern North Sea, where the majority of riverine input enters the North Sea. However, the riverine contribution represents just 0.5% of the water budget and 0.7% of the carbon budget in the North Sea [*Thomas et al.*, 2005a], which is insufficient to cause the change recorded in DIC or pCO_2, although it may have contributed to the observed variability.

The northern North Sea is sufficiently deep to develop a summer thermocline, thus facilitating phytoplankton blooms during the productive period, which are maintained in the surface mixed layer. Using the maximum water column value of a representative northern station of the Brunt-Väisäilä frequency as an indicator of the mixed layer depth, we observe a
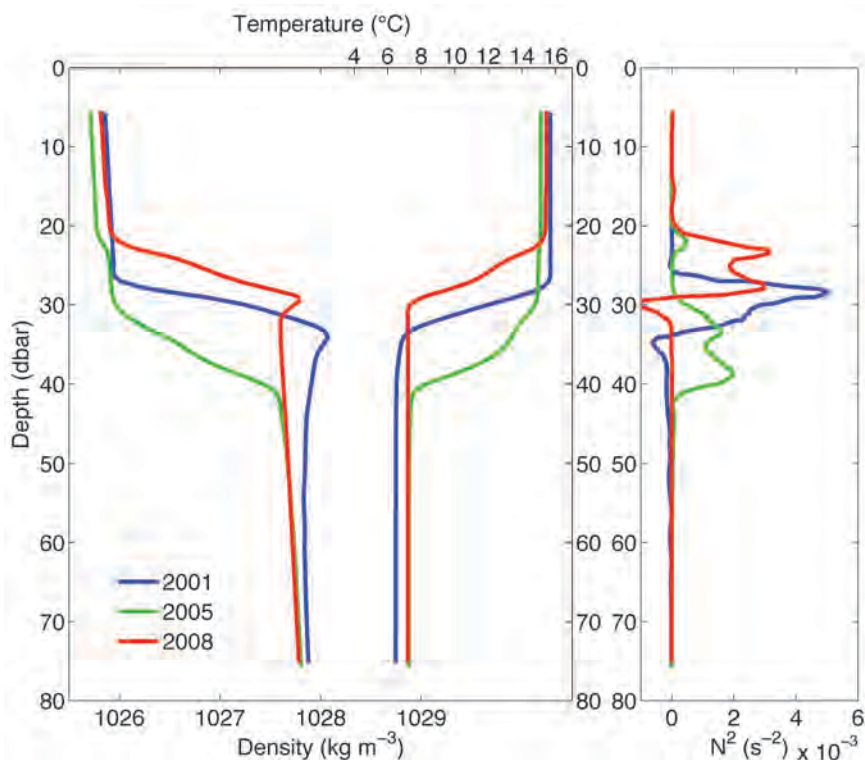

Figure 5. Stratification at 57ºN, 2.25ºE. (a) Vertical profiles of density and temperature for 2001 (blue), 2005 (green) and 2008 (red). (b) Brunt-Väisälä frequency squared profile for 2001 (blue), 2005 (green) and 2008 (red).

very stable, but shallower stratification with a surface mixed layer of approximately 30m in 2001 compared to 40m in 2005 (Figure 5). Since the residence time of the waters in the North Sea is of less than one year, there is no accumulation of metabolic DIC (previous years primary production has no effect on the current state of the North Sea). If the NCP were the same, as it was indicated in our datasets by AOU, a change in mixed-layer depth (MLD) would impact the observed pCO_2. While the biological pCO_2 drawdown was on the order of 300-330 µatm in 2001 [*Thomas et al.,* 2005b], a similar NCP would have caused a pCO_2 drawdown of 200-250 µatm in 2005, characterized by a mixed layer depth of 40m. This would lead to a difference of 50-130 µatm between the two years, which is in line with the observed increase of 51 µatm of temperature-normalized pCO_2 (Figure 4) in the northern North Sea. Taking the observed salinity change into account, such an increase would correspond to a pH decrease of 0.056.

Kühn et al., [2010] have modeled a greater CO_2 sink in the northern North Sea during years of NAO- (2001) compared to years of NAO+, which they attributed to weaker stratification facilitating greater upward transport of nutrients. The highest pH values and lowest pCO_2 values recorded are observed in the northern North Sea during years of NAO-, however we cannot ascribe this to weaker stratification. The weaker stratification in 2005, associated with cooler temperatures, demonstrates that the expression of pH and CO_2 can be exaggerated or masked by physical conditions within the North Sea. The variability of the mixed layer depth in the North Sea is controlled by a combination of temperature and NAO [*Lenhart et al.*, 2004] and we propose the latter affects it through two possible processes. Firstly, a stronger North Atlantic inflow weakens the thermocline in years of neutral and positive NAO, leading to less stable stratification as found in 2005 and 2008. Alternatively, weaker winds may allow the thermocline to rise during more negative NAO conditions. In 2008 a stronger warming of the surface waters resulted in a more stable water column with a shallower mixed layer. This situation enhanced the NCP effect on the surface layer pCO_2. Simultaneously the warmer waters experienced in 2008 raised the pCO_2, eventually leading to comparable pCO_2 conditions in 2005 and 2008, with 2008 showing the warmer and shallower surface layer.

In summary our results indicate that under conditions of NAO+, as in 2008, the North Sea shelf pump is more efficient than under NAO- due to increased rates of Atlantic and Baltic inflow into the North Sea and a strengthened anti-clockwise circulation. The strengthened biogeochemical divide between the northern and southern North Sea means that more carbon is exported from the northern North Sea out of the Norwegian Trench without coming into

contact with the atmosphere, which limits subsequent out gassing of remineralized CO_2 making the shelf pump more effective. When NAO+ occurs in conjunction with a year of higher SST, shoaling of the thermocline allows intense areas of primary production to develop. This causes lower pCO_2 and higher pH in surface waters of the northern North Sea, however, this is not shown to have any effect on total carbon uptake. In addition, any changes to the biogeochemical content or quantity of the source water masses contributing to the North Sea can intensify or diminish these expressions.

Acknowledgements

References

Anderson, L. A., and J. L. Sarmiento (1994). Redfield ratios of remineralization determined by nutrient data analysis. *Global Biogeochem. Cycles.* 8, 65-80.

Artioli, Y., J.C. Blackford, M. Butenschön, J.T. Holt, S.L. Wakelin, H. Thomas, A.V. Borges and J.I. Allen (2012). The carbonate system in the North Sea: Sensitivity and model validation. *J. Mar. Syst.* 102-104, 1-13.

Bates, N.R. (2001). Interannual variability of oceanic CO_2 and biogeochemical properties in the western North Atlantic subtropical Gyre. *Deep Sea Res. II* 48, 1507-1528.

Borges, A.V., and M. Frankignoulle (1999). Daily and seasonal variations of the partial pressure of CO_2 in surface seawater along Belgian and southern Dutch coastal areas. *J. Mar. Syst.* 19, 251-266.

Borges, A.V., and M. Frankignoulle (2002). Distribution and air-water exchange of carbon dioxide in the Scheldt plume off the Belgian coast. *Biogeochemistry* 59, 41-67.

Borges, A.V., and N. Gypens (2010). Carbonate chemistry in the coastal zone responds more strongly to eutrophication than to ocean acidification. *Limnol. Oceanogr.* 55, 346-353.

Bozec, Y., H. Thomas, K. Elkalay, and H.J.W. de Baar (2005). The continental shelf pump for CO_2 in the North Sea - evidence from summer observation. *Mar. Chem.* 93, 131-147.

Bozec, Y., H. Thomas, L.–S. Schiettecatte, A.V. Borges, K. Elkalay and H.J.W. de Baar (2006). Assessment of the processes controlling the seasonal variations of dissolved inorganic carbon in the North Sea. *Limnol. Oceanogr.* 51, 2746-2762.

Cai, W.–J., H. Xinping, W.–J. Huang, M.C. Murrell, J.C. Lehrter, S.E. Lohrenz, W.–C. Chou, W. Zhai, J.T. Hollibaugh, Y. Wang, P. Zhao, X. Guo, K. Gundersen, Dai, M., and G.–C. Gong (2011). Acidification of subsurface coastal waters enhanced by eutrophication. *Nature Geosci.* 4, 766-770.

Dickson, A.G., and F.J. Millero (1987). A comparison of the equilibrium constants for the dissociation of carbonic acid in seawater media. *Deep Sea Res.* 34, 1733-1743.

Dickson, A.G., C.L. Sabine, and J.R. Christian (2007). Guide to best practices for ocean CO_2 measurements. PICES Special Publication, 3, Sidney.

Dooley, H. D. (1974). Hypotheses concerning the circulation of the northern North Sea. *J. Cons. Cons. Int. Explor. Mer.* 36, 54-61.

Fofonoff, P., and R.C. Millard Jr. (1983). Algorithms for computation of fundamental properties of seawater. *Unesco Technical Papers in Marine Science* 44, 42-43.

Frankignoulle, M., and A.V. Borges (2001). European continental shelf as a significant sink for atmospheric carbon dioxide. *Global. Biogeochem. Cycles* 15, 569-576.

Gattuso, J.-P., M. Frankignoulle, and R. Wollast (1998). Carbon and carbonate metabolism in coastal aquatic ecosystems. *Annu. Rev. Ecol. Syst*. 29, 405–434.

Greatbatch, R.J. (2000). The North Atlantic Oscillation. *Stochastic Environ. Res. Risk Assess.* 14, 213–242.

Greatbatch, R.J. (2000). The North Atlantic Oscillation. *Stochastic Environ. Res. Risk Assess.* 14, 213–242.

Gypens, N., G. Lacroix, C. Lancelot, and A.V. Borges (2011). Seasonal and inter-annual variability of air-sea CO_2 fluxes and seawater carbonate chemistry in the Southern North Sea. *Prog. Oceanogr.* 88, 59–77.

Hjalmarsson, S., K. Wesslander, L.G. Anderson, A. Omstedt, M. Perttilä and L. Mintrop (2008). Distribution, long-term development and mass balance calculation of total alkalinity in the Baltic Sea. *Cont. Shelf Res.* 28, 593-601.

Hordoir, R., and H.E.M. Meier (2010). Freshwater fluxes in the Baltic Sea: A model study. *J. Geophys. Res.* 115, C08028.

Hurrell, J.W. (1995). Decadal trends in the North Atlantic Oscillation: Regional temperatures and precipitation. *Science* 269, 676–679.

Hurrel, J., and H. van Loon (1997). Decadal variations in climate associated with the North Atlantic Oscillation. *Clim. Change* 36, 301-336.

Hurrel, J.W. (2003). Climate: North Atlantic and Arctic Oscillation (NAO/AO), in *Encyclopedia of Atmospheric Sciences*, edited by J. Holton, J. Pyle, and J. Curry, pp. 439-445, Academic Press, New York.

ICES (1983). International Council For The Exploration Of The Sea, Flushing times of the North Sea, *ICES Cooperative Research Report* 123.

Ionita, M., N. Rimbu, and G. Lohmann (2011). Decadal variability of the Elbe River streamflow. *Int. J. Climatol.* 31, 22-30.

Kempe, S., and K. Pegler (1991). Sinks and sources of CO_2 in coastal seas: the North Sea. *Tellus* 43B, 224-235.

Körtzinger, A., H. Thomas, B. Schneider, N. Gronau, L. Mintrop and J.C. Duinker (1996). At-sea intercomparison of two newly designed underway pCO_2 systems - Encouraging results. *Mar. Chem.* 52, 133-145.

Kühn, W., J. Pätsch, H. Thomas, A.V. Borges, L.–S. Schiettecatte, Y. Bozec and A.E.F. Prowe (2010). Nitrogen and carbon cycling in the North Sea and exchange with the North Atlantic-A model study, Part II: Carbon budget and fluxes. *Cont. Shelf Res.* 30, 1701-1716.

Lenhart, H.J., J. Pätsch, W. Kühn, A. Moll, and T. Pohlmann (2004). Investigation on the trophic state of the North Sea for three years (1994-1996) simulated with the ecosystem model ERSEM – the role of a sharp NAOI decline. *Biogeosciences Discuss.* 1, 725-754.

Lorkowski, I., J. Pätsch, A. Moll, and W. Kühn (2012). Interannual variability of carbon fluxes in the North Sea from 1970 to 2006 – Competing effects of abiotic and biotic

drivers on the gas-exchange of CO_2. *Estuar. Coast. Shelf S.* 100, 38-57.

Levine, N.M., S.C. Doney, I. Lima, R. Wanninkhof, N.R. Bates and R.A. Feely (2011). The impact of the North Atlantic Oscillation on the uptake and accumulation of anthropogenic CO_2 by North Atlantic Ocean mode waters. *Global Biogeochem. Cycles* 25, GB3022.

McKinley, G.A., A.R. Fay, T. Takahashi, and N. Metzl (2011). Convergence of atmospheric and North Atlantic carbon dioxide trends on multidecadal timescales. *Nat. Geosci.* 4, 606-610.

Mehrbach, C., C.H. Culberson, J.E. Hawley, and R.M. Pytkowicz (1973). Measurement of the apparent dissociation constants of carbonic acid in seawater at atmospheric pressure. *Limnol. Oceanogr.* 18, 897-907.

Omar, A.M., A. Olsen, T. Johannessen, M. Hoppema, H. Thomas, and A.V. Borges (2010). Spatiotemporal variations of fCO_2 in the North Sea. *Ocean Sci.* 6, 77-89.

Otto, L., J.T.F. Zimmerman, G.K. Furnes, M. Mork, R. Saetre and G. Becker (1990). Review of the physical oceanography of the North Sea. *Neth. J. Sea Res.* 26, 161-238.

Pätsch, J., and W. Kühn (2008). Nitrogen and carbon cycling in the North Sea and exchange with the North Atlantic—a model study. Part I. Nitrogen budget and fluxes. *Cont. Shelf Res.* 28, 767–787.

Pérez, F.F., M. Vázquez-Rodríguez, H. Mercier, A. Velo, P. Lherminier, and A.F. Ríos (2010). Trends of anthropogenic CO_2 storage in North Atlantic water masses. *Biogeosciences* 7, 1789-1807.

Prowe, A.E.F., H. Thomas, J. Pätsch, W. Kühn, Y. Bozec, L.–S. Schiettecatte, A.V. Borges, and H.J.W. de Baar (2009). Mechanisms controlling the air–sea CO_2 flux in the North Sea. *Cont. Shelf Res.* 29, 1801-1808.

Santana-Casiano, J.M., M. González-Dávila, M.–J. Rueda, O. Llinás and E.–F. González-Dávila (2007). The interannual variability of oceanic CO_2 parameters in the northeast Atlantic subtropical gyre at the ESTOC site. *Global Biogeochem. Cycles* 21, GB1015.

Schiettecatte, L.-S., F. Gazeau, C. van der Zee, N. Brion, and A.V. Borges (2006). Time series of the partial pressure of carbon dioxide (2001-2004) and preliminary inorganic carbon budget in the Scheldt plume (Belgian coast waters). *Geochem. Geophys. Geosyst.* 7, Q06009.

Schiettecatte, L.-S., H. Thomas, Y. Bozec and A.V. Borges (2007). High temporal coverage of carbon dioxide measurements in the Southern Bight of the North Sea. *Mar. Chem.* 106, 161-173.

Schuster, U., and A.J. Watson (2007). A variable and decreasing sink for atmospheric CO_2 in the North Atlantic. *J. Geophys. Res.* 112, C11006.

Schuster, U., A.J. Watson, N.R. Bates, A. Corbiere, M. Gonzalez-Davila, N. Metzl, D. Pierrot, and M. Santana-Casiano (2009). Trends in North Atlantic sea-surface fCO_2

from 1990 to 2006. *Deep-Sea Res. II* 56, 620-629.

Shadwick, E., H. Thomas, Y. Gratton, D. Leong, S.A. Moore, T. Papakyriakou, and A.E.F. Prowe (2011). Export of Pacific carbon through the Arctic Archipelago to the North Atlantic. *Cont. Shelf Res.* 31, 806-816.

Takahashi, T., J. Olafsson, J.G. Goddard, D.W. Chipman, and S.C. Sutherland (1993). Seasonal-variation of CO_2 and nutrients in the high-latitude surface oceans – a comparative study. *Global Biogeochem. Cycles* 7, 843-878.

Thomas, H., and B. Schneider (1999). The seasonal cycle of carbon dioxide in Baltic Sea surface waters. *J. Mar. Syst.* 22, 53-67.

Thomas, H., Y. Bozec, K. Elkalay, and H.J.W. de Baar (2004). Enhanced open ocean storage of CO_2 from shelf sea pumping. *Science* 304, 1005-1008.

Thomas, H., Y. Bozec, H.J.W. de Baar, K. Elkalay, M. Frankignoulle, L.-S. Schiettecatte, G. Kattner, and A.V. Borges (2005). The carbon budget of the North Sea. *Biogeosciences* 2, 87-96.

Thomas, H., Y. Bozec, K. Elkalay, H.J.W. de Baar, A.V. Borges, and L.–S. Schiettecatte (2005). Controls of the surface water partial pressure of CO_2 in the North Sea. *Biogeosciences* 2, 323-334.

Thomas, H., A.E.F. Prowe, S. van Heuven, Y. Bozec, H.J.W. de Baar, L.–S. Schiettecatte, K. Suykens, M. Koné, A.V. Borges, I.D. Lima and S.C. Doney (2007). Rapid decline of the CO_2 buffering capacity in the North Sea and implications for the North Atlantic Ocean. *Global Biogeochem. Cycles* 21, GB4001.

Thomas, H., A.E.F. Prowe, I.D. Lima, S.C. Doney, R. Wanninkhof, R.J. Greatbatch, U. Schuster and A. Corbière (2008). Changes in the North Atlantic Oscillation influence CO_2 uptake in the North Atlantic over the past 2 decades. *Global Biogeochem. Cycles* 22, GB4027.

Thomas, H., D. Unger, J. Zhang, K.-K. Liu and E.H. Shadwick (2008). Biogeochemical cycling. In: Urban E., Sundby B., Malanotte-Rizzoli, P. and Melillo, J. (eds) Watersheds, *Bays and Bounded Seas* (SCOPE No. 70). Island Press, Washington, D. C., pp. 169-190.

Thomas, H., L.-S. Schiettecatte, K. Suykens, Y.J.M. Koné, E.H. Shadwick, A.E.F. Prowe, Y. Bozec, H.J.W. de Baar, and A.V. Borges (2009). Enhanced ocean carbon storage from anaerobic alkalinity generation in coastal sediments. *Biogeosciences* 6, 267-274.

Tsunogai, S., S. Watanabe, and T. Sato (1999). Is there a "continental shelf pump" for the absorption of atmospheric CO_2? *Tellus* 51B, 701–712.

Wakelin, S.L., J.T. Holt, J.C. Blackford, J.I. Allen, M. Butenschön and Y. Artioli (2012). Modelling the carbon fluxes of the northwest European continental shelf: Validation and budgets. *J. Geophys. Res.* 117, C05020.

Watson, A.J., U. Schuster, D.C.E. Bakker, N.R. Bates, A. Corbière, M. González-Dávila, T.

Friedrich, J. Hauck, C. Heinze, T. Johannessen, A. Körtzinger, N. Metzl, J. Olafsson, A. Olsen, A. Oschlies, X.A. Padin, B. Pfeil, J.M. Santana-Casiano, T. Steinhoff, M. Telszewski, A.F. Rios, D.W.R. Wallace and R. Wanninkhof (2009). Tracking the variable North Atlantic sink for atmospheric CO_2. *Science* 326 (5958), 1391–1393.

Winther, N.G. and J.A. Johannessen (2006). North Sea circulation: Atlantic inflow and its destination. *J. Geophys. Res.* 111, C12018.

Wollast, R. (1998). Evaluation and comparison of the global carbon cycle in the coastal zone and in the open ocean, p. 213-252. In K.H. Brink and A.R. Robinson (eds.), The Global Coastal Ocean. John Wiley & Sons.

Chapter 5

Direct observations of diel biological CO_2 fixation on the Scotian Shelf, northwestern Atlantic Ocean

Helmuth Thomas, William Burt, Susanne Craig, Blair J. W. Greenan, Gerhard J. Herndl, Simon Higginson, Lesley Salt, Elizabeth H. Shadwick, and Jorge Urrego-Blanco

Abstract

Much of the variability in the surface ocean's carbon cycle can be attributed to the availability of sunlight, triggering surface heat flux and photosynthesis, which in turn regulate the biogeochemical cycling of carbon over a wide range of time scales. The critical processes of this carbon cycle regulation, occurring at time scales of a day or less, however, have undergone few investigations, most of which have been limited to time spans of several days to months. Optical methods have helped to infer short-term biological variability, but complementing investigations of the oceanic CO_2 system are lacking. We employ high-frequency CO_2 and optical observations covering the full seasonal cycle on the Scotian Shelf, northwestern Atlantic Ocean, in order to unravel diel periodicity of the surface ocean carbon cycle and its effects on annual budgets. Significant diel periodicity in the surface CO_2 system occurs only if the water column is sufficiently stable as observed during seasonal warming. During that time biological CO_2 drawdown, or net community production (NCP), is delayed for several hours relative to the onset of photosynthetically available radiation (PAR), due to diel cycles in chlorophyll *a* concentration and to grazing. In summer NCP decreases by more than 90%, coinciding with the seasonal minimum of the mixed layer depth, and resulting in the disappearance of the diel CO_2 periodicity in the surface waters.

1 Introduction

Shelf and marginal seas play a crucial role in the global carbon cycle as they link terrestrial, marine and atmospheric compartments (Ciais et al., 2008; Thomas et al., 2008; Chen and Borges, 2009). As a consequence of their role as an integral link between the compartments, the spatial and temporal variability of the carbon cycle in marginal seas is generally higher than in open ocean environments (Thomas and Schneider, 1999; Schiettecatte et al., 2006; Chen and Borges, 2009; Omar et al., 2010). In addition to natural drivers, anthropogenic processes perturbing natural cycles in each of the carbon cycle compartments affect variability in shelf and marginal seas. Examples of such perturbations include eutrophication, ocean acidification and atmospheric nitrogen deposition (Doney et al., 2007; Thomas et al., 2009; Borges and Gypens, 2010; Cai et al., 2011).

Physical, biological and chemical processes govern the variability of the carbon cycle and the air-sea exchange of CO_2. Although these processes are evident at many temporal and spatial scales, they interact at high frequency local scales, eventually yielding diurnal, seasonal and longer-term periodicity. Our understanding of the monthly to seasonal variability in the carbon cycle in several shelf and marginal seas has improved, in particular with respect to attaining full annual observational coverage (Chen and Borges 2009; Thomas et al., 2004, Omar et al., 2010; Shadwick et al., 2010, 2011). At shorter time scales, optical methods have helped to infer short-term biological variability (Siegel et al., 1989; Stramska and Dickey, 1992; Cullen et al., 1992; Gernez et al., 2011; Dall'Olmo et al., 2011). However, corresponding investigations of the oceanic CO2 system are largely lacking. A few recent studies have focused on time scales of several days to months (Hood et al., 2001; Bates et al., 2001; Copin Montegut 2004; Lefevre et al., 2008; Boutin and Merlivat, 2009; Leinweber et al., 2009; Bozec et al., 2011; Lefevre and Merlivat, 2012). Investigations of processes at the rate of their occurrence in shelf and marginal seas are still sparse when it comes to full seasonal coverage (Vandemark et al., 2011).

The Scotian Shelf region is located at the eastern Canadian continental shelf at the boundary between the subpolar and subtropical gyres. This region is thus influenced by water masses of Arctic origin via the Labrador and Newfoundland Shelves, by low-salinity waters emanating from the Gulf of St. Lawrence, and by the Gulf Stream (Urrego-Blanco and Sheng, 2012). One of the dominant characteristics on the shelf is the large seasonal amplitude in sea surface temperature (SST) between subzero temperatures in winter to approximately 20ºC during summer (Shadwick and Thomas, 2011)(Fig. 1). Recent studies have identified this region as a strong source for atmospheric CO_2 at the annual scale, with an intense, but brief period of CO_2 uptake during the spring bloom, which occurs at the

annual SST minimum in late March to early April (Shadwick et al., 2011a)(Fig. 1). Controls of the seasonal to interannual variability of the surface CO_2 system in the Scotian Shelf region have been inferred from satellite observations, and include the intensity of autumn and winter storms, winter nutrient levels, and the onset of post-winter water column stratification (Greenan et al., 2004, 2008; Shadwick et al., 2010). The processes controlling the variability of the carbon cycle at time scales shorter than the monthly to seasonal scale remain poorly understood, which is the case for most regions of the open oceans, as well as for shelf and marginal seas. This study sheds light on the role of high frequency processes in controlling the carbon cycle in the surface waters of the Scotian Shelf region over a complete annual cycle. In particular, we investigate the occurrence of processes with diel periodicity, how their occurrence is controlled and how they contribute to seasonal and annual patterns of the surface water CO_2 system on the Scotian Shelf.

2 Material and methods

Investigations of the carbon cycle on the Scotian Shelf were initiated in 2006, and comprise shipboard observations of the carbon cycle and complementary parameters through the entire water column, as well as deployment of a CARIOCA buoy. Sporadically, these observations were paralleled by the deployment of the SeaHorse profiler, as detailed below. In-depth descriptions of the buoy location and the corresponding sampling activities have been given in Shadwick et al. (2011a). Here, we employ observations from the CARIOCA buoy, deployed since April 2007, that records surface water pCO_2, SST, salinity, and complementary parameters at an hourly rate and at a depth of approximately 2m. Details of the CARIOCA sensor have been reported, for example, by Bates et al. (2000, 2001), Bakker et al. (2001) and Hood and Merlivat (2001). In order to avoid data gaps due to maintenance, we reconstruct an annual cycle using different years of observations (Fig. 1). We focus on three key periods of the annual cycle: firstly, winter (pre-spring bloom to spring bloom transition); secondly, late spring to early summer, i.e., the warming period; and thirdly, the autumn to winter transition (Fig. 1). Diel cycles in pCO_2 with hourly resolution were established by removing the 48-point moving average from the (hourly) observations, which is similar to the approach pursued by Leinweber et al. (2009). We corrected the in-situ pCO_2 observations ($pCO_2,_{obs}$) for each day to the daily mean temperature ($pCO2,_{temp}$) of that day using the full suite of carbonate system equations via the CO2SYS program (Lewis and Wallace, 1998) with the constants by Dickson and Millero (1987). As discussed in Sect. 3, the difference between these values reveals the biologically driven change of pCO_2 ($pCO_2,_{bio}$):

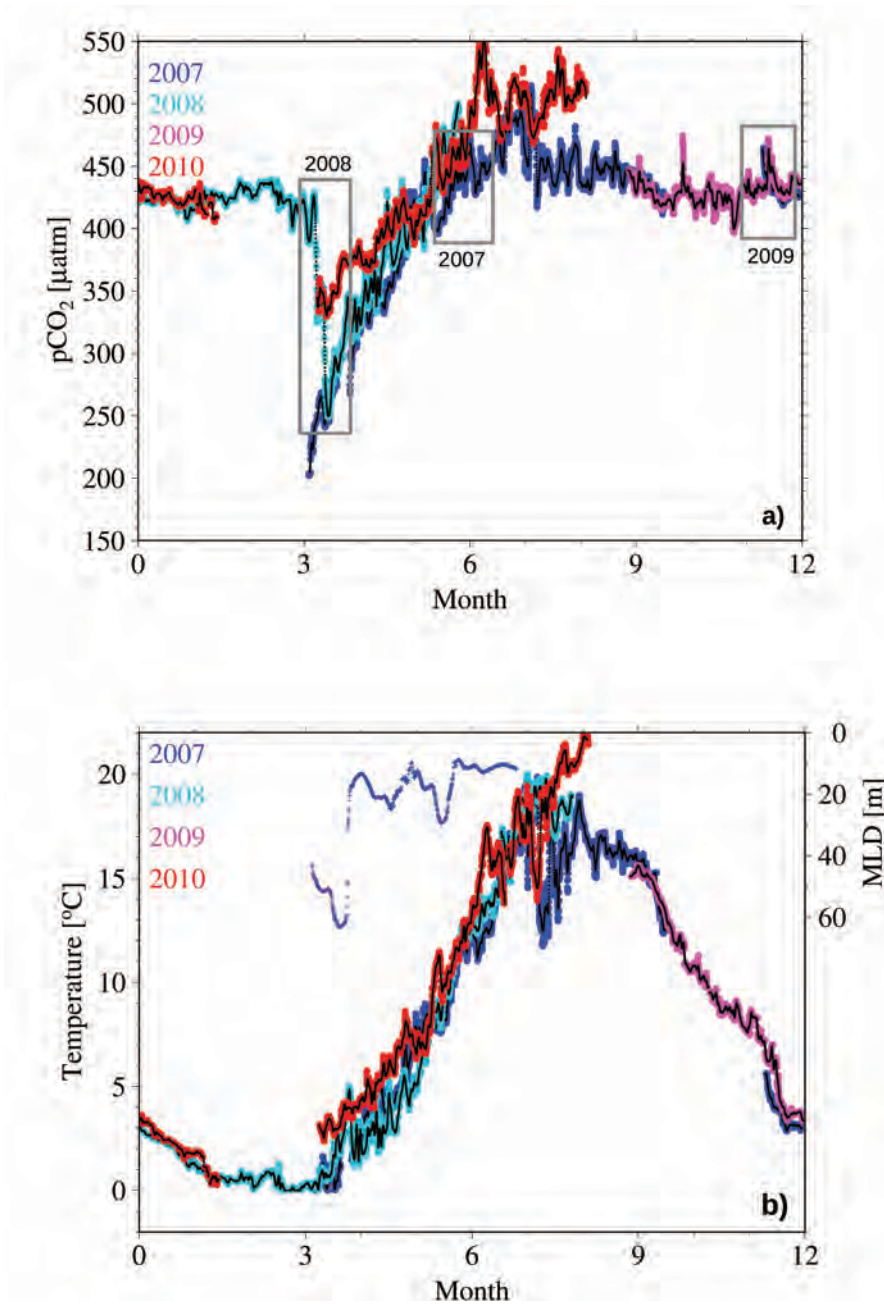$$pCO_2,_{obs} - pCO_2,_{temp} = pCO_2,_{bio}. \qquad (1)$$

Figure 1. Composite of available pCO_2 (a) and temperature data (b) for the years 2007-2010, recorded by the CARIOCA buoy. For the further study we evaluate data from June/July 2007, April 2008 and November/December 2009 as indicated by the gray boxes in a), assuming a climatological annual cycle. The black lines indicate the 24-point moving average. In (b), the depth of the maximum of the Brunt-Väisälä frequency is shown as measure of the mixed layer depth (MLD), computed from the Seahorse data, deployed between April 2007 and July 2007.

Mean diel cycles for the spring period (days 160-200 representing the period, when surface waters warm) were computed as the corresponding 40-day average of each hour of the day (Figs. 2a, b, 4d). Under consideration of the salinity records of the CARIOCA buoy and the salinity-alkalinity relationship reported by Shadwick et al. (2011a), we computed dissolved inorganic carbon (DIC) concentrations as a function of pCO_2 and alkalinity using CO2SYS (Lewis and Wallace, 1998) and the carbonate system constants by Dickson and Millero (1987). The integration of the biological component of the diel DIC cycles yielded the estimates of the biological rates.

In order to investigate the crucial period between spring and summer, when the waters are warming (Fig. 1), we combine the CARIOCA data with observations from the SeaHorse, an autonomous profiler (Greenan et al., 2004, 2008), which records water column profiles of temperature, salinity, photosynthetically active radiation (PAR), and downwelling irradiance ($E_d(\lambda)$) between 3-80m depth. Profiles were recorded with approximately 0.5 m vertical resolution approximately every 2 h between 4 April 2007 and 27 July 2007. The comparison of the diel temperature anomaly recorded at the sea surface by the CARIOCA buoy and the SeaHorse, respectively, shows good agreement of both instruments in timing and amplitude (Fig. 2a). The obtained diel cycle in surface temperature with an amplitude of 0.2 - 0.3ºC is the result of incoming solar radiation of approximately 500 W m^{-2} over 10 - 12h per day in a mixed layer depth (MLD) of 10-20m.

In an attempt to resolve the contribution of phytoplankton to NCP during the warming period, we derived chlorophyll a concentrations between 5 and 6m from profiles of SeaHorse $E_d(\lambda)$ using the model of Nahorniak et al. (2001). This depth range was chosen to be as close to the depth of the CARIOCA sensors (2m) as possible,
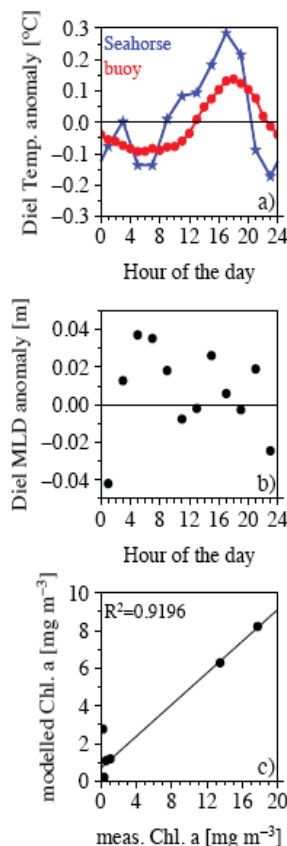

Figure 2. (a) Comparison of the diel temperature anomaly recorded by the CARIOCA buoy (red) and the SeaHorse profiler (blue), shown as average of the days 160-200. (b) Diel MLD anomaly, shown as average of the days 160-200, computed from the maximum of the Brunt-Väisälä frequency as measure of the MLD. (c) Correlation between the Chl α concentrations measured and modeled after Nahorniak et al. (2001).

whilst preventing the inclusion of noisy E_d data due to surface light wave focusing. The model required that the attenuation of E_d is calculated at three wavelengths (412, 443, 555 nm) over a depth interval (5 – 6m). Since the sensor wavelengths (379.3, 442.9, and 491 nm) did not exactly match the wavelengths required by the model, $E_d(\lambda)$ was first interpolated to model wavelengths. Modelled chlorophyll α (Chl$_{mod}$; mg m^{-3}) at an average depth of 5.5m (i.e. halfway between 5 and 6m) was then calculated using Nahorniak et al.'s (2001) formulations that include spectral coefficients to describe the absorption properties of water, phytoplankton and coloured dissolved organic matter and assume a value of 0.8 for the average cosine of downwelling light, μ_d (dimensionless). Chl$_{mod}$ values were compared with discrete, fluorometrically determined chlorophyll α values obtained at the same time and depth from ship-based water samples (Fig. 2c), and R^2, root mean square error (RMSE; mg m^{-3}) and bias (mg m^{-3}) values of 0.92, 4.31 mg m^{-3}, and -1.76 mg m^{-3} ($N = 8$), respectively, were obtained. These values were then grouped into periods 1-3 as described above, and averaged into time bins to give climatological values for Chl$_{mod}$ every two hours during the hours of daylight when reliable $E_d(\lambda)$ measurements could be made, which, at this time of year and latitude corresponded to times between ~06:00-16:00 local time.

3   Results and discussion

The spectral analysis of the buoy data (Fig. 3a, b) revealed a 24-h periodicity for the parameters pCO$_2$ and SST that occurs only when the waters are warming, i.e. between April and late August. Both pCO$_2$ and SST also showed significant coherent patterns during this time of the year (Fig. 3b, bottom panel, Fig. 3c) and are the focus of this paper. Outside of this period, periodicity and significant coherence were only observed, if detected, at longer time scales (several days), which mirrors the typical frequency of winter storms in the region (Fig. 3c). Other parameters, such as salinity, do not show significant 24-h periodicity, which means that tidal, lateral and other effects are either not identifiable, or act on timescales longer than 24 h. Such processes would be captured by the 48-point moving average, and do not influence the diel cycles. We also verified the potential role of daily cycles in MLD, which could lead to an intrusion of CO$_2$-rich water into the surface layer, if the MLD deepens. Boutin and Merlivat (2009) suggested that this process is an important driver of the diel pCO$_2$ anomaly. Leinweber et al. (2009), however, suggest that the deepening of the MLD is of minor importance due to the absence of a strong vertical gradient in DIC at their study site. The computation of the diel MLD anomaly for our location did not reveal a significant diel pattern, with variability, on the order of a few tens of centimeters (Fig. 2b), given a MLD of 10-20m. We therefore consider the influence of
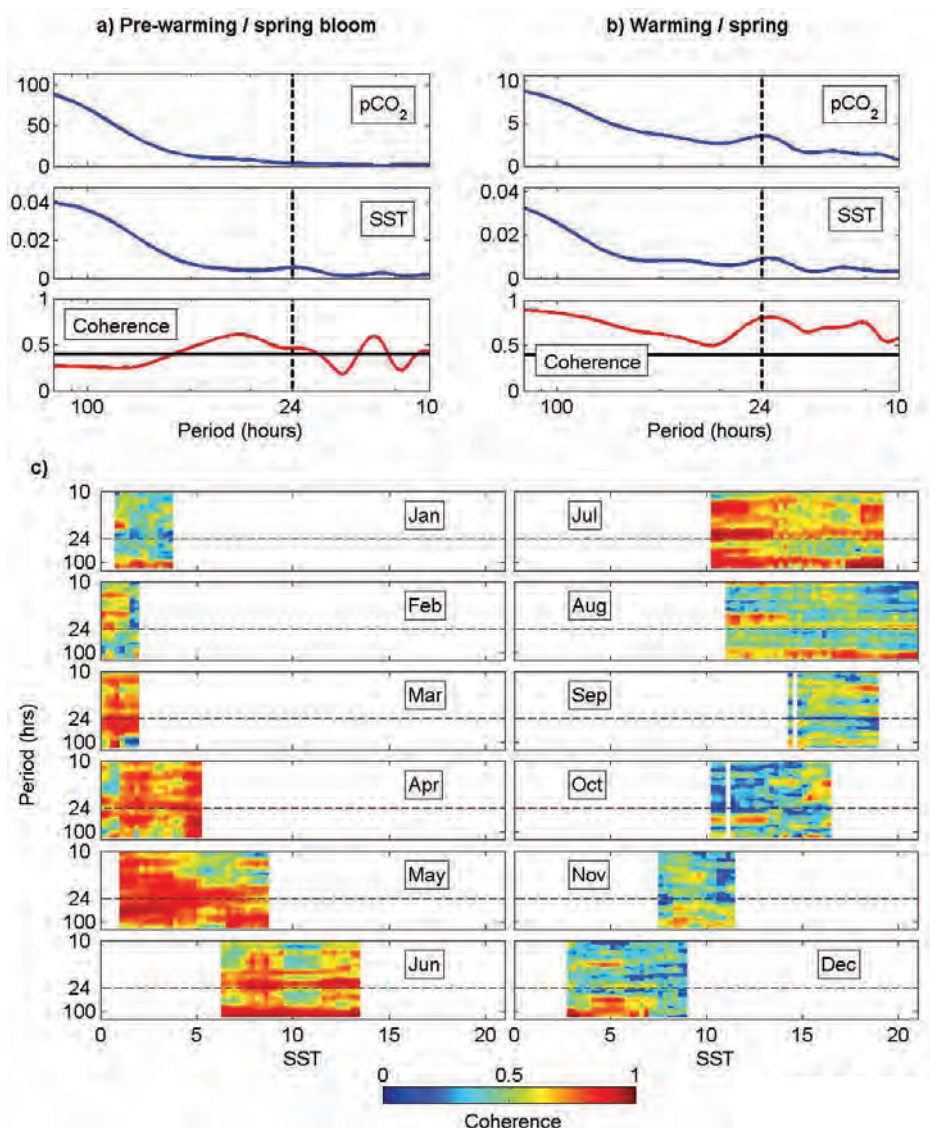
Figure 3. Spectral analysis of pCO_2 and SST data from the CARIOCA buoy. Power spectra of pCO_2 and SST and their coherence are shown for two periods: a) the pre-warming/spring bloom period and b) the warming period (see Figure 1a gray boxes). The dashed line on each plot indicates the 24 h period, and the horizontal solid line on the coherence plots shows the 5% significance level based on the degrees of freedom of the cross-spectral estimators. The coherence between pCO_2 and SST is plotted as a function of SST in monthly composites (c), illustrating the temporal evolution of the coherence. The color scale indicates the level of coherence between pCO_2 and SST, and the dashed line shows the 24 h period. High coherence at the 24 h period occurs only during the period when the water is warming.

temperature-driven diel variability in MLD as negligible in our case. The CO_2 air-sea fluxes play a very minor role in the surface layer DIC concentrations at the 24h timescale, such that the feedback between pCO_2 and CO_2 air-sea fluxes is negligible in our study.

Surface heat fluxes cause variability in SST at diel and seasonal time scales (Umoh and Thompson, 1994), which in turn drive some of the observed variability of the pCO_2, primarily because of the temperature dependence of the Henry constant. We corrected the observed pCO_2 data ($pCO_{2,\,obs}$) to a daily mean temperature to give $pCO_{2,\,temp.}$, The difference between $pCO_{2,\,obs}$ and $pCO_{2,\,temp}$ yielded pCO_2 data that were governed by processes other than temperature within a 24 h period. Since we did not detect processes other than SST variability acting on the 24 h period, the remaining pCO_2 variability was ascribed to biological activity ($pCO_{2,\,bio}$, Eq. 1). The daily and diel variability of the $pCO_{2,\,obs}$ and $pCO_{2,\,bio}$ for three periods of the year is shown in Fig. 4. In the winter period (days 80-95, Fig. 4a), the amplitude of the diel oscillation was small and the pCO_2 relatively constant. With the onset of the spring bloom, at approximately day 95 (see also Shadwick et al., 2011a, their Figs. 4 and 16), the diel amplitude drastically increased (Fig. 4a). Throughout both of these periods, $pCO_{2,\,obs}$ and $pCO_{2,\,bio}$ were in phase and tracked each other closely indicating that temperature was not the main driver for the short-term variability during this time of the year. Similarly, in the autumn to winter (Fig. 4b) transition, $pCO_{2,\,obs}$ and $pCO_{2,\,bio}$ again revealed in-phase patterns, though with a higher amplitude in autumn (days 305-345) than in winter (days 80-95), which can be ascribed to deepening of the mixed layer and an intrusion of high pCO_2 subsurface waters into the surface mixed layer (Shadwick et al., 2011a). Between the days 160-200 (end of June until end of July), i.e. later in the season of surface water warming, the amplitude of the diel oscillation was reduced compared to that observed during the spring bloom (Fig. 4a-c). More importantly, a phase shift was detectable between $pCO_{2,\,obs}$ and $pCO_{2,\,bio}$, with the latter occurring approximately 3h earlier than the $pCO_{2,\,obs}$ (Fig. 4c, d). We postulate that the cause for this phase shift might be diel cycles in biological activity. Such diel cycles were only visible, when the water column was sufficiently stable, such as during thermal stratification (Fig. 1b; Shadwick et al., 2011a, their Fig. 9). Outside the warming period, several processes have the potential to obscure or prevent diel signals or their detection: For example, during the autumn and winter periods, thermal stratification breaks down due to cooling air temperatures and increased wind-driven mixing resulting in a deepening of the mixed layer and greatly decreased photosynthetic activity, meaning that the diel cycles easily detectable during the warming period are difficult to detect or are completely absent in autumn and winter.

We can consider the diel cycle of pCO_2 as a composite of a temperature-driven component, which follows the diel cycle of SST (Fig. 4d), and a biologically driven component,
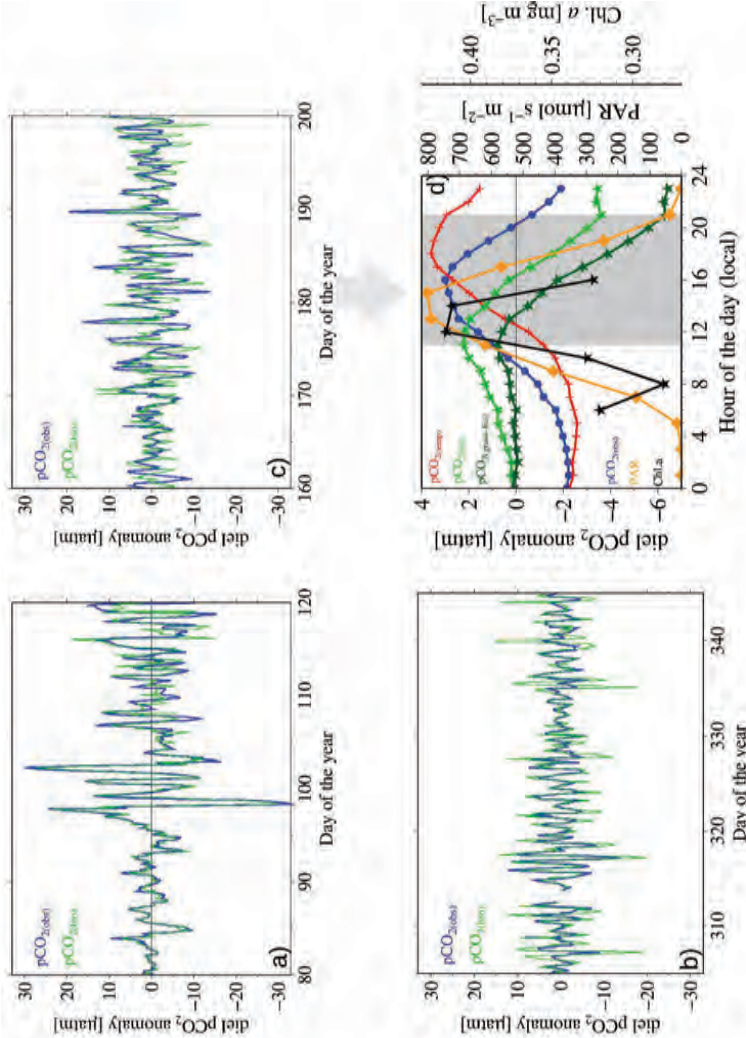
Figure 4. Diel anomalies and daily cycles of observed pCO_2, biologically controlled pCO_2, PAR, and Chl. *a*. Shows diel anomalies of $pCO_{2,\,obs}$ (blue) and $pCO_{2,\,bio}$ (green) for three periods of the year (a-c) as depicted in Fig. 1. Note the phase shift in the warming period (a, b) both parameters show the same timing (i.e., they are independent). Average diel anomalies or daily cycles compiled for the 40-day period from days 160-200 (see Fig. 1) observed pCO_2 ($pCO_{2,\,obs}$, blue), biologically controlled pCO_2 ($pCO_{2,\,bio}$, green), temperature-only controlled pCO_2 ($pCO_{2,\,temp}$, red), $pCO_{2,\,bio}$ corrected for respiratory activity ($pCO_{2,\,gross-bio}$, dark green) and photosynthetic active radiation (PAR, orange). Chlorophyll a (Chl. *a*, black) is shown for the hours (6.00h-16.00h), when reliable $E_d(\lambda)$ measurements can be made by the Seahorse. The gray-shaded box indicates the period when net carbon fixation occurs. The respiration rate has been computed from the slope of the $pCO_{2,\,bio}$ during night time conditions and production rates have been computed from the slopes of $pCO_{2,\,bio}$ and $pCO_{2,\,gross-bio}$ during daytime (gray-shaded area).

117

controlled by the balance of production and respiration of organic matter. The diel biological cycle obtained here can be considered a net biological signal, which shows an increase of the $pCO_{2, bio}$, i.e. net respiration, beginning in the evening (approx. 21:00h) and ending in the morning hours (10:00h-11:00h), when net community production (NCP) begins to exceed community respiration. NCP, indicated by a negative gradient in the pCO_2 anomaly (Fig. 4d), dominates the system until dusk. Subtracting the respiration signal, computed from the slope of the $pCO_{2(bio)}$ during nighttime conditions, allows us to estimate the diurnal cycle of gross primary production (GPP). The corresponding respiration rate, assumed to be constant throughout the day, is estimated to be 0.05 µmol C $(L\ h)^{-1}$; the rates of NCP and GPP are 0.26 µmol C $(L\ h)^{-1}$ and 0.31 µmol C $(L\ h)^{-1}$, respectively, both lasting approximately 10 h per day. This compares well with the GPP estimates given by Forget et al. (2007, their Table 2), which, when combined with an assumed 30m in MLD, yield GPP rates of 13 µmol C $(1\ d)^{-1}$. It must be noted, however, that their station is somewhat further offshore at the shelf break than the mooring location of the CARIOCA buoy and the SeaHorse. Somewhat more difficult to compare are the daily production rates reported by Boutin and Merlivat (2009), which range between 1.8 µmol C $(1\ d)^{-1}$ and 4.8 µmol C $(1\ d)^{-1}$. While their method of estimating NCP is similar to our approach, the data were obtained in the Southern Ocean at comparable latitude, but from a drifting instrument.

The onset of the net photosynthetic CO_2 drawdown occurred approximately 4-5 h after sunrise, near the period maximum of PAR (Fig. 4d) - a phenomenon that has been frequently documented but surprisingly has rarely been discussed or addressed in detail. Stramska and Dickey (1992), Siegel et al. (1989) and Gernez et al. (2011) report a phase shift of several hours between the onset of PAR and maximum values of either the beam attenuation coefficient (c_p) or dissolved oxygen (O_2) concentrations. The latter two are mirroring the build up of photosynthetic organic matter and reveal phasing throughout the diurnal cycle, which is comparable to the phasing of $pCO_{2, bio}$. Bozec et al. (2011, their Fig. 5) also show a similar phase shift between dissolved O_2 and pCO_2, relative to PAR. They conclude, however, that pCO_2 and PAR are out of phase by 180 degrees and O_2 is in phase with PAR. Leinweber et al. (2009) report similar but shorter time lags between their pCO_2 parameters, which tend to reveal stronger diel amplitudes than we observed. Overall, it appears that the temperature control of their system is more pronounced than on the Scotian Shelf, as evident from the higher diel temperature amplitude of 4°C in the Santa Monica Bay (Leinweber et al., 2009), compared to 0.2°C on the Scotian Shelf (Fig. 2a). Lefevre and Merlivat (2012) report for the tropical eastern Atlantic a time lag between PAR and SST; however, the relationship with chemical parameters (DIC, oxygen) appears complex and variable, likely because of physical processes. In summary, it appears that there is sufficient evidence in the literature to suggest that the signal of net biological carbon fixation in the water column, as

revealed by pCO_2, O_2 or beam attenuation measurements, is detectable at or around peak PAR, which is the ultimate energy source for the biological carbon fixation.

In order to determine whether this reported periodicity in metrics of phytoplankton photosynthetic activity occurred at our study site, we binned averaged Chl_{mod} over the 40-day warming period (days 160-200). This revealed a diel cycle with a difference of approximately 30% (0.13 mg Chl α m^{-3}) between minimum and maximum values, with the lowest values corresponding to low PAR levels during early morning and late afternoon, and maximum values to peak PAR at around noon (Fig. 4d). Please note that the daily Chl_{mod} excursion is small compared to the RMSE of 4.31 mg m^{-3} (Fig. 2c), indicating that quantitative interpretation of Chl_{mod} results should be made with caution. However, even if not a truly quantitative estimate of Chl α, the diel, i.e. relative Chl_{mod} pattern, observed at our study site is significant and, furthermore, is very similar to those observed in other studies of optical signals that have been interpreted as the combined effects of processes including daily primary production, phytoplankton sinking, and zooplankton grazing (Gardner et al., 1993; Marra, 1997; Stramska and Dickey, 1992; Gernez et al., 2011). When compared with the pCO_2 diel cycles, it was observed that the onset of net CO_2 drawdown, indicated by the change in slope of $pCO_{2, bio}$ from positive to negative, coincided with the time of the maximum Chl_{mod} values (Fig. 4d). In other words, our data suggest that a threshold Chl α concentration must first be attained during the growth phase before the system achieves net CO_2 drawdown. Others have also reported diel signals in either Chl *a* or photosynthetic parameters (Cullen et al., 1992; Bruyant et al., 2005), with peak values around noon. It should also be noted that photoinhibition may depress photosynthetic rate at high irradiances , especially around noon, potentially further modulating the exact occurrence of net CO_2 drawdown with respect to PAR levels.

Another process that may have contributed to the patterns in Chl_{mod} is phytoplankton diel vertical migration, whereby cells migrate to well lit surface waters during daylight hours and to deeper, nutrient rich waters at night. At this time of year (June-July), the phytoplankton community was dominated by flagellates (Harrison et al., 2008), which are well known to exhibit diel vertical migration patterns (Eppley et al., 1968; MacIntyre et al., 1997; Hall and Paerl, 2011), making it likely that this process contributed, at least in part, to both the accumulation of biomass during daylight hours and to the lag time between PAR and NCP, when the flagellates first have to move upward to reach the well lit surface during the early morning hours.

Both our results and those reported in the literature are consistent with the notion of a phase shift between the onset of PAR at dawn and of net carbon fixation at

approximately solar noon. Meso- and microzooplankton, which are active during nighttime, might still exert grazing pressure on phytoplankton during the early morning hours and thereby keep the abundance of phytoplankton low during the initial hours of daylight (Siegel et al. 1989). In addition to grazing effects, the diurnal variability in phytoplankton photosynthetic activity itself also contributes to delaying net carbon fixation until PAR has reached approximately maximum values as discussed above. Furthermore, in order to detect net carbon fixation as a change in the pCO_2 (or O_2 concentrations) in the water column, primary producers have to compensate for the respiratory activity of the heterotrophs, which in turn might exhibit relatively constant activity rates throughout the diel cycle (Cullen et al., 1992; Gernez et al., 2011). Based on our analysis, we suggest that grazing and the dependence of the photosynthetic rate on PAR lead to a net-autotrophic system just before, or at, maximum PAR values (Fig. 4d). As mentioned earlier, in our study we were not able to identify any diurnal variability in the water column structure, i.e. in strength and depth of stratification, which might have provoked the phase shift between PAR and $pCO_{2,\,bio}$.

We have revealed the seasonal dynamics of NCP by integrating the hourly $pCO_{2,\,bio}$ values (Fig. 5), yielding the biologically driven DIC concentration change, or under consideration of the MLD, the NCP inventory. The maximum value of NCP is 3.4 mol C m^{-2} or 271 µmol C L^{-1}, which is with respect to temporal evolution and magnitude of NCP similar to the results reported by Shadwick et al. (2011a), thus underpinning the importance of biological processes in the surface layer DIC variability. The integration of hourly values provides further evidence for the ongoing biological CO_2 fixation after the spring bloom as a significant contributor to annual CO_2 fixation (Shadwick et al., 2011a, b). Of particular interest is the observation that the carbon fixation rate, i.e. the DIC uptake rate by phytoplankton, is fairly constant from the onset of the spring bloom (approx. day 100) to approximately day 180, with DIC uptake rates of approximately 2.5 µmol C (L d)$^{-1}$, corresponding to a NCP rate of 0.26 µmol C (L h)$^{-1}$, assuming a 10-hour photoperiod per day (Fig. 4d). Again, this compares well with the GPP rates of 1-3 µmol C (L d)$^{-1}$ as reported
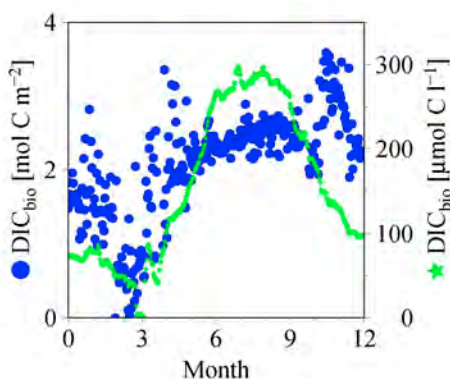

Figure 5. Annual cycle of biological DIC uptake. We show the annual cycle of biological DIC uptake, integrated from hourly values, i.e. accumulated diel changes. The mixed layer inventory of biological DIC uptake was obtained by dividing the biological DIC concentration change by the MLD as reported by Shadwick et al. (2011a). The production rates were computed from the slopes of the DIC uptake.

by Forget et al. (2007) for this period. Charette et al. (2001) reported ^{14}C-based GPP rates, determined for the area in September 1997, of 0.9-13 μmol C $(L\ d)^{-1}$, assuming a 30m MLD. These GPP rates were given without estimates of water column respiration, hindering a direct comparison to our data. The production rate decreases to about 0.1 μmol C $(L\ d)^{-1}$ (Fig. 5), when the mixed layer depth reaches its minimum. Thereafter, a combination of dramatically reduced availability of nutrients and photoinhibition of photosynthesis reduces NCP substantially in autumn.

4   Conclusions

In summary, we observed a statistically significant diurnal periodicity of the CO_2 system in surface waters only during the period when the water is warming. The corresponding increase in water column stability during warming facilitates the appearance of the diurnal cycle. The unravelled diurnal cycles of the surface pCO_2 reveal that net photosynthetic carbon fixation, i.e. NCP, begins approximately 4-5 h after onset of PAR. Grazing and transitional metabolic rates are likely the responsible processes for this phase shift, eventually allowing the ecosystem to be autotrophic for approximately 10 h out of 16 h of daylight during spring and early summer.

References

Bates, N.R., Samuels, L. and Merlivat, L. (2001).Biogeochemical and physical factors influencing seawater fCO2 and air-sea CO2 exchange on the Bermuda coral reef. Limnol. Oceanogr., 46(4), 833–846.

Bozec, Y., Merlivat, L., Baudoux, A.-C., Beaumont, L. Blain, S., Bucciarelli, E., Danguy, t. Grossteffan, E., Guillot, A., Guillou, J., Répécaud, M., Tréguer, P. (2011). Diurnal to inter-annual dynamics of pCO2 recorded by a CARIOCA sensor in a temperate coastal ecosystem (2003–2009). Mar. Chem. 126, 13-26.

Borges A. V. & N. Gypens (2010). Carbonate chemistry in the coastal zone responds more strongly to eutrophication than to ocean acidification, Limnology and Oceanography, 55, 346-353.

Bruyant, F. and others 2005. Diel variations in the photosynthetic parameters of Prochlorococcus strain PCC 9511: Combined effects of light and cell cycle. Limnology and Oceanography **50:** 850-863.

Cai, W.-J., Hu, X. , Huang, W.-J., Murrell, M. C., Lehrter, J. C., Lohrenz, S. E., Chou, W.-C., Zhai, W., Hollibaugh, J. T., Wang, Y., Zhao, P., Guo, X., Gundersen, K., Dai, M., and Gong, G.-C. (2011). Acidification of subsurface coastal waters enhanced by eutrophication, Nature Geoscience, 4, 766-770.

Chen C.T.A. & A.V. Borges (2009) Reconciling opposing views on carbon cycling in the coastal ocean: continental shelves as sinks and near-shore ecosystems as sources of atmospheric CO2, Deep-Sea Research II, 56 (8-10), 578-590.

Ciais P., A.V. Borges, G. Abril, M. Meybeck, G. Folberth, D. Hauglustaine & I.A. Janssens (2008) The impact of lateral carbon fluxes on the European carbon balance, Biogeosciences, 5, 1259-1271.

Copin-Montegut, C., Begovic, M. and Merlivat, L. (2004). Variability of the partial pressure of CO2 on diel to annual time scales in the Northwestern Mediterranean Sea. Mar. Chem. 85 169 – 189.

Cullen, J. J., Lewis, M., Davis, C. O. and Barber, R. (1992). Photosynthetic characteristics and estimated growth rates indicate grazing is the proximate control of primary production in the Equatorial Pacific. J. Geophys. Res. 97: 639–655, doi:10.1029/91JC01320.

Dall'Olmo, G., Boss, E., Behrenfeld, M. J., Westberry, T. K., Courties, C. Prieur, L., Pujo-Pay, M., Hardman-Mountford, N., and Moutin, T. (2011). Inferring phytoplankton carbon and eco-physiological rates from diel cycles of spectral particulate beam-attenuation coefficient, Biogeosciences, 8, 3423-3440.

Doney, S. C., Mahowald, N., Lima, I, Feely, R. A., Mackenzie, F. T., Lamarque, J.-

F., and Rasch, P. J.: Impact of anthropogenic atmospheric nitrogen and sulphur deposition on ocean acidification and the inorganic carbon system, P. Natl. Acad. Sci., 104, 14580–14585, 2007.

Gernez, P., Antoine, D. and Huot, Y. (2011). Diel cycles of the particulate beam attenuation coefficient under varying trophic conditions in the northwestern Mediterranean Sea: Observations and modeling, Limnol. Oceanogr., 56(1), 17–36.

Greenan, B.J.W., Petrie, B.D. Harrison, W.G. and Oakey, N.S. (2004). Are the Spring and Fall Blooms on the Scotian Shelf Related to Short-Term Physical Events? Cont. Shelf Res., 24, 603-625, doi:10.1016/j.csr.2003.11.006.

Greenan, B. J. W., Petrie, B. D., Harrison, W. G., and Strain, P. M. (2008). The Onset and Evolution of a Spring Bloom on the Scotian Shelf, Limnol. Oceanogr., 53, 1759.

Hood. E.M., Wanninkhof, R. and Merlivat. L. (2001). Short timescale variations of fCO2 in a North Atlantic warm-core eddy: Results from the Gas-Ex 98 carbon interface ocean atmosphere (CARlOCA) buoy data. J. Geophys Res., 106, 2561-2575.

Lefevre, N., A. Guillot, L. Beaumont, and T. Danguy (2008), Variability of fCO2 in the Eastern Tropical Atlantic from a moored buoy, J. Geophys. Res., 113, C01015, doi:10.1029/2007JC004146.

Nahorniak, J. S., M. R. Abbott, R. M. Letelier, and W. S. C. Pegau. 2001. Analysis of a method to estimate chlorophyll-a concentration from irradiance measurements at varying depths. J. Atmos. Ocean. Technol. **18:** 2063-2073.

Omar, A. M., A. Olsen, T. Johannessen, M. Hoppema, H. Thomas, and A.V. Borges (2010). Spatiotemporal variations of *f*CO2 in the North Sea, *Ocean Science*, 6, 77-89.

Schiettecatte L.-S., F. Gazeau, C. Van der Zee, N. Brion & A.V. Borges (2006). Time series of the partial pressure of carbon dioxide (2001-2004) and preliminary inorganic carbon budget in the Scheldt plume (Belgian coast waters), Geochemistry, Geophysics, Geosystems (G3), VOL. 7, Q06009, doi:10.1029/2005GC001161.

Shadwick, E.H., Thomas, H., Comeau, A., Craig, S.E., Hunt, C.W. and Salisbury, J.E. (2010). Air-Sea CO2 fluxes on the Scotian Shelf: seasonal to multi-annual variability, Biogeosciences, 7, 3851-3867, 2010, doi:10.5194/bg-7-3851-2010.

Shadwick, E.H., Thomas, H., Azetsu-Scott, K., Greenan, B.J.W., Head, E and Horne, E. (2011a). Seasonal variability of dissolved inorganic carbon and surface water pCO_2 in the Scotian Shelf region of the Northwestern Atlantic, *Marine Chemistry,* 124, 23–37, doi:10.1016/j.marchem.2010.11.004.

Shadwick, E.H., and Thomas, H. - 2011 - Carbon Dioxide in the Coastal Ocean: A Case Study in the Scotian Shelf Region - in: Ocean Year Book, 25, A. Chircop, S. Coffen-Smout, and M. McConnell, M. (eds.), Martinus Nijhoff, Leiden/Boston, 171-204.

Siegel, D. A., Dickey, T. D., Washburn, L., Hamilton, M. K. and Mitchell, B. G. (1989). Optical determination of particulate abundance and production variations in the oligotrophic ocean. Deep-Sea Res. 36: 211–222.

Stramska, M., and Dickey, T. D. (1992). Variability of bio-optical properties of the upper ocean associated with diel cycles in phytoplankton population. J. Geophys. Res. 97: 17873–17887, doi:10.1029/92JC01570.

Thomas, H., and B. Schneider (1999). The seasonal cycle of carbon dioxide in Baltic Sea surface waters, *J. of Mar. Sys., 22*, 53-67.

Thomas, H., Y. Bozec, K. Elkalay and H.J.W. deBaar (2004). Enhanced open ocean storage of CO_2 from shelf sea pumping. *Science*, 304, 5673, 1005-1008. DOI: 10.1126/science.1095491.

Thomas, H., D. Unger, J. Zhang, K.-K. Liu and E.H. Shadwick (2008). Biogeochemical cycling. In: Urban E., Sundby B., Malanotte-Rizzoli, P. and Melillo, J. (eds) Watersheds, Bays and Bounded Seas (SCOPE No. 70). Island Press, Washington, D. C., 169-190.

Thomas, H., L.-S. Schiettecatte, K. Suykens, Y.J.M. Koné, E.H. Shadwick, A.E.F. Prowe, Y. Bozec, H.J.W. de Baar, and A.V. Borges - 2009 - Enhanced ocean carbon storage from anaerobic alkalinity generation in coastal sediments - *Biogeosciences*, 6, 267-274.

Umoh, J. U., Thompson, K. R., 1994. Surface heat flux, horizontal advection, and the seasonal evolution of water temperature on the Scotian Shelf. J. Geophys. Res. 99 (20), 403–420.

Urrego-Blanco, J. and Sheng, J. (2011). Interannual variability of circulation and hydrography over the Eastern Canadian Continental Shelf, *Atmosphere-Ocean*, submitted.

Vandemark, D., J. E. Salisbury, C. W. Hunt, S. M. Shellito, J. D. Irish, W. R. McGillis, C. L. Sabine, and S. M. Maenner, J., Temporal and spatial dynamics of CO2 air-sea flux in the Gulf of Maine, Geophys. Res., 116, C01012, doi:10.1029/2010JC006408, 2011.

Chapter 6

Rapid acidification of mode and intermediate waters in the southwest Atlantic Ocean

Lesley A. Salt, Steven M.A.C. van Heuven, Maaike E. Claus, Elizabeth M. Jones, and Hein J.W. de Baar.

Abstract

Observations along the southwest Atlantic WOCE A17 line made during the Dutch GEOTRACES-NL program (2010-11) were compared with historical data from 1994 to quantify the changes in the anthropogenic component of the total pool of dissolved inorganic carbon (ΔC_{ant}). Application of the extended Multi Linear Regression (eMLR) method shows that the ΔC_{ant} from 1994 to 2011 has largely remained confined to the upper 1000 dbar. The greatest changes occurred in the upper 200 dbar in the SubAntarctic Zone (SAZ), where a maximum increase of 37 μmol kg^{-1} is found. South Atlantic Central Water (SACW) experienced the highest rate of increase in C_{ant}, at 0.99 ± 0.14 μmol kg^{-1} y^{-1}, resulting in a rate of decrease in pH of -0.0016 yr^{-1}. The highest rates of acidification relative to ΔC_{ant}, however, were found in SubAntarctic Mode Water (SAMW) and Antarctic Intermediate Water (AAIW). The low buffering capacity of SAMW and AAIW combined with their relatively high rates of C_{ant} increase of 0.53 ± 0.11 μmol kg^{-1} y^{-1} and 0.36 ± 0.06 μmol kg^{-1} y^{-1}, respectively, has, and will continue to cause rapid acidification in the SAZ and simultaneously reduce the chemical buffering capacity of this significant CO_2 sink.

1 Introduction

The Atlantic Ocean contains the largest store of anthropogenic carbon (C_{ant}) of all the world's oceans, accounting for approximately 38% of the total C_{ant} inventory (Sabine et al., 2004). Within the Atlantic, the North Atlantic is currently responsible for the majority of the uptake of C_{ant} (Levine et al., 2011), due to the formation of North Atlantic Deep Water (NADW). However, a recent Atlantic basin inventory analysis indicates that in the past decade the South Atlantic has been more effective at sequestering C_{ant} (Wanninkhof et al., 2010) than the North Atlantic. These authors calculated a rate of increase of the North Atlantic inventory of 1.9 Pg C decade^{-1}, whereas the South Atlantic inventory grew at a rate of 3.0 Pg C decade^{-1}. Calculations by Ríos et al. (2012) indicate that the southwestern Atlantic Ocean dominates the South Atlantic sink of C_{ant}, with a storage rate of 0.25±0.035 Pg C decade^{-1}. Quantifying the exact rate of increase in anthropogenic carbon in ocean waters is inherently problematic due to the highly variable nature of dissolved inorganic carbon (DIC) within the ocean and the relatively small fraction that the anthropogenic component represents (~3%; Ríos et al., 2010). In the past decade a number of methods for calculating the increase in C_{ant} (ΔC_{ant}) between reoccupations of ocean transects have been developed (e.g. TrOCA, $\varphi C_T{}^0$, eMLR). Despite the differing approaches and assumptions, there is overall coherence in the determinations of the C_{ant} in the world's oceans (Lee et al., 2003; Peng et al., 2003; Álvarez et al., 2009; Wanninkhof et al., 2010).

The southwest Atlantic has been occupied several times over the past 20 years and several techniques to determine C_{ant} have been applied to the WOCE '94 A17 transect by Ríos et al. (2010). All methods confirmed maximum C_{ant} concentrations in South Atlantic Central Water (SACW), however, south of 40°S discrepancies between the methods (ΔC^* (Gruber et al., 1996), Tracer combining Oxygen, inorganic Carbon and total Alkalinity (TrOCA)(Touratier et al., 2007), $\varphi CT°$ (Vázquez-Rodríguez et al., 2009a), Transit Time Distributions (TTD)(Waugh et al., 2006)) is significant. Generally, the TrOCA method provided the highest estimate, followed by $\varphi CT°$ and TTD, however all show great conformity in latitudinal behavior.

The presence of the western boundary current in the South Atlantic Ocean means that the C_{ant} signal penetrates deeper and is larger in the western half of the basin compared to the eastern half (Wanninkhof et al., 2010; Ríos et al., 2010; Vázquez-Rodríguez et al., 2009). Murata et al. (2008) show that the C_{ant} signal in SubAntarctic Mode Water (SAMW) can be ~7 μmol kg^{-1} higher west of 15°W compared to the east. The major pathways of C_{ant} into the South Atlantic ocean interior are by means of the formation of mode and intermediate waters (McNeil et al., 2001; Sabine et al., 2004). The SAMW is formed in the SubAntarctic Zone

(SAZ), between the Subtropical Front (STF) and subAntarctic Front (SAF), where a calculated anthropogenic CO_2 uptake of $0.07 - 0.08$ PgC yr^{-1} occurs (Sabine et al., 1999; McNeil et al., 2001). A total CO_2 sink of 1.1 Pg C yr^{-1} has been calculated by McNeil et al. (2007) for the SAZ, making it the largest CO_2 sink in the Southern Ocean and a significant sink for anthropogenic atmospheric CO_2.

The increase in DIC that results from the uptake of anthropogenic CO_2 from the atmosphere leads to increasing proton, bicarbonate ion and carbon dioxide concentrations ($[H^+]$, $[HCO_3^-]$, $[CO_2]$) and decreasing carbonate concentrations ($[CO_3^{2-}]$), a process referred to as *ocean acidification*. Sabine et al. (2004) state that approximately 50% of the total amount of C_{ant} in the world's oceans resides in the upper 400 m. The associated decrease in pH has been calculated as -0.1 pH units in the surface ocean relative to pre-industrial times (Royal Society, 2005; Orr et al., 2005). In the North Atlantic Ocean acidification rates of -0.0016±0.0001 yr^{-1} and -0.0012±0.002 yr^{-1}, for SubArctic Intermediate Water (SAIW) and SubPolar Mode Water (SPMW), respectively, have been reported (Vázquez-Rodríguez et al., 2012). Data from the European Time Series in the Canary Islands (ESTOC) station shows significantly higher rates of pH decrease in surface waters of -0.0017 ± 0.0004 yr^{-1}, for the time period 1995 to 2004, with notable influence from regional climatic forcing (Santana-Casiano et al., 2007). Acidification rates that deviate from the rate expected from C_{ant} increases alone have been observed in upper Labrador Sea Water (uLSW), SAIW, and eastern North Atlantic Central Water (eNACW) (Vázquez-Rodríguez et al., 2012). These variations have been attributed to a combination of climatic and biological effects. The greater sensitivity of some water masses to acidification has been well documented by González-Dávila et al. (2011) through the application of the buffering factors described by Egleston et al. (2010) and previously Frankignoulle (1994). González-Dávila et al. (2011) showed that waters originating at high latitudes are particularly sensitive to increases in the concentration of dissolved CO_2 ($[CO_2 (aq)]$), in particular Antarctic Intermediate Water (AAIW) and upper Circumpolar Deep Water (*u*CDW) due to low total alkalinity (A_T) to DIC ratios.

A number of the biological consequences of ocean acidification are related to the changes in $[CO_3^{2-}]$, and thus the concentration of calcium carbonate ($[CaCO_3]$). Carbonate and bicarbonate ions are used by marine calcifying organisms to form both varieties of calcium carbonate: aragonite (e.g. by pteropods) and calcite (e.g. by coccolithophores and foraminifera). Aragonite is the less metastable form of $CaCO_3$ resulting in a saturation horizon ($\Omega_{Ar}=1$) approximately 2 km shallower than that of calcite ($\Omega_{Ca}=1$) in the South Atlantic Ocean. Below these depths the respective forms of $CaCO_3$ are no longer present in particulate form. It follows that organisms which use aragonite are much more vulnerable to

decreases in $[CO_3^{2-}]$ driven from surface increases in $[CO_2]$ than organisms using calcite. A number of experiments have observed shell dissolution in pteropods incubated at elevated partial pressure of CO_2 (pCO_2) (Orr et al., 2005; Lischka et al., 2011) associated with a lowering of the aragonite saturation state (Ω_{Ar}). Recently similar results have been observed *in situ* in the Southern Ocean (Bednaršek et al., 2012), indicating that species are already being affected by C_{ant} accumulation.

This study examines the increase of C_{ant} in the southwest Atlantic Ocean between two occupations of the WOCE A17 line, which took place in 1994 and 2010/11. We calculate the changes in C_{ant} (ΔC_{ant}) in the different water masses and subsequently examine the pH changes driven by the invasion of anthropogenic carbon between WOCE '94 A17 and GEOTRACES-NL (2010/2011). These results are furthermore put into context with regard to the differing buffering capacities of individual water masses.

2   Data and Method

2.1   Datasets

The two datasets used in this study are the results from the CO_2 survey data from the WOCE '94 A17 section (public data at: http://cdiac.ornl.gov/oceans/woce_a17c .html) and the Dutch West Atlantic GEOTRACES program, completed in 2011 (GEOTRACES-NL (2010/2011). The respective cruise tracks and stations are shown in Fig. 1. The GEOTRACES-NL (2010/2011) section was carried out in two parts. The shown stations north of the equator were occupied in July 2010 by the Dutch RV Pelagia (expedition 64PE321, from Hamilton, Bermuda to Fortaleza, Brazil), and the southern hemisphere was sampled during March 2011 by the British RRS James Cook (JC057, from Punta Arenas, Chile to Las Palmas, Gran Canaria). The WOCE '94 A17 section was similarly carried out in austral autumn and this data has undergone rigorous quality control (Key et al., 2010). The data report is available from 'http://cdiac.ornl.gov/ oceans/ndp_084/' (Ríos et al., 2005b), where an offset of -8 μmol kg^{-1} in the A_T data has been reported and
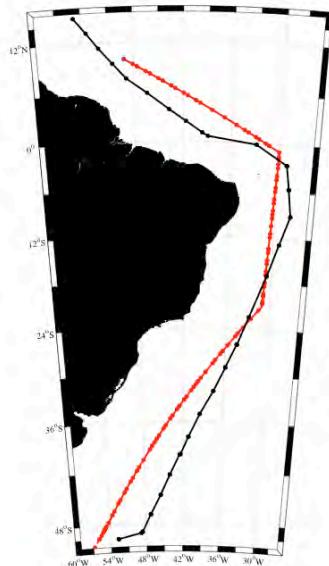

Figure 1. Cruise tracks from both cruises with used stations (black represents the WOCE '94 A17 line, red represents the GEOTRACES-NL (2010/2011) expeditions).

corrected for in this study. For a detailed analysis of the WOCE occupation we refer the reader to Ríos et al. (2010).

2.2   GEOTRACES-NL (2010/11) measurements

2.2.1 Dissolved inorganic carbon and total alkalinity

During the GEOTRACES-NL (2010/2011) cruises, for measurements of DIC and A_T, water samples of 600 ml were collected from throughout the water column, from 24 Niskin samplers mounted onto a CTD rosette, following standard operating procedures (Dickson et al., 2007). At least two duplicates samples were collected at each station, from different parts of the profile. Samples were analyzed immediately after collection on a VINDTA 3C (Versatile INstrument for the Determination of Total Alkalinity, Marianda, Kiel) instruments, simultaneously. These systems determine DIC by coulometric titration using a coulometer (Johnson et al., 1987) and determine A_T by potentiometric titration with 0.1M hydrochloric acid (Mintrop et al., 2000). Quality control was performed through regular measurements of certified reference material (CRM, Batch #100) supplied by Dr. Andrew Dickson at Scripps Institute of Oceanography (San Diego, California). Based on the measurements performed on the CRM, DIC was measured with a precision of one standard deviation of 1.0 µmol kg^{-1} and the precision of A_T had one standard deviation of 1.1 µmol kg^{-1}.

2.2.2 Ancillary parameters

Dissolved oxygen samples were collected from a minimum of three depths throughout the water column for CTD sensor calibration. The samples were collected in 120 ml borosilicate glass bottles and treated following the Winkler method (Winkler, 1888) and analyzed spectrophotometrically on a Hitachi U-1100 Spectrophotometer, following Pai et al., (1993). The precision, estimated from 123 replicates, was ±0.98 µmol l^{-1}.

Inorganic nutrients (PO_4, $Si(OH)_4$, NO_3) were analyzed following the methods of Grasshoff et al. (1983). In every run a control and a natural sterilized, Reference Nutrient Sample (RMNS Kanso, Japan) were measured. Precision was estimated to be ± 0.01, 0.2, and 0.2 µmol l^{-1} for PO_4, $Si(OH)_4$, and NO_3, respectively. Values of salinity are reported on the practical salinity scale.

2.2.3 pH Calculations

From DIC, A_T and supplementary data (salinity, temperature, pressure, $Si(OH)_4$, PO_4), the pH and pCO_2 were also calculated in-situ for both datasets using CO2_SYS (Lewis and Wallace, 1998) adapted for Matlab (van Heuven, 2011a), applying the carbonic acid

dissociation constants of Mehrbach et al. (1973), (refit by Dickson and Millero, 1987), and the KSO_4 constant of Dickson (1990). The same calculation was carried out for both the WOCE '94 A17 and GEOTRACES-NL (2010/2011) datasets with the resulting pH reported on the total pH scale.

2.3   Deepwater consistency between WOCE and GEOTRACES

In a later section, we employ the eMLR method (Friis et al., 2005) to infer ΔC_{ant} between the two cruises. The eMLR method considers various biogeochemical properties (in this case, salinity (S), DIC, NO_3, $Si(OH)_4$ and apparent oxygen utilization ($AOU=[O_2]_{sat}-[O_2]_{obs}$)) and is particularly sensitive to large scale (*secular*) changes in the distributions of these properties, as well as to analytical biases in their measurement. In order to assess the magnitude and distributions of these changes, we gridded the values of S, DIC, NO_3, $Si(OH)_4$ and AOU of each dataset and subtracted the grids from each other. Grid spacing was every 2 degrees of latitude, with 80 layers in the vertical direction, with increased density towards the surface. The differences deeper than 400 dbar (i.e. the deepest extent of the winter mixed layer; Dong et al. 2008) are very modest, having average values (for S, DIC, NO_3, $Si(OH)_4$ and AOU) of 0.004±0.047; 1.5±12.2 µmol kg^{-1}; 2.15±6.37 µmol kg^{-1}; -3.7±11.5 µmol kg^{-1}; 1.2±15.0 µmol kg^{-1}, respectively. Due to greater seasonality one would expect larger variability in the upper 400m, which we do see, however, the differences remain of a similar order of magnitude with average differences of 0.122±0.404; 6±18 µmol kg^{-1}; 3.51±8.02 µmol kg^{-1}; 1.4±3 µmol kg^{-1}; 0.9±19 µmol kg^{-1} for S, DIC, NO_3, $Si(OH)_4$ and AOU, respectively.

2.4   eMLR and C_{ant} Calculations

There are two general carbon data-based approaches for studying the increasing oceanic C_{ant}. The first approach uses back-calculation techniques (e.g. φC_T, ΔC^*, TrOCA) to obtain an estimate of pre-industrial DIC concentration against which to compare current measurements. Methods from the second approach aim to determine the part of change in DIC between two specific time periods that is attributable to anthropogenic CO_2 invasion (e.g. multi-linear regression, time series residuals). One example of each approach is employed in this study [eMLR (Friis et al., 2005) and φC_T (Vázquez-Rodríguez et al., 2009a, 2009b)]. Various comparison and evaluations of these and other methods are available in the literature (Levine et al., 2008; Yool et al., 2010; van Heuven et al., 2011b; Sabine and Tanhua, 2010).

2.4.1 ΔC_{ant} from eMLR

The multi-linear regression approach to estimating anthropogenic CO_2 invasion was introduced by Wallace (1995). It involves using a number of biogeochemical properties,

known to be related to DIC, to obtain a model of the observed DIC. As the relationships between DIC and these properties are not expected to change over time, the same statistical relationships can be applied to a second dataset of later date. Differences between the model 'predicted' DIC and the observed DIC are attributed to the invasion of anthropogenic CO_2. In the extended version (eMLR), which is applied here, the DIC from both datasets is fitted to the same selection of properties from both datasets, and the difference between parameter coefficients is assumed to be predictive of the difference in C_{ant} between the two cruises:

$$\Delta C_{ant}{}^{eMLR} = DIC^{MLR2,t2} - DIC^{MLR1,t1} \tag{1}$$

$$= (a_2 - a_1) + (b_2 - b_1) S_{t2} + (c_2 - c_1) SiO_{2t2} + (d_2 - d_1) NO_{3t2}$$
$$+ \dots (e_2 - e_1) T_{t2} + (f_2 - f_1) AOU_{t2}. \tag{2}$$

Using a stepwise regression the most significant terms for the WOCE A17 '94 dataset were determined as, in order of decreasing importance: S, SiO_2, NO_3, T, and AOU. These properties predict DIC with an R^2 value of 0.99 and a root mean square error (rmse) of 6.66 µmol kg^{-1}. For the GEOTRACES-NL (2010/2011) dataset, the order of importance was: S, SiO_2, NO_3, T and AOU, with an R^2 of 0.98 and rmse of 9.87 µmol kg^{-1} (Fig. 2).
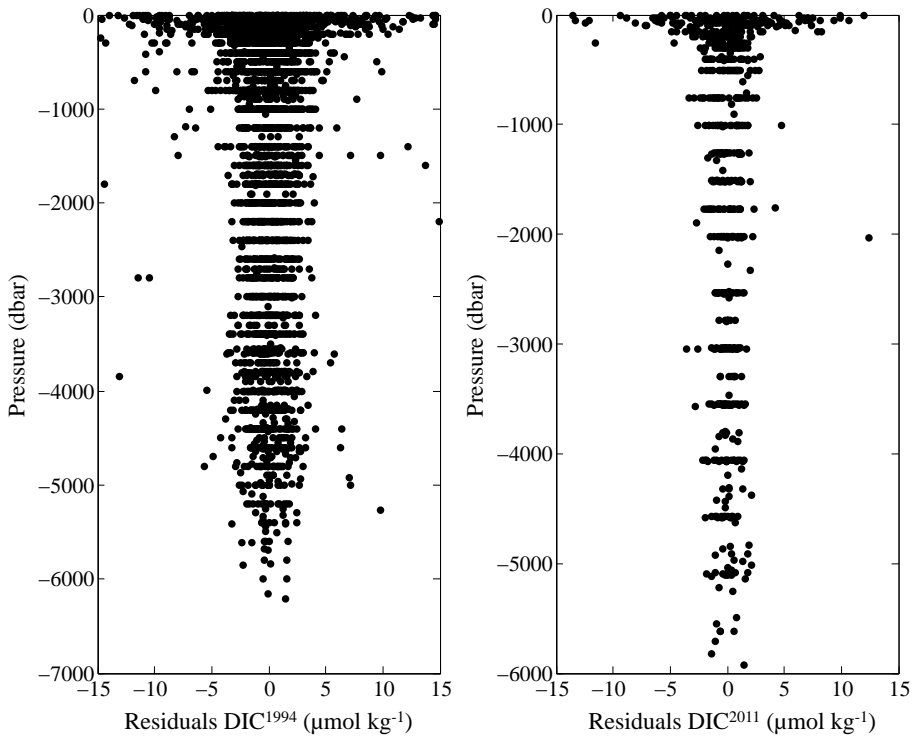

Figure 2. The residuals of the MLR fits of the (a) WOCE '94 A17 and (b) GEOTRACES-NL (2010/2011) datasets.

Table 1. Differences between the fitted coefficients for the two data sets obtained on the WOCE '94 A17 and the GEOTRACES-NL (2010/2011) cruises. The listed parameters were fitted to DIC for the applied eMLR method at various density intervals.

Min density	Max density	Mean Layer Depth	a	Si(OH)$_4$	NO$_3$	S	Theta	AOU	Pressure	rmse	R^2	n
						Sigma-θ						
20.00	23.50	31	132	5.67	-130.26	-12.47	10.73	-0.12	0.16	7.61	0.98	40
23.50	24.50	50	-190	-6.97	15.19	2.30	3.63	0.15	0.04	6.26	0.95	30
24.50	25.00	53	899	23.25	-12.86	-31.74	8.84	0.23	0.37	4.98	0.99	12
25.00	25.40	57	549	3.32	-0.64	-18.85	4.47	-0.21	0.31	5.54	0.99	18
25.40	26.20	107	-603	6.54	0.36	17.33	-2.68	-0.21	0.05	3.78	0.99	31
26.20	26.40	160	-109	0.97	1.57	1.68	1.42	-0.15	0.03	2.11	1.00	21
26.40	26.60	196	139	0.93	-0.13	-4.83	0.68	0.05	0.01	2.35	1.00	33
26.60	26.80	259	77	1.31	1.51	-4.29	3.40	-0.17	0.01	1.65	1.00	30
26.80	27.00	310	288	1.33	1.70	-10.90	5.14	-0.19	0.01	1.64	1.00	42
27.00	27.15	431	82	-0.12	-0.97	-1.59	-2.97	0.16	0.00	1.14	1.00	50
27.15	27.35	672	730	0.21	-1.29	-20.88	0.74	0.16	0.00	2.07	0.99	37
27.35	27.45	991	-1466	-0.01	1.77	42.62	-0.63	-0.35	-0.01	1.37	0.98	22
						Sigma-2						
27.45	36.70	1108	-141	-0.24	3.84	2.11	5.01	-0.52	0.01	1.50	0.99	40
36.70	36.75	1279	-199	-0.35	4.05	4.88	-0.92	-0.50	0.00	0.98	1.00	21
36.75	36.85	1531	-3210	-0.67	4.15	92.33	-17.46	-0.15	-0.01	1.25	1.00	20
36.85	36.90	1614	-1563	-0.29	3.42	44.16	-6.22	-0.25	0.00	1.15	1.00	16
36.90	37.00	1946	-3314	-0.75	6.28	93.81	-14.05	-0.33	0.00	2.27	1.00	48
37.00	37.05	2586	-3038	-0.54	4.80	85.85	-9.70	-0.20	0.00	0.74	1.00	95
						Sigma-4						
37.05	45.90	3050	-474	0.18	1.33	11.41	13.33	-0.12	0.01	0.73	0.99	29
45.90	45.98	3730	-51	0.35	2.02	0.07	13.57	-0.54	0.00	1.18	1.00	61
45.98	46.02	4195	22023	-0.34	-1.72	-628.87	20.07	-0.80	0.00	1.43	1.00	18
46.02	46.10	4582	7689	-0.33	0.93	-219.90	9.91	-0.38	0.00	1.04	0.99	28
46.10	60.00	5108	-47999	0.63	1.291	1385.48	-55.32	-1.04	-0.01	1.09	0.89	25

The eMLR regressions were applied along isopycnals intervals, consistent with the idea that the preferred method of water movement from the surface into the ocean interior is along surfaces of constant density. It thus follows that waters occupying the same density band share a common formation history and can be described by a single equation. Isopycnal bands were chosen based on temperature-salinity plots of the water masses and the number of data points occupying each interval. The coefficients and accompanying statistics from each isopycnal interval are displayed in Table 1. The residuals of each fit are shown in Fig. 2, with the 2011 dataset showing a maximum average residual of 7 μmol kg^{-1}, in the surface layer and an overall average of 2.1 μmol kg^{-1} including the deeper waters (>2000 dbar). In comparison, the WOCE '94 A17 dataset shows a water column average residual of 3.17 μmol kg^{-1}, which we attribute to less precise measurements in the earlier dataset. Pressure was included in the regression to avoid skewing (over depth) of the residuals of the MLR by the relatively large amount of samples located towards the surface, as mentioned by Hauk et al. (2010).

2.4.2 C_{ant} from $\varphi C_T°$

The $\varphi C_T°$ method is a back-calculation approach that uses stoichiometric ratios from biogeochemical processes to account for the addition of DIC in the water column resulting from organic matter remineralization and calcium carbonate dissolution, since the time of water formation. It is based on the general principle of 'preformed DIC' (or $C_T°$) of Brewer (1978) and ΔC^* of Gruber et al. (1996). The main advantage of this method is that it considers the non- steady state of A_T and pCO_2 in the subsurface reference layer.

2.5   Buffer Factors

The Revelle factor was originally described by Revelle and Suess (1957) and quantified the attenuated response of increasing DIC impacted by increasing pCO_2, or vice versa. This work has been built upon by Frankignoulle (1994) and more recently by Egleston et al. (2010), who outlined six expressions that define how $[CO_2]$, $[H^+]$, and Ω_{Ar} or Ω_{Ca}, are impacted by changes in DIC or A_T. The following three equations, taken from Egleston et al. (2010), are the expressions for the three buffer factors relating to DIC which were applied to the GEOTRACES-NL (2010/2011) southwest Atlantic section:

$$\gamma DIC = (\partial \ln[CO_2]/\partial DIC)^{-1} \quad = DIC - Alk_C{}^2/S, \tag{3}$$

$$\beta DIC = (\partial \ln[H^+]/\partial DIC)^{-1} \quad = DIC \times S - Alk_c{}^2/Alk_C, \tag{4}$$

$$\omega DIC = (\partial \ln\Omega/\partial DIC)^{-1} \quad = DIC - \{Alk_C \times P/[HCO_3^-]\}, \tag{5}$$

where
$$DIC = [CO_2] + [HCO_3^-] + [CO_3{}^{2-}], \tag{6}$$

$$Alk_C = [HCO_3^-] + 2[CO_3{}^{2-}], \tag{7}$$

$$P = 2[CO_2] + [HCO_3^-], \tag{8}$$

$$S = [HCO_3^-] + 4[CO_3^{2-}] + [H^+] + [OH^-] + \ldots$$
$$\{[H^+][B(OH)_4^-]/Khb + [H^+]\} \tag{9}$$

and Ω refers to the saturation state of sea water with respect to aragonite or calcite. These equations quantify the resistance to change of $[CO^2]$ (represented by γDIC), $[H^+]$(βDIC) and Ω(ωDIC) in a water mass to changes in DIC. The concentrations used for the calculations were obtained from CO2SYS (Lewis and Wallace, 1998, adapted for Matlab by van Heuven, 2011a) using the same input conditions as previously mentioned (Sect. 2.2.3).

3   Hydrography of the South Atlantic Ocean

The distributions of potential temperature, salinity, AOU, silicate, A_T, and DIC of the GEOTRACES-NL (2010/2011) section are shown in Fig. 3(a-f). The large water masses have been described elsewhere (Mémery et al., 2000; Ríos et al., 2010; Wanninkhof et al., 2010), thus here the treatment is relatively brief. Located deeper than 4500 dbar throughout the section is Antarctic Bottom Water (AABW), characteristic in its high DIC and AOU. Values for DIC in this water mass range from 2243 to 2267 µmol kg^{-1}, and AOU values occupy a narrow band between 111 to 128 µmol kg^{-1}. The DIC maximum (2267 µmol kg^{-1}) and potential temperature minimum (-0.16°C) of the entire section are both found in this water mass, which also shows the greatest A_T value (2369 µmol kg^{-1}), occurring below the upper 1000m. These characteristics are all representative of the old age of the water mass and are caused by the large amount of organic matter remineralization which has taken place within it. The AABW can, most easily, be distinguished from the overlying *lower* Circumpolar Deep Water (*l*CDW), by the high silicate concentrations, which reach values greater than 120 umol kg^{-1} in AABW. Silicate concentrations in the deep waters (>4000 dbar) demonstrate a strong covariance with A_T (R^2=0.95), which has been previously noted (Broecker and Peng, 1982; Ríos et al., 1995; Pérez et al., 2002) and stems from the simultaneous dissolution of opaline and calcium carbonate shells from the hard tissue of organisms (Pérez et al., 2002).

The *l*CDW has a core at approximately 3500 dbar at 50ºS, above which it merges into *upper* Circumpolar Deep Water (*u*CDW), with its respective core identified by an oxygen minimum at approximately 1500 m (Mémery et al., 2000). Both branches of CDW display properties similar to that of AABW, as they represent a mixture of AABW and Weddell Sea Deep Water (Wong et al., 1998; Orsi et al., 1999). The *u*CDW and *l*CDW share isopycnals with *upper* North Atlantic Deep Water (*u*NADW) and *lower* North Atlantic Deep Water

(*l*NADW), respectively, in the northern half of the section. The *u*CDW and *u*NADW occupy the density band between $\sigma_\theta > 27.4$ and $\sigma_3 < 41.47$, with the front between the two water masses found at approximately 26ºN (Mémery et al., 2000). The NADW has been more recently ventilated than CDW and can thus be distinguished by lower AOU values of ~60 µmol kg^{-1} and DIC values lower than 2200 µmol kg^{-1}. The deeper *l*NADW can be separated from *u*NADW through higher silicate values, which rise to 40 µmol kg^{-1}, whereas *u*NADW has maximum silicate concentrations of 20 µmol kg^{-1} (Fig. 3d). The A_T values are also lower (~20 µmol kg^{-1}) in *u*NADW compared to *l*NADW.

The Antarctic Intermediate Water (AAIW) enters the section at 200 dbar just south of 48°S, identifiable as a tongue of water with very low salinity and A_T (minima of 34.05 and 2275 µmol kg^{-1}, respectively). The AAIW lies above *u*CDW and below SubAntarctic Mode Water (SAMW) (Peterson and Whitworth, 1989). This water mass is carried northward at intermediate depths between $\sigma_\theta > 27.1$ and $\sigma_\theta < 27.4$ (Ríos et al., 2012) from south of the SAF. In the southwestern Atlantic Ocean AAIW extends further north than in other oceans, due to the western boundary current along the coast of South America (Talley, 1996). The AAIW is a relatively young water mass and has AOU values comparable to NADW (~50 – 100 µmol kg^{-1}), however, it can be distinguished from *u*NADW, in its northward reaches, by its elevated silicate concentrations. Situated above the AAIW, the SAMW can be considered a component of the AAIW (McCartney, 1977). This water mass can be easily identified by the tracer Si* = [Si(OH)$_4$]-[NO$_3^-$] which has values from -10 to -15 µmol kg^{-1} in regions of SAMW formation (Sarmiento et al., 2004). The SAMW formation region is located just south of 47ºS in the Subantarctic Zone (SAZ), north of the SAF (McCartney, 1977) where deep winter mixing forms this high-oxygen water mass.

We estimate the Subtropical Front (STF) at ~41°S, where there is a steep gradient in salinity in the surface 200 dbar. North of the STF, in the surface, and extending northward to a density of $\sigma_\theta < 26.5$ kg m^{-3}, is South Atlantic Central Water (SACW; Ríos et al., 2012), which is heavily depleted in silicate, and has elevated salinity and A_T. Against this background, the two Amazon plumes are very distinct at 5°N and 15°N with salinity and A_T values as low as 34.11 and 2265 µmol kg^{-1}, and 32.3 and 2157 µmol kg^{-1}, respectively. The maximum values of both salinity and A_T correspond with South Atlantic Central Water (SACW) in the subtropics (17°S), reaching absolute maxima of 37.5 and 2456 µmol kg^{-1}, respectively, at 50 dbar depth. The subtropical part of the SACW that features high salinity and A_T is often referred to as the Salinity Maximum Water (SMW). In this study we make no distinction between SMW and SACW.

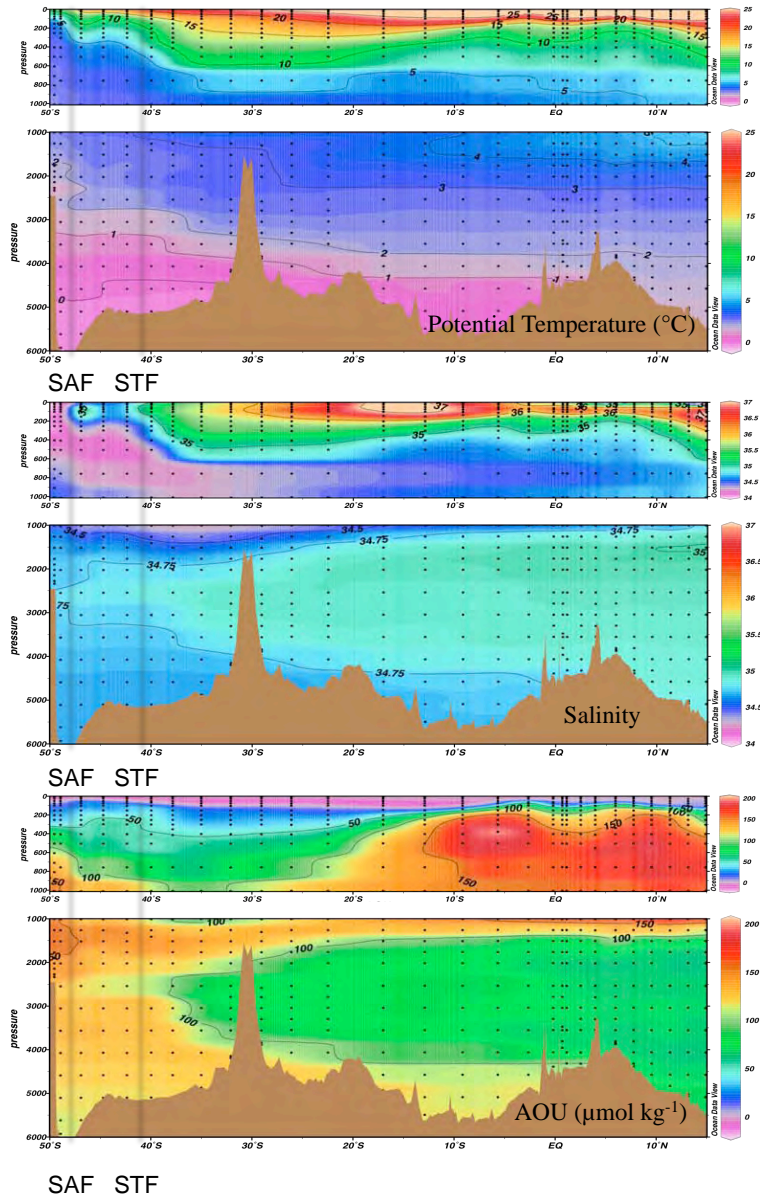**Figure 3**. Section distributions of (a) temperature (ºC), (b) salinity, (c) AOU (µmol kg^{-1}), collected on the GEOTRACES-NL (2010/11) cruises. Black solid lines represent the SubAntarctic front (SAF) and Subtropical Front (STF) at the surface.

Figure 3. Section distributions of (d) silicate (μmol kg^{-1}), (e) A$_T$ (μmol kg^{-1}) and (f) DIC (μmol kg^{-1}), collected on the GEOTRACES-NL (2010/11) cruises. Black solid lines represent the SubAntarctic front (SAF) and Subtropical Front (STF) at the surface.
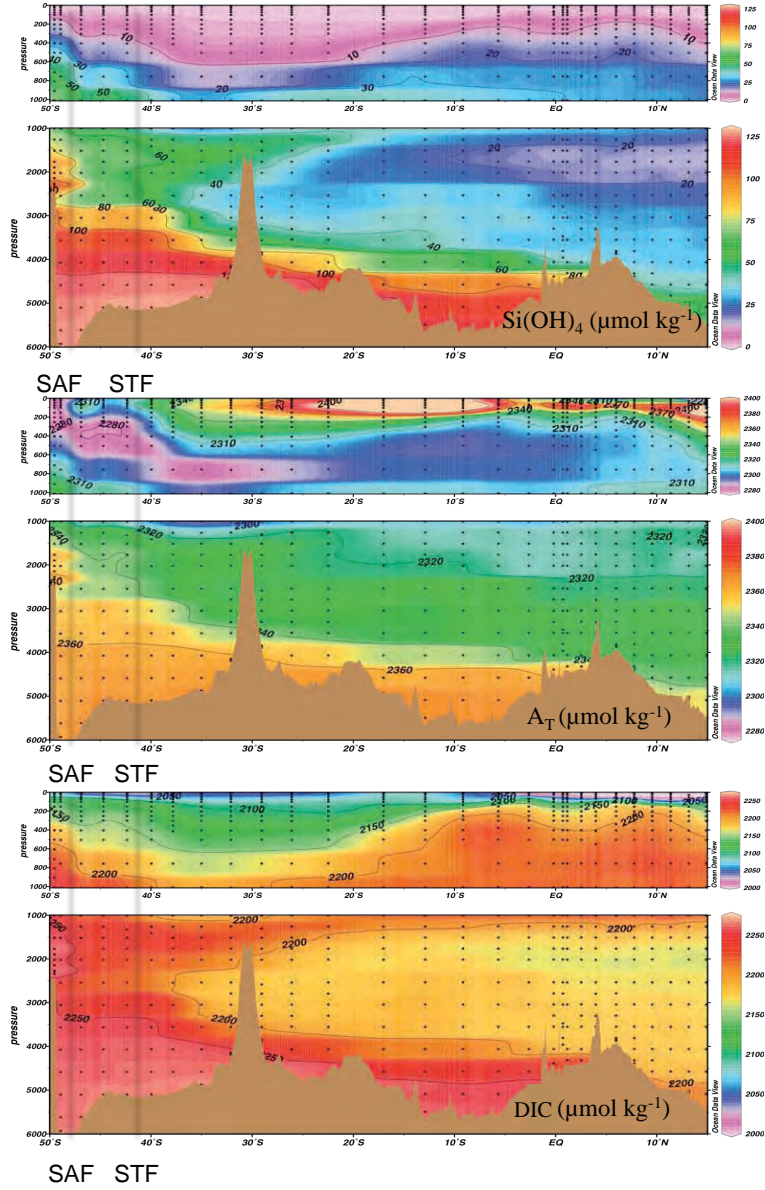
4 Results

4.1 ΔC_{ant} from eMLR

The increase in C_{ant} (ΔC_{ant}) from 1994 to 2011, obtained from an eMLR analysis, is shown in Fig. 4a. The general pattern is that from 1994 to 2011 the most evident increase in C_{ant} occurred in the upper 1000 dbar, particularly in the southern half of the section. The largest increases (up to 36 µmol kg^{-1}) were found in the surface waters of the SAZ, just south of 45°S. In the surface waters (<100 dbar) of the section the ΔC_{ant} gradually decreases northwards in a linear relationship with latitude ($R^2 = -0.74$) to a concentration of 0 µmol kg^{-1} just north of the equator (~5°N). This follows the pattern expected from surface water temperature, which plays a large role in determining the surface ocean pCO_2 and contributes to the role of the equatorial region acting as a source of CO_2 to the atmosphere during austral summer (Takahashi et al., 2009). The steepest vertical gradient of ΔC_{ant} is found at ~47°S just north of the SAF, where over the depth range from 600 to 0 dbar the ΔC_{ant} increases from 0 to 36 µmol kg^{-1}.

South of 15°S the deepest penetration of positive ΔC_{ant} values is found at 1200 dbar in the STZ, between 25ºS and 40ºS. The ΔC_{ant} zero-contour shoals southward of 35°S to ~600 dbar at 50ºS, coinciding with the lower limits of AAIW, as has been noted in other ocean basins (Sabine et al., 2004). In the northern half of the section, the deepest limit of ΔC_{ant} penetration in AAIW reaches a depth of ~700 dbar at 15ºS and north of the equator the AAIW signal becomes distorted as it mixes with NADW. The NADW shows near-zero concentrations of ΔC_{ant} throughout its extent, with the exception of the *u*NADW in the equatorial region, which show ΔC_{ant} values up to 5 µmol kg^{-1}. In *l*NADW, and the other deep and bottom waters (AABW, *l*CDW), ΔC_{ant} shows no change or a tendency to negative values.

Water Mass	Density Range	Latitude	Pressure (dbar)	δC_{ant} (µmol yr^{-1})	[a]δC_{ant} (µmol yr^{-1})	δpH yr^{-1}
SACW	$\sigma^\theta 20.0$-$\sigma^\theta 26.8$	23 - 18°S	90-160	0.99±0.14	0.90±0.04	-0.0016
SAMW	$\sigma^\theta 26.5$-$\sigma^\theta 27.1$	48 - 50°S	90-160	0.53±0.11	0.53±0.02	-0.0014
AAIW	$\sigma^\theta 27.1$-$\sigma^\theta 27.4$	48 - 50°S	360-450	0.36±0.06	0.36±0.02	-0.0010
***u*CDW**	$\sigma^\theta 27.4$-$\sigma^3 41.47$	49 - 50°S	1400-1800	0.33±0.07	0.16±0.04	-0.0010
***u*NADW**	$\sigma^\theta 27.4$-$\sigma^3 41.47$	10 – 15°N	1600-1800	0.20±0.03	0.16±0.04	-0.0005
***l*CDW**	$\sigma^3 41.47$-$\sigma^4 45.9$	48 - 50°S	3250-3750	0.00±0.06	0.08±0.04	0.0000
***l*NADW**	$\sigma^3 41.47$-$\sigma^4 45.9$	10 - 15°N	3000-3500	0.00±0.02	0.08±0.04	0.0000

Table 2. The calculated rates of increase of C_{ant} and pH along the section, listed per water mass. The identification criteria for each water mass are provided. Error represents $2\sigma/N^{0.5}$. [a]Values from Ríos et al. (2012).

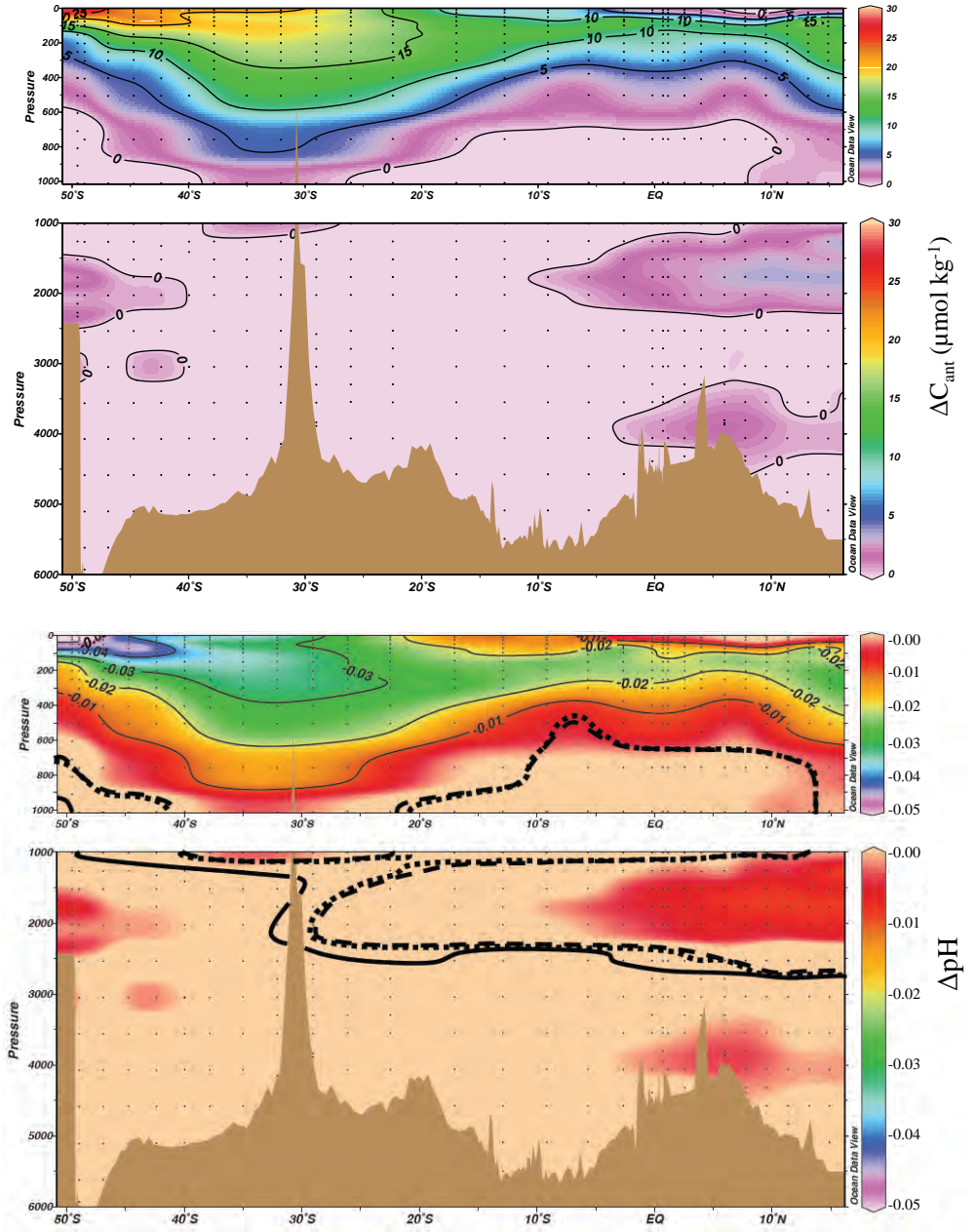**Figure 4**. (a) Distribution of $\Delta C_{ant}^{1994\text{-}2011}$ (µmol kg^{-1}), calculated using the eMLR approach. (b) Distribution of the $\Delta pH^{1994\text{-}2011}$ associated with $\Delta C_{ant}^{1994\text{-}2011}$. The aragonite saturation horizon (ΩAr) is marked on for pre-industrial times (solid line), 1994 (dashed line) and 2011 (dotted line).

To estimate the rate of increase of C_{ant} in each water mass we identified their respective cores using the water mass descriptions given in Mémery et al. (2000) and Ríos et al. (2012) and averaged their values of ΔC_{ant}. Assuming a constant yearly increase, we then divided this total increase by 17 to obtain the rate of yearly increase of C_{ant} over the period 1994 to 2011. The calculated values are shown in Table 2 with those of Ríos et al. (2012) for comparison. The highest rates of increase were found in SACW and SAMW with C_{ant} increase rates of 0.99 ± 0.14 µmol kg^{-1} y^{-1} and 0.53 ± 0.11 µmol kg^{-1} y^{-1}, respectively. The latter value shows good consistency with that calculated by Ríos et al. (2012; 0.53 ± 0.02 µmol kg^{-1} y^{-1}). However, there is a notable difference of 0.09 µmol kg^{-1} y^{-1} between the increase for SACW calculated here and that of 0.90 ± 0.04 µmol kg^{-1} y^{-1} (Ríos et al., 2012). As this is a surface water mass, and our study utilized data collected 6 years after that used for comparison in Ríos et al. (2012), we corrected the ΔC_{ant} as follows. Assuming complete equilibration between the atmosphere and ocean we corrected our ΔC_{ant} value for the additional DIC increase caused solely by atmospheric increases over the last 6 years, assuming constant salinity and A_T. The resulting calculated $C_{ant}^{1994-2005}$ increase rate was 0.92 ± 0.14 µmol kg^{-1} y^{-1}, making our result consistent with the previous estimate. As such, we attribute the difference in ΔC_{ant} increase rates in SACW to changing atmospheric pCO_2 concentrations between sampling times. Despite the similarities in formation history between SAMW and AAIW, the latter shows a much lower increase rate of 0.37 ± 0.06 umol kg^{-1} yr^{-1}. Increase rates of 0.33 ± 0.07 µmol kg^{-1} y^{-1} and 0.20 ± 0.03 µmol kg^{-1} y^{-1} were calculated for *u*CDW and *u*NADW, respectively. The *l*NADW, *l*CDW and AABW all show no significant increases.

4.2   Changes to pH and buffering capacity

Assuming no changes of A_T between the WOCE '94 A17 and GEOTRACES-NL (2010/2011) occupations, we use the calculated ΔC_{ant} and the measured A_T during GEOTRACES-NL (2010/2011) to calculate the anthropogenic driven change in pH from 1994 to 2011 ($\Delta pH^{1994-2011}$). From the application of the φC_T^0 method of anthropogenic carbon determination (Vázquez-Rodríguez et al., 2009a, 2009b; Sect. 2.3.2) we obtain the C_{ant} signal since pre-industrial times, which allows the calculation of the decline in pH, which has occurred since pre-industrial times (ΔpH)(Fig. 4b). The average surface (<250 dbar) ΔpH, across the section, from pre-industrial times to 1994, calculated using the $\varphi C_T°$ method, was -0.08, which is just under the predicted, general surface ocean decrease of 0.1 (Orr et al., 2005). The ocean interior experienced relatively small ΔpH, however, the change was accompanied by a significant shoaling of the aragonite saturation horizon, most notably in the southern half of the section (Fig. 4b). South of the SAF, at ~49°S, the aragonite saturation horizon rose by ~250 m, whereas further north, at 25°S, it had risen just 200 m. The change was almost imperceptible north of the Equator. From 1994 to 2011 the surface pH shows an averaged, further decline of 0.03, making the total surface ΔpH -0.11 since pre-

industrial times. Thus, of the total decrease since pre-industrial times to the present day, 27% occurred within the past 17 years. However, we can detect no notable change to the aragonite saturation state during this latter period. Historically, the uptake of C_{ant} by the surface ocean was relatively gradual, which allowed it to be well distributed throughout the water column. The effects of the recently, steeply decreasing anthropogenic acidification have not yet significantly penetrated into the deeper ocean.

The distribution of $\Delta pH^{1994\text{-}2011}$ across the section broadly follows the C_{ant} increases (compare Figs 4a, 4b), as expected under the assumption of a constant A_T. If we further assume a constant decrease over the 17 years, the yearly acidification rates were calculated from $\Delta pH^{1994\text{-}2011}$ and identified for each water mass core, as done for the yearly C_{ant} increases (Table 2). The highest rates of acidification were found in the surface waters, where we also observe the greatest rates of C_{ant} increase, with SACW showing a pH rate of decrease of -0.0016 yr^{-1}. The latter value is in line with that calculated for the same water mass on the eastern side of the North Atlantic Ocean at the ESTOC site (-0.0017 yr^{-1}) for the period 1995 to 2004 (Santana-Casiano et al., 2007; González-Dávila et al., 2010). The SAMW demonstrates the next greatest rate of decline with -0.0014 y^{-1}, followed by AAIW and *u*CDW both showing acidification rates of -0.001 yr^{-1}, which are comparable with values from other recently ventilated water masses in the North Atlantic: acidification rates of -0.0019 yr^{-1} and -0.0012 yr^{-1} have been reported for SubArctic Intermediate Water and SubPolar Mode Water, respectively (Vázquez-Rodríguez et al., 2012). The lowest non-zero acidification rate of -0.0005 yr^{-1} is found in *u*NADW.

5   Discussion

The distribution of ΔC_{ant} and the increase rates of C_{ant} calculated here show good consistency with previous studies (Ríos et al., 2010; Wanninkhof et al., 2010; Ríos et al., 2012). In contrast to our calculated ΔC_{ant}, a number of studies have found increasing concentrations of C_{ant} in AABW (Murata et al., 2008; Vázquez-Rodríguez et al., 2009; Brown et al., 2010). However, it has been noted previously that it is absent in eMLR analyses (Wanninkhof et al., 2010). The distributions of C_{ant} in AABW presented in Vázquez-Rodríguez et al. (2009) also indicate that C_{ant} concentrations have not yet spread further north than 50ºS, potentially explaining its absence in our calculations. Analysis of changes in the surface waters are usually overlooked due to the larger residuals associated with the presence of biological activity and seasonal variability (Friis et al., 2005), however, here we give these results validation.

The SAZ is typically under-saturated with respect to CO_2 (Metzl et al., 1999) due to a

combination of low temperatures and biological activity (McNeil et al., 2007). Calculation of pCO_2 using DIC and A_T shows that during both the WOCE '94 A17 and GEOTRACES-NL (2010/11) cruises the surface waters in the SAZ were under-saturated with respect to atmospheric pCO_2, at 311.5 µatm and 355.2 µatm, respectively (atmospheric pCO_2 was 359 µatm in 1994 and 392 µatm in 2011, ftp://ftp.cmdl.noaa.gov/ccg/co2/trends/co2_annmean_ mlo.txt). The two years thus show relative consistency in ΔpCO_2 (pCO_{2ocean} – $pCO_{2atm.}$), with an average under-saturation of -47.5 µatm in 1994 and -38.8 µatm in 2011. Using average salinity, A_T, temperature and pressure in this region, this computes as a DIC difference of 4.4 µmol kg^{-1} between the two years. Furthermore, principally the variability in both temperature and biology should be accounted for in the eMLR because of the use of temperature and biology-representative variables used (i.e. temperature, NO_3 and $Si(OH)_4$). However, the conceivably variable carbon export between the two time periods (due to variably dominant phytoplankton groups) may have lead to variation in the chemical stoichiometry, which could not be accounted for.

To corroborate our observations of surface ΔC_{ant} obtained using eMLR by another approach, we follow Lee et al. (1997) to derive a linear relationship between temperature and salinity normalized-DIC (NDIC=DIC*(35/S)) for surface waters (<100 dbar) with a temperature greater than, or equal to, 19°C (T≥19) and lower than 19°C (T<19). We derive such relationships for both WOCE '94 A17 and GEOTRACES-NL (2010/2011) data, with the resulting equations given below with those of Lee et al. (1997):

Lee et al. (1997):	T≥19°C:	NDIC = 2136.3 – 6.97T	(10)
	T<19°C:	NDIC = 2163.2 – 9.15T	(11)

WOCE (1994):	T≥19°C:	NDIC = 2141 – 6.99T (R^2=0.86)	(12)
	T<19°C:	NDIC = 2209 – 10.69T (R^2=0.96)	(13)

GEOTRACES (2011):	T≥19°C:	NDIC = 2160 – 7.02T (R^2=0.85)	(14)
	T<19°C:	NDIC = 2246 – 11.09T (R^2=0.99)	(15)

For T≥19°C the gradient, or slope, between temperature and NDIC is almost identical for all three datasets, varying from 6.90 to 7.02, which would result in a maximum NDIC difference of 2.6 µmol kg^{-1} at 29.3°C (the maximum temperature recorded of both datasets). These temperatures cover the tropics to the mid-latitudes, reaching 40°S. The resulting equations, from the WOCE '94 A17 and GEOTRACES-NL (2010/2011) datasets, show an increasing intercept of NDIC of 19 (2160-2141) µmol kg^{-1} from 1994 to 2011, which is consistent with the increase anticipated solely by increasing atmospheric pCO_2 (+20 µmol kg^{-1}). The

increase of intercept is also consistent with the ΔC_{ant} calculated using eMLR between latitudes $0°$ to $40°S$ (14 to 27 μmol kg^{-1}). North of the equator inconsistencies emerge between the estimated ΔC_{ant} values from the derived equation and from the eMLR analysis. In this region the pCO_2 of the ocean often exceeds that of the atmosphere (Takahashi et al., 2009), thus changes in temperature or other physical processes may exert controls undetectable by our analysis.

The colder temperature range ($<19°C$), encompassing the higher latitudes ($>46°S$), shows a slight steepening of the slope over the years in addition to an increased intercept. The observed increase in the intercept of 37 (2246-2209) μmol kg^{-1} corresponds with the highest value of ΔDIC calculated using an eMLR (37 μmol kg^{-1} at $49°S$) at a temperature of $11.2°C$. The variation in the slope (11.09-10.69=0.4) leads to a maximum difference of ±7.6 μmol kg^{-1} DIC at $18.9°C$ between the calculated NDIC values from 1994 to 2011. This comparison increases our confidence in our ΔC_{ant} values calculated in the surface waters, however, we note that in the high latitude regions there is the potential for greater errors.

The continuing uptake of atmospheric CO_2 gradually depletes the naturally available carbonate ion in the surface ocean thereby decreasing the capacity to *buffer* further CO_2 uptake and leading to the gradual acidification of the seawater. The extent to which the pH is affected by the increase of DIC is dependent upon several properties, including temperature, pressure, and A_T, which together determine its *buffering* capacity. As DIC increases, assuming no other changes take place, the buffering capacity of the water is reduced as $[CO_3^{2-}]$ decreases and $[CO_2]$ increases. The A_T is not altered by the flux of atmospheric CO_2 into the ocean, however, it is affected by biological processes, notably the dissolution and formation of calcium carbonate, with dissolution dominating in deep waters and formation playing a more important role in the surface. Table 2 quantifies the extent to which the calculated ΔC_{ant} have impacted pH in the water masses of the southwest Atlantic Ocean. Examination of this table clearly shows that the rate of acidification per μmol kg^{-1} of DIC is not equal between water masses. The SAMW, a relatively fresh, low alkalinity water mass, has an acidification rate of -0.0014 yr^{-1}, which is 88% of that of SACW, a warmer, more saline water mass. However, the C_{ant} increase rate of SAMW is only 54% that of SACW. The AAIW shows the same rate of acidification as *u*CDW, however, the increase of C_{ant} in *u*CDW is 10% lower than that of AAIW. These differences can be attributed to the varying buffering capacities of the water masses.

The distributions of the sensitivities of $[H^+]$(βDIC), $[CO_2]$(γDIC) and Ω_{CaCO3} (ωDIC) to changes in DIC for the southwest Atlantic are shown in Fig. 5. The greatest sensitivities to increasing DIC (denoted by low values in figures 5a, 5b, and high values in 5c) were

generally found in the deep waters. That is to say that for a given increase in DIC these waters will show large resultant changes in $[H^+]$, $[CO_2]$ and $[CO_3^{2-}]$, or aragonite and calcite saturation (Ω_{Ar}, Ω_{Ca}). Both uCDW and lCDW show very similar behavior – as expected from their similar formation history – however, interestingly, there is a notable difference between the buffering capacities of the two limbs of NADW. The difference is most noticeable in ωDIC, likely caused by the slightly higher A_T/DIC ratio in lNADW. A lower βDIC in uNADW denotes a greater sensitivity to acidification in response to increasing DIC concentrations. More rapid acidification in uNADW, compared to lNADW, has been observed by Vázquez-Rodríguez et al. (2012) and attributed to mixing with Labrador Sea Water (LSW), which exhibits a strong decreasing pH trend with time. The lower pH of LSW and its contribution to uNADW could account for the reduced buffering capacity calculated in this water mass in the southwest Atlantic Ocean.

The highest βDIC values are found in SACW, and SAMW which both have relatively low concentrations of DIC compared to the other water masses but the highest concentrations of A_T. The three water masses with the greatest response in pH relative to ΔC_{ant} were AAIW, uCDW and lCDW, with βDIC values of 0.148 mmol kg^{-1}, 0.141 mmol kg^{-1}, and 0.143 mmol kg^{-1}, respectively. These water masses show the highest DIC/A_T ratios along the section as they all originate in the Southern Ocean (SO) where upwelling brings deep waters rich in $[CO_2(aq)]$ and low in $[CO_3^{2-}]$ to the surface. In addition, these waters have slightly lower salinities and thus lower borate concentrations, which further diminish their buffering capacity. With the current calculated rate of increase of C_{ant}, aragonite will become under-saturated in AAIW around the year 2100, when DIC concentrations reach 2208 µmol kg^{-1}. This could happen even sooner, as wintertime, storm-driven upwelling entrainment of deep waters into the surface in the SO is predicted to cause seasonal aragonite under-saturation in the region as soon as 2030, when atmospheric CO_2 levels reach ~450 ppm (McNeil and Matear, 2008).

To quantify the differences between water masses in the context of increasing DIC, we calculate the respective changes in $[H^+]$, $[CO_3^{2-}]$ and pH in response to a 10 µmol kg^{-1} increase in DIC in SACW and uCDW. In SACW such an increase would lead to a 3.87% increase in $[H^+]$ and a 2.51% decrease in $[CO_3^{2-}]$ with a pH decline of -0.0165. In contrast, the same increase in uCDW leads to a +7.3% increase in $[H^+]$, -6.26% decrease in $[CO_3^{2-}]$ with pH decreasing by 0.0306 units. This makes uCDW twice as susceptible to pH changes from increasing DIC than SACW and three times more susceptible to $[CO_3^{2-}]$ decreases and thus under-saturation of aragonite and calcite.
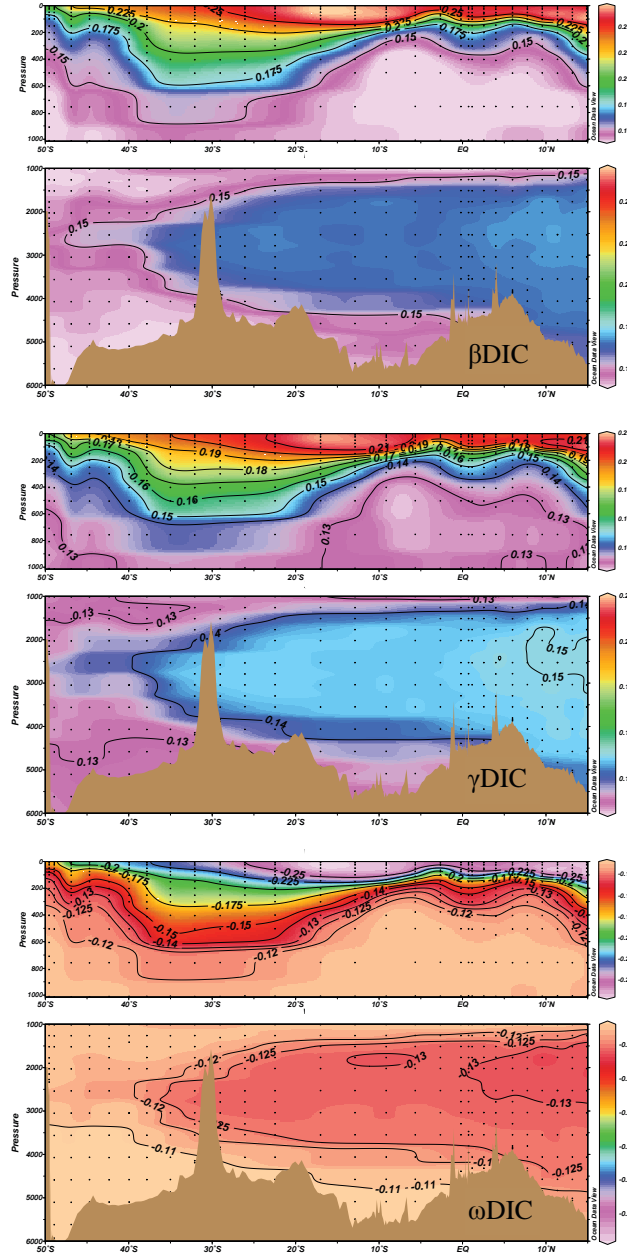
Figure 5. Distribution of the three buffering factors relating to DIC; βDIC, γDIC, and ωDIC (mmol kg^{-1}).

The buffering capacity of each water mass will be further reduced by increasing the DIC concentrations. To investigate how the buffering capacities of the different water masses in this section have changed over time, and will continue to do so, the DIC buffer factors of each water mass were calculated and plotted against DIC concentration (Fig. 6). Due to the large relative error of the calculated ΔC_{ant} increases in the deeper waters, these were not included. The high rate of uptake of C_{ant} by SACW means that this water mass has seen the largest decrease in buffering capacity since pre-industrial times. The βDIC value has decreased from 0.281 to 0.247 mmol kg^{-1} and Ω_{Ar} has decreased from 4.1 to 3.3. In contrast, *u*CDW has shown relatively little change due to the low values of C_{ant}. However, extrapolating our calculated C_{ant} rates of increase we predict a 33 μmol kg^{-1} increase in this water mass over the next century, which will result in a significant reduction in buffering and a pH decrease of -0.102. The SAMW and AAIW follow the same relationship, however, SAMW contains a greater proportion of subtropical water than AAIW, thus it maintains a slightly higher buffering capacity than AAIW. Both AAIW and *u*CDW will see a similar increase in C_{ant} over the next century (37 and 33 μmol kg^{-1}, respectively), however, the decline in Ω_{Ar} will be 1.6 times greater in AAIW, leading to under-saturation. The SAMW will see approximately 54% of the increase in C_{ant} that SACW will experience, however will undergo 84% of the associated pH decline. These changes highlight the vulnerability of SAMW and AAIW to increasing C_{ant}, as noted by Gonzalez-Davila et al. (2010).

The observed pattern of ΔC_{ant} in the southwest Atlantic clearly identifies the SAZ as the most effective entry point of C_{ant} into the ocean. In addition, the buffering factors of Egleston et al. (2010) explicitly show that by the end of this century the two dominant water masses in this area (SAMW and AAIW) will be the most sensitive to further C_{ant} increases. Whilst it is clear that this will accelerate the rate of acidification in these water masses, it is unclear how it will affect the CO_2 uptake in the SAZ. Assuming no changes to primary production, the increased sensitivity of SAMW to DIC changes will lead to much greater seasonal variability in the carbonate system of this water mass between the productive and non-productive period. The biological uptake of DIC in the SAZ in austral spring and summer would lead to a more dramatic decrease in surface water pCO_2, allowing a greater air-sea pCO_2 flux. Conversely, the acidification and decline in Ω_{Ar} may be detrimental to calcifying organisms in the area, as observed in the Southern Ocean (Bednarsek et al., 2012), thus limiting export via the biological pump. Additionally, SAMW plays a vital role in the ventilation and supply of nutrients to the thermocline (Karstensen and Quadfasel, 2002; Sarmiento et al., 2004) with models suggesting that this source of nutrients sustains almost three-quarters of primary production in the low latitudes (Sarmiento et al., 2004). As such, reductions to production and export in these regions may have significant consequences for other areas of the ocean as well.
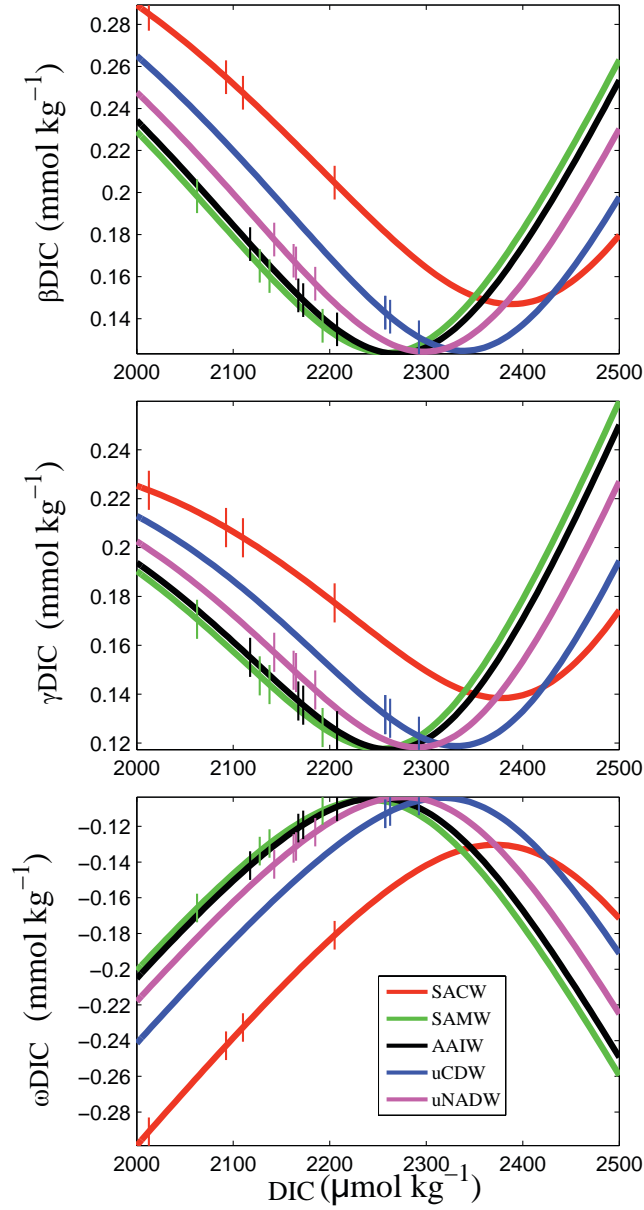
Figure 6. The DIC buffer factors of each water mass over a range of DIC concentrations. The vertical lines denote the DIC concentration in pre-industrial times, 1994, 2011 and the projected concentration in 2110.

The water masses SAMW and AAIW both risk further reduction in their buffering capacities by long-term variability to their physical properties. On decadal time scales a freshening of AAIW has been observed in the Pacific and Indian sectors of the Southern Ocean (Wong et al., 1999). Decadal variability has also been noted in temperature, salinity and biogeochemical parameters of SAMW (Bindoff et al., 2007; Alvarez et al., 2011), which could further diminish or enhance the buffering capacity of this water mass and thus the C_{ant} driven acidification. Variations on decadal time scales have been related to the Southern Annular Mode (Álvarez et al., 2011), the dominant climate forcing over the region. Similarly in the North Atlantic, the North Atlantic Oscillation exerts a degree of control over the carbonate system variables and C_{ant} uptake (Santana-Casiano et al., 2007; Pérez et al., 2010). Such external controls will cause irregular C_{ant} uptake over time, as has been observed by Brown et al. (2010), making it difficult to accurately predict future C_{ant} uptake.

6 Conclusion

The continuing uptake of C_{ant} in the southwest Atlantic has been assessed through application of eMLR to two datasets collected in 1994 and 2011. The distribution of ΔC_{ant} is comparable with previous studies of C_{ant} accumulation in the region (Ríos et al., 2010). The largest increases are found in the SAZ, just north of the SAF; a previously identified substantial CO_2 sink (Metzl et al., 1999). The SACW (0.99 ± 0.14 µmol kg^{-1} y^{-1}), SAMW (0.53 ± 0.11 µmol kg^{-1} y^{-1}) and AAIW (0.36 ± 0.06 µmol kg^{-1} y^{-1}) are responsible for the greatest C_{ant} uptake, consistent with earlier studies showing them to be an effective pathway of C_{ant} into the ocean interior (Álvarez et al., 2009). The lower extent of AAIW demarks the greatest depth of penetration of C_{ant} into the ocean in the past 17 years indicating that future uptake will similarly be largely concentrated within the surface 1000m.

The increase in C_{ant} in the southwest Atlantic has led to acidification of water masses. The calculated C_{ant}-driven acidification is greatest in SACW, where a current rate of pH decline of 0.0016 yr^{-1} is found. However, the acidification response per µmol kg^{-1} increase in DIC is greatest in the intermediate and mode waters. We identify SAMW as the water mass with the greatest risk of rapid acidification, due to a combination of its high C_{ant} uptake and its limited buffering capacity. AAIW, on the other hand, is more at risk of aragonite under-saturation due its low A_T values and resultant high ωDIC values. Continued increase of C_{ant} at the current rate calculated will lead to aragonite under-saturation in the core of AAIW by 2104.

References

Álvarez, M., C. Lo Monaco, T. Tanhua, A. Yool, A. Oschlies, J.L. Bullister, C. Goyet, N. Metzl, F. Touratier, E. McDonagh, and H.L. Bryden (2009). Estimating the storage of anthropogenic carbon in the subtropical Indian Ocean: a comparison of five different approaches. *Biogeosciences* 6, 681-703.

Álvarez, M., T. Tanhua, H. Brix, C. Lo Monaco, N. Metzl, E.L. McDonagh, and H.L. Bryden (2011). Decadal biogeochemical changes in the subtropical Indian Ocean associated with Subantarctic Mode Water. *J. of Geophys. Res.* 116, C09016.

Anderson, L.A., and J.L. Sarmiento (1994). Redfield ratios of remineralization determined by nutrient data analysis. *Global Biogeochem. Cycles.* 8, 65-80.

Bednarsek, N., G. A. Tarling, D.C.E. Bakker, S. Fielding, E.M. Jones, H.J. Venables, P. Ward, A. Kuzirian, B. Lézé, R. A. Feely and E.J. Murphy (2012). Extensive dissolution of live pteropods in the Southern Ocean. *Nat. Geosc.* 5, 881-885.

Bindoff, N.L., J. Willebrand, V. Artale, A, Cazenave, J. Gregory, S. Gulev, K. Hanawa, C. Le Quéré, S. Levitus, Y. Nojiri, C.K. Shum, L.D. Talley and A. Unnikrishnan, (2007), *Observations: Oceanic Climate Change and Sea Level. In: Climate Change 2007: The Physical Science Basis. Contribution of Working Group I to the Fourth Assessment Report of the Intergovernmental Panel on Climate Change* [Solomon, S., D. Qin, M. Manning, Z. Chen, M. Marquis, K.B. Averyt, M. Tignor and H.L. Miller (eds.)]. Cambridge University Press, Cambridge, United Kingdom and New York, NY, USA.

Broecker, W.S., and Peng, T.-H. (1982) Tracers in the Sea. Columbia University, Eldigio Press, New York, 690pp.

Brown, P.J., D.C.E. Bakker, U. Schuster, and A.J. Watson (2010). Anthropogenic carbon accumulation in the subtropical North Atlantic. *J. Geophys. Res.* 115, C04016.

Caldeira, K., and Wickett, M.E. (2005). Ocean model predictions of chemistry changes from carbon dioxide emissions to the atmosphere and ocean. *J. Geophys. Res.* 110, C09S04.

Chung, S. -N., K. Lee, R.A. Feely, C.L. Sabine, F.J. Millero, R. Wanninkhof, J.L. Bullister, R.M. Key and T.-H. Peng (2003). Calcium carbonate budget in the Atlantic Ocean based on water column inorganic carbon chemistry. *Global Biogeochem. Cycles* 17(4), 1093.

Dickson, A.G., and F.J. Millero (1987). A comparison of the equilibrium constants for the dissociation of carbonic acid in seawater media. *Deep Sea Res.* 34, 1733-1743.

Dickson, A.G. (1990). Standard potential of the reaction: $AgCl(s)+1/2H_2(g)=Ag(s)+HCl(aq)$, and the standard acidity constant of the ion HSO_4^- in synthetic seawater from 273.15 to 318.15 K. *J. Chem. Thermodyn.* 22, 113-127.

Dickson, A.G., Sabine, C.L., and Christian, J.R. (Eds.) (2007). Guide to best practices for

ocean CO_2 measurements. *PICES Special Publications 3*, pp. 191.

Dong, S., J. Sprintall, S.T. Gille, and L. Talley (2008). Southern Ocean mixed-layer depth from Argo float profiles. *J. Geophys. Res.* 113, C06013.

Egleston, E.S., C.L. Sabine, and M. Morel (2010). Revelle revisited: Buffer factors that quantify the reponse of ocean chemistry to changes in DIC and alkalinity. *Global Biogeochem. Cycles*, 24, GB1002.

Frankignoulle, M. (1994). A complete set of buffer factors for acid/base CO_2 system in seawater, *J. Mar. Syst.* 5, 111-118.

Friis, K., A. Körtzinger, J. Patsch, and D.W.R. Wallace (2005). On the temporal increase of anthropogenic CO_2 in the subpolar North Atlantic. *Deep Sea Res. Part I* 52, 681-698.

González-Dávila, M., J.M. Santana-Casiano, R.A. Fine, J. Happell, B. Delille, and S. Speich (2011). Carbonate system in the water masses of the Southeast Atlantic sector of the Southern Ocean during February and March 2008. *Biogeosciences* 8, 1401-1413.

Grasshof, K., M. Ehrhardt, and K. Kremling (1983). Methods of seawater analysis. Verlag Chemie GmbH, Weinheim.

Gruber, N., J.L. Sarmiento, and T.F. Stocker (1996). An improved method for detecting anthropogenic CO_2 in the oceans. *Global Biogeochem. Cycles* 10, 809-837.

Gruber, N. (1998). Anthropogenic CO_2 in the Atlantic Ocean. *Global Biogeochem. Cycles* 12, 165-191.

Hartin, C.A., R.A. Fine, B.M. Sloyan, L.D. Talley, T.K. Chereskin and J. Happell (2011). Formation rates of Subantarctic mode water and Antarctic intermediate water within the South Pacific. *Deep-Sea Res. I* 58, 524-534.

Hauck, J., M. Hoppema, R.G.J. Bellerby, C. Völker, and D. Wolf-Gladrow (2010). Data-based estimation of anthropogenic carbon and acidification in the Weddell Sea on a decadal timescale. *J. Geophys. Res.* 115, C03004.

van Heuven, S., D. Pierrot, E. Lewis, and D. W. R. Wallace (2011). MATLAB Program Developed for CO2 System Calculations. ORNL/CDIAC-105b. Carbon Dioxide Information Analysis Center, Oak Ridge National Laboratory, U.S. Department of Energy, Oak Ridge, Tennessee.

van Heuven, S.M.A.C., M. Hoppema, O. Huhn, H.A. Slagter, and H.J.W. de Baar (2011). Direct observation of increasing CO_2 in the Weddell Gyre along the Prime Meridian during 1973-2008. *Deep-Sea Res. II* 58, 2613-2635.

Hoppema, M., M.H.C. Stoll and H.J.W. De Baar (2000). CO_2 in the Weddell Gyre and Antarctic Circumpolar Current: austral autumn and early winter. *Mar. Chem.* 72, 203-220.

Johnson, K.M., J.M. Sieburth, P.J. Williams and L. Brändström (1987). Coulometric total carbon dioxide analysis for marine studies: Automation and calibration. *Mar. Chem.* 21, 117-133.

Karstensen, J., and D. Quadfasel (2002). Water subducted into the Indian Ocean subtropical gyre. *Deep Sea-Res. Part II* 49, 1441-1457.

Key, R.M., T. Tanhua, A. Olsen, M. Hoppema, S. Jutterström, C. Schirnick, S. van Heuven, A. Kozyr, X. Lin, A. Velo, D.W.R Wallace and L. Mintrop (2010). The CARINA data synthesis project: Introduction and overview. *Earth Syst. Sci. Data* 2, 105–121.

Lee, K., F.J. Millero, and R. Wanninkhof (1997). The carbon dioxide system in the Atlantic Ocean. *J. Geophys. Res.* 102, 15,693-15,707.

Lee, K., S.-D. Choi, G.-H. Park, R. Wanninkhof, T.-H. Peng, R.M. Key, C.L. Sabine, R.A. Feely, J.L. Bullister, F.J. Millero and A. Kozyr (2003). An updated anthropogenic CO_2 inventory in the Atlantic Ocean. *Global Biogeochem. Cycles* 17(4), 1116.

Levine, N.M., S.C. Doney, R. Wanninkhof, K. Lindsay and I.Y. Fung (2008). Impact of ocean carbon system variability on the detection of temporal increases in anthropogenic CO_2. *J. Geophys. Res.* 113, C03019.

Levine, N.M., S.C. Doney, I. Lima, R. Wanninkhof, N.R. Bates, and R.A. Feely (2011). The impact of the North Atlantic Oscillation on the uptake and accumulation of anthropogenic CO_2 by North Atlantic Ocean mode waters. *Global Biogeochem. Cycles* 25, GB3022.

Lewis, E.L., and D.W.R. Wallace (1998). Program developed for CO_2 system calculations, ORNL/CDIAC-105. Carbon dioxide information analysis center, Oak Ridge National Laboratory, U.S. Department of Energy, Oak Ridge.

Lischka, S., J. Büdenbender, T. Boxhammer, and U. Riebesell (2011). Impact of ocean acidification and elevated temperatures on early juveniles of the polar shelled pteropod Limacina helicina: mortality, shell degradation, and shell growth. *Biogeosciences* 8, 919-932.

Lo Monaco, C., C. Goyet, N. Metzl, A. Poisson and F. Touratier (2005). Distribution and inventory of anthropogenic CO_2 in the Southern Ocean: Comparison of three data-based methods. *J. Geophys. Res.* 110, C09S02.

McNeil, B.I., B. Tilbrook, and R. Matear (2001). Accumulation and uptake of anthropogenic CO_2 in the Southern Ocean, south of Australia between 1968 and 1996, *J. Geophys. Res.* 106, 31,431-31,445.

McNeil, B.I., N. Metzl, R.M. Key, R.J. Matear, and A. Corbiere (2007). An empirical estimate of the Southern Ocean air-sea CO_2 flux, *Global. Biogeochem. Cycles* 21, GB3011.

McNeil, B.I., and R.J. Matear (2008). Southern Ocean acidification: A tipping point at 450-ppm atmospheric CO_2. *Proc. Natl. Acad. Sci.* 105, 18860-18864.

Mehrbach, C., C.H. Culberson, J.E. Hawley, and R.M. Pytkowicz (1973). Measurement of the apparent dissociation constants of carbonic acid in seawater at atmospheric pressure. *Limnol. Oceanogr.* 18, 897-907.

Mémery, L., M. Arhan, X.A. Alvarez-Salgado, M.-J. Messias, H. Mercier, C.G. Castro, and A.F. Ríos (2000). The water masses along the western boundary of the south and equatorial Atlantic. *Prog. Oceanogr.* 47, 69-98.

Millero, F.J., K. Lee, and M. Roche (1998). Distribution of alkalinity in the surface waters of the major oceans. *Mar. Chem.* 60, 111-130.

Mintrop, L., F.F. Perez, M. Gonzalez-Davila, M.J. Santana-Casiano, and A. Kortzinger (2000). Alkalinity determination by potentiometry: intercalibration using three different methods. *Cienc. Marinas* 26, 23-37.

Molleri, G.S.F., Novo, E.M. L. De M, and Kampel, M. (2010). Space-time variability of the Amazon River plume based on satellite ocean color. *Cont. Shelf Res.* 30, 342-352.

Murata, A., Y. Kumamoto, K.'I. Sasaki, S. Watanabe, and M. Fukasawa (2008). Decadal increases of anthropogenic CO_2 in the subtropical South Atlantic Ocean along 30°S. *J. Geophys. Res.* 113, C06007.

Orsi, A.H., G.C. Johnson and J.L. Bullister (1999). Circulation, mixing, and production of Antarctic Bottom Water. *Prog. Oceanogr.* 43, 55-109.

Pai, S.–C., Gong, G., Liu, K.–K. (1993). Determination of dissolved oxygen in seawater by direct spectrophotometry of total iodine. *Mar. Chem.* 41, 343-351.

Peng, T.-H., R. Wanninkhof, and R.A. Feely (2003). Increase of anthropogenic CO_2 in the Pacific Ocean over the last two decades. *Deep-Sea Res. II* 50, 3065-3082.

Peng, T.-H., and R. Wanninkhof (2010). Increase in anthropogenic CO_2 in the Atlantic Ocean in the last two decades. *Deep-Sea Res. I* 57, 755-770.

Pérez, F.F., Álvarez, M., and Ríos, A.F. (2002). Improvements on the back-calculation technique for estimating anthropogenic CO_2. *Deep-Sea Res. I* 49, 859-875.

Pérez, F.F., M. Vázquez-Rodríguez, H. Mercier, A. Velo, P. Lherminier, and A.F. Ríos (2010). Trends of anthropogenic CO_2 storage in North Atlantic water masses. *Biogeosciences* 7, 1789-1807.

Peterson, R.G., and T. Whitworth (1989). The Subantarctic and Polar Fronts in relation to deep water masses through the Southwestern Atlantic. *J. Geophys. Res.* 94, 10817-10838.

Revelle, R. and H. Suess (1957). Carbon dioxide exchange between atmosphere and ocean and the question of an increase of atmospheric CO_2 during the past decades. *Tellus* 9, 18-27.

Ríos, A.F., Anderson, T.R., and F.F. Pérez (1995). The carbonic system distribution and fluxes in the NE Atlantic during Spring 1991. *Progress in Oceanography*, 35, 295-314.

Ríos, A.F., F.F. Pérez, M. Álvarez, L. Mintrop, M. González-Dávila, J.M. Santana Casiano, N. Lefèvre and A.J. Watson (2005). Seasonal sea-surface carbon dioxide in the Azores area. *Mar. Chem.* 96, 35-51.

Ríos, A.F., K.M. Johnson, X.A. Alvarez-Salgado, L. Arlen, A. Billant, L.S. Bingler, P. Branellec, C.G. Castro, D.W. Chipman, G. Roson and D.W.R. Wallace (2005). Carbon Dioxide, Hydrographic, and Chemical Data Obtained During the R/V Maurice Ewing Cruise in the South Atlantic Ocean (WOCE Section A17, 4 Janurary-21 March 1994), Carbon Dioxide Information Analysis Center, Oak Ridge National Laboratory, ORNL/CDIAC-148, NDP-084, pp. 1-27.

Ríos, A.F., Vázquez-Rodríguez, M., Padin, X.A., and Pérez, F.F. (2010). Anthropogenic carbon dioxide in the South Atlantic western basin. *J. Mar. Syst.* 83, 38-44.

Ríos, A.F., A. Velo, P.C. Pardo, M. Hoppema and F.F. Pérez (2012). An update of anthropogenic CO_2 storage rates in the western South Atlantic basin and the role of Antarctic Bottom Water. *J. Mar. Syst.* 94, 197-203.

Sabine, C.L., R.A. Feely, N. Gruber, R.M. Key, K. Lee, J.L. Bullister, R. Wanninkhof, C.S. Wong, D.W.R. Wallace, B. Tilbrook, F.J. Millero, T.-H. Peng, A. Kozyr, R. Ono and A.F. Ríos (2004). The Oceanic Sink for Anthropogenic CO_2. *Science* 305, 367-371.

Sabine, C.L. and T. Tanhua (2010). Estimation of Anthropogenic CO_2 Inventories in the Ocean.
Ann. Rev. Mar. Sci. 2(1), 175–198.

Santana-Casiano, J.M., M. González-Dávila, M.-J. Rueda, O. Llinás, and E.-F. González-Dávila (2007). The interannual variability of oceanic CO_2 parameters in the northeast Atlantic subtropical gyre at the ESTOC site. *Global Biogeochem. Cycles* 21, GB1015.

Sarmiento, J.L., N. Gruber, M.A. Brzezinski and J.P. Dunne (2004). High-latitude controls of thermocline nutrients and low latitude. *Nature* 427, 56-60.

Sievers, H.A. and W.D. Nowlin (1984). The stratification and water masses at Drake Passage. *J. Geophys. Res.* 89, 489-514.

Sloyan, B.M., and S.R. Rintoul (2001). Circulation, Renewal, and Modification of Antarctic Mode and Intermediate Water. *J. Phys. Oceanogr.* 31, 1005-1030.

Takahashi, T., W.S. Broecker, and S. Langer (1985). Redfield ratio based on chemical data from isopycnal surfaces. *J. Geophys. Res.* 90, 6907-6924.

Takahashi, T., S.C. Sutherland, R. Wanninkhof, C. Sweeney, R.A. Feely, D.W. Chipman, B. Hales, G. Friederich, F. Chavez, C. Sabine, A. Watson, D.C.E. Bakker, U. Schuster, N. Metzl, H. Yoshikawa-Inoue, M. Ishii, T. Midorikawa, Y. Nojiri, A. Kortzinger, T. Steinhoff, M. Hoppema, J. Olafsson, T.S. Arnarson, B. Tilbrook, T. Johannessen, A. Olsen, R. Bellerby, C.S. Wong, B. Delille, N.R. Bates, H.J.W. de Baar (2009). Climatological mean and decadal change in surface ocean pCO_2, and net sea-air CO_2 flux over the global oceans. *Deep-Sea Res. II* 56, 554-577.

Talley, L.D. (1996). Antarctic intermediate water in the South Atlantic. In: Wefer, G., Berger, H.H., Siedler, G., Webb, D. (Eds.), The South Atlantic: Present and Past Circulation. Springer-Verlag.

Ternon, J.F., C. Oudot, A. Dessier, and D. Diverres (2000). A seasonal tropical sink for atmospheric CO_2 in the Atlantic ocean: the role of the Amazon River discharge. *Mar. Chem.* 68, 183-201.

Touratier, F., and C. Goyet (2004). Definition, properties, and Atlantic Ocean distribution of the new tracer TrOCA. *J. Mar. Syst.* 46, 169-179.

Touratier, F., and C. Goyet (2004). Applying the new TrOCA approach to assess the distribution of anthropogenic CO_2 in the Atlantic Ocean. *J. Mar. Syst.* 46, 181-197.

Touratier, F., L. Azouzi, and C. Goyet (2007). CFC-11, $\Delta^{14}C$ and ^3H tracers as a means to assess anthropogenic CO_2 concentrations in the ocean. *Tellus 59B,* 318-325.

Vázquez-Rodríguez, M., F. Touratier, C. Lo Monaco, D.W. Waugh, X.A. Padin, R.G.J. Bellerby, C. Goyet, N. Metzl, A.F. Ríos, and F.F. Pérez (2009). Anthropogenic carbon distributions in the Atlantic Ocean: data-based estimates from the Arctic to the Antarctic. *Biogeosciences* 6, 439-451.

Vázquez-Rodríguez, M., X.A. Padin, A.F. Ríos , R.G.J. Bellerby, and F.F. Pérez (2009). An upgraded carbon-based method to estimate the anthropogenic fraction of dissolved CO_2 in the Atlantic Ocean. *Biogeosciences Discuss.* 6, 4527-4571.

Vázquez-Rodríguez, M., F.F. Pérez, A. Velo, A.F. Ríos, and H. Mercier (2012). Observed acidification trends in North Atlantic water masses. *Biogeosciences* 9, 5217-5230.

Wallace, D. (2001). Storage and transport of excess CO_2 in the ocean: The JGOFS/WOCE global CO_2 survey, in *Ocean Circulation and Climate*, edited by G. Siedler et al., pp. 489-521, Academic, San Diego, California.

Wanninkhof, R., S.C. Doney, J.L. Bullister, N.M. Levine, M. Warner, and N. Gruber (2010). Detecting anthropogenic CO_2 changes in the interior Atlantic Ocean between 1989 and 2005. *J. Geophys. Res*. 115, C11028.

Waugh, D.W., T.M. Hall, B.I. McNeil, R. Key, and R.J. Matear (2006). Anthropogenic CO_2 in the oceans estimated using transit time distributions. *Tellus 58B*, 376-389.

Winkler, L.W. (1888). Die Bestimmung des im Wasser gelösten Sauerstoffes, *Chem. Berichte, 27*, 2843-2855.

Wong, A.P.S., N.L. Bindoff, and J.A. Church (1999). Large-scale freshening of intermediate waters in the Pacific and Indian oceans. *Nature* 400, 440-443.

Yool, A., A. Oschlies, A.J.G. Nurser, and N. Gruber (2010). A model-based assessment of the TrOCA approach for estimating anthropogenic carbon in the ocean. *Biogeosciences* 7, 723-751.

Chapter 7

Summary and Recommendations

7.1 Summary

Objectives

The object of this research was to investigate the buffering capacity of coastal and ocean systems of the Atlantic Ocean in light of the uptake of anthropogenic atmospheric carbon dioxide in these regions. A combination of data collected from nine cruises, a moored pCO_2 instrument and a three-year, on-going time-series have facilitated the analysis presented here. The different approaches to monitoring the oceanic carbonate system reflect the amount of variability in the different systems, which also present different challenges to discern the anthropogenic CO_2 trends from natural trends. The synthesis of all these approaches provides a comprehensive study of carbon dynamics in the Atlantic Ocean.

Internal Consistency

The fundamental thermodynamic principles governing the carbonate system in the ocean were published by Park in 1969. The equations outlined in this body of work were written primarily for use in deep waters, which are not in contact with the atmosphere or in the presence of substantial biological activity. The subsequent application of these equations to other marine environments is thus likely to introduce errors into the calculations as some of the governing assumptions no longer apply. It is thus not surprising perhaps, that when calculating a carbonate system parameter from two others, there is always an associated error (Wanninkhof et al., 1999; McElligott et al., 1998). In Chapter 2 we find that the error between calculated and measured parameters in the coastal ocean is approximately two times greater than that of the open ocean (Lee et al., 1997).

The diverse environments provided by the North Sea were successfully used to examine how the internal consistency varies between them. The most significant result was potentially the increasing difference between the performance of different carbonic acid dissociation constants in low salinity waters compared to high salinity waters. In the open ocean the differences are not noticeable, however, in coastal regions where the salinity falls below typical ocean values, the recommended constants of Mehrbach et al. (1973), refit by Dickson and Millero (1987) are no longer the most representative. Due to the increasingly large amount of work being carried out in coastal regions, this has large implications for future calculations of the carbonate system in these areas.

In higher salinity waters, which constitute the majority of the North Sea, the differences in internal consistency observed between different K_1 and K_2 parameterizations became insignificant compared to that caused by the input combinations for the calculations. All seasons displayed a similar level of internal consistency, with the exception of spring, which

was significantly worse. This is consistent with the findings of Koeve et al. (2011) and Hoppe et al. (2012) who both observe poor internal consistency in algal cultures and waters of high biological activity, which has been attributed to the contribution of organic matter to alkalinity. Here we show the same effect in a natural environment, however, again using the different biogeochemical regimes provided by the North Sea – the northern North Sea and southern North Sea – we find greater internal consistency in the south, which is associated with higher organic matter, indicating that this is not the primary cause of non-consistency in calculations. Instead, we can link this north-south pattern in internal consistency to the ratio of A_T:DIC, as noted by Lee et al. (1996). This study could not conclusively prove the source of errors in the calculations, and we find that this is an area, which would benefit from further work to better understand the carbonate system in coastal regions.

Terrestrial Significance

The influence of near-shore systems on coastal waters cannot be underestimated in studies of the carbon cycle. An example of this in the North Sea is the considerable influence of the Wadden Sea, which supplies large amounts of DIC and A_T to the southern North Sea throughout the year (Brasse et al., 1999; Thomas et al., 2009). In 2008 a time-series of A_T and DIC measurements was started in the Marsdiep basin – the largest basin of the Wadden Sea, facilitating an investigation into the controls of these parameters throughout the year (Chapter 3). Both DIC and A_T demonstrate a clear seasonal signal, with decreasing values throughout spring to late summer, and increasing values from summer to mid-winter. Whilst this pattern for DIC is easily explained by the annual cycle of photosynthesis, the A_T cycle shows the direct inverse to that of the adjacent southern North Sea and other coastal systems (Hydes et al., 2012). We deduce that the A_T fluctuations appear to be predominantly an effect of redox reactions within the nitrogen cycle highlighting the close interaction between nitrogen and carbon in the coastal environment. Furthermore, the magnitude of A_T generation between years appears to be linked to the initial diatom bloom, whose size is likely determined by the wintertime silicate concentration. The close interaction of sediment, water column and atmosphere in the Marsdiep leads to a high level of codependence between the carbonate system and phytoplankton succession and associated remineralization processes. The time series data presented is complemented by the collection of a broad range of chemical parameters facilitating such analysis. Despite this, a large number of assumptions must be made to localize the processes taking place in the carbon and nitrogen cycles. Further understanding of this system requires additional research into sedimentological processes and their impact on the water column, as in the Wadden Sea benthic remineralization can constitute up to 50% of remineralization (van Beusekom et al., 1999).

The Ocean Signal

The other significant influence on coastal regions, such as the North Sea, is the dominating ocean signal. Observations obtained in the late summer of 2001 and 2005 indicated a large decrease in the air-sea partial pressure difference of CO_2 (ΔpCO_2), which is consistent with a decrease in the buffering capacity of the ocean. The same phenomenon was also observed in the adjacent North Atlantic Ocean (Lefèvre et al., 2004; Schuster and Watson, 2007; Thomas et al., 2008), indicating that it was not a local effect. An additional dataset collected in the late summer of 2008 complicated the matter by demonstrating no further change in buffering capacity or disproportionate ΔpCO_2 thus leaving the reduction in buffering capacity between 2001 and 2005 unexplained. The change observed in the North Atlantic Ocean was attributed to the effects of the North Atlantic Oscillation Index, a measure of atmospheric pressure difference between the Azores and Iceland. The NAO was shown to exert significant control on the carbonate system in the North Atlantic Ocean, which thus supplies the majority of water and carbon to the North Sea, making it vital to understand these effects on a large scale so that we can anticipate the effects on a coastal scale.

The third occupation of the North Sea in 2008 facilitated the analysis of the effects of different NAO states on the carbonate system in the North Sea, as 2001, 2005 and 2008 coincided with years of negative, neutral and positive NAO indices, respectively (Chapter 4). The effects of NAO on the carbonate system in the North Sea are not all direct, as NAO influences precipitation patterns and water column stratification, which affect riverine runoff and phytoplankton blooms. The NAO also causes changes in the hydrographic properties of seawater, such as salinity and temperature, which directly impact the carbonate system. Within the North Sea, between the three years, we observed an increase in the DIC North Atlantic end member from 2001 to 2005 coinciding with a decrease in the DIC Baltic Sea end member. The latter being driven by greater precipitation over Scandinavia, the former being driven by changes in salt and heat exchange in the subtropical gyre of the North Atlantic Ocean. These changes led to an overall increase in the carbon inventory of the North Sea. From 2005 to 2008, which signified a change from neutral to positive NAO, there was no significant changes to the end members, however, the warmer summer combined with stronger North Atlantic inflow led to differences in mixing and mixed-layer depth and caused a strong gradient of pH between the southern North Sea and the northern North Sea. The sheer number of ways in which the NAO affects the North Sea make each change difficult to constrain and taking into account the varying time scales on which they operate complicates things further. However, we conclusively show that these effects are large enough to completely mask the expected increase in CO_2 driven by anthropogenic atmospheric increases.

Short-scale Perturbations

On the other side of the North Atlantic Ocean, the Scotian Shelf is a coastal system with more direct ocean influence. Chapter 5 sees the use of high-frequency CO_2 data to explain the diel carbon cycle throughout the year on the Scotian Shelf. Despite falling within the temperate latitude band, the Scotian Shelf constitutes an annual source of CO_2 to the atmosphere (Shadwick et al., 2011). During periods of warming (from April to August) a clear diel signal becomes apparent. Temperature-normalization was used to separate the temperature and biological controls on pCO_2 allowing us to identify the onset of net photosynthetic drawdown of CO_2, which lags the onset of photosynthetically available radiation (PAR) by up to 5 hours. The pCO_2 change attributed to biology was then further used to compute net community production (NCP). The maximum NCP calculated was 3.4 mol C m^{-2}, however NCP demonstrated a reduction up to 90% during summer time associated with the minimum in mixed layer depth. These results emphasize the significance of taking diel variability into account when working with pCO_2 data, as extrapolation of a value from different times of day can lead to substantial error margins.

Long-term Perturbations

On long time scales (>10 years) the ocean's role in anthropogenic carbon sequestration becomes much more significant than that of the coastal ocean. The Atlantic Ocean contains the highest proportion of global oceanic anthropogenic CO_2 per surface area (Sabine et al., 2004) and recent basin-wide inventories indicate that, currently, more effective uptake of Cant occurs in the southern half of the basin (Wanninkhof et al., 2010). The reoccupation of the historical WOCE A17 (1994) cruise track in 2010/11 facilitated a study of increasing Cant in the southwest Atlantic Ocean over more than a decade (Chapter 6). Using a combined approach of eMLR and ϕC_T^0 methods, we quantified the increase in Cant, which took place between 1994 and 2010/11 and calculated the associated change in pH. The largest C_{ant} increase of 37 $\boldsymbol{\mu}$mol kg^{-1} occurred in the SubAntarctic Zone, which is a well-documented CO_2 sink, whereas the deep waters (Antarctic Bottom Water, lower North Atlantic Deep Water, and lower Circumpolar Deep Water) showed no significant increases. Comparison of the calculated changes in Cant to changes in pH reveal the lowest buffering capacities, of the present water masses, lie in the mode and intermediate water masses. Thus, the increases in DIC have greater impact on pH in these two water masses. The significant Cant accumulation in these regions, accompanied by their high sensitivity to CO_2 increases, has caused a rapid drop in pH. If the current, calculated rate of increase of C_{ant} continues, we predict that these waters will be under-saturated with respect to aragonite by the year 2104.

Conclusions

This thesis has shown the importance of a multi-faceted approach to studying the ocean carbonate system. In temperate, coastal regions high frequency measurements are required in addition to measurements taken over longer time scales. The large amount of primary production which is supported in these regions mean that significant changes can occur over a few years, thus to put these changes in the context of change driven by anthropogenic forcing, a multitude of scales is necessary.

7.2   Recommendations

This thesis was designed to build upon previous work undertaken in the North Sea, using the datasets to quantitatively and qualitatively describe the changes in the North Sea carbonate system caused by anthropogenic CO_2 invasion. Due to the highly variable nature of coastal regions, this work was complemented by a time-series of carbon measurements adjacent to the North Sea, which began at the start of this PhD, and additional datasets from the Atlantic Ocean.

Limitations in oceanic carbon studies due to lack of internal consistency in the thermodynamic calculations remains a problem in this field. In this work we present the findings from the first internal consistency study conducted in a coastal environment on a seasonal scale (see Chapter 2). Our results support previous findings of a significant decrease in consistency between measured and calculated parameters in waters of high biological activity, which occur seasonally in temperate environments. Furthermore, even in abiotic waters, the internal consistency of coastal waters never reaches the same reproducibility found in open ocean waters. The presence of unaccounted for contributors to alkalinity is a very likely source of errors here. The field would greatly benefit from dedicated research in this area, as such a large number of studies rely on measuring two carbonate parameters and calculating one or two of the carbonate parameters. This is also an issue in lab environments, where algal cultures are grown in different CO_2 concentrations. In these experiments the quantity of water available for analysis is often limited, leading to analysis of two carbonate parameters and calculation of the remaining two.

One of the greatest challenges in temperate, coastal regions is to accurately constrain the CO_2 fluxes between the atmosphere and surface waters. The diversity of coastal regions means that each area is distinctly unique in behavior, thus making it impossible to extrapolate the results from one region to another. Whilst cruises offer excellent data coverage over an area, they are temporally limited as they offer just a 'snapshot' of the system at a particular time. The seasonal variability in temperate, coastal environments severely limits the use of such data to examine long-term CO_2-driven trends, or even annual deductions as to whether an area is an overall source or sink of CO_2 to the atmosphere. In the North Sea this problem has been largely helped by expeditions carried out in all four seasons. It is further resolved by the time-series measurements carried out at the NIOZ jetty. Until these time-series reach the maturity at which they can capture the natural variation exerted by climate forcing, there is a strong reliance on models to fill in the temporal gaps.

Modeling is one branch of investigation, which is not explored in this thesis, however, should not be overlooked. The ability of models to accurately represent the natural world provides a valuable tool against which to validate theories and to predict possible future scenarios. To facilitate the most correct portrayal it is vital to have a sound understanding of the underlying processes and how, and under what conditions they occur. As such, one should not neglect the importance of simple process studies, to determine the rates and pathways of carbon through the various pools (e.g. dissolved inorganic carbon, particulate inorganic carbon…) in coastal regions. Whilst this is not dealt with in this thesis, it is an area, which currently lacks quantitative information. The cycling of carbon in different environments is as varied as air-sea CO_2 fluxes, and thus efforts should also be made to understand the rates, and timescales, at which these processes operate.

An invaluable tool, which I would recommend here, would be the deployment of a continuous, underway monitoring device, such as a pCO_2 sensor, or pH measurement device. There has been a community-wide effort to develop such autonomous instruments over the past twenty years with great success. The data collected from such a device in the Scotian Shelf (see Chapter 5) has shown how valuable this data can be in capturing high-frequency data and determining the drivers of annual CO_2 fluxes in a region. Such data helps us to understand the dominant controls of air-sea CO_2 fluxes and thus better able to predict them in the future. The frequency of such measurements also allows us to examine processes occurring over a wide-range of time scales. A valuable, additional extension of such work is to relate the high-frequency CO_2 signal, with additional measured parameters, such as temperature, PAR, to satellite ocean colour measurements to extrapolate relationships between these parameters. The use of ocean color and satellite derived measurements to help quantify CO_2 fluxes and biological production holds great potential for future research, as it offers global coverage for relatively small monetary and time investments.

Since the production of certified reference material for dissolved inorganic carbon and total alkalinity there has been a substantial increase in the inter-comparability of carbon measurements between cruises and laboratories. Such improvements have facilitated the application of methods of anthropogenic carbon determination (e.g. TrOCA, ϕC_T^0) as well as the accurate quantification of changes in inorganic carbon between two measurement times (e.g. eMLR, ΔC^*). Such analyses are becoming increasingly popular and provide valuable insight to the destination of atmospheric anthropogenic CO_2, however, Brown et al. (2010) have shown that climatic forcing in the North Atlantic Ocean exerts a significant control on the annual CO_2 sink. It is likely that a similar process affects the uptake in other ocean basins, again stressing the importance of multiple occupations coupled with long time-series measurements.

On a global scale the Atlantic Ocean is the most studied Ocean with regards to the carbonate system. This could partly be because it contains the highest proportion of anthropogenic carbon of all the oceans, however, it is more likely due to the fact that it is bordered by the worlds' wealthiest countries, which have a vested interest in it. It thus follows that the seas and coasts of the worlds' poorest countries remain somewhat of a 'black box' with regards to carbon observations. Some of these systems are located in significant upwelling systems, and may provide further insight into the cycling, distribution and fate of carbon in the coastal region. Whilst a number of programs are in place to aid the development of science and facilitate research in these regions, I recommend further efforts to fill in these spatial holes in ocean carbon research and hopefully, simultaneously, holes in knowledge.

References

Brasse, S., A. Reimer, R. Seifert, and W. Michaelis (1999). The influence of intertidal mudflats on the dissolved inorganic carbon and total alkalinity distribution in the German Bight, southeastern North Sea. *J. Sea Res.* 42, 93-103.

Brown, P.J., D.C.E. Bakker, U. Schuster, and A.J. Watson (2010). Anthropogenic carbon accumulation in the subtropical North Atlantic. *J. Geophys. Res.* 115, C04016.

van Beusekom, J.E.E.., U.H. Brockmann, K.-J. Hesse, W. Hickel, K. Poremba, U. Tillmann, (1999). The importance of sediments in the transformation and turnover of nutrients and organic matter in the Wadden Sea and German Bight. *Ger. J. Hydrogr.* 51, 245-266.

Hoppe, C.J.M., G. Langer, S.D. Rokitta, D.A. Wolf-Gladrow and B. Rost (2012). Implications of observed inconsistencies in carbonate chemistry measurements for ocean acidification studies. *Biogeosciences* 9, 2401-2405.

Hydes, D.J., Kelly-Gerreyn, B.A., Le Gall, A.C., Proctor, R., (1999), The balance of supply of nutrients and demands of biological production and denitrification in a temperate latitude shelf sea – a treatment of the southern North Sea as an extended estuary. Marine Chemistry, 68, 117-131.

Kempe, S., and K. Pegler (1991). Sinks and sources of CO2 in coastal seas: the North Sea. *Tellus* 43B, 224-235.

Koeve, W., H.-C. Kim, K. Lee, and A. Oschlies (2011). Potential impact of DOC accumulation on fCO2 and carbonate ion computations in ocean acidification experiments. *Biogeosciences Discuss.* 8, 3797-3827.

Lee, K., F.J. Millero, and D.M. Campbell (1996). The reliability of the thermodynamic constants for the dissociation of carbonic acid in seawater. *Mar. Chem.* 55, 233-245.

Lee, K., F. Millero, and R. Wanninkhof (1997). The carbon dioxide system in the Atlantic Ocean. *J. Geophys. Res.* 102, 15693-15707.

Lefèvre, N., A.J. Watson, A. Olsen, A.F. Rios, F.F. Perez, and T. Johannessen (2004). A decrease in the sink for atmospheric CO_2 in the North Atlantic. *Geophys. Res. Lett.* 31, L07306.

McElligott, S., R.H. Byrne, K. Lee, R. Wanninkhof, F.J. Millero, and R.A. Feely (1998). Discrete water column measurements of CO2 fugacity and pHT in seawater: A comparison of direct measurements and thermodynamic calculations. *Mar. Chem.* 60, 63-73.

Park, K. P. (1969). Oceanic CO2 System: An evaluation of ten methods of investigation. *Limnol. Oceanogr.* 14, 179-186.

Pérez, F.F., M. Vázquez-Rodríguez, H. Mercier, A. Velo, P. Lherminier, and A.F. Ríos (2010). Trends of anthropogenic CO_2 storage in North Atlantic water masses. *Biogeosciences* 7, 1789-1807.

Schuster, U., and A. J. Watson (2007). A variable and decreasing sink for atmospheric CO_2 in the North Atlantic, *J. Geophys. Res.* 112, C11006.

Shadwick, E.H., H. Thomas, K. Azetsu-Scott, B.J.W. Greenan, E. Head and E. Horne (2011). Seasonal variability of dissolved inorganic carbon and surface water pCO2 in the Scotian Shelf region of the Northwestern Atlantic. *Mar. Chem.* 124, 23-37.

Thomas, H., Y. Bozec, K. Elkalay, H.J.W. de Baar, A.V. Borges and L.-S. Schiettecatte (2005). Controls of the surface water partial pressure of CO2 in the North Sea. *Biogeosciences* 2, 323-334.

Thomas, H., A.E.F. Prowe, I.D. Lima, S.C. Doney, R. Wanninkhof, R.J. Greatbatch, U. Schuster and A. Corbière (2008). Changes in the North Atlantic Oscillation influence CO2 uptake in the North Atlantic over the past 2 decades. *Global Biogeochem. Cycles* 22, GB4027.

Thomas, H., L.-S. Schiettecatte, K. Suykens, Y.J.M. Koné, E.H. Shadwick, A.E.F. Prowe, Y. Bozec, H.J.W. de Baar, A.V. Borges (2009). Enhanced ocean carbon storage from anaerobic alkalinity generation in coastal sediments. *Biogeosciences* 6, 267-274.

Vázquez-Rodríguez, M., F.F. Pérez, A. Velo, A.F. Ríos, and H. Mercier (2012). Observed acidification trends in North Atlantic water masses. *Biogeosciences* 9, 5217-5230.

Wanninkhof, R., E. Lewis, R.A. Feely, and F.J. Millero (1999). The optimal carbonate dissociation constants for determining surface water pCO2 from alkalinity and total inorganic carbon. *Mar. Chem.* 65, 291 - 301.

Wanninkhof, R., S.C. Doney, J.L. Bullister, N.M. Levine, M. Warner, and N. Gruber (2010). Detecting anthropogenic CO2 changes in the interior Atlantic Ocean between 1989 and 2005. *J. Geophys. Res.* 115, C11028.

Nederlandse samenvatting

Koolstof is de meest fundamentele bouwsteen van het leven op deze planeet en het vierde meest overvloedige element in het universum. Met het begin van de Industriële Revolutie aan het einde van de 18e eeuw, de mens heeft versneld kooldioxide (CO_2) uitgestoten aan de atmosfeer door verbranding van fossiele organische koolstof welke voorheen voor lange termijn lagen opgeslagen. In de 20e eeuw is de atmosferische CO_2-concentratie met meer dan 20% gestegen, en het stijgingspercentage neemt nog steeds toe. Een groot deel van deze CO_2 wordt opgenomen door de oceanen, veranderen de chemie van zeewater in het proces, die kan potentieel hebben ontzettende gevolgen voor organismen leven in de oceaan en voor de toekomstige beperking van verdere atmosferische CO_2-stijgingen.

Eén van de belangrijkste vragen is hoeveel CO_2 wordt opgenomen door de oceanen en in welke gebieden dit het meest effectief gebeurt? Van continentale zeeën is al langer bekend dat hun bijdrage aan de primaire productie met betrekking tot hun oppervlakte onevenredig groot is, waardoor onderzoek in deze gebieden van groot belang is. Voor dit proefschrift is het carbonaat-systeem in de continentale zeeën, de kustwateren, en de open Atlantische Oceaan onderzocht om het lot en gevolgen van antropogene emissies van CO_2 in elk van deze omgevingen te bepalen.

Voordat we kunnen bepalen hoeveel en welk soort koolstof er in de oceanen is, moeten we begrijpen hoe goed onze metingen de werkelijkheid vertegenwoordigen. De thermodynamische grondbeginselen voor het carbonaat-systeem in de oceaan werden gepubliceerd door Park in 1969. De vergelijkingen die hierin werden voornamelijk geschreven voor gebruik in diepe wateren, die niet in contact zijn geweest met de atmosfeer en waarin weinig biologische activiteit plaatsvindt. Verdere toepassing van deze vergelijkingen in andere mariene milieus zal dus waarschijnlijk fouten introduceren in de berekeningen gezien sommige van de regerende veronderstellingen niet langer van toepassing zijn. Hier vinden we dat de fout tussen berekende en gemeten parameters in de kust gebieden ongeveer twee keer groter is dan die van de open oceaan.

De uiteenlopende milieus van de Noordzee werden vervolgens gebruikt om aan te tonen dat er een toenemend verschil is tussen de werking van verschillende koolzuurdissociatieconstanten in lager zoutgehalte wateren in vergelijking met hoge zoutgehalte wateren. In de open oceaan, zijn die verschillen zijn niet merkbaar, echter in kustregio's waar het zoutgehalte lager is dan typische oceaanwaarden, zijn de aanbevolen constanten van Mehrbach et al. (1973), refit Dickson en Millero (1987), niet langer de meest representatieve. Vanwege de steeds grotere hoeveelheid onderzoek dat wordt verricht in de kustregio's, heeft dit grote gevolgen voor de toekomstige berekening van het carbonaat-systeem in deze gebieden.

Terrestrische betekenis

De invloed van estuarine en getijden systemen mag in studies naar de koolstofcyclus in kustwateren niet worden onderschat. In 2008 startte een serie van A_T en DIC metingen in het Marsdiepbekken – de grootste bekken van de Waddenzee, om onderzoek naar de regulatie van deze parameters gehele jaar (hoofdstuk 3) te vergemakkelijken. Zowel DIC als A_T tonen een duidelijk seizoensgebonden signaal, met dalende waarden gedurende de lente tot de late zomer, en de oplopende waarden van zomer naar midwinter. Terwijl dit patroon voor DIC gemakkelijk te verklaren is door de jaarlijkse cyclus van fotosynthese verklaren is, toont de A_T-cyclus de directe inverse aan van de aangrenzende zuidelijke Noordzee. De schommelingen in de A_T-cyclus wordt veroorzaakt door een overheersend effect van redoxreacties binnen de stikstofcyclus en laten daarmee de nauwe interactie tussen stikstof en koolstof in de kust omgeving zien. Deze tijdreeksen zijn aangevuld met een breed scala aan chemische parameters ter vergemakkelijking van een dergelijke analyse. Ondanks dit, moet een groot aantal veronderstellingen worden gemaakt om processen die plaatsvinden in de koolstof en stikstofcycli te lokaliseren. Verder begrip van dit systeem vereist extra onderzoek naar sedimentologische processen en hun impact op de waterkolom.

Het signaal van de oceaan

De andere significante invloed op kustregio's, zoals de Noordzee, is het overheersende oceaansignaal. Drie bezettingen van de Noordzee tijdens perioden met een positieve, negatieve en neutrale Noord Atlantische Oscillatie index (NAO) vergemakkelijkt de analyse van de effecten van verschillende NAO regimes op het carbonaat-systeem in de Noordzee (hoofdstuk 4). De invloeden van de NAO op het carbonaat-systeem in de Noordzee zijn niet altijd direct, zoals bijvoorbeeld de NAO invloeden op neerslagpatronen en stratificatie van de waterkolom, die weer gevolgen hebben voor afvoer door rivieren en fytoplanktonbloeien. Daarnaast zorgt de NAO ook voor wijzigingen in de hydrografische eigenschappen van zeewater, zoals zoutgehalte en temperatuur, die rechtstreeks van invloed zijn het carbonaat-systeem. Tussen de drie verschillende jaren zien we dat in de Noordzee dat een DIC toename in het Noord Atlantische-aandeel van 2001 tot 2005 samenvalt met een daling in DIC in het Oostzee-aandeel. Het Oostzee-aandeel wordt veroorzaakt door meer neerslag over Scandinavië, terwijl het Noord Atlantische-aandeel wordt veroorzaakt door veranderingen in zout- en warmte-uitwisseling in de subtropische gyre van de Noord-Atlantische oceaan.

Deze veranderingen leidden tot een algemene toename van de koolstofvoorraad koolstof in de Noordzee. Van 2005 tot 2008, dat een overgang van neutrale naar positieve NAO betekende, was er geen significante veranderingen in de DIC concentratie van de verschillende water aandelen. Echter, de warmere zomer in 2008, gecombineerd met sterkere Noord-Atlantische instroom leidde tot verschillen in mengen en de diepte van de in de diepte

van de gemengde laag en veroorzaakte een sterke verloop van pH tussen de zuidelijke en de noordelijke Noordzee. Het aantal manieren waarop de NAO invloed heeft op de Noordzee maakt het moeilijk elke wijziging te beperken en rekeninghoudend met de verschillende tijdschalen waarop ze opereren bemoeilijkt de analyse nog meer. Echter blijkt onomstotelijk dat deze effecten groot genoeg zijn om de verwachte toename in CO_2, gedreven door antropogene atmosferische verhogingen, volledig te maskeren.

Korte termijn verstoringen

Aan de andere kant van de Noord-Atlantische oceaan ligt de Scotian plat, een kustsysteem met meer directe invloed van de oceaan. Hoofdstuk 5 laat het gebruik van hoge-frequentie CO_2-gegevens zien om de dagelijkse koolstofcyclus gedurende het hele jaar op de Scotian plat om uit te leggen. Ondanks dat the Scotion plat op op een gematigde latitude ligt, vormt de Scotian plat een jaarlijkse bron van CO_2 naar de atmosfeer (Shadwick et al., 2011). Tijdens perioden van opwarming van de aarde (van April tot augustus) wordt er een duidelijk diel signaal zichtbaar. Temperatuur-normalisatie werd gebruikt om de temperatuur en biologische effect op pCO_2 te onderscheiden, waardoor het mogelijk is het begin van de netto fotosynthetische vermindering van CO_2 te bepalen, ondanks dat deze tot 5 uren achterloopt op het begin van fotosynthetische beschikbaar straling (PAR). De pCO_2 verandering toegeschreven aan biologie werd vervolgens verder gebruikt voor het berekenen van netto community productie (NCP). De maximale NCP berekend was 3.4 mol C m^{-2}, maar NCP liet een vermindering tot 90% tijdens de zomer, welke wordt geassocieerd met een minimum in de diepte van de gemengde laag. Deze resultaten benadrukken het belang om de diel variabiliteit mee te nemen bij het werken met pCO_2 gegevens, omdat extrapolatie van een waarde uit verschillende tijden van de dag tot substantiële fout marges leiden kan.

Lange termijn verstoringen

Op lange termijn (> 10 jaar) wordt de rol van de oceaan in het vastleggen van antropogeen koolstofveel belangrijker dan de rol van de kustgebieden. De Atlantische oceaan bevat het hoogste percentage van globale oceanische antropogene CO_2 emissies (Sabine et al., 2004) en recente inventarisaties van voorraden geven aan dat op dit moment meer C_{ant} effectief wordt opgenomen in de zuidelijke helft van het bekken (Wanninkhof et al., 2010). De herbezetting van de historische WOCE A17 (1994) cruise track in 2010/11 maakt een studie naar toenemende C_{ant} in de zuidwestelijke Atlantische oceaan over een tijdsperiode langer dan een dan een decennium mogelijk (hoofdstuk 6). Met behulp van een gecombineerde aanpak van eMLR en ϕC_T^0 methoden, is de toename van C_{ant}, die plaatsvond tussen 1994 en 2010/11 en de bijbehorende wijziging in pH gekwantificeerd. De grootste C_{ant} toename van 37 µmol kg^{-1} is opgetreden in de SubAntarctic Zone, die een goed gedocumenteerde CO_2-opslag is. Anderzijds blijkt dat de diepe wateren (Antarctische Bottom lower North Atlantic

Deep Water en lower Circumpolar Deep Water) geen significante toenames heeft plaatsgevonden.

Een vergelijking van de berekende veranderingen in C_{ant} ten opzichte van veranderingen in de pH laten zien dat de laagste buffercapaciteit van de huidige water massa, liggen in de mode en intermediate watermassa's. De stijging van DIC het dus een grotere impact op de pH in deze twee watermassa's. De aanzienlijke C_{ant} accumulatie in deze regio's, vergezeld met hun hoge gevoeligheid om CO_2 te laten toenemen, heeft geleid tot een snelle daling in pH. Als de huidige, berekende stijgingspercentage van C_{ant} constant blijft, voorspellen we dat deze wateren onderverzadigd met betrekking tot aragoniet zullen worden in 2104.

Conclusies

Dit proefschrift heeft het belang aangetoond van een veelzijdige aanpak bij het bestuderen van de oceaan carbonaatsysteem. In gematigde, kustgebieden zijn hoogfrequente metingen vereist naast metingen die op langere tijdschalen worden verricht. De grote hoeveelheid primaire productie die wordt ondersteund in deze regio's betekenen dat aanzienlijke wijzigingen kunnen plaatsvinden in een paar jaar. Om deze veranderingen in de context van verandering gedreven door antropogene invloeden te plaatsen zijn metingen op verschillende tijdshalen essentieel.

References

Al-Raei, A.M., K. Bosselmann, M.E. Böttcher, B. Hespenheide, F. Tauber (2009). Seasonal dynamics of microbial sulfate reduction in temperature intertidal surface sediments: controls by temperature and organic matter. *Ocean Dynamics* 59, 351-370.

Álvarez, M., C. Lo Monaco, T. Tanhua, A. Yool, A. Oschlies, J. L. Bullister, C. Goyet, N. Metzl, F. Touratier, E. McDonagh, and H. L. Bryden (2009). Estimating the storage of anthropogenic carbon in the subtropical Indian Ocean: a comparison of five different approaches. *Biogeosciences* 6, 681-703.

Álvarez, M., T. Tanhua, H. Brix, C. Lo Monaco, N. Metzl, E. L. McDonagh, and H. L. Bryden (2011). Decadal biogeochemical changes in the subtropical Indian Ocean associated with Subantarctic Mode Water. *J. of Geophys. Res.* 116, C09016.

Anderson, L. A., and J. L. Sarmiento (1994). Redfield ratios of remineralization determined by nutrient data analysis. *Global Biogeochem. Cycles* 8, 65-80.

Archer, D. (2005). Fate of fossil fuel CO_2 in geologic time. *J. of Geophys. Res.* 110, C09S05.

Artioli, Y., J. C. Blackford, M. Butenschön, J. T. Holt, S. L. Wakelin, H. Thomas, A. V. Borges and J. I. Allen (2012). The carbonate system in the North Sea: Sensitivity and model validation. *J. of Mar. Syst.* 102-104, 1-13.

Averyt, K.B., M. Tignor and H.L. Miller. Cambridge University Press, Cambridge, United Kingdom and New York, NY, USA, 996 pp.

Bakker, C., P.M.J. Herman, and M. Vink (1994). A new trend in the development of the phytoplankton in the Oosterschelde (SW Netherlands) during and after the construction of a storm-surge barrier. *Hydrobiologia* 283, 79-100.

Barth, S. (1998). [11]B/[10]B variations of dissolved boron in a freshwater-seawater mixing plume (Elbe Estuary, North Sea). *Mar. Chem.* 62, 1 - 14.

Bates, N. R. (2001). Interannual variability of oceanic CO_2 and biogeochemical properties in the Western North Atlantic subtropical gyre. *Deep-Sea Res. II* 48, 1507-1528.

Bates, N.R., L. Samuels and L. Merlivat (2001). Biogeochemical and physical factors influencing seawater fCO_2 and air-sea CO_2 exchange on the Bermuda coral reef. *Limnol. Oceanogr*. 46(4), 833–846.

Beck, M., and H. –J. Brumsack (2012). Biogeochemical cycles in sediment and water column of the Wadden Sea: The example Spiekeroog Island in a regional context. *Ocean and Coastal Management* 68, 102-113.

Bednaršek, N., G. A. Tarling, D.C.E. Bakker, S. Fielding, E.M. Jones, H.J. Venables, P. Ward, A. Kuzirian, B. Lézé, R. A. Feely and E.J. Murphy (2012). Extensive dissolution of live pteropods in the Southern Ocean. *Nature Geoscience* 5, 881-885.

Beldowski, J., A. Löffler, B. Schneider and L. Joensuu (2010). Distribution and biogeochemical control of total CO_2 and total alkalinity in the Baltic Sea. *Journal of Marine Systems* 81, 252-259.

Belkin, I. M. (2004). Propagation of the "Great Salinity Anomaly" of the 1990s around the Northern Atlantic. *Geophys. Res. Lett.* 31, L08306.

van Beusekom, J. E. E., U. H. Brockmann, K.-J. Hesse, W. Hickel, K. Poremba, U. Tillmann (1999). The importance of sediments in the transformation and turnover of nutrients and organic matter in the Wadden Sea and German Bight. *German Journal of Hydrography* 51, 245-266.

van Beusekom, J. E. E., De Jong, V. N., 2002. Long-term changes in Wadden Sea nutrient cycles: importance of organic matter import from the North Sea. *Hydrobiologia* 475/476, 185-194.

van Beusekom, J. E. E., M. Loebl, P. Martens (2009). Distant riverine nutrient supply and local temperature drive the long-term phytoplankton development in a temperate coastal basin. *J. of Sea Res.* 61, 26-33.

van Beusekom, J. E. E., de Jonge, V. N., 2012. Dissolved organic phosphorus: An indicator of organic matter turnover? *Est. Coast. and Shelf Sci.* 108, 29-36.

Bindoff, N.L., J. Willebrand, V. Artale, A, Cazenave, J. Gregory, S. Gulev, K. Hanawa, C. Le Quéré, S. Levitus, Y. Nojiri, C.K. Shum, L.D. Talley and A. Unnikrishnan (2007). Observations: Oceanic Climate Change and Sea Level. In: Climate Change 2007: The Physical Science Basis. Contribution of Working Group I to the Fourth Assessment Report of the Intergovernmental Panel on Climate Change [Solomon, S., D. Qin, M. Manning, Z. Chen, M. Marquis, K.B. Averyt, M. Tignor and H.L. Miller (eds.)]. Cambridge University Press, Cambridge, United Kingdom and New York, NY, USA.

van Boekel, W.H.M., F.C. Hansen, R. Riegman, R.P.M. Bak (1992). Lysis-induced decline of a *Phaeocystis* spring bloom and coupling with the microbial foodweb. *Mar. Ecol. Prog. Ser.* 81, 269-276.

Borges, A. V., and M. Frankignoulle (1999), Daily and seasonal variations of the partial pressure of CO_2 in surface seawater along Belgian and southern Dutch coastal areas, *J. Mar. Syst. 19*, 251-266.

Borges, A. V., and M. Frankignoulle (2002). Distribution and air-water exchange of carbon dioxide in the Scheldt plume off the Belgian coast. *Biogeochemistry* 59, 41-67.

Borges, A.V., B. Delille and M. Frankignoulle (2005). Budgeting sinks and sources of CO_2 in the coastal ocean: Diversity of ecosystems counts. *Geophys. Res. Lett.* 32, L14601.

Borges, A. V., L. -S. Schiettecatte, G. Abril, B. Delille, and F. Gazeau (2006). Carbon dioxide in European coastal waters. *Estuar. Coast. Shelf S.* 70, 375-387.

Borges, A. V., and N. Gypens (2010). Carbonate chemistry in the coastal zone responds more strongly to eutrophication than to ocean acidification. *Limnol. Oceanogr.* 55(1), 346-353.

Bozec, Y., H. Thomas, K. Elkalay, and H. J. W. de Baar (2005). The continental shelf pump for CO_2 in the North Sea - evidence from summer observation. *Mar. Chem.* 93, 131-147.

Bozec, Y., H. Thomas, L. –S. Schiettecatte, A. V. Borges, K. Elkalay and H. J. W. de Baar (2006). Assessment of the processes controlling the seasonal variations of dissolved inorganic carbon in the North Sea. *Limnol. Oceanogr.* 51, 2746-2762.

Bozec, Y., L. Merlivat, A.-C. Baudoux, L. Beaumont, S. Blain, E. Bucciarelli, T. Danguy, E. Grossteffan, A. Guillot, J. Guillou, M. Répécaud and P. Tréguer (2011). Diurnal to inter-annual dynamics of pCO_2 recorded by a CARIOCA sensor in a temperate coastal ecosystem (2003-2009). *Mar. Chem.* 126, 13 – 26.

Brasse, S., A. Reimer, R. Seifert, and W. Michaelis (1999). The influence of intertidal mudflats on the dissolved inorganic carbon and total alkalinity distribution in the German Bight, southeastern North Sea. *J. Sea Res.* 42, 93-103.

Brockmann, U., R.W.P.M. Laane, and J. Postma (1990). Cycling of nutrient elements in the North Sea. *Neth. J. Sea Res.* 26, 239-264.

Broecker, W.S., and T.-H. Peng (1982). Tracers in the Sea. Columbia University, Eldigio

Press, New York, 690pp.

Brown, P. J., D. C. E. Bakker, U. Schuster, and A. J. Watson (2010). Anthropogenic carbon accumulation in the subtropical North Atlantic. *J. Geophys. Res.* 115, C04016.

Bruyant, F., M. Babin, B. Genty, O. Prasil, M.J. Behrenfeld, H. Claustre, A. Bricaud, L. Garczarek, J. Holtzendorff, M. Koblizek, H. Dousova and F. Partensky (2005). Diel variations in the photosynthetic parameters of Prochlorococcus strain PCC 9511: Combined effects of light and cell cycle. *Limnol. Oceanogr.* 50**,** 850-863.

Burkill, P. H., S. D. Archer, C. Robinson, P. D. Nightingale, S. B. Groom, G. A. Tarran, and M. V. Zubkov (2002). Dimethyl sulphide biogeochemistry within a coccolithophore bloom (DISCO): an overview. *Deep-Sea Res. II* 49, 2863-2885.

Cadée, G.C. (1992). Phytoplankton variability in the Marsdiep, The Netherlands. ICES *Mar. Sci. Symp.* 195, 213-222.

Cadée, G.C.and J. Hegeman (2002). Phytoplankton in the Marsdiep at the end of the 20th century; 30 years monitoring biomass, primary production, and Phaeocystis blooms. *J. Sea Res.* 48, 97-110.

Cai, W. (2011). Estuarine and Coastal Ocean Carbon Paradox: CO_2 Sinks or Sites of Terrestrial Carbon Incineration? *An. Rev. Mar. Sci.* 3**,** 123-145.

Cai, W.–J., H. Xinping, W. –J. Huang, M. C. Murrell, J. C. Lehrter, S. E. Lohrenz, W.–C. Chou, W. Zhai, J. T. Hollibaugh, Y. Wang, P. Zhao, X. Guo, K. Gundersen, Dai, M., and G.–C. Gong (2011). Acidification of subsurface coastal waters enhanced by eutrophication. *Nature Geosci. 4*, 766-770.

Caldeira, K., and M. E. Wickett (2003). Anthropogenic carbon and ocean pH, *Nature*, 425, 365.

Caldeira, K., and M. E. Wickett (2005). Ocean model predictions of chemistry changes from carbon dioxide emissions to the atmosphere and ocean. *J. Geophys. Res.* 110, C09S04.

Canadell, J. G., C. Le Quere, M. R. Raupach, C. B. Field, E. T. Buitenhuis, P. Ciais, T. J. Conway, N. P. Gillett, R. A. Houghton and G. Marland (2007). Contributions to accelerating atmospheric CO_2 growth from economic activity, carbon intensity, and efficiency of natural sinks. *P. Natl. Acad. Sci.* 104 (47), 18866-18870.

Chen, C.-T.A., R.M. Pytkowicz, and E.J. Olson (1982). Evaluation of the calcium problem in the South Pacific. *Geochem. J.* 16, 1-10.

Chen, C.-T.A., S.-L. Wang (1999). Carbon, alkalinity and nutrient budgets on the East China Sea continental shelf. *J. Geophys. Res.* 104, 20675-20686.

Chen, C.-T.A. (2002). Shelf-vs. dissolution-generated alkalinity above the chemical lysocline. *Deep-Sea Res. II* 49, 5365-5375.

Chen, C.-T.A., and A.V. Borges (2009). Reconciling opposing views on carbon cycling in the coastal ocean: Continental shelves as sinks and near-shore ecosystems as sources of atmospheric CO_2. *Deep-Sea Res. II* 56, 578-590.

Chung, S.-N., K. Lee, R.A. Feely, C.L. Sabine, F.J. Millero, R. Wanninkhof, J.L. Bullister, R.M. Key, and T.-H. Peng (2003). Calcium carbonate budget in the Atlantic Ocean based on water column inorganic carbon chemistry. *Global Biogeochem. Cycles* 17(4), 1093.

Ciais P., A.V. Borges, G. Abril, M. Meybeck, G. Folberth, D. Hauglustaine and I.A. Janssens (2008). The impact of lateral carbon fluxes on the European carbon balance.

Biogeosciences 5, 1259-1271.

Clayton, T.D., R.H. Byrne, J.A. Breland, R.A. Feely, F.J. Millero, D.M. Campbell, P.P. Murphy, M.F. Lamb (1995). The role of pH measurements in modern oceanic CO_2-system characterizations: precision and thermodynamic consistency. *Deep-Sea Res.* 42, 411-431.

Copin-Montegut, C., M. Begovic, and L. Merlivat (2004). Variability of the partial pressure of CO_2 on diel to annual time scales in the Northwestern Mediterranean Sea. *Mar. Chem.* 85, 169 – 189.

Corbière, A., N. Metzl, G. Reverdin, C. Brunet and T. Takahashi (2007). Interannual and decadal variability of the oceanic carbon sink in the North Atlantic subpolar gyre. *Tellus,* 59B, 168-178.

Cullen, J. J., M. Lewis, C.O. Davis and R. Barber (1992). Photosynthetic characteristics and estimated growth rates indicate grazing is the proximate control of primary production in the Equatorial Pacific. *J. Geophys. Res.* 97, 639–655.

Dall'Olmo, G., E. Boss, M.J. Behrenfeld, T.K. Westberry, C. Courties, L. Prieur, M. Pujo-Pay, N. Hardman-Mountford, and T. Moutin (2011). Inferring phytoplankton carbon and eco-physiological rates from diel cycles of spectral particulate beam-attenuation coefficient. *Biogeosciences* 8, 3423-3440.

Dickson, A.G. (1981). An exact definition of total alkalinity and a procedure for the estimation of alkalinity and total inorganic carbon from titration data. *Deep-Sea Res.* 28A (6), 609-623.

Dickson, A.G., and F.J.A. Millero (1987). A comparison of the equilibrium constants for the dissociation of carbonic acid in seawater media. *Deep-Sea Res.* 34, 1733-1743.

Dickson, A.G. (1990). Standard potential of the reaction: AgCl(s)+1/2H$_2$(g)= Ag(s)+HCl(aq), and the standard acidity constant of the ion HSO_4^- in synthetic seawater from 273.15 to 318.15 K. *J. Chem. Thermodyn. 22*, 113-127.

Dickson, A. G., Sabine, C. L., and Christian, J. R. (Eds.) (2007). Guide to best practices for ocean CO_2 measurements. *PICES Special Publications 3*, 191 pp, Sidney.

Doney, S. C., N. Mahowald, I. Lima, R.A. Feely, F.T. Mackenzie, J.-F. Lamarque, and P.J. Rasch (2007). Impact of anthropogenic atmospheric nitrogen and sulphur deposition on ocean acidification and the inorganic carbon system. *P. Natl. Acad. Sci.* 104, 14580–14585.

Doney, S.C., V.J. Fabry, R.A. Feely and J.A. Kleypas (2009). Ocean acidification: the other CO_2 problem, *Ann. Rev. Mar. Sci.,* 1, 169-192.

Dong, S., J. Sprintall, S. T. Gille, and L. Talley (2008). Southern Ocean mixed-layer depth from Argo float profiles. *J. Geophys. Res.* 113, C06013.

Dooley, H. D. (1974). Hypotheses concerning the circulation of the northern North Sea. *J. Cons. Cons. Int. Explor. Mer.* 36, 54-61.

Dugdale, R.C., and J.J. Goering (1967). Uptake of new and regenerated forms of nitrogen in primary production. *Limnol. Oceanogr.* 12, 196-206.

Dunne, J.P., J.L. Sarmiento, and A. Gnanadesikan (2007). A synthesis of global particle export from the surface ocean and cycling through the ocean interior and on the seafloor. *Global Biogeochem. Cycles* 21, GB4006.

Egleston, E. S., C. L. Sabine, and M. Morel (2010). Revelle revisited: Buffer factors that quantify the reponse of ocean chemistry to changes in DIC and alkalinity. *Global Biogeochem. Cycles* 24, GB1002.

van Engeland, T., K. Soetaert, A. Knuijt, R.W.P.M. Laane, and J.J. Middelburg (2010). Dissolved organic nitrogen dynamics in the North Sea: A time series analysis (1995-2005). *Estuar. Coast. Shelf S.* 89, 31-42.

Fabry, V.J., B.A. Seibel, R.A. Feely, and J.C. Orr (2008). Impacts of ocean acidification on marine fauna and ecosystem processes. ICES *J. Mar. Sci.* 65, 414-432.

Fennel, K. (2010). The role of continental shelves in nitrogen and carbon cycling: Northwestern North Atlantic case study. *Ocean Sci.* 6, 539-548.

Finlayson-Pitts, B.J., and J.N. Pitts (1999). *Chemistry of the Upper and Lower Atmosphere*. Academic Press: New York, 1999.

Fofonoff, P., and R. C. Millard Jr. (1983). Algorithms for computation of fundamental properties of seawater. *Unesco Technical Papers in Marine Science.* 44, 42-43.

Fraga, F., and X.A. Alvarez Salgado (2005). On the variation of alkalinity during phytoplankton photosynthesis. Ciencias Marinas, Universidad Autonoma de Baja California.

Frankignoulle, M. (1994). A complete set of buffer factors for acid/base CO_2 system in seawater. *J. Mar. Syst.* 5, 111-118.

Frankignoulle, M., and A. V. Borges (2001). European continental shelf as a significant sink for atmospheric carbon dioxide. *Global. Biogeochem. Cycles* 15(3), 569-576.

Friis, K., A. Körtzinger and D.W.R. Wallace (2003). The salinity normalization of marine inorganic carbon chemistry data. *Geophys. Res. Lett.* 30(2), 1085.

Friis, K., A. Körtzinger, J. Patsch, and D.W.R. Wallace (2005). On the temporal increase of anthropogenic CO_2 in the subpolar North Atlantic. *Deep Sea Res. Part I.* 52, 681-698.

Gao, H., F. Schreiber, G. Collins, M.M. Jensen, O. Svitlica, J.E. Kostka, G. Lavik, D. de Beer, H.Y. Zhou, and M.M. Kuypers (2010). Aerobic denitrification in permeable Wadden Sea sediments. *ISME Journal* 4(3), 417-426.

Gattuso, J.-P., M. Frankignoulle, and R. Wollast (1998). Carbon and carbonate metabolism in coastal aquatic ecosystems. *Annu. Rev. Ecol. Syst.* 29, 405–434.

Greatbatch, R. J. (2000). The North Atlantic Oscillation. *Stochastic Environ. Res. Risk Assess. 14*, 213 – 242.

Gernez, P., D. Antoine, and Y. Huot (2011). Diel cycles of the particulate beam attenuation coefficient under varying trophic conditions in the northwestern Mediterranean Sea: Observations and modeling. *Limnol. Oceanogr.* 56(1), 17–36.

González-Dávila, M., J. M. Santana-Casiano, R. A. Fine, J. Happell, B. Delille, and S. Speich (2011). Carbonate system in the water masses of the Southeast Atlantic sector of the Southern Ocean during February and March 2008. *Biogeosciences* 8, 1401-1413.

Goyet, C. and A. Poisson (1989). New determination of carbonic acid dissociation constants in seawater as a function of temperature and salinity. *Deep Sea Res. I* 36, 1635-1654.

Grasshof, K., M. Ehrhardt, and K. Kremling (1983). Methods of seawater analysis. Verlag Chemie GmbH, Weinheim.

Greenan, B.J.W., B.D. Petrie, W.G. Harrison, and N.S. Oakey (2004). Are the Spring and Fall Blooms on the Scotian Shelf Related to Short-Term Physical Events? *Cont. Shelf Res.* 24, 603-625.

Greenan, B. J. W., B.D. Petrie, W.G. Harrison and P.M. Strain (2008). The Onset and Evolution of a Spring Bloom on the Scotian Shelf. *Limnol. Oceanogr.* 53, 1759.

Gripenberg, S. (1960). On the Alkalinity of Baltic Waters. *ICES J. Mar. Sci.* 26(1), 5-20.

Grover, J.P. (1997). Resource competition. London: Chapman and Hall, 342.

Gruber, N., J.L. Sarmiento, and T.F. Stocker (1996). An improved method for detecting anthropogenic CO_2 in the oceans. *Global Biogeochem. Cycles* 10, 809-837.

Gruber, N. (1998). Anthropogenic CO_2 in the Atlantic Ocean. *Global Biogeochem. Cycles*, 12, 165-191.

Gypens, N., G. Lacroix, C. Lancelot, and A. V. Borges (2011). Seasonal and inter-annual variability of air-sea CO$_2$ fluxes and seawater carbonate chemistry in the Southern North Sea. *Prog. Oceanogr.* 88, 59–77.

Hansson, I. (1973). A new set of acidity constants for carbonic acid and boric acid in sea water. *Deep Sea Res. I* 20, 461-478.

Hartin, C. A., R. A. Fine, B. M. Sloyan, L. D. Talley, T. K. Chereskin and J. Happell (2011), Formation rates of Subantarctic mode water and Antarctic intermediate water within the South Pacific, *Deep-Sea Res. I, 58*, 524-534.

Hauck, J., M. Hoppema, R. G. J. Bellerby, C. Völker, and D. Wolf-Gladrow (2010). Data-based estimation of anthropogenic carbon and acidification in the Weddell Sea on a decadal timescale. *J. Geophys. Res.* 115, C03004.

Heip, C.H.R., N.K. Goosen, P.M.J. Herman, J. Jromkamp, J.J. Middelburg and K. Soetaerd (1995). Production and consumption of biological particles in temperate tidal estuaries. *Oceanography and Marine Biology: an Annual Review* 33, 1-149.

Hernandez-Ayon, J. M., A. Zirino, A.G. Dickson, T. Camiro-Vargas and E. Valenzuela-Espinoza (2007). Estimating the contribution of organic bases from microalgae to the titration alkalinity in coastal seawaters. *Limnol. Oceanogr-meth* 5, 225-232.

van Heuven, S., D. Pierrot, E. Lewis, and D.W.R. Wallace (2009). MATLAB Program developed for CO$_2$ system calculations. ORNL/CDIAC-105b. Carbon dioxide information analysis center. Oak Ridge National Laboratory, U.S. Department of Energy, Oak Ridge, Tennessee.

van Heuven, S., D. Pierrot, E. Lewis, and D. W. R. Wallace (2011a), MATLAB Program Developed for CO$_2$ System Calculations. ORNL/CDIAC-105b. Carbon Dioxide Information Analysis Center, Oak Ridge National Laboratory, U.S. Department of Energy, Oak Ridge, Tennessee.

van Heuven, S. M. A. C., M. Hoppema, O. Huhn, H. A. Slagter, and H. J. W. de Baar (2011). Direct observation of increasing CO$_2$ in the Weddell Gyre along the Prime Meridian during 1973-2008. *Deep-Sea Res. II*, 58, 2613-2635.

Hjalmarsson, S., K. Wesslander, L. G. Anderson, A. Omstedt, M. Perttilä and L. Mintrop (2008). Distribution, long-term development and mass balance calculation of total alkalinity in the Baltic Sea. *Cont. Shelf Res.* 28, 593-601.

Hofmann, A.F., F. J. R. Meysman, K. Soetaert, and J.J. Middelburg (2009). pH modelling in aquatic systems with time-variable acid-base dissociation constants applied to the turbid, tidal Scheldt estuary. *Biogeosciences* 6(8), 1539-1561.

Hood. E.M., R. Wanninkhof, and L. Merlivat (2001). Short timescale variations of fCO$_2$ in a North Atlantic warm-core eddy: Results from the Gas-Ex 98 carbon interface ocean atmosphere (CARlOCA) buoy data. *J. Geophys Res.* 106, 2561-2575.

Hoppe, C. J. M., G. Langer, S.D. Rokitta, D.A. Wolf-Gladrow, and B. Rost (2012). Implications of observed inconsistencies in carbonate chemistry measurements for ocean acidification studies. *Biogeosciences* 9, 2401-2405.

Hoppema, J.M.J. (1990). The Distribution and Seasonal Variation of Alkalinity in the Southern Bight of the North Sea and in the Western Wadden Sea. *Neth. J. Sea Res.* 26(1), 11-23.

Hoppema, J. M. J. (1991). The Carbon Dioxide System and Dissolved Oxygen in the Coastal Waters of the Netherlands. Rijsuniversiteit Groningen.

Hoppema, M. (1991). The seasonal behaviour of carbon dioxide and oxygen in the coastal North Sea along the Netherlands. *Neth. J. Sea Res.*, 28(3), 167-179.

Hoppema, J.M.J. (1993). Carbon-dioxide and oxygen disequilibrium in a tidal basin (Dutch-Wadden Sea). *Neth. J. Sea Res.* 31, 221-229.

Hoppema, M., M. H. C. Stoll and H. J. W. De Baar (2000). CO_2 in the Weddell Gyre and Antarctic Circumpolar Current: austral autumn and early winter. *Mar. Chem.* 72, 203-220.

Hordoir, R., and H.E.M. Meier (2010). Freshwater fluxes in the Baltic Sea: A model study. *J. Geophys. Res.* 115, C08028.

Houghton, S. D. (1991). Coccolith sedimentation and transport in the North Sea. *Mar. Geol.* 99(1-2), 267-274.

Huertas, I.E., G. Navarro, S. Rodríguez-Gálvez and L. M. Lubián (2006). Temporal patterns of carbon dioxide in relation to hydrological conditions and primary production in the northeastern shelf of the Guld of Cadiz (SW Spain). *Deep-Sea Res. II* 53, 1344-1362.

Hurrell, J. W. (1995). Decadal trends in the North Atlantic Oscillation: Regional temperatures and precipitation. *Science,* 269, 676–679.

Hurrel, J., and H. van Loon (1997). Decadal variations in climate associated with the North Atlantic Oscillation. *Clim. Change* 36, 301-336.

Hurrel, J. W. (2003). Climate: North Atlantic and Arctic Oscillation (NAO/AO), in *Encyclopedia of Atmospheric Sciences*, edited by J. Holton, J. Pyle, and J. Curry, pp. 439-445, Academic Press, New York.

Hurrell, J. W. and C. Deser (2010). North Atlantic climate variability: The role of the North Atlantic. *J. Marine Syst.* 79, 231-244.

Hydes, D.J., B.A. Kelly-Gerreyn, A.C. Le Gall, and R. Proctor (1999). The balance of supply of nutrients and demands of biological production and denitrification in a temperate latitude shelf sea – a treatment of the southern North Sea as an extended estuary. *Mar. Chem.* 68, 117-131.

ICES (1983). International Council For The Exploration Of The Sea, Flushing times of the North Sea, *ICES Cooperative Research Report* 123.

Ionita, M., N. Rimbu, and G. Lohmann (2011). Decadal variability of the Elbe River streamflow. *Int. J. Climatol.* 31, 22-30.

IPCC (2007). Climate Change 2007: The Physical Science Basis. Contribution of Working Group I to the Fourth Assessment. Report of the Intergovernmental Panel on Climate Change. Edited by: S. Solomon, D. Qin, M. Manning, Z. Chen, M. Marquis.

Ishii, M., N. Kosugi, D. Sasano, S. Saito, T. Midorikawa and H. Y. Inoue (2011). Ocean acidification off the south coast of Japan: A result from time series observations of CO_2 parameters from 1994 to 2008. *J. Geophys. Res.* 116, C06022.

Jin, X., N. Gruber, J. P. Dunne, J. L. Sarmiento, and R. A. Armstrong (2006). Diagnosing the contribution of phytoplankton functional groups to the production and export of particulate organic carbon, $CaCO_3$, and opal from global nutrient and alkalinity distributions. *Global Biogeochem. Cycles* 20, GB2015.

Johnson, K. M., J. M. Sieburth, P. J. Williams, and L. Brändström (1987). Coulometric total carbon dioxide analysis for marine studies: Automation and calibration. *Mar. Chem.* 21, 117-133.

Johnson, K.M., K.D. Wills, D.B. Butler, W.K. Johnson and C.S. Wong (1993). Coulometric total carbon dioxide analysis for marine studies: maximizing the performance of an automated gas extraction system and coulometric detector. *Mar. Chem.* 44, 167-188.

de Jonge, V.N. (1990). Response of the Dutch Wadden Sea ecosystem to phosphorus

discharges from the river Rhine. *Hydrobiologia* 195, 49-62.

de Jonge, V.N. (1997). High remaining productivity in the Dutch western Wadden Sea despite decreasing nutrient inputs from riverine sources. *Mar. Poll. Bull.* 34(6), 427-436.

Karstensen, J., and D. Quadfasel (2002). Water subducted into the Indian Ocean subtropical gyre. *Deep Sea-Res. Pt II* 49 (7-8), 1441-1457.

Kempe, S., and K. Pegler (1991). Sinks and sources of CO_2 in coastal seas: the North Sea. *Tellus,* 43B, 224-235.

Key, R.M., T. Tanhua, A. Olsen, M. Hoppema, S. Jutterström, C. Schirnick, S. van Heuven, A. Kozyr, X. Lin, A. Velo, D.W.R Wallace and L. Mintrop (2010). The CARINA data synthesis project: Introduction and overview. *Earth Syst. Sci. Data* 2, 105–121.

Kieskamp, W.M., L. Lohse, E. Epping, and W. Helder (1991). Seasonal variation in denitrification rates and nitrous oxide fluxes in intertidal sediments of the western Wadden Sea. *Mar. Ecol. Prog. Ser.* 72, 145-151.

Klaas, C., and D. E. Archer (2002). Association of sinking organic matter with various types of mineral ballast in the deep sea: Implications for the rain ratio. *Global Biogeochem. Cycles* 16(4), 1116.

Koeve, W., H. -C. Kim, K. Lee, and A. Oschlies (2011). Potential impact of DOC accumulation on fCO2 and carbonate ion computations in ocean acidification experiments. *Biogeosciences Discussions* 8, 3797-3827.

Körtzinger, A., H. Thomas, B. Schneider, N. Gronau, L. Mintrop and J. C. Duinker (1996). At-sea intercomparison of two newly designed underway pCO2 systems - Encouraging results. *Mar. Chem.* 52, 133-145.

Kowalski, N., O. Dellwig, M. Beck, M. Grunwald, C.-D. Dürselen, T.H. Badewien, H.-J. Brumsack, J.E.E. van Beusekom, and M.E. Böttcher (2012). A comparative study of manganese dynamics in the water column and sediments of intertidal systems of the North Sea. *Estuar. Coast. Shelf S.* 100, 3-17.

Kühn, W., J. Pätsch, H. Thomas, A. V. Borges, L. –S. Schiettecatte, Y. Bozec and A. E. F. Prowe (2010). Nitrogen and carbon cycling in the North Sea and exchange with the North Atlantic-A model study, Part II: Carbon budget and fluxes. *Cont. Shelf Res.,* 30, 1701-1716.

Lamb, M.F., C.L. Sabine, R.A. Feely, R. Wanninkhof, R.M. Key, G.C. Johnson, F.J. Millero, K. Lee, T.-H. Peng, A. Kozyr, J.L. Bullister, D. Greenley, R.H. Byrne, D.W. Chipman, A.G. Dickson, C. Goyet, P.R. Guenther, M. Ishii, K.M. Johnson, C.D. Keeling, T. Ono, K. Shitashima, B. Tilbrook, T. Takahashi, D.W.R. Wallace, Y.W. Watanabe, C. Winn and C.S. Wong (2002). Consistency and synthesis of Pacific Ocean CO_2 survey data. *Deep-Sea Res. II* 49, 21-58.

Lee, K., and F. Millero (1995). Thermodynamic studies of the carbonate system in seawater. *Deep-Sea Res. I* 42, 2035-2061.

Lee, K., F. J. Millero, and D.M. Campbell (1996). The reliability of the thermodynamic constants for the dissociation of carbonic acid in seawater. *Mar. Chem.* 55, 233-245.

Lee, K., F. J. Millero, and R. Wanninkhof (1997). The carbon dioxide system in the Atlantic Ocean. *J. of Geophys. Res.* 102, 15,693-15,707.

Lee, K., F. J. Millero, R.H. Byrne, R.A. Feely, and R. Wanninkhof (2000). The recommended dissociation constants for carbonic acid in seawater. *Geophys. Res. Lett.* 27(2), 229-232.

Lee, K., S.-D. Choi, G.-H. Park, R. Wanninkhof, T.-H. Peng, R.M. Key, C.L. Sabine, R.A. Feely, J.L. Bullister, F.J. Millero and A. Kozyr (2003). An updated anthropogenic

CO$_2$ inventory in the Atlantic Ocean. *Global Biogeochem. Cycles* 17(4), 1116.

Lee, K., C. L. Sabine, T. Tanhua, T.–W. Kim, R.A. Feely and H.–C. Kim (2011). Roles of marginal seas in absorbing and storing fossil fuel CO$_2$. *Energy Environ. Sci.* 4, 1133.

Lefèvre, N., A.J. Watson, A. Olsen, A.F. Rios, F.F. Perez, and T. Johannessen (2004). A decrease in the sink for atmospheric CO$_2$ in the North Atlantic. *Geophys. Res. Lett.* 31, L07306.

Lefèvre, N., A. Guillot, L. Beaumont, and T. Danguy (2008). Variability of fCO$_2$ in the Eastern Tropical Atlantic from a moored buoy. *J. Geophys. Res.* 113, C01015.

Lenhart, H.J., J. Patsch, and G. Radach (1996). Daily nutrient loads of the European continental rivers for the years 1977-1993. Berichte aus dem Zentrum fur Meeres- und Klimaforschung. Reihe B: *Ozeanographie* 22, 1-159.

Lenhart, H.J., J. Pätsch, W. Kühn, A. Moll, and T. Pohlmann (2004). Investigation on the trophic state of the North Sea for three years (1994-1996) simulated with the ecosystem model ERSEM – the role of a sharp NAOI decline. *Biogeosciences Discuss. 1*, 725-754.

Levine, N.M., S.C. Doney, R. Wanninkhof, K. Lindsay and I.Y. Fung (2008). Impact of ocean carbon system variability on the detection of temporal increases in anthropogenic CO$_2$. *J. Geophys. Res.*, 113, C03019.

Levine, N.M., S.C. Doney, I. Lima, R. Wanninkhof, N.R. Bates, and R.A. Feely (2011). The impact of the North Atlantic Oscillation on the uptake and accumulation of anthropogenic CO$_2$ by North Atlantic Ocean mode waters. *Global Biogeochem. Cycles* 25, GB3022.

Lewis, E.L. (1980). The practical salinity scale 1978 and its antecedents. IEEE *Journal of Oceanic Engineering* OE-5 (1), 3-8.

Lewis, E. L., and D.W.R. Wallace (1998). Program developed for CO$_2$ system calculations, ORNL/CDIAC-105. Carbon dioxide information analysis center, Oak Ridge National Laboratory, U.S. Department of Energy, Oak Ridge.

Lischka, S., J. Büdenbender, T. Boxhammer, and U. Riebesell (2011). Impact of ocean acidification and elevated temperatures on early juveniles of the polar shelled pteropod Limacina helicina: mortality, shell degradation, and shell growth. *Biogeosciences* 8, 919-932.

Liss, P. S. and M.J. Pointon (1973). Removal of dissolved boron and silicon during estuarine mixing of sea and river waters. *Geochim. Cosmochim. Ac.* 37, 1493-1498.

Loebl, M., T. Dolch, and J.E.E. van Beusekom (2007). Annual dynamics of pelagic primary production and respiration in a shallow coastal basin. *J. Sea Res.* 58, 269-282.

Loebl, M., F. Colijn, J.E.E. van Beusekom, J.G. Baretta-Bekker, C. Lancelot, C.J.M. Philippart, V. Rousseau, K.H. Wiltshire (2009). Recent patterns in potential phytoplankton limitation along the Northwest European continental coast. *J. Sea Res.* 61, 34-43.

Lo Monaco, C., C. Goyet, N. Metzl, A. Poisson and F. Touratier (2005). Distribution and inventory of anthropogenic CO$_2$ in the Southern Ocean: Comparison of three data-based methods. *J. Geophys. Res.* 110, C09S02.

Lorkowski, I., J. Pätsch, A. Moll, and W. Kühn (2012). Interannual variability of carbon fluxes in the North Sea from 1970 to 2006 – Competing effects of abiotic and biotic drivers on the gas-exchange of CO$_2$. *Estuar. Coast. Shelf S.* 100, 38-57.

Lueker, T. J., A.G. Dickson, and C.D. Keeling (2000). Ocean pCO$_2$ calculated from dissolved inorganic carbon, alkalinity, and equations for K$_1$ and K$_2$: validation based

on laboratory measurements of CO_2 in gas and seawater at equilibrium. *Mar. Chem.* 70, 105-119.

Macfarling Meure, C., D. Etheridge, C. Trudinger, P. Steele, R. Langenfelds, T. van Ommen, A. Smith and J. Elkins (2006). Law Dome CO_2, CH_4 and N_2O ice core records extended to 2000 years BP. *Geophys. Res. Lett.* 33, L14810.

Mackin, J.E., and K.T. Swider (1989). Organic matter decomposition pathways and oxygen consumption in coastal marine sediments. *J. Mar. Res.* 47, 681-716.

Maybeck, M. (1982). Carbon, nitrogen, and phosphorus transport by world rivers. *Am. J. Sci.* 282, 401-450.

Maybeck, M. (1993). Riverine transport of atmospheric carbon: sources, global typology and budget. *Water Air Soil Poll.* 70, 443-463.

McElligott, S., R.H. Byrne, K. Lee, R. Wanninkhof, F.J. Millero, and R.A. Feely (1998). Discrete water column measurements of CO_2 fugacity and pH_T in seawater: A comparison of direct measurements and thermodynamic calculations. *Mar. Chem.* 60, 63-73.

McKinley, G.A., A.R. Fay, T. Takahashi, and N. Metzl (2011). Convergence of atmospheric and North Atlantic carbon dioxide trends on multidecadal timescales, *Nat. Geosci.* 4, 606-610.

McNeil, B. I., B. Tilbrook, and R. Matear (2001). Accumulation and uptake of anthropogenic CO_2 in the Southern Ocean, south of Australia between 1968 and 1996. *J. Geophys. Res.* 106, 31,431-31,445.

McNeil, B. I., N. Metzl, R. M. Key, R. J. Matear, and A. Corbiere (2007). An empirical estimate of the Southern Ocean air-sea CO_2 flux. *Global. Biogeochem. Cycles* 21, GB3011.

McNeil, B. I., and R. J. Matear (2008). Southern Ocean acidification: A tipping point at 450-ppm atmospheric CO_2. *Proc. Natl. Acad. Sci.* 105, 18860-18864.

Mehrbach, C., C.H. Culberson, J.E. Hawley, and R.M. Pytkowicz (1973). Measurement of the apparent dissociation constants of carbonic acid in seawater at atmospheric pressure. *Limnol. Oceanogr.* 18, 897-907.

Mémery, L., M. Arhan, X.A. Alvarez-Salgado, M.-J. Messias, H. Mercier, C.G. Castro, and A.F. Ríos (2000). The water masses along the western boundary of the south and equatorial Atlantic. *Prog. Oceanogr.* 47, 69-98.

Millero, F. J., R.H. Byrne, R. Wanninkhof, R. Feely, T. Clayton, P. Murphy and M.F. Lamb (1993). The internal consistency of CO_2 measurements in the equatorial Pacific. *Mar. Chem.* 44, 269-280.

Millero, F. J., K. Lee, and M. Roche (1998). Distribution of alkalinity in the surface waters of the major oceans. *Mar. Chem.* 60, 111-130.

Millero, F., D. Pierrot, K. Lee, R. Wanninkhof, R. Feely, C.L. Sabine, R.M. Key and T. Takahashi (2002). Dissociation constants for carbonic acid determined from field measurements. *Deep-Sea Res. II* 49, 1705-1723.

Millero, F. J., T.B. Graham, F. Huang, H. Bustos-Serrano and D. Pierrot (2006). Dissociation constants of carbonic acid in seawater as a function of salinity and temperature. *Mar. Chem.* 100, 80-94.

Mintrop, L., F.F. Perez, M. Gonzalez-Davila, M.J. Santana-Casiano, and A. Kortzinger (2000). Alkalinity determination by potentiometry: intercalibration using three different methods. *Cienc. Marinas* 26, 23-37.

Mojica-Preito F.J. and F.J. Millero (2002). The values of pK_1 and pK_2 for the dissociation of

carbonic acid in seawater. *Geochim. Cosmochim. Ac.* 66(14), 2529-2540.

Molleri, G.S.F., E.M.L. Novo, M. De and M. Kampel (2010). Space-time variability of the Amazon River plume based on satellite ocean color. *Cont. Shelf Res. 30,* 342-352.

Mosley, L. M., B. M. Peake and K.A. Hunter (2010). Modelling of pH and inorganic carbon speciation in estuaries using the composition of the river and seawater end members. *Environ. Modell. Softw.* 25, 1658-1663.

Muller F.L.L. and B. Bleie (2008). Estimating the organic acid contribution to coastal seawater alkalinity by potentiometric titrations in a closed cell. *Anal. Chim. Acta* 619, 183-191.

Murata, A., Y. Kumamoto, K.'I. Sasaki, S. Watanabe, and M. Fukasawa (2008). Decadal increases of anthropogenic CO_2 in the subtropical South Atlantic Ocean along 30°S. *J. Geophys. Res.*, 113, C06007.

Nahorniak, J.S., M.R. Abbott, R.M. Letelier, and W.S.C. Pegau (2001). Analysis of a method to estimate chlorophyll-a concentration from irradiance measurements at varying depths. *J. Atmos. Ocean. Technol.* 18, 2063-2073.

Omar, A.M., A. Olsen, T. Johannessen, M. Hoppema, H. Thomas, and A.V. Borges (2010). Spatiotemporal variations of fCO_2 in the North Sea. *Ocean Sci.* 6, 77-89.

Orr, J.C., V.J. Fabry, O. Aumont, L. Bopp, S.C. Doney, R.A. Feely, A. Gnanadesikan, N. Gruber, A. Ishida, F. Joos, R.M. Key, K. Lindsay, E. Maier-Reimer, R. Matear, P. Monfray, A. Mouchet, R.G. Najjar, G.-K. Plattner, K.B. Rodgers, C.L. Sabine, J.L. Sarmiento, R. Schlitzer, R.D. Slater, I.J. Totterdell, M.-F. Weirig, Y. Yamanaka and A. Yool (2005). Anthropogenic ocean acidification over the twenty-first century and its impact on calcifying organisms. *Nature,* 437, 681-686.

Raven, J. (2005). Ocean acidification due to increasing atmospheric carbon dioxide, Document No. 12/05, The Royal Society, London, 2005.

Orsi, A.H., G.C. Johnson and J.L. Bullister (1999). Circulation, mixing, and production of Antarctic Bottom Water. *Prog. Oceanogr.* 43, 55-109.

Osterroht, C. (1993). Extraction of dissolved fatty acids from sea water. *Fresenius J Anal Chem.* 345, 773-779.

Otto, L., J.T.F. Zimmerman, G.K. Furnes, M. Mork, R. Saetre and G. Becker (1990). Review of the physical oceanography of the North Sea. *Neth. J. Sea Res.* 26(2-4), 161-238.

Pai, S. –C., G. Gong, K.–K. Liu (1993). Determination of dissolved oxygen in seawater by direct spectrophotometry of total iodine. *Mar. Chem.* 41, 343-351.

Park, K.P. (1969). Oceanic CO_2 System: An evaluation of ten methods of investigation. *Limnol. Oceanogr.* 14(2), 179-186.

Pätsch, J., W. Kühn, G. Radach, J.M. Santana Casiano, M. Gonzalez Davila, S. Neuer, T. Freudenthal and O. Llinas (2002). Interannual variability of carbon fluxes at the North Atlantic Station ESTOC. *Deep-Sea Res. II* 49, 253-288.

Pätsch, J., and H.J. Lenhart (2004). Daily Loads of Nutrients, Total Alkalinity, Dissolved Inorganic Carbon and Dissolved Organic Carbon to the European Continental Rivers for the Years 1977-2002. Berichte aus dem Zentrum für Meeres- und Klimaforschung, Reihe B, Ozeanographie, 48, 159 pp.

Pätsch, J., and W. Kühn (2008). Nitrogen and carbon cycling in the North Sea and exchange with the North Atlantic—a model study. Part I. Nitrogen budget and fluxes. *Cont. Shelf Res.* 28, 767–787.

Peng, T.-H., R. Wanninkhof and R. A. Feely (2003). Increase of anthropogenic CO_2 in the Pacific Ocean over the last two decades. *Deep-Sea Res. II* 50, 3065-3082.

Peng, T.-H., and R. Wanninkhof (2010). Increase in anthropogenic CO_2 in the Atlantic Ocean in the last two decades. *Deep-Sea Res. I* 57, 755-770.

Pérez, F.F., M. Álvarez, and A.F. Ríos (2002). Improvements on the back-calculation

technique for estimating anthropogenic CO_2. *Deep-Sea Res. I* 49, 859-875.

Pérez, F.F., M. Vázquez-Rodríguez, H. Mercier, A. Velo, P. Lherminier, and A.F. Ríos (2010). Trends of anthropogenic CO_2 storage in North Atlantic water masses. *Biogeosciences* 7, 1789-1807.

Peterson, R.G., and T. Whitworth (1989). The Subantarctic and Polar Fronts in relation to deep water masses through the Southwestern Atlantic. *J. Geophys. Res. 94*, 10,817-10,838.

Petit, J.R., J. Jouzel, D. Raynaud, N.I. Barkov, J.–M. Barnola, I. Basile, M. Benders, J. Chappellaz, M. Davis, G. Delaygue, M. Delmotte, V.M. Kotlyakov, M. Legrand, V.Y. Lipenkov, C. Lorius, L. Pépin, C. Ritz, E. Saltzman and M. Stievenard (1999). Climate and atmospheric history of the past 420,000 years from the Vostok ice core, Antarctica. *Nature* 399, 429-436.

Philippart, C.J.M., and G.C. Cadée (2000). Was total primary production in the western Wadden Sea stimulated by nitrogen loading? *Helgol. Mar. Res.* 54, 55-62.

Philippart, C.J.M., G. C. Cadée, W. van Raaphorst, and R. Riegman (2000). Long-term phytoplankton-nutrient interactions in a shallow coastal sea: algal community structure, nutrient budgets, and denitrification potential. *Limnol. Oceanogr.* 45, 131-144.

Philippart, C.J.M., J.J. Beukema, G.C. Cadée, R. Dekker, P.W. Goedhart, J.M. van Iperen, M.F. Leopold, and P.M.J. Herman (2007). Impacts of nutrient reduction on coastal communities. *Ecosystems* 10, 95-118.

Prieto, F.J.M., and F.J. Millero (2002). The values of pK_1 and pK_2 for the dissociation of carbonic acid in seawater. *Geochim. Cosmochim. Ac.* 66(14), 2529 - 2540.

Prowe, A.E.F., H. Thomas, J. Pätsch, W. Kühn, Y. Bozec, L.–S. Schiettecatte, A.V. Borges, and H.J.W. de Baar (2009). Mechanisms controlling the air–sea CO_2 flux in the North Sea. *Cont. Shelf Res*. 29, 1801-1808.

Proctor, R., J.T. Holt, J.I. Allen, and J. Blackford (2003). Nutrient fluxes and budgets for the North West European Shelf from a three-dimensional model. *Science of the Total Environment* 314-316, 769-785.

Raven, J. (2005). Ocean acidification due to increasing atmospheric carbon dioxide, Document No. 12/05, The Royal Society, London, 2005.

Reimer, A., S. Brasse, R. Doerfer, C.-D. Dürselen, S. Kempe, W. Michaelis, H.-J. Rick and R. Seifert (1999). Carbon cycling in the German Bight: An estimate of transformation processes and transport. *German Journal of Hydrography* 51, 313-329.

Revelle, R. and H. Suess (1957). Carbon dioxide exchange between atmosphere and ocean and the question of an increase of atmospheric CO_2 during the past decades. *Tellus, 9*, 18-27.

Richards, F.A., J.D. Cline, W.W. Broenkow, and L.P. Atkinson (1965). Some consequences of the decomposition of organic matter in Lake Nitinat, an Anoxic Fjord. *Limnol. Oceanogr.* 10, 185-201.

Ridderinkhof, H., J.T.F. Zimmerman, and M.E. Philippart (1990). Tidal exchange between the North Sea and Dutch Wadden Sea and mixing time scales of the tidal basins. *Neth. J. Sea Res.* 25(3), 331-350.

Riegman, R., B.R. Kuipers, A.A.M. Noordeloos, and H.J. Witte (1993). Size-differential control of phytoplankton and the structure of plankton communities, *Neth. J. Sea Res.* 31, 255-265.

Ríos, A.F., Anderson, T.R., and F.F. Pérez (1995). The carbonic system distribution and fluxes in the NE Atlantic during Spring 1991. *Prog. Oceanogr. 35,* 295-314.

Ríos, A.F., F.F. Pérez, M. Álvarez, L. Mintrop, M. González-Dávila, J.M. Santana Casiano, N. Lefèvre and A.J. Watson (2005). Seasonal sea-surface carbon dioxide in the Azores area. *Mar. Chem.* 96, 35-51.

Ríos, A.F., K. M. Johnson, X.A. Alvarez-Salgado, L. Arlen, A. Billant, L.S. Bingler, P. Branellec, C.G. Castro, D.W. Chipman, G. Roson and D.W.R. Wallace (2005). Carbon Dioxide, Hydrographic, and Chemical Data Obtained During the R/V Maurice Ewing Cruise in the South Atlantic Ocean (WOCE Section A17, 4 Janurary-21 March 1994), Carbon Dioxide Information Analysis Center, Oak Ridge National Laboratory, ORNL/CDIAC-148, NDP-084, pp. 1-27.

Ríos, A.F., M. Vázquez-Rodríguez, X.A. Padin, and F.F. Pérez (2010). Anthropogenic carbon dioxide in the South Atlantic western basin. *J. Mar. Syst. 83,* 38-44.

Ríos, A.F., A. Velo, P.C. Pardo, M. Hoppema and F.F. Pérez (2011). An update of anthropogenic CO_2 storage rates in the western South Atlantic basin and the role of Antarctic Bottom Water. *J. Mar. Syst.* 94, 197-203.

Ríos, A.F., A. Velo, P.C. Pardo, M. Hopema and F.F. Pérez (2012). An update of anthropogenic CO_2 storage rates in the western South Atlantic basin and the role of Antarctic Bottom Water. *J. Mar. Syst.* 94, 197-203.

Roy, R.N., L.N. Roy, M. Lawson, K.M. Vogel, C.P. Moore, W. Davis and F.J. Millero (1993). Determination of the ionization constants of carbonic acid in seawater. *Mar. Chem.* 44, 249-259.

Sabine, C.L., R.A. Feely, N. Gruber, R.M. Key, K. Lee, J.L. Bullister, R. Wanninkhof, C.S. Wong, D.W.R. Wallace, B. Tilbrook, F.J. Millero, T.–H. Peng, A. Kozyr, T. Ono and A.F. Ríos (2004). The Oceanic Sink for Anthropogenic CO_2. *Science* 305, 367-371.

Sabine, C.L. and T. Tanhua (2010). Estimation of Anthropogenic CO_2 Inventories in the Ocean. *Ann. Rev. Mar. Sci.* 2(1), 175–198.

Santana-Casiano, J.M., M. González-Dávila, M.–J. Rueda, O. Llinás and E.–F. González-Dávila (2007). The interannual variability of oceanic CO_2 parameters in the northeast Atlantic subtropical gyre at the ESTOC site, *Global Biogeochem. Cycles* 21, GB1015.

Sarmiento, J.L., N. Gruber, M.A. Brzezinski and J.P. Dunne (2004). High-latitude controls of thermocline nutrients and low latitude. *Nature* 427, 56-60.

Schiettecatte, L.-S., F. Gazeau, C. van der Zee, N. Brion, and A.V. Borges (2006). Time series of the partial pressure of carbon dioxide (2001-2004) and preliminary inorganic carbon budget in the Scheldt plume (Belgian coast waters). *Geochem. Geophys. Geosyst.* 7, Q06009.

Schiettecatte, L.-S., H. Thomas, Y. Bozec and A.V. Borges (2007). High temporal coverage of carbon dioxide measurements in the Southern Bight of the North Sea. *Mar. Chem.* 106, 161-173.

Schlesinger, W.H. (1997). Biogeochemistry: An Analysis of Global Change, 2nd ed. Academic Press, San Diego. 588pp.

Schoemann, V., H.J.W. de Baar, J.T.M. de Jong, and C. Lancelot (1998). Effects of phytoplankton blooms on the cycling of manganese and iron in coastal waters. *Limnol. Oceanogr.* 43, 1427-1441.

Schoemann, V.S., S. Becquevort, J. Stefels, V. Rousseau and C. Lancelot (2005). *Phaeocystis* blooms in the global ocean and their controlling mechanisms: A review.

J. Sea Res. 53, 43-66.

Schuster, U., and A.J. Watson (2007). A variable and decreasing sink for atmospheric CO_2 in the North Atlantic. *J. Geophys. Res.* 112, C11006.

Schuster, U., A.J. Watson, N.R. Bates, A. Corbiere, M. Gonzalez-Davila, N. Metzl, D. Pierrot, and M. Santana-Casiano (2009). Trends in North Atlantic sea-surface fCO_2 from 1990 to 2006. *Deep-Sea Res. II* 56(8-10), 620-629.

Seidel, M.P., M.D. DeGrandpre, and A.G. Dickson (2008). A sensor for in situ indicator-based measurements of seawater pH. *Mar. Chem.* 109, 18-28.

Shadwick, E.H., H. Thomas, A. Comeau, S.E. Craig, C.W. Hunt and J.E. Salisbury (2010). Air-Sea CO_2 fluxes on the Scotian Shelf: seasonal to multi-annual variability. *Biogeosciences* 7, 3851-3867.

Shadwick, E., H. Thomas, Y. Gratton, D. Leong, S.A. Moore, T. Papakyriakou, and A.E.F. Prowe (2011). Export of Pacific carbon through the Arctic Archipelago to the North Atlantic. *Cont. Shelf Res.* 31, 806-816.

Shadwick, E.H., H. Thomas, K. Azetsu-Scott, B.J.W. Greenan, E. Head and E. Horne (2011). Seasonal variability of dissolved inorganic carbon and surface water pCO_2 in the Scotian Shelf region of the Northwestern Atlantic. *Mar. Chem.* 124, 23-37.

Shadwick, E.H., and H. Thomas (2011). Carbon Dioxide in the Coastal Ocean: A Case Study in the Scotian Shelf Region - in: Ocean Year Book, 25, A. Chircop, S. Coffen-Smout, and M. McConnell, M. (eds.), Martinus Nijhoff, Leiden/Boston, 171-204.

Siegel, D.A., T. D. Dickey, L. Washburn, M.K. Hamilton and B.G. Mitchell (1989). Optical determination of particulate abundance and production variations in the oligotrophic ocean. *Deep-Sea Res.* 36, 211–222.

Sievers, H.A. and W.D. Nowlin (1984). The stratification and water masses at Drake Passage, *J. Geophys. Res.* 89, 489-514.

Sloyan, B.M., and S.R. Rintoul (2001). Circulation, Renewal, and Modification of Antarctic Mode and Intermediate Water. *J. Phys. Oceanogr.* 31, 1005-1030.

Stedmon, C.A., C.L. Osburn and T. Kragh (2010). Tracing water mass mixing in the Baltic-North Sea transition zone using the optical properties of coloured dissolved organic matter. *Est. Coast. Shelf Sci.* 87, 156-162.

Stramska, M., and T.D. Dickey (1992). Variability of bio-optical properties of the upper ocean associated with diel cycles in phytoplankton population. *J. Geophys. Res.* 97, 17873–17887.

Takahashi, T., W.S. Broecker and S. Langer (1985). Redfield ratio based on chemical data from isopycnal surfaces. *J. Geophys. Res.* 90, 6907-6924.

Takahashi, T., J. Olafsson, J.G. Goddard, D.W. Chipman, and S.C. Sutherland (1993). Seasonal-variation of CO_2 and nutrients in the high-latitude surface oceans – a comparative study. *Global Biogeochem. Cycles* 7, 843-878.

Takahashi, T., S.C. Sutherland, C. Sweeney, A. Poisson, N. Metzl, B. Tilbrook, N.R. Bates, R. Wanninkhof, R.A. Feely, C.L. Sabine, J. Olafsson, and Y. Nojiri (2002). Global sea-air CO_2 flux based on climatological surface ocean CO_2, and seasonal biological and temperature effects. *Deep Sea. Res. II* 49, 1601-1622.

Takahashi, T., S.C. Sutherland, R. Wanninkhof, C. Sweeney, R.A. Feely, D.W. Chipman, B. Hales, G. Friederich, F. Chavez, C. Sabine, A. Watson, D.C.E. Bakker, U. Schuster, N. Metzl, H. Yoshikawa-Inoue, M. Ishii, T. Midorikawa, Y. Nojiri, A. Kortzinger, T. Steinhoff, M. Hoppema, J. Olafsson, T.S. Arnarson, B. Tilbrook, T. Johannessen, A. Olsen, R. Bellerby, C.S. Wong, B. Delille, N.R. Bates, H.J.W. de Baar (2009). Climatological mean and decadal change in surface ocean pCO_2, and net sea-air CO_2 flux over the global oceans. *Deep-Sea Res. II* 56, 554-577.

Talley, L.D. (1996). Antarctic intermediate water in the South Atlantic. In: Wefer, G., Berger, H.H., Siedler, G., Webb, D. (Eds.), The South Atlantic: Present and Past Circulation. Springer-Verlag.

Ternon, J.F., C. Oudot, A. Dessier and D. Diverres (2000). A seasonal tropical sink for atmospheric CO_2 in the Atlantic ocean: the role of the Amazon River discharge. *Mar. Chem.* 68, 183-201.

Thomas, H., V. Ittekkot, C. Osterroht, and B. Schneider (1999). Preferential recycling of nutrients – the ocean's way to increase new production and to pass nutrient limitation? *Limnol. Oceanogr.* 44, 1999-2004.

Thomas, H., and B. Schneider (1999). The seasonal cycle of carbon dioxide in Baltic Sea surface waters. *J. Mar. Syst.* 22, 53-67.

Thomas, H., Y. Bozec, K. Elkalay, and H.J.W. de Baar (2004). Enhanced open ocean storage of CO_2 from shelf sea pumping. *Science,* 304, 1005-1008.

Thomas, H., Y. Bozec, H.J.W. de Baar, K. Elkalay, M. Frankignoulle, L.-S. Schiettecatte, G. Kattner, and A.V. Borges (2005). The carbon budget of the North Sea. *Biogeosciences* 2, 87-96.

Thomas, H., Bozec, Y., Elkalay, K., de Baar, H.J.W., Borges, A.V., and Schiettecatte, L.-S., (2005). Controls of the surface water partial pressure of CO_2 in the North Sea. *Biogeosciences* 2, 323-334.

Thomas, H., A.E.F. Prowe, S. van Heuven, Y. Bozec, H.J.W. de Baar, L.–S. Schiettecatte, K. Suykens, M. Koné, A.V. Borges, I.D. Lima and S.C. Doney (2007). Rapid decline of the CO_2 buffering capacity in the North Sea and implications for the North Atlantic Ocean. *Global Biogeochem. Cycles* 21, GB4001.

Thomas, H., A.E.F. Prowe, I.D. Lima, S.C. Doney, R. Wanninkhof, R.J. Greatbatch, U. Schuster and A. Corbière (2008). Changes in the North Atlantic Oscillation influence CO_2 uptake in the North Atlantic over the past 2 decades. *Global Biogeochem. Cycles* 22, GB4027.

Thomas, H., D. Unger, J. Zhang, K.-K. Liu and E.H. Shadwick (2008). Biogeochemical cycling. In: Urban E., Sundby B., Malanotte-Rizzoli, P. and Melillo, J. (eds) Watersheds, *Bays and Bounded Seas* (SCOPE No. 70). Island Press, Washington, D. C., pp. 169-190.

Thomas, H., L.-S. Schiettecatte, K. Suykens, Y.J.M. Koné, E.H. Shadwick, A.E.F. Prowe, Y. Bozec, H.J.W. de Baar, and A.V. Borges (2009). Enhanced ocean carbon storage from anaerobic alkalinity generation in coastal sediments. *Biogeosciences* 6, 267-274.

Thomas, H., S.E. Craig, B.J.W. Greenan, W. Burt, S. Herndl, L. Salt, E.H. Shadwick, and J. Urrego-Blanco (2012). Direct observations of diel biological CO_2 fixation in the oceans. *Biogeosciences Discussions* 9, 2153 - 2168.

Touratier, F., and C. Goyet (2004). Definition, properties, and Atlantic Ocean distribution of the new tracer TrOCA, *J. Mar. Syst.* 46, 169-179.

Touratier, F., and C. Goyet (2004). Applying the new TrOCA approach to assess the distribution of anthropogenic CO_2 in the Atlantic Ocean. *J. Mar. Syst.* 46, 181-197.

Touratier, F., L. Azouzi, and C. Goyet (2007). CFC-11, Δ^{14}C and ^{3}H tracers as a means to assess anthropogenic CO_2 concentrations in the ocean. *Tellus* 59B*,* 318-325.

Tsunogai, S., S. Watanabe, and T. Sato (1999). Is there a "continental shelf pump" for the absorption of atmospheric CO2? *Tellus* 51B, 701-712.

Umoh, J.U., and K.R. Thompson (1994). Surface heat flux, horizontal advection, and the seasonal evolution of water temperature on the Scotian Shelf. *J. Geophys. Res.* 99, 403–420.

Uppstrom, L.R. (1974). The boron/chlorinity ratio of deep-sea water from the Pacific Ocean. *Deep-Sea Res.* 21, 161-162.

Urrego-Blanco, J. and J. Sheng (2011). Interannual variability of circulation and hydrography over the Eastern Canadian Continental Shelf. *Atmosphere-Ocean*, submitted.

Vandemark, D., J.E. Salisbury, C.W. Hunt, S.M. Shellito, J.D. Irish, W.R. McGillis, C.L. Sabine, and S.M. Maenner. Temporal and spatial dynamics of CO_2 air-sea flux in the Gulf of Maine. *Geophys. Res*. 116, C01012.

Vázquez-Rodríguez, M., F. Touratier, C. Lo Monaco, D.W. Waugh, X.A. Padin, R.G.J. Bellerby, C. Goyet, N. Metzl, A.F. Ríos and F.F. Pérez (2009). Anthropogenic carbon distributions in the Atlantic Ocean: data-based estimates from the Arctic to the Antarctic. *Biogeosciences* 6, 439-451.

Vázquez-Rodríguez, M., X. A. Padin, A. F. Ríos , R. G. J. Bellerby, and F. F. Perez (2009). An upgraded carbon-based method to estimate the anthropogenic fraction of dissolved CO_2 in the Atlantic Ocean, *Biogeosciences Discusion* 6, 4527-4571.

Vázquez-Rodríguez, M., F.F. Pérez, A. Velo, A.F. Ríos, and H. Mercier (2012). Observed acidification trends in North Atlantic water masses. *Biogeosciences* 9, 5217-5230.

Wakelin, S.L., J.T. Holt, J.C. Blackford, J.I. Allen, M. Butenschön and Y. Artioli (2012). Modelling the carbon fluxes of the northwest European continental shelf: Validation and budgets. *J. Geophys. Res.*, 117, C05020.

Wallace, D. (2001). Storage and transport of excess CO_2 in the ocean: The JGOFS/WOCE global CO_2 survey, in *Ocean Circulation and Climate*, edited by G. Siedler et al., pp. 489-521, Academic, San Diego, California.

Wanninkhof, R., Lewis, E., Feely, R.A., and Millero, F.J. (1999). The optimal carbonate dissociation constants for determining surface water pCO_2 from alkalinity and total inorganic carbon. *Mar. Chem.* 65, 291-301.

Wanninkhof, R., S.C. Doney, J.L. Bullister, N.M. Levine, M. Warner, and N. Gruber (2010). Detecting anthropogenic CO_2 changes in the interior Atlantic Ocean between 1989 and 2005. *J. Geophys. Res*. 115, C11028.

Watson, A.J., U. Schuster, D.C.E. Bakker, N.R. Bates, A. Corbière, M. González-Dávila, T. Friedrich, J. Hauck, C. Heinze, T. Johannessen, A. Körtzinger, N. Metzl, J. Olafsson, A. Olsen, A. Oschlies, X.A. Padin, B. Pfeil, J.M. Santana-Casiano, T. Steinhoff, M. Telszewski, A.F. Rios, D.W.R. Wallace and R. Wanninkhof (2009). Tracking the variable North Atlantic sink for atmospheric CO_2. *Science,* 326 (5958), 1391–1393.

Waugh, D.W., T.M. Hall, B.I. McNeil, R. Key, and R.J. Matear (2006). Anthropogenic CO_2 in the oceans estimated using transit time distributions. *Tellus 58B*, 376-389.

Winkler, L.W. (1888). Die Bestimmung des im Wasser gelösten Sauerstoffes, *Chem. Berichte, 27*, 2843-2855.

Winther, N.G. and J.A. Johannessen (2006). North Sea circulation: Atlantic inflow and its destination. *J. Geophys. Res.* 111, C12018.

Wolf-Gladrow, D.A., R.E. Zeebe, C. Klaas, A. Kortzinger, and A.G. Dickson (2007). Total alkalinity: The explicit conservative expression and its application to biogeochemical processes. *Mar. Chem.* 106, 287-300.

Wollast, R. (1991). The coastal organic carbon cycle: fluxes, sources and sinks. In: Mantoura, R.F.C., Martin, J.M., Wollast, R. (Eds.), Ocean Margin Processes in Global Change, Wiley, Chichester, pp.365-382.

Wollast, R. (1998). Evaluation and comparison of the global carbon cycle in the coastal zone and in the open ocean, p. 213-252. In K.H. Brink and A.R. Robinson (eds.), The Global Coastal Ocean. John Wiley & Sons.

Wong, A.P.S., N.L. Bindoff, and J.A. Church (1999). Large-scale freshening of intermediate waters in the Pacific and Indian oceans. *Nature* 400, 440-443.

Wootton, J.T., C.A. Pfister, and J.D. Forester (2008). Dynamic patterns and ecological impacts of declining ocean pH in a high-resolution multi-year dataset. *Proc. Natl. Acad. Sci.* 105, 18848-18853.

Yool, A., A. Oschlies, A.J.G. Nurser and N. Gruber (2010). A model-based assessment of the TrOCA approach for estimating anthropogenic carbon in the ocean. *Biogeosciences* 7, 723-751.

van der Zee, C., and L. Chou (2005). Seasonal cycling of phosphorus in the southern bight of the North Sea. *Biogeosciences* 2, 27-42.

Zeebe, R.E. and D. Wolf-Gladrow (2001). CO_2 in Seawater: Equilibrium, Kinetics, Isotopes, Amsterdam: Elsevier Science, B.V. pp 346.

Chapter 9

CV and Bibliography of Author

Curriculum Vitae

Lesley Salt was born on the 7th March 1986 in Nottingham, England. After attending secondary school in one of the villages *furthest* from any coastline in the UK, she attended the University of Southampton, where she studied Oceanography at an undergraduate level. Preferring the chemical aspect of Ocean sciences, her first Bachelors project examined the role of natural iron limitation on phytoplankton community structure around the Crozet Islands. After another year of biogeochemistry lectures, she completed her Masters project examining the carbonate system of the (Sub-) tropical Northeast Atlantic. In June 2008 she received her Masters degree from the University of Southampton and in the same month moved to the Netherlands to start the PhD project at the Royal Netherlands Institute for Sea Research. Having used two datasets collected by others at sea for her undergraduate and masters work, she has since taken every opportunity to be the one doing the sea-going work and has thus participated in 9 scientific cruises totaling 10 months at sea. At the time of writing Lesley is now working for the Centre National de la Recherche Scientifique at the Station Biologique de Roscoff, in France, in the Chimie Marine group of Dr. Yann Bozec.

Bibliography

Salt, **L. A.**, S. M. A. C. van Heuven, M. E. Claus, E. M. Jones, and H. J. W. de Baar (2014), Rapid acidification of mode and intermediate waters in the southwest Atlantic. *Submitted to Biogeosciences.*

Salt, L. A., H. Thomas, F. Prowe, A.V. Borges, Y. Bozec and H.J.W. de Baar (2013), Variability of North Sea pH and CO_2 pumping in response to North Atlantic Oscillation forcing, *Published in Journal of Geophysical Research, 118,* 1-9.

Thomas, H., S.E. Craig, B.J.W. Greenan, W. Burt, G.J. Herndl, S. Higginson, **L. Salt**, E.H. Shadwick, and J. Urrego-Blanco (2012), Direct observations of diel biological CO_2 fixation on the Scotian Shelf, northwestern Atlantic Ocean, *Biogeosciences, 9*, 2301-2309.

de Baar, H.J.W., H.A.J. Meijer, H. Thomas, P. Ruardij, T. Johannesen, H.J. Zemmelink, A.M. Omar, I.T. van der Laan-Luijkx, **L. Salt**, K. Elkalay, Y. Bozec and A. Prowe (2010). Uptake of CO_2 by the North Sea in interaction with plankton blooms, pp. 94-107. In *Land-Ocean Interactions in the Coastal Zone (LOICZ)*. Editors Carlo Heip and Remi Laane.

Acknowledgements

"From the standpoint of daily life, however, there is one thing we do know: that we are here for the sake of each other - above all for those upon whose smile and wellbeing our own happiness depends, and also for the countless unknown souls with whose fate we are connected by a bond of sympathy. Many times a day I realize how much my own outer and inner life is built upon the labors of my fellow men, both living and dead, and how earnestly I must exert myself in order to give in return as much as I have received."

Albert Einstein.

Firstly, and foremost, I would like to thank my promotor, Hein de Baar. Thank you for the opportunity to undertake this research, for your support and guidance throughout it and for the flexibility to follow the avenues of research that really interested me. It has been a hugely educative and fun adventure. Many additional thanks for facilitating a large amount of international travel in the name of science, and ironically, CO_2 research.

To my second promotor, Helmuth Thomas, thank you so much for the significant amount of time and work you have invested in this thesis, without your help I'm confident I would still be writing (Chapter 1…). Furthermore, I would like to thank you for your hospitality during my time in Canada, both in and outside of work. People are still impressed I managed to get an office **with** a window at Dal.

Over the past five years I've had the privilege to meet some wonderful people whom have all contributed something to my life or my thesis. In chronological order, firstly to Henk Zemmelink and Josje Snoek, whom made my introduction and integration into the NIOZ so easy, for which I am very grateful. To Steven van Heuven, whose mobile number is forever engrained in my brain since that first year of my PhD in which you helped me a ridiculous amount. I don't think I've ever had a more educative year and I am so grateful for it. Further thanks to Rob, Charlie, Maarten, Charlotte, Marie and Claire, whom all welcomed me to Texel and the NIOZ and made my first year on the island so much warmer and friendlier.

In Halifax, I owe a big thanks to CO_2-colleagues Elizabeth and Will, and also to Cayla, Hamish, and Kelly for the roadtrips, ice hockey games and all the fun times had. Here I will also add a big thanks to Jess and Teurai, for the encouragement, support, and much needed thesis-breaks throughout the years. (Hopefully the next time either of you ask if you can call me Dr.Salt yet, the answer will be yes!).

A very special thanks to all my housemates over the years who had to put up with my unorthodox working hours, unpredictable presence/absences, and severe arachnophobia. In Den Burg - Darci (and temporarily Niamh), I'm proud to still hold the record for 'quickest departure from the Potvis' with you. In Halifax - Jen, I still miss our summer evening swims in the lake and (too-) late night chats. On Texel - Sabine, thanks for all the delicious stuff you baked, Arno, thanks for being the most chilled out person, ever, and Olga, thanks for the general good mood you bring to the house (every second week ;)). The Potvis #6 has a history of good housemates, so I'm proud to be amongst them. In Groningen - Maaike, Johan, Piedie and Lynn – I really enjoyed the strongbow-balcony, avond spelletjes, Read-Steady-Cook and an AH open past 8pm, even if it was only for a short time. The endless Frisian coffee at Emmastraat was definitely responsible for chapters 3 and 6! Occasional Den Hoorn housemate – Lenny, thank you so much for the bed and breakfast during my trips to Texel. I hope casa de Lenny, featuring the terracotta dome and world gin bar, opens somewhere near me one day.

I have also had the good fortune of participating in a total of 9 cruises throughout my time at the NIOZ. Each one stands out for various reasons, characterized largely by the people onboard. Here I would like to say a special thanks to all my cruise-buddies, who helped make those times so special. To Libby, with whom I spent ~4 months at sea from 03-2011 to 03-2012 – we were practically living together! Over the five years we've met in Paris, Punta Arenas, Las Palmas, Cape Town and Barcelona, I hope to keep this up for the next 5 years. To Nikki, my most recent CO2 cruising buddy, thanks for making these past few months on Texel, in the Med, Black Sea, Istanbul and Lisbon so much fun. After two months of sharing a cabin with you, and so (so) many broken boundaries, its needless to say, I'll(mo) miss your face.

Additional thanks to the nutrients department at the NIOZ, for the wonderful job they do. Special thanks to Karel for all the help with oxygen measurements over the years and to Sharyn for all the additional help you end up giving us and for your cherished company onboard. To the guys in the workshop for all the help over the years and good times onboard, especially to Ruud, John, Leon, Jan Dirk and Edwin. Thank you to the crew of the Pelagia whom always make sailing so much fun, in particular Bert, Roel, Cor, Sjaak, Klaas, Alex, Ger, Jaap, Jose, Pieter, Rik, Freddy, Martijn, and Inno, whom I have had the pleasure to sail with a number of times now.

I owe a particularly huge thank you to my two paranimfs, whom have both helped me through the past years. To Astrid, my fellow PhD, office mate, and for two years, my only CO_2 colleague. You have been with me throughout this PhD and I like to think we have helped and counseled each other, and your companionship has meant a tremendous deal to me. I cannot thank you enough and I wish you, and your family, nothing but happiness and success in the future and hope I will be there to see it. To Maaike, you have been my student, cruise-buddy, housemate, and friend and suffered with me through the hardest part of any PhD – the end. I will never forget all the support (and coffee and koek!!!) you gave me and I hope one day I can return the favour.

Finally, I'd like to thank Mum, Dad, Michelle and Matt (and Will). You have all witnessed the trials and tribulations over the past half-decade, with amusement, bemusement and more recently, possibly, some concern. Thank you all for giving me endless support, perspective, advice, a sense of humor, and a roof over my head, as and when needed.

Texel, 18th August, 2013.